University of Naples Federico II

Polytechnic and Basic Sciences School

Ph.D. in Chemical Sciences

XXXIV Cycle

Capsular polysaccharides and lipopolysaccharides from psychrophiles: structural characterization and biological activity.

Ph.D. candidate:
Rossella Di Guida

Supervisor:
Prof. Maria Michela Corsaro

Examiner:
Prof. Alessio Cimmino

Coordinator: Prof. Angela Lombardi

Index

Abbreviations

AA	Alditol Acetate
Ac_2O	Acetic anhydride
AFP	Antifreeze proteins
Amp	Ampicillin
BLPs	Braun Lipoproteins
CaCo-2	Human colon adenocarcinoma cells
Cm	Chloramphenicol
COSY	Double Quantum-Filtered Correlation spectroscopy
CPS	Capsular polysaccharide
CRC	Colorectal cancer
CTR	Untreated cells
D,D-Hep	D-*glycero*-D-*manno*-heptose
DEPT-HSQC	Distortionless Enhancement by Polarization Transfer-Heteronuclear Single Quantum Coherence
DOC-PAGE	Sodium deoxycholate PolyAcrylamide Gel Electrophoresis
DMEM	Dulbecco Modified Eagle medium
EB	Eluition buffer
EDTA	Ethylenediaminetetraacetic acid
EPS	Extracellular polysaccharide
FBS	Fetal-bovine serum
Gal	Galactose
GalA	Galacturonic acid
GalN	2-Amino-2-deoxy-galactose
GAPDH	Glyceraldehyde-3-phosphate dehydrogenase
GC-MS	Gas chromatography-Mass spectrometry
Glc	Glucose
GlcA	Glucuronic acid
GlcN	2-Amino-2-deoxy-glucose
GulNA	Gulosaminuronic acid
HCT-116	Human colon rectal carcinoma cells
HF	Hydrofluoric acid
HMBC	Heteronuclear multiple bond correlation
HPLC	High Performance Liquid Chromatography
HSQC	Heteronuclear Single Quantum Correlation
IBPs	Ice binding proteins

IL-6	Interleukin 6
IM	Inner membrane
Ino	Inositol
IRI	Ice Recrystallization Inibition
Kdo	3-Deoxy-D-*manno*-oct-2-ulosonic acid
Kdo8N	8-Amino-8-deoxy-*manno*-oct-2-ul-osonic acid
L,D-Hep	L-*glycero*-D-*manno*-heptose
LB	Luria Bertani
LBP	LPS-binding protein
LOS	Lipooligosaccharide
LPS	Lipopolysaccharide
MALDI-TOF	Matrix Assisted Laser Desorption Ionization – Time Of Flight
Man	Mannose
ManN	2-Amino-2-deoxy-mannose
ManNAc	2-Acetamido-2-deoxy-mannose
ManNAcA	2-Acetamido-2-deoxy-mannuronic acid
MB	Marine broth
MD-2	myeloid differentiation protein 2
MGA	Methyl glycoside acetylated
MGS	Mean grain size
MLVs	Multilamellar vesicles
MyD88	Myeloid differentiation primary-response protein 88
NF-κB	Nuclear factor kappa B
NMR	Nuclear Magnetic Resonance
NOE	Nuclear Overhauser Effect
NOESY	Nuclear Overhauser enhancement spectroscopy
OM	Outer membrane
OMPs	Outer Membrane Proteins
OS	Oligosaccharide
PCP	Phenol/Chloroform/Petroleum ether
PCR	Polymerase chain reaction
PEtN	Phosphoethanolamine
PG	Peptidoglycan
PMAA	Partially Methylated Alditol Acetate
POPE	1-palmitoyl-2-oleoyl-sn-glycero-3-phosphoethanolamine
POPG	1-palmitoyl-2-oleoyl-sn-glycero-3-phospho-(1′-*rac*-glycerol)
Py	Pyridine
qRT-PCR	Quantitative real-time polymerase chain reactions
Qui2NAc	2-Acetamido-2,6-dideoxy-D-glucose
Rha	Rhamnose
Rif	Rifampin
R-LPS	Rough-Lipopolysaccharide
ROESY	Rotating frame Overhauser effect spectroscopy

RPMI	Roswell Park Memorial Institute
SDS	Sodium dodecyl sulfate
S-LPS	Smooth-Lipopolysaccharide
SUVs	Small unilammellar vesicles
TAE	Tris-acetate-EDTA
TBST	Tris-buffered saline and 0.05% Tween-20
TEM	Trasmission Electronic Microscopy
TFA	Trifluoroacetic acid
THAP	2,4,6-Trihydroxyacetophenone
TLR	Toll-like receptor
TRIF	TIR-domain-containing adaptor protein
TOCSY	Total correlation spectroscopy
TSP	3-Trimethylsilyl-propanoate
TTBS	Tris-buffered saline and 0.05% v/v Tween-20

Abstract

Microorganisms that inhabit the cold biosphere, called cold-adapted or psychrophiles, represent a significant portion of the biomass of the planet (Siddiqui K.S. et al., 2013; De Maayer P. et al., 2014). These microorganisms (bacterial and archaeal communities) have developed many strategies to survive, including structural modification of molecules belonging to the external layer (such as lipopolysaccharides, LPSs) and the production of molecules of biotechnological interest, including carbohydrate-based polymers (extracellular polysaccharides, EPS) (Poli A. et al., 2011; Casillo A. et al., 2018). In literature, few studies regarding the relationship between the structure of molecules belonging to the external layer of cellular membranes and cold adaptation mechanisms are reported. Low temperatures decrease the membrane fluidity, resulting in the phase transition from its normal liquid-crystalline state to a more rigid gel-like state. It is reported that microbial cells counteract the lowering temperature by incorporating unsaturated and short fatty acids to restore optimal fluidity (Cavicchioli R. et al., 2006; D'Amico S. et al., 2006).

LPSs is the major component of Gram-negative bacterial outer membrane and possess a pivotal role in bacterial survival increasing the strength of the cell envelope and mediating the contacts with the external environment. Therefore, it is reasonable to assume that structural modifications could occur in the LPS of cold-adapted bacteria. The LPS general structure can be divided into three distinct regions: Lipid A, core oligosaccharide and O-specific chain, which differ in their structure and biosynthetic pathways (Raetz and Whitfield, 2002; Yethon and Whitfield, 2001). The lipid A is a highly conserved glycolipid domain that anchors the molecule to the OM, therefore its structure is crucial for membrane integrity. The core oligosaccharide is constituted by the inner core and the outer core regions. The inner core, directly linked to the lipid A, is more conserved and contains peculiar sugars such as Kdo (3-deoxy-D-*manno*-oct-2-ulosonic acid) and heptoses. Usually, the outer core contains common monosaccharides and displays a higher variability. The O-specific chain

polysaccharide (O-antigen) is the most variable moiety of the LPS. It can be a homo- or heteropolymer composed of a variable number (up to 40) of repeating units, each one can contain up to 10 sugars. The O-antigen is not always expressed, and in this case, the LPS is named Rough-LPS or lipooligosaccharide (LOS).

The LPSs represent the major virulence factor of Gram-negative bacteria. It is able to elicit host immune response through the TLR4/MD-2 receptor complex expressed on the surface of a wide number of different (immune and non-immune) cells. The excessive exposure or excessive host responses to LPS can lead to an uncontrolled inflammation process and finally to septic shock. The biological activity of this molecule, that varies from highly endotoxic (agonist) to antiinflammatory (antagonist), is due to the lipid A primary structure. TLR-mediated immunomodulatory therapy was found to be a promising strategy for the treatment of acute and chronic disorders, ranging from infectious diseases and sepsis to autoimmune syndromes and cancer. In addition, the vaccines require a co-administration of immune-stimulating agents to improve immune response. The recent advances in the development of fully synthetic conjugated vaccines highlight the urgent need for novel TLR-dependent vaccine adjuvants (Adanitsch F.et al., 2018).

Some bacteria can synthesize homo- or heteropolysaccharides, that can be divided into capsular polysaccharides (CPSs) and medium released exopolysaccharides (MRPs). CPSs are linked to the bacterial surface both via a covalent bond to phospholipids or lipid-A molecules and may be associated directly with the cell without any membrane anchor (Fresno S. et al., 2006; Whitfield and Valvano 1993). CPS constitutes the outermost layer of the bacterial cell and mediates its direct interaction with the environment. These molecules showed cryoprotectant abilities inhibiting the ice crystal growth (Casillo A. et al., 2017) and influence the physical properties of the ice matrix, promoting the cell aggregation and facilitating the biofilm formation (Glud et al., 2014; Fernández-Méndez et al.; 2014). In pathogenic Gram-negative bacteria, capsular polysaccharides are one of the most important virulence

factors that protect the bacterium from the innate immune response. Bacterial polysaccharides are biocompatible, biodegradable, and generally non-toxic molecules with different useful properties. They can be used in many fields such as cosmetics, drug delivery systems, emulsifiers, food additives, heavy metal removal, and thickeners. Some polysaccharides have shown various bioactivities including antimicrobial, antiviral, anticancer, antioxidant, and immunomodulatory activities.

During this PhD project, the LPSs and CPSs from cold-adapted Gram-negative bacteria have been extracted, purified, and characterized by chemical analyses, mass spectrometry and NMR spectroscopy. The structural characterization of these molecules is aimed both at the comprehension of cold-adaptation mechanisms and at the investigation of their biological activity.

Shewanella vesiculosa HM13 is a psychrotolerant bacterium, isolated from the intestine of a horse mackerel (*Trachurus japonicus*), able to produce extracellular membrane vesicles (EMVs) with a single major protein (P49) as cargo. This strain was selected as a host for the secretory production of foreign proteins at low temperatures (Chen et al., 2020). EMVs generally have a spherical structure, with a size ranging from 20 to 250 nm in diameter and are originated from the bacterial outer membrane (Kulp and Kuehn, 2010; Schwechheimer and Kuehn, 2015). Due to their origin, the vesicles mainly contain lipopolysaccharides, phospholipids, outer membrane proteins, and periplasmic contents. The research group of Prof. Kurihara (Kyoto University) demonstrated that genes involved in the biosynthesis of surface glycoconjugates are included in the P49 gene cluster. The deletion of some of these genes affected the loading of the P49 into the vesicles.

To go deeper into the involvement of surface glycolipids in the P49 association, the surface glycoconjugates from the cells and EMVs have been isolated and characterized, starting from *Shewanella vesiculosa* HM13 wild-type.

We extracted the LPS from *S. vesiculosa* HM13 cells grown at 4 °C. The analysis revealed the rough nature of the isolated LPS, as already observed for other *Shewanella* species (Vinogradov E. et al., 2003; Vinogradov E. et al., 2004; Moule A.

L. et al., 2004). The oligosaccharide moiety (Figure 1) showed structural features already reported for *Shewanella* strains, such as the presence of the Kdo8N instead of the usual Kdo. In addition, the presence of a phosphoethanolamine group substituting the O-4 position of the Kdo8N, agrees with other oligosaccharide structures from *Shewanella* species (Vinogradov E. et al., 2003; Silipo A. et al., 2005). Unfortunately, the low number of vesicles secreted at 4 °C prevented the characterization of the LPS. To overcome this problem, *Shewanella vesiculosa* was grown at 18 °C. The LOS isolated from the vesicles at 18 °C revealed the same structure of that reported for the cells. This result agrees with the budding biogenesis of the EMVs from the outer membrane (Kamasaka K. et al 2020).

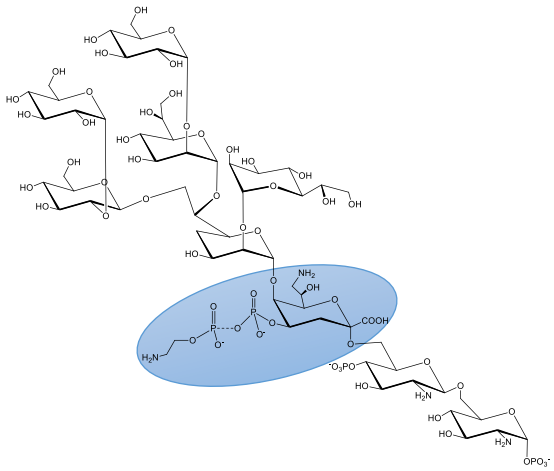

Figure 1 – Core oligosaccharide structure of the LOS from *Shewanella vesiculosa* HM13

In addition, *S. vesiculosa* HM13 produces a capsular polysaccharide isolated from both cells and vesicles. The chemical analyses and NMR spectra of the purified CPS suggested that the polysaccharides from cells and EMVs share the same structure. The CPS consists of a highly hydrophobic branched pentasaccharidic repeating unit (Figure 2). This feature is due to the presence of novel monosaccharide (shewanosamine, ShewN), which was isolated and characterized.

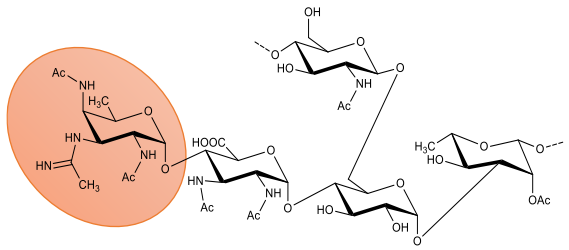

Figure 2 – CPS repeating unit from *S. vesiculosa* HM13

Successively, was investigated *S. vesiculosa* HM13 HM3343-mutant that defects in a gene (HM3343) encoding a protein homologous to Wzx. The deletion of HM3343 gene resulted in a marked decrease of cellular P49 levels and disappearance of P49 from EMVs. All the analyses suggested that the LOSs isolated from the cells and EMVs of the HM3343-mutant are identical to those obtained for the wild-type. Moreover, chemical analysis and NMR experiments suggested that the CPSs isolated from the cells and EMVs of the mutant and wild type are identical. The only difference observed is the lower amount of CPS with respect to the wild type. This finding could suggest that the protein encoding by the HM3343 is involved in the membrane translocation of the repeating units of this polysaccharide, which in turn is implicated in the P49 association to the vesicles.

Thanks to the collaboration with Prof. Paduano group, adhesion assays of CPS from *S. vesiculosa* HM13 on bacterial mimic vesicles showed its ability to aggregate around the vesicles with a driving force attributable to hydrophobic interaction. This result could suggest a key role of this hydrophobic polysaccharide in the aggregate formation and attachment to surfaces for biofilm formation. This propriety makes the polysaccharide a promising molecule for the development of new adhesive materials avoiding health hazardous chemicals and dependence on petroleum resources used for the obtainment of components of commercial adhesives (Haag A. P. et al., 2006).

Pseudoalteromonas nigrifaciens Sq02 is a psychrotrophic bacterium, isolated from the intestine of a fish species (*Seriola quinqueradiata*). DOC-PAGE analysis of the extracts indicated the rough nature of LPS and the presence of a CPS. The LOS was

fully deacylated to resolve the primary structure. NMR experiments together with chemical analyses and MALDI-TOF experiments suggested that this bacterium shares the same oligosaccharide with *Pseudoalteromonas haloplanktis* TAC125 (Corsaro M. M. et al., 2001) (Figure 3). Moreover, it was observed that the lipid A possesses the same fatty acids composition and heterogeneity already reported for other *Pseudoalteromonas* species (Corsaro M. M. et al., 2002; Krasikova I. N. et al.; 2003, Volk A. S. et al 2007; Carillo S. et al., 2011). In particular, the main lipid A species is a di-phosphorylated penta-acylated glycoform, carrying four C12:0(3-OH) and one C12:0 residue, substituting the non-reducing GlcN, as found in *P. haloplanktis* TAB 23 (Carillo S. et al., 2011) and *P. haloplanktis* ATCC 14393T (Krasikova I. N. et al., 2004) (Figure 3).

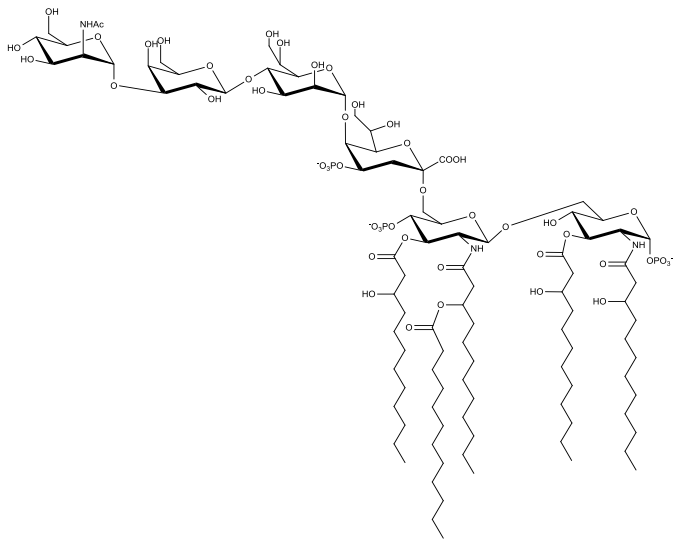

Figure 3 – LOS structure from *Pseudoalteromonas nigrifaciens* Sq02

To purify the CPS from the LOS, the water extract was treated with 1% acetic acid and the supernatant was fractionated through gel filtration chromatography. Chemical analyses and NMR experiments allowed to establish the structure of the CPS, that is made up only of *N*-acetylated aminosugars and contains the rare 2-acetamido-2-deoxy-D-mannuronic acid (D-MaNAcA) (Figure 4).

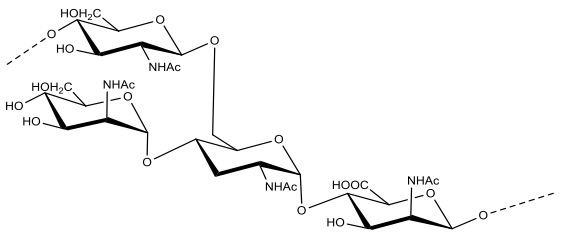

Figure 4 – CPS repeating unit from *P. nigrifaciens* Sq02

In collaboration with prof. Schiraldi group the immunomodulatory effect of the molecules isolated from *P. nigrifaciens* Sq02 on colon cancer cell lines was also investigated. LPS and the lipid A, on differentiated CaCo-2 cells, showed a similar action to the LPS from *E. coli* and *S. minnesota*. In particular TLR-4 expression increases, at both mRNA and protein levels, as well as NF-κB and cytokines (Kaszowska M. et al., 2017; Nyati K. K. et al., 2017). A possible anti-cancer activity of the isolated CPS against two colon cancer cell lines (CaCo-2 and HTC-116) was also preliminarily evaluated. The results suggested a significant reduction in cell viability, especially on HCT-116 cells, after 72h. The mechanism of CPS action was identified by evaluation of four specific markers (Bax, Caspase 3, Caspase 9, Bcl-2) associated with the apoptosis pathway.

Pseudomonas sp. ANT_J38B is a psychrotolerant bacterium isolated from a sample soil collected from King George Island (Antarctica) (Romaniuk K. et al., 2018). The LPS from this bacterium was extracted from the cells grown at 4 °C and analyzed by DOC-PAGE. After silver staining the experiment allowed to establish the smooth nature of LPS. Chemical analyses and NMR experiments allowed us to identify the structure of the O-chain repeating unit (Figure 5). The latter consists of a disaccharide containing the 2-acetamido-2,6-di-deoxyglucopyranose (β-D-3-QuipNAc) and 2-acetamido-2-deoxy-gulopyranuronamide acetylated at O-3 position (α-L-4-GulpNAc3OAcAN). The presence of a high number of acetyl substituent confers a high hydrophobic to the molecule.

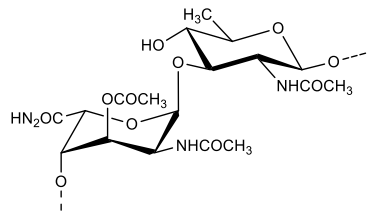

Figure 5 – O-Chain repeating unit from *Pseudomonas* sp. ANT_J38B

The psycrotolerant bacteria *S. vesiculosa* HM13 and *P. nigrifaciens* Sq02 produce a R-LPS. This feature is common among the LPS structures from cold-adapted bacteria analyzed up to now (Casillo A. et al., 2019). The lack of the O-chain could enhance the outer membrane flexibility and stability at low temperatures (Corsaro M. M. et al., 2017). In addition, the LPS showed the presence mainly of fatty acids with a short chain (from 10 to 15) confirming the trend commonly found in cold-adapted bacteria. *Pseudomonas* sp. ANT_J38B is an example of cold-adapted bacterium that produce an S-LPS at low temperature. Previously, S-LPSs have been found exclusively for cold-adapted bacteria grown at temperatures above 20 °C. However, a common feature of O-chain from psychrophilic bacteria is the presence of uronic acids, amino sugars (Kilcoyne M. et al., 2004; Hoffman J. et al., 2012) and acyl substituents.

To find a possible correlation between the O-chain expression and cold adaptation, molecular biology experiments should be performed. It was observed that *Photobacterium profundum* FL26 mutant is not able to produce S-LPS and is a cold sensitive phenotype (Lauro F. M. et al., 2008). *Pseudomonas extremaustralis wapH* mutant is not able to grow at 8 °C and produces a higher amount of S-LPSs and a lower amount of low molecular weight glycoforms (Benforte F. C. et al., 2018). These experiments have suggested that the LPS structure is essential for bacterial cold adaptation but is not possible to speculate about the O-chain role. For this reason, further studies will be necessary. Based on the molecular biology methodologies acquired during the exchange period in the research group of Prof. Susana Merino (University of Barcelona), I tried to obtain a deletion of the gene encoding a putative

O-antigen ligase for the psychrotolerant bacterium *Idiomarina zobellii* KMM 231^T, able to produce a S-LPS. The experiments are still ongoing.

Finally, to evaluate a possible involvement of two CPSs isolated in cold survival by conferring cryoprotection to the cells Ice Recrystallization Inhibition (IRI) assays were performed, in collaboration with Prof. Gibson. The results have demonstrated that the CPS does not display IRI activity (Biggs C. I. et al., 2019).

Papers related to this thesis work

1. Casillo, R. Di Guida, S. Carillo, C. Chen, K. Kamasaka, J. Kawamoto, T. Kurihara, M. M. Corsaro "Structural Elucidation of a Novel Lipooligosaccharide from the Cold-Adapted Bacterium OMVs Producer *Shewanella* sp. HM13" Mar. Drugs, 17 (2019) 34.

2. R. Di Guida, A. Casillo, F. Yokoyama, J. Kawamoto, T. Kurihara, M. M. Corsaro, "Detailed structural characterization of the lipooligosaccharide from the extracellular membrane vesicles of *Shewanella vesiculosa* HM13" Mar. Drugs, 18 (2020) 231.

3. R. Di Guida, A. Casillo, M. M. Corsaro, "O-specific polysaccharide structure isolated from the LPS of the Antarctic bacterium *Pseudomonas* ANT_J38B" Carbohydr. Res., 497 (2020) 108125.

4. R. Di Guida, A. Casillo, A. Stellavato, C. di Meo, S. Kawai, J. Kawamoto, T. Ogawa, T. Kurihara, C. Schiraldi, M. M. Corsaro "Complete lipooligosaccharide structure from *Pseudoalteromonas nigrifaciens* Sq02-Rif^r and study of its immunomodulatory activity." Mar. Drugs., 19(11) (2021) 646.

5. R. Di Guida, A. Casillo, A. Stellavato, S. Kawai, T. Ogawa, C. di Meo, J. Kawamoto, T. Kurihara, C. Schiraldi, M. M. Corsaro "Capsular Polysaccharide from a fish-gut bacterium induces/promotes apoptosis of colon cancer cells in vitro through Caspases' pathway activation." Carbohydr. Polym. 278 (2022) 118908.

The author of the present PhD thesis acknowledges: Prof. Corsaro M. M., Dr. Casillo A., Prof. Kurihara T., Prof. Merino S., Prof. Tutino M. L., Prof. Parrilli E, Dr. Colarusso A., Dr. Lauro C., Prof. Gibson M. I., Prof. Paduano L., Prof. Schiraldi C. and Dr. Delbarre-Ladrat C. for the scientific support.

Chapter I: Introduction

1.1 Gram-negative bacteria

Gram-negative bacteria are members of the *Bacteria* domain, one of the three domains of life (Figure 1.1) in which all the organisms on Earth are classified, besides *Archaea* and *Eukaryota*. They are prokaryotic organisms, which are single-celled with a simple structure that lacks membrane-bound organelles, and a membrane-bound nucleus. They contain a DNA floating freely in a mass called nucleoid. Many prokaryotes also contain additional circular DNA molecules called plasmids, with additional cell functions, such as encoding proteins able to inactivate antibiotics.

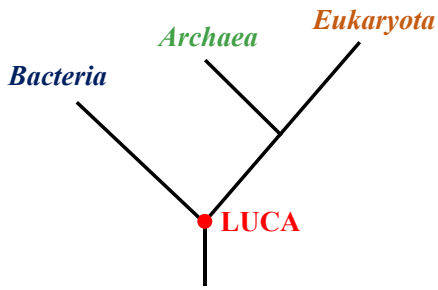

Figura 1.1 Phylogenetic tree of life, where "LUCA" is the last universal common ancestor.

Bacteria are currently classified according to their characteristics, such as morphology and temperature required for their optimal growth. In the 1884 Christian Gram developed a staining procedure that allowed to classify the bacteria into two main groups, based on the structural differences in their cell envelope. The possibility to use the Gram staining to categorize bacteria suggests that a basic organization is conserved. After this colorimetric assay, some bacteria are coloured in purple (Figure 1.2b), and for this reason named Gram-positive, while the others, termed Gram-negative, appear pink (Figure 1.2b). The reason why this iodine stain is not retained by the Gram-negative bacteria is that they possess a peptidoglycan (PG) layer much thinner than in Gram-positive (Figure 1.2a) (Beveridge T. J. and Graham L. L., 1991).

The PG is a rigid layer that encloses the cytoplasmic membrane (or inner membrane, IM), consisting in a network of alternating chains of *N*-acetylglucosamine and *N*-acetylmuramic acid that are cross-linked by penta-peptide chains. This layer confers shape and osmotic strength to the bacterial cell. The IM is a symmetric glycerophospholipid bilayer, which surrounds the cytosol and contains several proteins with essential functions, such as energy production, lipid and glycolipids biosynthesis, secretion, and transport. Moreover, in Gram-negative bacteria the thin PG layer is immersed in an aqueous space, termed periplasm, confined between the inner and outer membranes (OM) (Beveridge T. J. and Graham L. L., 1991).

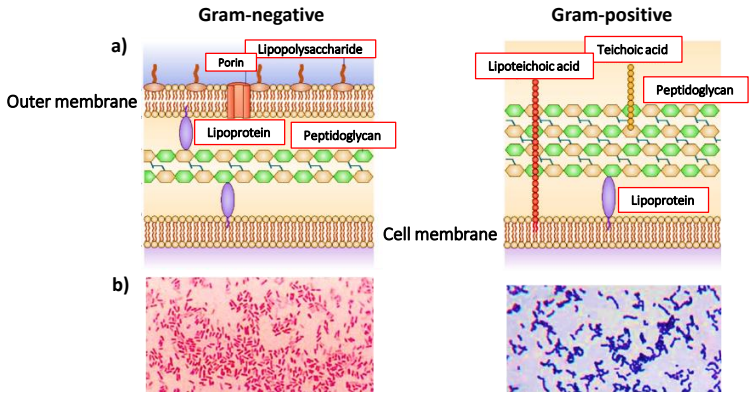

Figure 1.2 a) Cell wall architecture of Gram-negative bacteria and Gram-positive bacteria and b) Gram staining.

1.2 Gram-negative outer membrane

As previously mentioned, the outer membrane (OM) is a feature of Gram-negative bacteria. The OM represents the most external layer and consists in an asymmetrical lipid bilayer connected to the PG through peculiar lipoproteins, named Braun Lipoproteins (BLPs) (Sankaran K. and Wu H. C., 1994). This membrane contains glycerophospholipids in the inner leaflet, whereas the outer leaflet is principally composed of lipopolysaccharides (LPSs) (Kamio Y. and Nikaido H., 1976). The OM

also contains several proteins (Outer Membrane Proteins, OMPs), of which most of them are composed of amphipathic β-strands which adopt a β-barrel structure (Fairman et al., 2011; Schulz G. E., 2002). Among the OMPs an important class are the porins, which are integral membrane proteins forming channels for the passage of small hydrophilic molecules through the semipermeable membrane (Zeth K. and Thein M., 2010). In addition, on the cell surface of a wide range of bacterial species, polysaccharidic molecules named capsular polysaccharides (CPSs) or capsule are found. These macromolecules are linked to the bacterial cell surface via covalent attachment to either phospholipids or lipid-A molecules, while, in certain cases, it was observed that CPS may be associated directly with the cell without any membrane anchor (Fresno S. et al., 2006; Whitfield C., 1988; Whitfield C. and Valvano M. A., 1993). When is present, the capsule constitutes the outermost layer of the bacterial cell and therefore mediates its direct interaction with the environment.

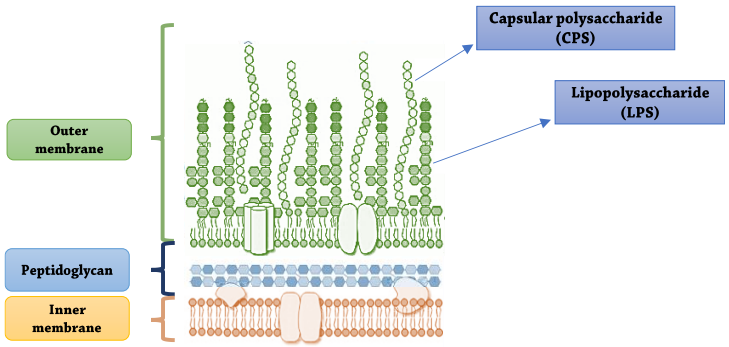

Figure 1.3 Architecture of Gram-negative cell wall.

1.3 Lipopolysaccharide (LPS): structure and biosynthesis

The LPS is an extremely heat-stable amphiphilic macromolecule. Generally, is composed of three regions divided based on their genetics, structures, and function: a glycolipid portion (lipid A) covalently linked to an oligosaccharide moiety (core) which is, in turn, linked to an O-polysaccharide chain (O-chain) (Alexander C. and Rietschel E. T., 2001) (Figure 1.4). The LPS is termed smooth (S-LPS or simply LPS) when the O-chain is present since the microscope shows a smooth morphology of the colonies. On contrary, when the O-chain is absent is termed rough (R-LPS, lipooligosaccharide or LOS) due to the rough aspect of the colonies (Alexander C. and Rietschel E. T., 2001; Caroff M. and Karibian D., 2003). The LPS layer is stabilized by electrostatic interactions between the negatively charged groups present on LPS and divalent cations (as Ca^{2+} and Mg^{2+}). This leads to a highly ordered structure with low fluidity that can explain the low susceptibility to hydrophobic molecules and negatively charged antibiotic. However, is possible to increase the permeability of the OM by destabilizing the interactions of the LPSs and cations using group of polymyxin antibiotics, cationic proteins, and peptides or polyamines, and chelators like ethylenediaminotriacetic acid (EDTA) (Vaara M., 1992). Due to its location, the LPS is involved in all the interactions with the external environment such as adhesion, colonization, symbiosis, and virulence. In fact, in pathogenic Gram-negative bacteria the released LPSs, also called endotoxins, interact with the mammalian innate immune system activating the production of host pro-inflammatory cytokines. This can be beneficial to the host, enhancing resistance to infecting microbes, however if the production of pro-inflammatory cytokines is massive and uncontrolled can lead to septic shock and death (Alexander C. and Rietschel E. T., 2001; Caroff M. and Karibian D., 2003).

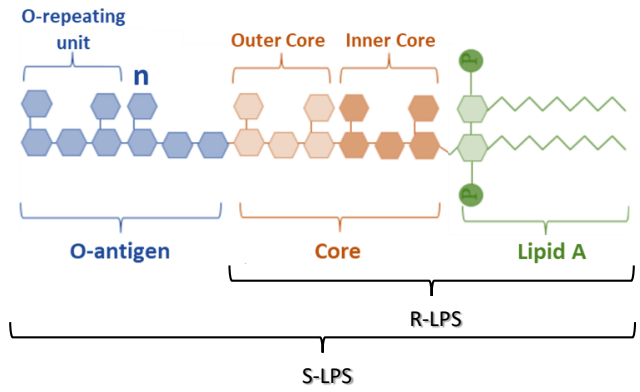

Figure 1.4 General chemical structure of LPS from Gram-negative bacteria

1.3.1 Lipid A

The lipid A is the glycolipid portion of the LPS, which is involved in hydrophobic interactions with the phospholipid bilayer composing the inner leaflet of the OM (Holst O. et al., 1996). Therefore, its structure is crucial for membrane integrity and stability. This moiety represents the most conserved moiety of the LPS and for this reason is possible to identify a common general structure. It is composed by a disaccharide backbone of two D-glucosamine β-(1→6) linked, which are substituted with 3-hydroxy fatty acid linked as amides at position 2 and as esters at position 3. The acyl groups directly linked to the sugar backbone are defined primary. Some of these fatty acids are further acylated at the hydroxy groups by secondary acyl chains. In addition, the reducing GlcN residue (GlcN I or proximal unit) is phosphorylated at position 1 and the non-reducing one (GlcN II or distal unit) at position 4' with the position 6' free, resulting the attachment site of the saccharide moiety of the LPS (Figure 1.5). Among the bacterial LPS, this general structure is conserved, but lipid A molecules possess a heterogeneity mainly due to the type, number, and position of fatty acids and to the phosphorylation patterns. Indeed, the phosphate groups can be absent or substituted by a second phosphate (giving rise to a pyrophosphate group), but

also by other polar substituents such as 4-amino-4-deoxy-L-arabinopyranose (Ara4N), 2-amino-ethanol group (EtN) or by acidic residues such as galacturonic acid (GalA) (Plötz B. M. et al., 2000). These substituents are usually present in non-stoichiometric amount.

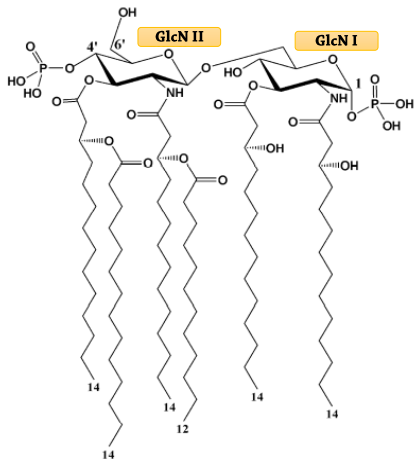

Figure 1.5 The structure of lipid A from the LPS of *E. coli*.

Lipid A represents the endotoxic principle of the LPS and its biological activity (agonist or antagonist) is due to its three-dimensional structure (Seydel U. et al., 2000). In particular, the molecular shape of the lipid A depends on the tilt angle between the disaccharide backbone and the acyl chains, since this influences the specificity of the binding with the immune receptors (Netea M. G. et al., 2002). The angle of inclination is determined by the grade of acylation and the fatty acid distribution between the two GlcN units (Figure 1.6). When the lipid A is bisphosphorylated and hexa-acylated with an asymmetric (4 + 2) distribution of acyl groups, as the *E. coli* lipid A in figure 1.5, displays a tilt angle >50° and a conical molecular shape. This leads to the highest immunostimulatory capacity in mammal's cell. In contrast, species with a tilt angle <25°, such as the tetra-acylated lipid IVA precursor of *E. coli* lipid A and the penta-acylated lipid A of *Rhodobacter sphaeroides* (Strittmatter W. et al., 1983) are endotoxically inactive

but can be antagonist. The molecular shape of these species is cylindrical. Species with a tilt angle between 25° and 50°, as monophosphorylated lipid A, have a lower bioactivity.

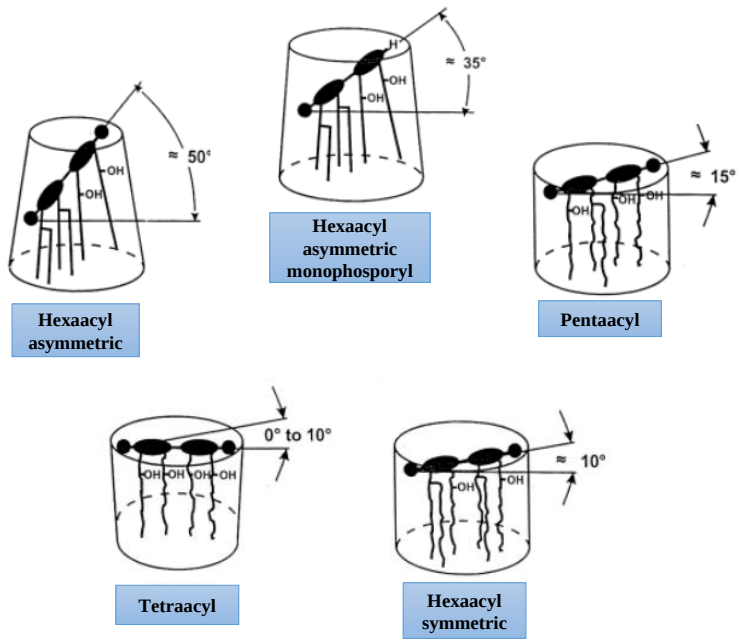

Figure 1.6 Tilte angle of different acylation patterns. Intrinsic conformations of asymmetric hexa-acylated lipid A, less active monophosporyl lipid A, and showing low activity, inactive or antagonistic penta- and tetra-acylated lipid A and symmetric hexa-acylated lipid A (Seydel U. et al., 2000).

1.3.2 Core region

The Core region is a linear or branched oligosaccharide domain characterised by up to fifteen monosaccharides (Holst O., 1999). Within a genus or family, the structure tends to be well conserved reflecting the importance of the core in outer-membrane integrity. Based on the monosaccharide composition the core can be distinguished in two different regions termed: inner and outer core (Holst O., 1999).The inner core is directly linked to the lipid A and contains uncommon sugar residues, constituted by eight or seven carbon atoms, such as the L-glycero-D-*manno*-heptose, the less common D-*glycero*-D-*manno*-heptose (De Soyza A.,

2008) and 3-deoxy-D-*manno* octulosonic acid (Kdo). This latter sugar is a marker of Gram-negative bacteria that connects the core oligosaccharide to the lipid A backbone with an α-configured ketosidic linkage. There are some exceptions in which the Kdo is replaced by its C-3 hydroxy-derivative D-*glycero*-D-*talo*-oct-2-ulosonic acid (Ko), like in some *Acinetobacter* (Vinogradov E. et al., 1997) or *Burkholderia* (Silipo A. et al., 2006) strains, or by its C-8 amino-derivative the 8-amino-8-deoxy-*manno*-oct-2-ul-osonic acid (Kdo8N), in *Shewanella* genus (Vinogradov E. et al. 2003; Silipo A. et al., 2005). The first L,D- or D,D-Hep residue is linked at the position 5 of the first Kdo and may be substituted by other heptose units. The Kdo is typically substituted at position 4 by a negative charged group, such as a phosphate, pyrophosphate or phosphorylethanolamine (PEtN), or a second Kdo unit. These substitutions are often present in non-stoichiometric amount. The outer core region is the most exposed portion and is characterised by a higher structural variability than the inner core region. It is typically composed of common neutral and acidic monosaccharides, as well as aminosugars.

1.3.3 O-Chain

The polysaccharide region, named O-specific chain or polysaccharide (OPS), is the most exposed portion of the LPS. The OPS is made of up to 50 oligosaccharide repeating units (O-units) consisting of two to eight different monosaccharide residues. Only a few bacterial strains or species contain homopolymeric O-chains. The repeating unit can be linear or branched and can contain many non-carbohydrate substituents such as phosphate, amino acids, and acetyl groups (Mayer H. et al. 1989). Bacterial polysaccharides can contain rare monosaccharides, such as the acidic monosaccharide termed Legionamminic acid (Leg) in the LPS from *Legionella pneumophila* (Knirel Y. A. et al., 1997) or in *Shewanella putrefaciens*, where the Shewanellose (She) was first isolated (Shashkov S. et al., 2002). A single bacterium produces LPSs with O-chains

characterised by a wide range of lengths because of incomplete synthesis of the polysaccharide chain (Raetz C. R. and Whitfield C., 2002). This different degree of polymerization is responsible for the "ladder-like" pattern, showed by SDS-PAGE (Sodium Dodecyl Sulphate - PolyAcrylamide Gel Electrophoresis) (Kittelberger R. and Hilbink F., 1993) typical of a smooth LPS. The O-polysaccharide is also referred to as the O-antigen because is the major antigen targeted by host antibody responses (Erridge C. et al., 2002). Indeed, is one of the most important virulence factors in the interaction of bacteria with humans and animals (Knirel Y. A., 2009). Is the most variable also within bacteria belonging to the same genus. The highly diversity in O-chain structure and composition may have developed during evolution in order to escape the host's immune system and to hide the common units, i.e. the lipid A and the inner core region attached to it. It has also an important biological role in the protection of the bacterial cells (Lerouge I. 2001; Rosenfeld Y. and Shai Y., 2006; Lindell K. et al., 2012).

1.3.4 LPS biosynthesis

The three regions of the LPS are synthesised through different and complex biosynthetic pathways. In the well-studied *E. coli* the biosynthesis of lipid A starts from the addition of one fatty acid to the UDP-GlcN molecule at position O-3 of the GlcNAc catalysed by the LpxA enzyme. Then the GlcNAc is de-N-acetylated by the LpxC de-acetylase. Therefore, the free nitrogen at position 2 is acetylated by a second fatty acid chain. The pyrophosphate linkage of some UDP-2,3-diacyl-glucosamine molecules is hydrolysed giving UMP and 1-phosphate-2,3-diacylglucosamine. A 1-6 linked disaccharide is then generated by the condensation of 1-phosphate-2,3-diacylglucosamine and another molecule of UDP-2,3-diacylglucosamine. A specific kinase next phosphorylates the 4 position of the disaccharide (Figure 2). This leads to a tetraacyl-disaccharide, the precursor of the lipid IVA (Raetz C. R. and Whitfield C., 2002; Trent M. S.,

2004). Next two Kdo units are transferred to the lipid A precursor, producing Kdo2-lipid A. Only after this step, two secondary acyl chains are added completing the lipid A biosynthesis. The core region is completed by sequential addition of sugars catalysed by specific glycosyltransferases. Finally, the core-lipid A precursor is flipped to the periplasmic face of the inner membrane, where the O-chain is added. For the O-antigen biosynthesis are currently known three different pathways: Wzy-dependent, ABC-transporter dependent, and synthase-dependent pathways (Raetz C. R. and Whitfield C., 2002). A common feature of the first two pathways is the first step which consists in the transfer of a sugar phosphate residue to a lipid carrier, called undecaprenolphosphate (Und-P), inserted in the inner membrane. Heteropolymers or branched polysaccharides are synthesized by Wzy-dependent pathway, while homopolysaccharides by ABC-transporter dependent pathway. In the first mechanism a single repeating unit is synthesized in the cytoplasm by sequential action of glycosyltransferases and then translocated to the periplasmic side of the inner membrane by Wzx (flippase). The nascent chain is added to the new translocated repeating unit by the Wzy O-antigen polymerase. In contrast during the second mechanism the chain is synthesized totally in the cytoplasm. Then the polymer is translocated into the periplasmic side of the membrane via the action of an ATP-binding cassette- transporter. These two processes are the most common, whereas the synthase pathway, peculiar of *Salmonella enterica* serovar Borreze (Keenleyside W. J. and Whitfield C., 1996), is very limited and only poorly characterized. Independently from the mechanism, once the undecaprenol-linked O-antigen is translocated to the periplasm, the O-chain is linked to the preformed lipid A-core by the action of the WaaL ligase only after the Und-P carrier is released and recycled, concluding the LPS biosynthesis.

1.4 Capsular polysaccharide: structure and biosynthesis

Capsular polysaccharides (CPSs), also named K antigens, are high-molecular-weight polymers of monosaccharide residues linked to each other by glycosidic bonds. CPSs can be homo- or heteropolymers, respectively constituted of one type or several types of monosaccharide. The repeating unit can be linear or branched and can display various types of inorganic and organic substituents. This molecule is linked to the bacterial cell surface via covalent attachment to either phospholipids or lipid-A molecules, while, in certain cases, may be associated directly with the cell without any membrane anchor (Fresno S. et al., 2006; Whitfield C. 1988; Whitfield C. and Valvano M. A. 1993). The CPS constitutes the outermost layer of the bacterial cell and mediates its interaction with the environment. In some *E. coli* strains isolated, this layer can extend from the cellular surface for 100–400 nm and is made of glycan chains with more than 200 sugars. A single species can produce structurally diverse CPSs, such as the 80 K antigens found in *E. coli* (Whitfield C., 2006), and these are the basis of serotyping system. The CPS could perform a wide range of biological functions, such as barrier against hydrophobic toxins, desiccation prevention (Whitfield C., 1988; Roberts I. S., 1996), promoting the biofilm formation and facilitating the colonization (Costerton J. W. et al. 1987; Merino S. and Tomas J. M. et al., 2010). Since these polymers are associated to the surface, they are the first bacterial structure encountered by the immune system upon infection. Indeed, in many bacteria the CPS is used to avoid the host immune system and was found that isolates without capsule are non-pathogenic.

Despite the variety of capsule structure, bacteria use a limited number of biosynthesis and assembly strategies. Two different biosynthetic pathways were identified: Wzy-dependent and ATP-binding cassette (ABC) transporter-dependent pathways (Whitfield C. et al., 2020). These two routes were proposed by studying the 80 different capsular serotypes of *E. coli*, which were divided into four groups based on the assembly system, organization of key genes, and regulatory characteristics. The Wzy-dependent pathway is used for groups 1 and 4 capsules, which are involved in

biofilm formation and are often found in bacteria able to cause gastrointestinal disease (Whitfield C. et al., 2020). This pathway (Figure 1.7a) involves the synthesis of polyprenol-linked CPS repeat units at the interface between the cytoplasm and the inner membrane (IM). Then this repeat unit is flipped across the IM by a Wzx protein and polymerized into the full-length CPS by a Wzy protein. To continue the polymerization a transphosphorylation of C-terminal tyrosine residues is necessary in the Wzc oligomer, member of the Polysaccharide CoPolymerase (PCP) family, and dephosphorylation by Wzb phosphatase. Then the polymer is translocated by an outer membrane polysaccharide protein (OPX), named Wza in *E. coli*, which acts as a channel. Finally, the polymer is assembled into a capsule structure on the cell surface, but it is not totally clear how CPSs are retained at the cell surface, and it is possible that the process is multifactorial (Bushell S. R. et al., 2013). The outer membrane protein Wzi, typically found in group 1 capsules from *E. coli* and *K. pneumoniae*, appears to be involved in the CPS surface association. Capsules belonging to 2 and 3 groups involve the ABC transporter-dependent assembly system. This system is found in a wide range of mucosal pathogens, as *N. meningitidis* and *H. influenzae*, where the CPS is involved in the virulence. These bacteria cause a wide range of diseases in humans, such as septicemia, urinary tract infections, meningitis, gastrointestinal infections, and a variety of respiratory infections in livestock. CPSs from ABC transporter-dependent pathways (Figure 1.7b) are synthesized at the cytoplasmic face of the IM through the concerted action of glycosyltransferases, starting from an unknown endogenous acceptor. Then the whole CPS, linked to diacylglycerophosphate or diacylglycerophosphate-Kdo, is exported across the IM via the ABC transporter (KpsM and KpsT in *E. coli*). and translocated across the periplasm and OM by PCP and OPX proteins (KpsE and KpsD in *E. coli*, respectively).

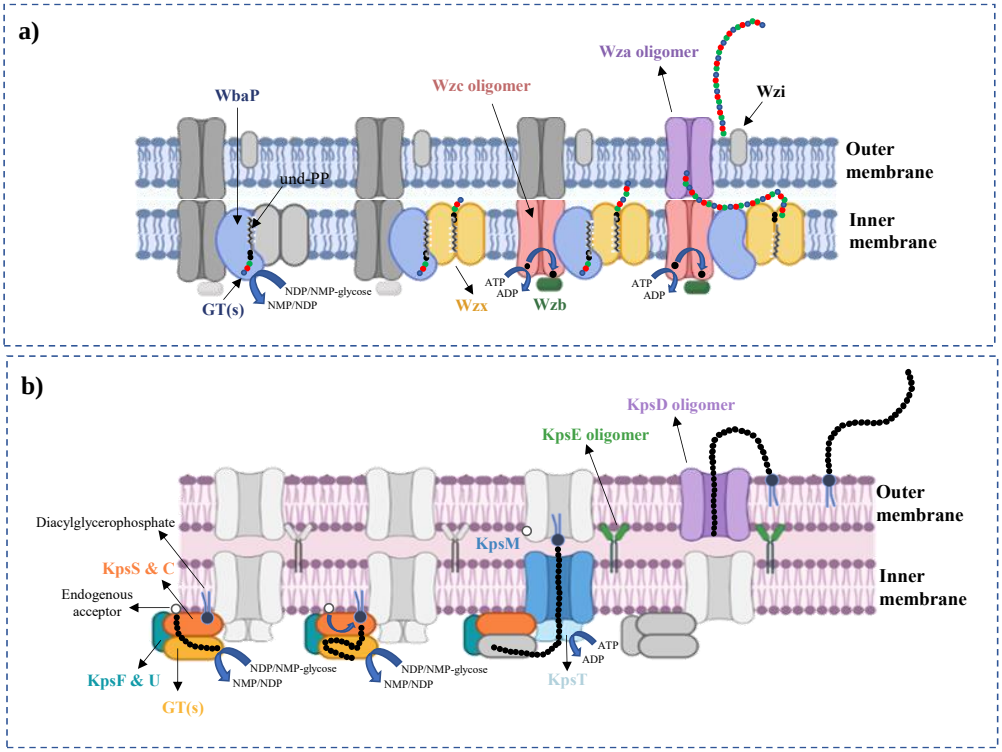

Figure 1.7. Proposed models for biosynthesis and assembly of group a) 1 and 4 b) 2 capsules in *E. coli* species. (Figure realized with Biorender)

1.5 Extracellular membrane vesicles

During normal or adverse growth conditions a wide range of Gram-negative bacteria release extracellular membrane vesicles (EMVs) (Schwechheimer C. and Kuehn M. J., 2015). EMVs are spherical bilayered particles, with a diameter of 20–250 nm, originated from a small portion of the bacterial outer membrane (OM). For this reason, they are primarily composed of lipopolysaccharides (LPSs), membrane phospholipids, and outer membrane proteins. LPSs and membrane phospholipids are the major components of the vesicles for their high surface-volume ratio. In addition, the vesicles can contain different cargoes such as DNA, RNA, many different periplasm and cytoplasm proteins and also toxins (Figure 1.8). These molecules and cargoes confer to the vesicles a role in diverse physiological and pathological functions (Kulp A. and Kuehn M. J., 2010). In fact, they are involved in bacterial pathogenesis via multiple mechanisms: they are targets for antibiotics and phages protecting the bacteria cell, interact with host cells delivering virulence factors into the cells and can also cross the mucus barrier in the gut and reach the intestinal epithelium, delivering bacterial antigens to the underlying macrophages, which triggers intestinal inflammation. The role of the vesicles in non-pathogenic bacteria is less studied and remains currently unclear. However, for these latter species many functions have been suggested, such as transfer of proteins between bacterial cells, cell-to-cell signalling, bacterial survival, biofilm formation and maintenance. To date, in Gram-negative bacteria four origins and mechanistic causes of vesicles biogenesis have been suggested (Mozaheb N. and Mingeot-Leclercq M. P., 2020):

1) Disruption of membrane integrity, due to the dissociation of the outer membrane in specific zones lacking crosslinks between Braun's lipoprotein (Lpp) and PG;
2) Activation of the SOS-response pathway, due to the presence of misfolded proteins accumulated in domains where crosslinks between peptidoglycans

and other components of the bacterial envelope are either locally depleted or displaced;

3) Perturbation of membrane symmetry, due to the accumulation of LPS, phospholipids or PG fragments in some areas of the outer membrane. This leads to the generation of microdomains in the OM with a differential curvature, fluidity, and charge. These have a propensity to bulge, resulting in increased MV production.
4) Prophage activation. In this case the vesiculation is the result of explosive cell lysis or bubbling cell death due to environmental stress as oxidative stress, UV radiation, nutrient reduction, temperature, pH, and antibiotic treatment.

EMVs have many potential applications, for their intrinsic characteristics, such as drug delivery vehicles, scaffold of enzymatic reaction (making OMVs natural nanoreactors), vaccines and adjuvants (Schwechheimer C. and Kuehn M. J., 2015; Cai W. et al., 2018).

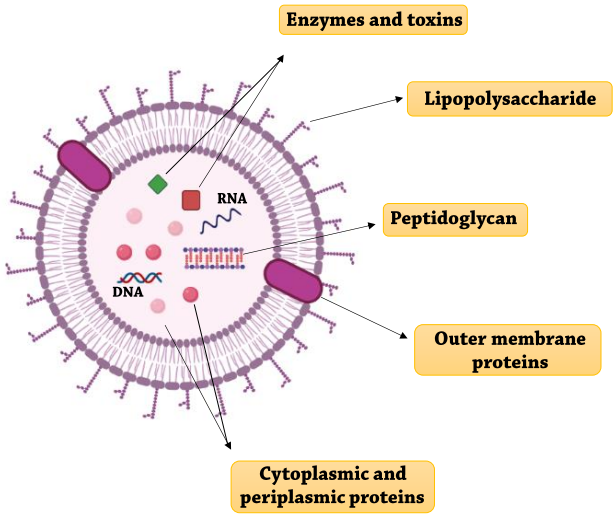

Figure 1.8 Structure and composition of Gram-negative EMVs. (Realized with Biorender)

1.6 Psychrophiles

The dominant part of the Earth's biosphere is cold, including aquatic and terrestrial ecosystems such as deep sea (90% of the ocean is below 5 °C), sea ice (13% of the earth's surface), lake ice, snow (35% of land cover) and glacial environments (10% of land cover), cold water lakes, permafrost (24% of land cover), cold soils and cold deserts (Collins T. and Margesin R. 2019). These regions are the natural habitat for cold-adapted organisms, belonging at all the three domains of life: *Bacteria*, *Archaea*, and *Eukarya*. For the first time, in 1902 Schmidt and Nielsen (Morita R. Y., 1975) defined the organisms able to reproduce at 0 °C as psychrophiles (from Greek, psukhros meaning 'cold' and philein, 'love'). This term had been coined only based on their minimum growth temperature. Successively Morita introduced the distinction between the term psychrophilic, when the minimum and the optimal growth temperatures are below 0 and 15 °C, respectively, and psychrotrophic (or psychrotolerant) for microorganisms able to survive at temperatures below 0 °C and that grow optimally at 20–25 °C (Morita R. Y., 1975). Psychrophiles and psychrotolerant have differences in their physiological and biochemical characteristics and ecological distribution. This is only one of the definitions still in common use today. In fact, other terms are currently used as 'eurypsychrophile' and 'stenopsychrophile' that describe a wide or narrow tolerance to cold, respectively (Cavicchioli R., 2006).

1.6.1 Molecular and physiological adaptation

Cold adapted species can thrive at low temperatures since have developed a wide range of physiological and structural adaptations (Siddiqui K. S. et al., 2013; Collins T. and Margesin R. 2019), many of which are only beginning to be understood. The discovery and understanding of these adaptation mechanisms are the keys to a more global view of the ecological roles of microbial communities in cold ecosystems. Additionally, these studies are a starting point for astrobiology, a scientific field that tries to give an answer to the following

questions: “How does life begin and evolve? Is there life beyond Earth?”. In fact, cold organisms can be considered as a model for the study of the origin and evolution of the life in the universe (Cavicchioli R. et al., 2002; Mastascusa, V. et al., 2014). Furthermore, the study of these organisms and their adaptation mechanisms is the basis of the research of extra-terrestrial life since their habitats are analogues of extra-terrestrial habitats (Cheptsov, V. S., et al., 2017).

The low temperatures induce physicochemical changing such as an increase in solvent viscosity and solubility of gasses, as the oxygen that leads to the increase of reactive oxygen species (ROS) and as consequence to oxidative stress, a decrease in the solubility of nutrients and solutes, increased osmotic stress, desiccation, reduced diffusion, and ice formation (De Maayer P. et al., 2014). The common features of the cold adaptation include the structural modification of enzymes, preservation of membrane fluidity, production of cold shock proteins, variation of the translation and transcription machinery and the occurrence of compatible solutes (Barria C. et al., 2013). Since the low temperatures lead to a negative effect on reaction rates, psychrophilic enzymes are usually characterized by a higher degree of structural flexibility, lower thermostability and higher specific activity at low temperatures than the mesophilic enzymes. The structural flexibility of these enzymes may be due to the active site and/or to other regions of the structure indirectly involved in activity (D’Amico S. et al., 2006). This flexibility improves the degree of complementarity between the catalytic site and substrate, decreasing activation energies and increasing substrate turnover rates (D’Amico S. et al., 2006). Different mechanisms are used to increase enzyme flexibility and activity, one of these is the reduction of arginine and proline content. These amino acids can form multiple hydrogen bonds and salt bridges reducing conformational flexibility (Huston A. L., 2008). Reduced alanine contents were found in proteins from psychrophilic *Shewanella spp*., while a lower content of both proline and arginine was detected for *Psychrobacter arcticus*, especially in proteins involved

in reproduction and cell division (Zhao J. S. et al. 2010, Ayala-del-Río H. L. et al., 2010). The ice formation is mainly limited to the extracellular space (Fonseca F. et al., 2016) and can lead to the exclusion of solutes and elimination of available liquid water. Thus, the elevate extracellular solute concentrations provokes intra and extra-cellular osmotic differences and dehydration of the cell interior. During temperature fluctuations, cells can also be subjected to ice recrystallization stress, a thermodynamically driven process causing ice crystal coalescence and growth of large, gravely damaging ice crystals at the expense of smaller crystals. Cold adapted microorganisms respond to these multiple stresses by production of a variety of molecules including, compatible solutes, ice-binding proteins (antifreeze and ice-nucleating proteins), and extracellular polymeric substances. Compatible solutes are low molecular mass, non-toxic organic compounds, such as glycine, betaine, glycerol, trehalose, sucrose, and mannitol (Ghobakhlou A. F. et al., 2015; Goordial J. et al., 2016; Mykytczuk N. C. S. et al. 2013). The accumulation of these molecules plays an important role in the restore the osmotic balance and cryoprotection, reducing the cytoplasmatic freezing point but also act as carbon, nitrogen, and energy sources (Methe B. A. et al. 2015). Furthermore, compatible solutes are supposed to be involved in scavenging free radicals and, due possibly to their preferential exclusion from protein surfaces and/or water entrapment effects, compacting effects on proteins and destabilising effects on the unfolded state, also play roles in preventing protein aggregation, enhancing protein folding and stabilising proteins and membranes at low temperatures. The trehalose disaccharide may avoid aggregation and denaturation of proteins, scavenge free radicals, and stabilize cellular membranes under cold temperatures (Kandror O. A. et al., 2002). In addition, a transcriptome analysis of *Escherichia coli* has shown that the trehalose biosynthetic genes otsA and otsB are induced under cold conditions (Phadtare S. et al., 2004). The ice binding proteins IBPs have an important role to counteract the low temperature and allow them to survive inside the ice

(Białkowska A. et al., 2020). They can be divided in ice-nucleating proteins (INPs) and antifreeze proteins (AFPs). INPs facilitate the formation of ice crystals at high subzero temperatures, providing a model for the ordering and stabilisation of water molecules in an ice-like structure, whereas AFPs can decrease the freezing point (thermal hysteresis) of fluids in organisms to avoid freezing.

1.6.2 Lipopolysaccharides and extracellular polysaccharides in cold adaptation

Low temperatures influence the membrane fluidity and consequently the cellular functioning and structural integrity. To restore membrane fluidity, bacteria have been shown to alter their fatty acids composition introducing steric restrictions that change the packing order or reduce the number of interactions in the membrane (D'Amico et al., 2006). In particular, the changing in the lipid composition consists in the increasing of unsaturated to saturated fatty acid ratios, size reduction, charge at lipid head groups (affecting packing of phospholipids), fatty acids with methyl-branches, trans-to cis-isomeric fatty acids conversion and/or a shorter acyl-chain length (D'Amico et al. 2006). For example, is well known that the mesophilic bacteria *E. coli* increases the amount of unsaturated fatty acids C16:1, C18:1 and C20:1 of the phospholipids, when grown at 15°C compared to 43°C (Cronan J. E. et al., 1975). In Gram-negative bacteria the alteration of fatty acids composition also involves the glycolipid domain of LPS. The lipid A is responsible for anchoring this macromolecule to the external leaflet of the OM. Therefore, its chemical structure is crucial in the maintenance of membrane integrity. In fact, when *E. coli* was grown at 12 °C the lipid A displays an approximately complete substitution of the C12:0 with C16:1 (Carty S. M. et al., 1999). Consistent with the observed modification in fatty acids in mesophiles at low temperature, the structures of the lipid As of the obligate psychrophiles *Colwellia psychrerythraea* 34H and *Psychromonas marina*

showed unsaturated acyl chains both as primary and/or secondary fatty acids (Casillo A. et al. 2017a, Sweet C. R. et al., 2014). Moreover, in the psychrotrophic bacterium *Pseudomonas syringae* the amount of hydroxylated fatty acids increases when was grown at 4 °C compared to that of fatty acids of the LPS from the bacterium grown at 22 °C (Kumar G. S. et al., 2002). The hydroxyl groups probably have the same role of the branched fatty acids, maintaining the homeoviscous state of the OM at low temperature. In addition, all the lipid As currently characterized from cold-adapted bacteria show shortened acyl chains with respect to mesophiles (Di Lorenzo F. et al., 2020, Casillo A. et al., 2019). Besides the modification in the fatty acid composition, it was found that the LPSs of the cold-adapted *Pseudomonas syringae* and *Pseudoalteromonas haloplanktis* TAC125 showed a phosphorylation degree that decreases when the temperature increases (Ray M. K. et al., 1994; Corsaro et al., 2004). In these molecules, the interaction between the phosphate groups and divalent cations, such as Ca^{2+} and Mg^{2+}, stabilizes the extracellular leaflet of the outer membrane (Kumar, G. S et al 2002, Ray, M. K. et al., 1994) and modulates its permeability.

Cold temperature induced significant structural modifications in the R-LPS structure of the mesophilic bacterium *Yersinia pestis* strain Yreka. In fact, the core structure of the LPS isolated at 6 °C differs from the structure at 37 °C and 25 °C in the replacement of terminal Glc with terminal D,D-Hep; phosphorylation of terminal Ko with phosphoethanolamine and a lower content of GlcNAc (Knirel Y. A. et al., 2005).

Many of the LPSs characterized from cold-adapted bacteria lack the O-chain (Casillo A. et al., 2019). Moreover, all the characterized S-LPSs have been isolated from cold adapted bacteria grown at temperatures above 20 °C. Evidence of the temperature correlation with the type/length of LPS produced is the LOS molecule of *Psychromonas arctica*, which is longer when the temperature shifts from 4 °C to 20 °C. Lack of the O-chain could improve the flexibility and

stability of the OM. However, to understand if the O-chain is involved in cold adaptation and its role, molecular biology experiments should be performed. To date this kind of experiments have been performed using two cold-adapted bacteria, *Photobacterium profundum* SS9 (Lauro F. M. et al. 2008) and *Pseudomonas extremaustralis* (Benforte F. C. et al, 2018).

Photobacterium profundum FL26 and FL25 mutants obtained by transposon mutagenesis are not able to express the O-antigen ligase and a putative LPS glycosyltransferase, respectively (Lauro F. M. et al. 2008). Both mutants are not able to produce S-LPS and have been demonstrated to be cold sensitive phenotypes. *Pseudomonas extremaustralis* was mutated in the *wapH* gene. *wapH* encods a glycosyltransferase which in *Pseudomonas aeruginosa* PAO1 adds a glucose residue to the outer core of the LPS. This mutant is not able to grow at 8 °C and produces a higher amount of S-LPSs and a lower amount of low molecular weight glycoforms (Benforte F. C. et al, 2018). Therefore, these mutations showed that the LPS structure is essential for the cold adaptation but is not possible to speculate about the O-chain role. For this reason, further studies will be necessary.

Psychrophiles are often surrounded by a polysaccharidic layer under cold conditions (Caruso C. et al., 2018; Marx J. G. et al., 2009; Casillo A. et al., 2018), leading to the modification of the physico-chemical environment of bacterial cells. These polysaccharides are identified as capsular polysaccharides (CPSs), if polymers are strictly associated with the cell membrane, and extracellular polysaccharide or exopolysaccharides (EPSs), if are released into the surrounding environment. Previously, the produced polysaccharides have been shown to be useful for protection against desiccation and reducing freezing damage (Ophir T. and Gutnick D. L. et al. 1994, Tamaru Y. et al., 2005). It has been hypothesized that one function of polysaccharides at low temperature might be as a cryoprotectant under freezing conditions (Marx J. C. et al., 2007). In fact, was found that the EPSs and the CPS isolated from the cold adapted *C.*

psychrerythraea 34H display a high ice recrystallization activity (Casillo A. et al., 2017b) suggesting a cryoprotectant effect for the cells at low temperature. Many studies on cold-adapted bacteria, like *Shewanella vesiculosa* M7, *Pseudoalteromonas antartica* NF3 and *Psychrobacter fozi* NF23, have demonstrated that the biofilm matrix is also composed of polysaccharides and membrane vesicles (Nevot M. et al., 2006; Frias A. et al., 2010; Perez-Cruz C. et al., 2013). The EPSs secreted by *P. antartica* are able to protect PC-liposomes from the activity of different detergents such as SDS (Cócera M. et al., 2000). This experiment suggests that EPSs, beside their role in cryoprotection, osmoprotection, adhesion and nutrient scavenging (Deming J. W. and Young J. N., 2017; Casillo A. et al., 2018; Lo Giudice A. et al., 2020), could also be involved in the stabilization of the released MVs.

1.6.3 Industrial and biotechnological applications

The study of cold adapted organisms has received great interest due to the promising biotechnological and industrial applications of these species and their biomolecules in a wide range of industry from pharmaceutical to cosmetic and food, and environmental biotechnology. Some of them have already found application in these industries. An example are psychrophilic enzymes characterized by a high activity at low temperature and often at moderate temperatures. These enzymes can decrease the temperature of the process reducing economics and environmental impact. In fact, is possible to carry out processes at ambient temperature, without the need of energy for heating or cooling, and to use lower quantities of enzyme compared to those adapted to higher temperatures. In the dairy industries, a variety of cold-adapted β-galactosidases, or lactases, have been used for the production of lactose free milk. Cold-adapted β-galactosidases offer the advantage of efficient hydrolysis at refrigeration temperatures which minimize problems associated with contamination and alteration of product organoleptic properties (Hoyoux A et al.,

2001; Ghosh M, et al., 2012). Other examples are cold adapted hydrolases used in detergents for cleaning at low-temperature (Sarmiento F. et al., 2015) and various enzymes (such as alkaline phosphate and nuclease) used in molecular biology for their easy inactivation and high activity (Barroca M. et al., 2017a). In the food industry are already employed AFPs for the preservation during freezing. They are used to preserve a smooth texture in ice creams and frozen yogurts and to reduce drip loss in frozen meats and fish, enhance frozen dough bread quality and enhance post-freezing quality of foods difficult to freeze as fruit and vegetables (Muñoz P. A. et al., 2017; Regand A. and Goff H. D., 2006; Voets I. K., 2017). They also have potential cryoprotective agents in medicine for the preservation of various types of biological materials. Instead, INPs are commercialised only for the artificial snow production (Cochet N. and Widehem P., 2000). They have other potential applications including the reduction of freezing energy costs in the food industry (Li J. et al. 1997) and in cloud seeding for climate control (Pummer B. G. et al. 2015). EPSs are biodegradable, bio-sustainable, non-toxic, and biocompatible biopolymers, recognised as potential alternatives to synthetic polymers in a number of applications. In the food industry, EPS can be used as thickening agents and emulsifiers, conferring improved stability and texture to foods and beverages. More recently, beneficial effects of EPS on human health via potential immunomodulatory, anti-coagulant, anti-inflammatory and anti-oxidant abilities have been indicated (Jouault S. C. et al. 2001; Leroy F. and De Vuyst L. 2016, J. Wang et al. 2019). Moreover, their capacity to bind heavy metals and organic pollutants combined with their flocculation properties for removal of suspended solids, organic matter EPS are useful as bioflocculants and bioabsorbants in soil and water bioremediation and decontamination as well as in wastewater and sludge treatment (More T. T. et al., 2014). The high emulsifying activity of some EPS indicates their potential as bioemulsifier agents (Caruso C. et al., 2018) while their role as bioadhesives was also suggested (Muralidharan J. and Jayachandran S., 2003). Their use as

cryoprotectants is also under study and an ability to improve the freeze–thaw survival of various Antarctic bacteria has already been shown (Caruso C. et al., 2018). Finally, several compatible solutes are commonly used in the stabilisation, preservation, and cryopreservation of diverse biological materials, ranging from enzymes to cells and tissues. Their use in increasing the freshness and stability of foods, in cosmetics and skin care products, as well as in increasing the growth performance of plants in saline, dry and low-temperature environments have also been investigated.

1.7 Aim of this work

In literature, few studies regarding the relationship between the structure of surface carbohydrate molecules, such as lipopolysaccharides (LPSs) and capsular polysaccharides (CPSs), and their involvement in cold adaptation mechanism are reported. The majority of LPSs from psychrophiles, grown at low temperatures and up to now, characterized are rough (Casillo A. et al., 2019). The lack of the O-chain portion could be a strategy for improving the functionality of membranes at low growth temperatures. In addition, EPSs of psychrophiles could possess the capability to protect the microorganisms from the low temperature by providing cryoprotection effect (Casillo A. et al., 2018). An example is the capsular polysaccharide secreted by the cold-adapted bacterium *Colwellia psychrerythraea* 34H that displays anti-freeze activity (Carillo S. et al., 2015). The activity of the CPS is probably attributable to its three-dimensional conformation.

The aim of this work was focused on the isolation, purification, and structural elucidation of LPSs and CPSs from psychrophilic Gram-negative bacteria, to understand the structural features involved into the adaptation to cold. Physico-chemical properties and activity have been examined, to evaluate their role in the bacterial physiology and to exploit their generally non-toxic, biocompatible, and biodegradable nature for possible industrial and medical applications.

The ability of these molecules to modulate the response of the immune system is considered an attractive strategy for the treatment of acute and chronic conditions, such as infectious diseases and sepsis, autoimmune disorders, and cancer. For this reason, *in vitro* immunomodulatory effect on intestinal epithelial cells and colon cancer cell lines has been also studied.

Finally, to shed light of the role of the O-chain in the bacterial survival at low temperature molecular biology experiments has been performed.

Chapter II: Methodology

2.1 Extraction and purification of LPS

The lipopolysaccharides are extracted from dried bacterial cells usually by using two different and complementary procedures, that may lead to selective isolation of S-LPS and R-LPS (LOS).

Typically, S-LPSs are extracted with the hot water-phenol (PhOH) protocol (Westphal O. and Jann K.., 1965), due to the presence of the O-polysaccharide that confers a higher hydrophilicity to the LPS. While R-LPSs are extracted with the phenol-chloroform-petroleum ether procedure (PCP) (Galanos C. et al., 1969), since the lacking of the O-chain moiety gives a greater hydrophobic character. These two methods can be performed in sequence, and in particular as first is applied the PCP methods.

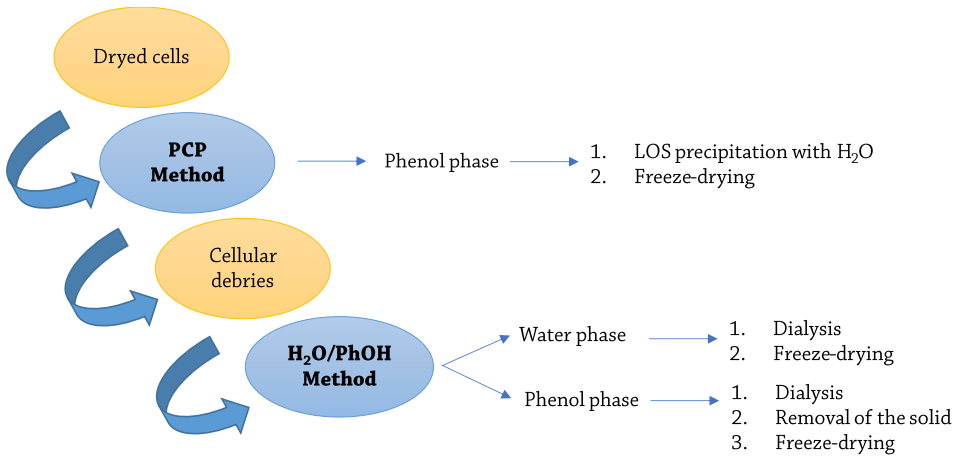

Figure 2.1 Schematic representation the PCP and hot phenol/water protocols for LPS extraction.

The PCP extraction consists in the treatment of dried cells with a mixture of phenol/chloroform/light petroleum (2:5:8, v:v:v). The lipophilic LPS in the solvent mixture, after removal of light solvents by evaporation, it is precipitated adding some drops of water to residual phenol. Usually, the sample obtained from this procedure

is free from nucleic acids and cytoplasmatic contaminants. After this extraction, the cellular residues were subjected to the hot phenol-water treatment with 90% phenol/water (1:1, v/v) at 68 °C, at this temperature the mixture is a mono-phase system. After centrifugation the water and phenol phases are separated. The LPSs are commonly recovered from the water phase together with nucleic acids, while the phenol phase generally contains proteins. Then the nucleic acids are removed from the water extract through an enzymatic treatment, with RNase, DNase and protease, followed by dialysis in order to remove digested material. However, the LPS can be recovered also in the phenol extract due to the occurrence within the repeating unit of hydrophobic groups. Typically, the LPS yields range from 0.1% to 6% (w_{LPS}/w_{dried_cells}), thus higher yields are related to contaminating substances.

Finally, to identify the nature of the LPS a polyacrylamide gel electrophoresis (PAGE) is performed by using denaturing agents sodium dodecyl sulfate (SDS) and sodium deoxycholate (DOC). For visualization of lipopolysaccharides and to define its purification degree the silver staining method is commonly used (Tsai C. M. and Frasch C. E., 1982). The presence of the typical "ladder-like" migration pattern suggests the smooth nature of the LPS molecules, differing in number of repeating units of the O-polysaccharide moiety. On the other end, the LOS corresponds to a fast-migrating band at the bottom of the gel, denoting the lower molecular weight of LOS lacking O-chain domain.

2.2 GC-MS methods for LPS analysis.

Preliminary information about the primary structure of the saccharide portion of the LPS are obtained by chemical analysis. These latter consist in the conversion of the monosaccharides into specific volatile derivates, since they are analysed though Gas-Chromatography coupled with Mass-Spectrometry (GC-MS).

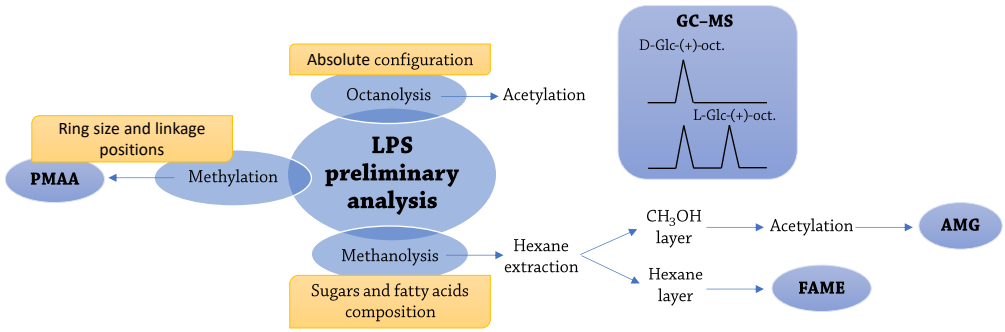

Figure 2.2 Strategies for GC-MS analysis of LPSs.

To obtain the monosaccharides composition of the LPS two different procedures can be applied. One of these consists in the LPS treatments with anhydrous methanolic HCl that leads to its solvolysis and the formation of O-methyl glycosides for each monosaccharide. During the reaction also methyl-esters derivatives of fatty acids are formed. These latter are extracted with hexane and analysed directly by GC-MS. Then the O-methyl glycosides are acetylated with acetic anhydride in pyridine obtaining the acetylated O-methyl glycosides (AMGs), that can be also injected and analysed by GC-MS. By comparison of the retention times, from the GC analysis, and the fragmentation pattern, from the MS spectra analysis, with authentic standards is possible to the identify the monosaccharide residues and the fatty acids. Quantification analysis of the sugars can be obtained by using an internal standard, usually the per-acetylated inositol.

Since this protocol provides a solvolysis in acid conditions, several isomers for each monosaccharide may form (pyranose and furanose either α or β anomers) resulting in the occurrence of many peaks in the corresponding chromatogram. This can be a problem, especially if a quantitative analysis is needed. The alternative approach, that avoids this drawback, is the derivatization of monosaccharides as alditol acetates. In this case, the LPS is subjected to a strong acid hydrolysis with trifluoroacetic acid (TFA) followed by the reduction of the carbonyl group with $NaBH_4$ and acetylation

of the free residues. This leads to the formation of a single peak for each monosaccharide. Generally, the fragmentation pattern of a methyl glycoside is more complex respect to the corresponding alditol acetate. If monosaccharides are substituted by a phosphate group, the sample is preliminary dephosphorylated with aqueous 48% HF to reveal the phosphorylated residue.

Another important step is the determination of the absolute configuration. The procedure consists in the LPS solvolysis with an enantiomerically pure alcohol as 2-(+)-octanol or 2-(+)-buthanol. Then the obtained diastereoisomeric glycosides are acetylated and injection to GC-MS. The comparison of the retention time of the acetyl 2-(+)-octylglycosides with the one of a standard mixture of O-2-(±)-octylglycosides of standard monoses in D or L configuration allows the assignment of the monosaccharide absolute configuration (Leontein K. et al., 1978).

Moreover, using chemical and GC-MS analysis, it is possible to obtain the ring size and linkage positions of each monosaccharide through derivatization as partially methylated alditol acetates (Ciucanu I. et al., 1984). The procedure consists in an extensively methylation of the LPS with CH_3I in DMSO and in strongly alkaline conditions. Then, the permethylated sample is hydrolysed under acid conditions and reduced with a marked reagent ($NaBD_4$). The obtained alditols have free hydroxyl groups at the positions previously involved in glycosidic linkages and cyclization, that can be acetylated. These partially methylated alditols acetates (PMAAs) are analysed by GC-MS and the fragments observed in the MS spectra are diagnostic for specific substitution patterns of acetyl and methoxyl groups. In particular, the position of the acetyl groups in the fragments indicates the linkage point or the cyclisation position of the pyranose or furanose cycle, while the methyl groups correspond to positions not involved in linkages. Furthermore, the reduction of the carbonyl group with $NaBD_4$ facilitates to distinguish the fragments derived from the reduced position (even masses) form those derived from the last position (odd masses) (Hakomori S., 1964). All the obtained information, confirmed by spectroscopic and spectrometric methods, will help in the structural elucidation.

2.3 Characterization of the lipooligo-/lipopolysaccharides.

The amphiphilic nature of the LPS determines its ability to form micelles with low solubility in both aqueous and apolar organic solvents. This makes the macromolecule difficult to study without any chemical modifications or degradation. The common strategy consists in the analysis of the lipid and saccharide moieties separately by using acid or alkaline hydrolysis.

2.3.1 Lipid A structure determination

A mild acid hydrolysis with 1% of acetic acid is sufficient to cleave selectively the labile glycosidic linkage between the Kdo and the non-reducing glucosamine of the lipid A (Figure 2.3) (De Castro C. et al., 2010). After the reaction the oligo-/polysaccharidic moiety, with an increased hydrophilic behaviour, is dissolved in the supernatant, while the hydrophobic lipid A portion is completely insoluble and recovered as precipitate.

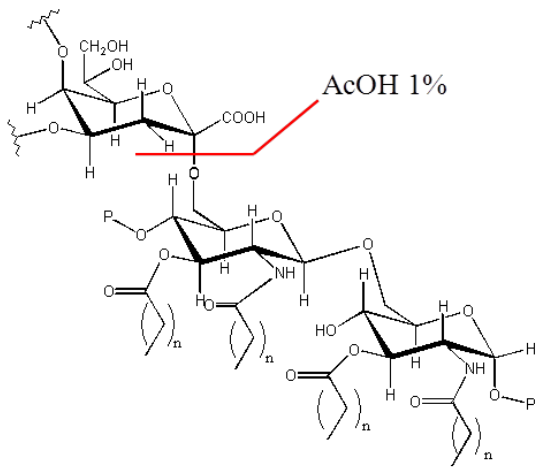

Figure. 2.3. Schematic illustration of the Kdo linkage cleavage during the mild acid treatment.

The structure of the lipid A is obtained with chemical analysis and mass spectrometry techniques (see paragraph 2.7) both on the native and selectively

degraded lipid A. As previously mentioned, fatty acids composition is achieved through GC-MS analysis of their methyl ester derivatives (FAMEs). MALDI-TOF data allow to gain insights into the number of lipid A species present in the fraction, the presence of polar heads and the distribution of acyl residues on each GlcN units of the disaccharide backbone (Que N. et al., 2000). The distribution of fatty acids on the disaccharidic backbone is obtained combining the information collected by the negative ion MALDI-TOF MS and MS/MS spectra of the intact lipid A and NH_4OH treatment product (Silipo A. et al., 2002). This procedure selectively cleaves the ester linked acyloxyacyl groups, leaving the amide-linked acyloxyacil groups. In particular, negative ions mass spectra of the ammonium treated lipid A allows the identification of the primary and secondary fatty acids linked on the amide functions of the sugar backbone (Que N. et al., 2000). It is possible also to selectively *O*-deacylated the lipid A, tipically with hydrazine. MALDI-TOF analysis of the *O*-deacylated products allows the determination of the amide linked fatty acids.

2.3.2 Core region determination

The mild acid hydrolysis leads to dehydration of Kdo with consequent formation of artefacts (Volk W. A. et al., 1972). This increase the sample heterogeneity and can make difficult the interpretation of NMR spectra, because the artefacts can be present in not negligible amount. Therefore, this procedure is avoided for the structural characterization of core region or rough-LPS. To overcomes this problem, the LPS is fully deacylated with a first de-O-acylation and a successive de-N-acylation (Figure 2.4), which leads to the isolation of the entire glycosidic portion of the LPS (Holst O., 2000). The first one is a mild alkaline hydrolysis using anhydrous hydrazine that removes the fatty acids linked as esters. A complete deacylation is obtained by a strong alkaline treatment with KOH 4M, that leave intact the phosphate groups but remove other substituents as acetyl and pyrophosphates substituents. The increased hydrophilic nature of the molecule

allowed to obtain structural information of the core from a R-LPS by NMR (see 2.8).

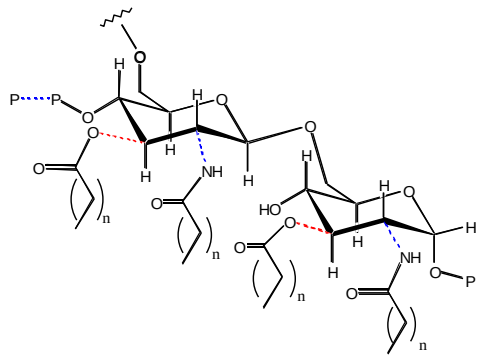

Figure 2.4. Schematic representation of the lipid A. Dotted red and blue lines indicates the linkages hydrolyzed during treatment with hydrazine or KOH, respectively.

2.3.3Characterization of the O-chain

The water-soluble polysaccharidic moiety, achieved from a S-LPS after a mild acid hydrolysis with 1% acetic acid, is subjected to NMR spectroscopic technique (see 2.8). It is possible to obtain the structural elucidation of the O-chain repeating unit since only its constituent monosaccharides are revealed thanks to their high relative abundance compared to the residues belonging to core region.

2.4 Isolation and purification of CPS

Capsular polysaccharides are strictly associated to the outer membrane, therefore are mainly recovered from the cells. The separation of cells from growth medium by centrifugation could lead to the distribution of some CPS molecules into the two phases. For this reason, the calculation of the capsule yield is quite complex. Then, the capsular polysaccharides are isolated from the dried cells usually by saline solution extraction (Casillo A. et al., 2018) or by the hot phenol/water method (Carillo S. et al., 2015). During the latter procedure LPSs and CPSs are extracted together. To isolate the CPSs from the LPSs an acetic acid hydrolysis is necessary, and the obtained

polysaccharide mixture is subjected to anionic exchange and/or gel filtration chromatography.

2.5 Microscopy for CPS visualisation

High-resolution microscopy techniques, such as atomic force microscopy (AFM) and transmission electron microscopy (TEM) are currently in use to detect and visualize bacterial capsules. Transmission electron microscopy is a great resource in microbiology for the high-resolution structural studies of bacteria and their components. In particular, the presence of CPSs on bacteria is revealed by thin sections TEM of the cells treated with cationic dyes, like Ruthenium red (RR), Alcian blue (Karlyshev A.V. et al., 2001), or cationized ferritin (Bayer M. E., 1990), in conjunction with fixatives in order to simultaneously stain and stabilise the capsular material. However, these staining requires a negative charge on CPS polymers and therefore it is not useful for CPS with a neutral, positive. Moreover, after the staining with a cationic dye, it is possible that the fragile nature of the capsule can result in the apparent absence of capsular material in up to 70% of encapsulated cells (Neo Y-L et al., 2010). Much more reliable for capsules observation is another TEM technique named freeze substitution (Graham L. L. et al., 1991; Korenevsky, A. A. et al., 2002). Such technique provides for a rapid physical vitrification of cells which fixes them in a fully hydrated state and results in very good preservation of the native structure of the cell. However, the laboriousness, time-consuming and the required of specialized equipment have limited the use of the freeze-substitution technique. Much more information comes from the atomic force microscopy (AFM), which is able to study the surface of single live bacterial cells in physiologically relevant environments. For this reason, AFM has been widely used to measure cell physical properties, such as membrane elasticity, and to explore the mechanical properties of cell surface polymers and to investigate cell adhesion through the interaction between an AFM tip and the bacterial surface (Velegol, S. B. and Logan, B. E. et al., 2002; Francius G. et

al., 2008). These studies have greatly enhanced our understanding of cell-surface interactions.

2.6 Preparative chromatography in the study of oligo/polysaccharides

Bacteria produce LPS molecules with a wide structural heterogeneity, leading to a glycosidic mixture after both acid and alkaline treatments. For this reason, the purification of the samples is important to simplify further analysis. Purification of oligo- and polysaccharide mixtures is generally achieved by using chromatographic techniques, such as size-exclusion chromatography when the mixture components show different molecular masses. In particular, the molecules that are too large to pass through the pores are excluded and traverse the column more rapidly. Smaller molecules instead, because they pass through gel pores, are eluted later. Different kinds of resins are commercially available with different range of pore sizes, differing also for the type of material, stability, chemical-physical properties and the selectivity. The most used resins are:

- Sephacryl: the matrix consists of allyl dextran and N,N'-methylenebisacrylamide. These resins are used to separate polysaccharides with a suitable buffer as eluent.
- Bio-gel P: the matrix is polyacrylamide with either water or a buffer as eluent.
- Sephadex: the matrix consists of allyl dextran. These resins are mainly used to desalt samples.

It is possible to elute the sample using buffers with high ionic strength in order to improve the chromatographic resolution, but in some cases even the only MilliQ water is an excellent eluent. The obtained fractions will be subjected to chemical, mass spectrometry and NMR analysis.

2.7 Mass spectrometry of oligo/polysaccharides

Mass spectrometry (MS) and tandem mass spectrometry (MS/MS or MS^2) are extensively used in LPS structural determination. Soft ionisation techniques like MALDI (Matrix Assisted Laser Desorption Ionisation) can provide information about the molecular mass of the intact molecules and the presence of different glycoforms, differing for the presence of one or more glycidic or non-glycidic residues. This methodology is based on a soft ionization of the sample that is suspended in a specific matrix that assists the analyte ionization when irradiated with laser pulses. The matrix consists in small organic molecules that have strong absorption at the laser wavelength used for the ionisation. The organic molecules protect the sample from the laser energy assuring a soft ionisation with formation of single charged ions. Usually, for carbohydrates, MALDI spectra are performed in negative ion mode, due to the presence of a great number of potentially ionising groups (hydroxyl or phosphate functions). High energy laser source is able to cleave the labile linkage between the Kdo and the glucosamine backbone lipid A. In case of LOS, in the deriving mass spectra there are three signals regions originated by the lipid A, the core oligosaccharide and the intact LOS. In LPS, due to the dispersion of molecular weight of the O-polysaccharide, information on the size of the repeating unit can be deduced. Using a MALDI-TOF system, it is possible to analyse the fragment ions generated by the precursor ions in the flight tube, when a higher laser intensity is applied. Moreover, when a spectrometer is equipped with a collision cell, it is possible to perform tandem mass spectrometry experiments, selecting an ion and inducing its fragmentation. With this technique it is possible to obtain the sequence of the monosaccharides and to identify branching locations by a series of product ions from glycosidic bond cleavages. The interpretation of fragmentation spectra of carbohydrates is not always easy, because fragmentation could not occur at each glycosidic linkage. Moreover, different fragment types can be formed, the identification of which is sometimes not immediate. Commonly, in mass spectrometry field the nomenclature introduced by Domon and Costello is used for oligosaccharide fragmentation, as shown in Figure

2.5 (Domon B. and Costello C. E., 1988). Fragment ions that contain a non-reducing end are labelled A, B, and C, while those contain the reducing-end of the oligosaccharide or the aglycon are named X, Y, and Z (Domon B. and Costello C. E., 1988; Spina E. et al., 2004). Subscript numbers indicate the number of monosaccharides present in the fragment. B, C, Y, and Z ions are originated from glycosidic bond cleavages. B and Y ions are cleaved at the non-reducing side of a glycosidic oxygen and C and Z ions are cleaved at the reducing side of a glycosidic oxygen. A and X ions resulted from glycosidic ring cleavages. They are labelled with superscript of two broken ring bond numbers that are assigned as shown in Figure 2.5.

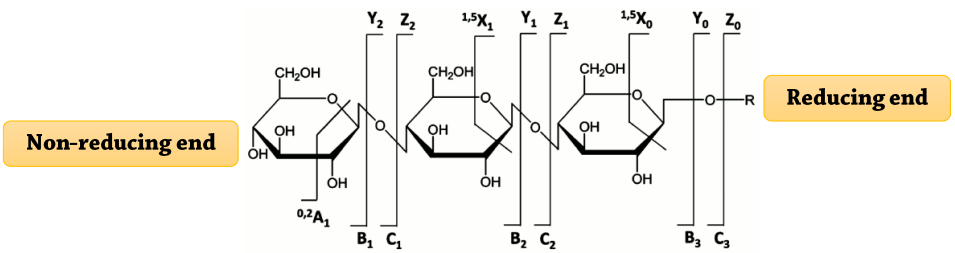

Figure 2.5. Domon and Costello nomenclature for glycoconjugate fragments generated by tandem MS/MS.

2.8 Nuclear Magnetic Resonance (NMR)

Nuclear Magnetic Resonance (NMR) spectroscopy is a fundamental technique for the structural elucidation of oligo-/polysaccharides. NMR allows to analyse carbohydrates in a native state, due to their good solubility in aqueous systems. Usually, the observed nuclei are ^{1}H and ^{13}C, as well as ^{31}P, to detect phosphate groups and unusual phosphorous containing substituents.

It is possible to divide a typical ^{1}H NMR spectrum of a carbohydrate in three regions:

- 5.5-4.0 ppm: anomeric proton signals. The number of signals in this region gives information on the number of aldopyranoses present in the molecule;

- 4.6-2.5 ppm: ring proton signals. This region, named carbinolic, is the most crowded and no information can be obtained using only mono-dimensional NMR spectrum;
- 2.5-1.0 ppm: deoxy position signals. In this region is possible to find the H3a,b diagnostic signals of the Kdo.

While the principal values of ^{13}C resonances are:

- 104-105 ppm: anomeric carbon atoms involved in a glycosidic linkage;
- 80-60 ppm: oxymethylene or carbinolic carbon atoms;
- 60-45 ppm: carbon atoms linked to nitrogen;
- ~ 30 ppm: aliphatic methylene carbons of deoxy-sugar residues;
- 20-17 ppm: methylene carbon atoms of 6-deoxy-sugar residues and of acetyl residues.

Anomeric proton and carbon chemical shifts can give information about anomeric configuration for each residue, since usually α-configured proton signals appear at lower fields respect to corresponding β-anomers, whereas the opposite situation occurs for carbon chemical shifts. In order to assign all the carbon and proton chemical shifts, the location and the nature of non-carbohydrate substituents and to characterise the monosaccharide sequence it is necessary to study different kind of two-dimensional NMR experiments at the same time. In detail, the study of $^{1}H,^{1}H$-TOCSY and $^{1}H,^{1}H$-COSY spectra permits the correct identification and assignment of all ring protons. In the TOCSY experiment a series of soft pulses transfer the magnetization in a measure that depends on the $^{3}J_{H,H}$ coupling constant. As a consequence, in the TOCSY spectrum, when a monosaccharide is *gluco*-configured all the signals of the residue will be present since possess a good transfer of magnetization. On the contrary, *manno* or *galacto*-configured residues present small coupling constant between H2-H3 and H4-H5 protons respectively, showing only 2 or 3 cross peaks correlated to anomeric proton signals. On the basis of the obtained proton resonances,

it is possible to assign all ^{13}C resonances from the analysis of the $^{1}H,^{13}C$-HSQC spectrum. This latter experiment allowed to identify also the linkage position of each residue due to glycosylation shift effect. Indeed, when a carbon is involved in a glycosidic linkage undergo a downfield shift of 8-10 ppm, while the adjacent carbons undergo an upfield shift of 1-3 ppm. Anomeric configurations are then confirmed by the $^{3}J_{H1,H2}$ and by $^{1}J_{C1,H2}$ values. In detail, in monosaccharides with the H-2 axial (as glucose, galactose), a $^{3}J_{H1,H2}$ around 8 Hz is indicative of a β-orientation, whereas below 3 Hz of an α-configuration. Sugars with the H-2 equatorial (as mannose) show both $^{3}J_{H1,H2}$ below 3 Hz. Moreover a $^{1}J_{C1,H2}$ below 165 indicates a β-anomer, above 170 Hz a α-anomer. To obtain the sequence of monosaccharides constituting the oligosaccharide (or the repeating unit of the polysaccharide) homonuclear and heteronuclear experiments are performed, such as $^{1}H,^{1}H$-NOESY, $^{1}H,^{1}H$-ROESY and $^{1}H,^{13}C$-HMBC. In the ROESY and NOESY experiments, which are built up by the NOE effect, dipolar interactions between nuclei give cross peaks due either to *intra*-molecular (giving information about the anomeric configurations of the residues) or *inter*-molecular couplings. While HMBC experiment displays long scalar correlations between ^{1}H and ^{13}C nuclei involved in glycosidic linkages. Finally, $^{1}H,^{31}P$-HSQC allows the localisation of the phosphorylation sites within the saccharide structure.

Results

Shewanella vesiculosa HM13

Shewanella is a genus of marine and freshwater Gram-negative *Gammaproteobacteria*, belonging to the family *Shewanellaceae*. The genus has only been recognized with its present name since 1985 (MacDonell M. T. and Colwell R. R., 1985), even if some species had already been known since 1931. The family, including only this genus, was proposed by Ivanova and co-workers since 2004 due to the lacking association with any other genus. *Shewanellaceae* family contains principally rod-shaped bacteria, both aerobic and facultative anaerobic. Members of this family have been isolated from coastal, open, and deep-sea waters and invertebrates or vertebrates from marine environments.

Shewanella vesiculosa HM13 is a cold-adapted bacterium, isolated from the intestine of a horse mackerel (*Trachurus japonicus*) (HM13 Horse Mackerel strain no. 13) (Chen C. et al., 2020). The growth temperature range of this bacterium is 4-25 °C, with optimum growth at 18 °C. This strain is able to secrete abundant amount of EMVs which contain a single major cargo protein (named P49) with an unknown function. This protein has been found also in the outer membrane and in the culture supernatant. Chen and co-workers have selected this bacterium since they were looking for novel cold-adapted bacteria suitable as host for secretory production of foreign proteins at low temperature (Chen C. et al., 2020). Several benefits involve recombinant proteins expression at low temperatures, such as overcome problems associated with heat denaturation of thermolabile proteins (Feller G., 2010) and with the production of enzymes that can act by damaging the host cell (since activities of such enzymes can be suppressed by low temperature) (Georlette D. et al., 2004). In addition, when secreted, the foreign proteins have the advantage of being separated by simple filtration or centrifugation.

To obtain information about the biogenesis mechanism of the P49-containing EMVs, the gene cluster containing the P49 gene was analysed (Kamasaka K. et al., 2020). The analysis revealed the presence of genes encoding homologs of surface glycolipid

biosynthesis proteins (Wza, WecA, LptA, and Wzx), components of type II secretion system (T2SS) (GspE, GspF, GspG, and GspK), glycerophosphodiester phosphodiesterase (GdpD), and nitroreductase (NfnB). Experiments on mutants that lack genes homologs of the T2SS components showed that P49 was not secreted. In addition, when *gdpD*, *wzx*, *lptA*, and *nfnB* were disrupted, P49 was not loaded to the EMVs and is released into the extracellular medium (Kamasaka K. et al., 2020). These results suggest that P49 is translocated across the outer membrane by a T2SS-like mechanism and then inserted into the vesicles through an interaction with its surface glycolipids. The aim of this chapter will be the isolation and the structural elucidation of surface glycolipids from the cells and the EMVs of *S. vesiculosa* HM13 to go deeper into the mechanism of EMVs biogenesis. In addition, a mutant of the bacterium that defects in a gene, which encodes a protein showing homology to Wzx (a flippase involved in membrane translocation of the repeating units constituting the LPS or CPS), will be investigated to understand how this gene is involved in the loading of P49 into the EMVs.

Fig. Genetic organization of the P49-containing gene cluster (Kamasaka K. et al., 2020).

Chapter III: *Shewanella vesiculosa* HM13 grown at 4 °C

3.1 LPS isolation and chemical analysis

The LPS was extracted from dried cells of *S. vesiculosa* HM13, grown in LB medium at 4 °C, by PCP (phenol/chloroform/light petroleum) method (Galanos C. et al., 1969) with a yield of 2.4%. Then the PCP precipitate was analyzed through sodium deoxycholate-polyacrylamide gel electrophoresis analysis (DOC-PAGE, Figure 3.1). After silver nitrate staining the gel revealed the presence of a fast-migrating species, indicating the rough nature of the LPS. The cellular debris were also extracted by the phenol/water method (Westphal O. and Jann K., 1965), obtaining the same fast migrating species together with proteins and nucleic acids (data not shown).

Figure 3.1. Analysis of the PCP precipitate (Lane **B**) from *S. vesiculosa* HM13 PCP extraction by 14% DOC-PAGE. The gel stained with silver nitrate indicates a Rough-LPS (LOS) by comparison with the Smooth-LPS from *E. coli* O127: B8 (Lane **A**).

The GC-MS analysis of monosaccharides, together with the absolute configuration determination, revealed the presence of D-glucose (D-Glc), 2-amino-2-deoxy-D-glucose (D-GlcN), L-*glycero*-D-*manno*-heptose (L,D-Hep), and D-*glycero*-D-*manno*-heptose (D,D-Hep). Methylation analysis, indicating the linkage position, showed the presence of terminal glucose, 2-substituted glucose, 2-substituted heptose, terminal heptose, and 2,6,7- tri-substituted heptose. In addition, GC-MS analysis of fatty acids as methyl esters revealed the presence of 3-hydroxydodecanoic C12:0(3OH), 3-hydroxytridecanoic C13:0(3OH), 3-hydroxytetradecanoic C14:0(3OH), dodecanoic

C12:0, tridecanoic C13:0, tetradecanoic C14:0, and pentadecanoic C15:0 as the major components (Table 3.1).

Table 3.1. Molar ratio percentage of fatty acids of the LOSs from *S. vesiculosa* HM13 cells, grown at 4 °C.

	C12:0	**C13:0**	**C12:3OH**	**C14:0**	**C13:3OH**	**C15:0**	**C14:3OH**
Cells	13.2%	24.7%	7.87%	7.37%	24.9%	19.4%	2.51%

3.2 Mass spectrometric analysis of the *O*-deacylated LOS

The LOS was de-*O*-acylated by mild hydrazinolysis and the product, named LOS-OH, was analyzed by negative ions MALDI-TOF in reflector mode (Figure 3.2). The mass spectrum, at higher molecular masses, revealed the presence of a signal at *m/z* 2298.6 assigned to a LOS-OH molecule with the following composition: $Hex_3Hep_3Kdo8NGlcN_2P_3$[C13:0(3OH)][C14:0(3OH)] (Calculated $[M-H]^-$ = 2298.84 Da), suggesting the presence of a 8-amino-3,8-dideoxy-*manno*-oct-2-ulosonic acid (Kdo8N) residue. This monosaccharide was reported for other LPSs from *Shewanella* species (Vinogradov, E. et al., 2002; Vinogradov, E. et al., 2003; Vinogradov, E. et al., 2008; Silipo, A. et al., 2005). Less intense is the signal at *m/z* 2422.6, that suggests the presence of a phosphoethanolamine group (PEtN, 123 Da). The LOS-OH ions cluster showed the differences of ±14 Da with respect to the two main signal at *m/z* 2298.6 and 2422.6, which were attributable to fatty acids with different chain length that substitute the two GlcN residues of the lipid A. Moreover, at low *m/z* values there are signals attributable to core oligosaccharide and lipid A, arising from an in-source β-elimination at the glycosidic bond between the Kdo8N and the lipid A (Gibson B.W., 1997). Signals at *m/z* 1360.8 and 1483.9, with the difference of 123 Da due to a phosphoethanolamine group, were both assigned to the core fragments. Finally, the signals at *m/z* 1316.8 and 1439.9 of decarboxylated core fragments were visible (B.W. Gibson et al., 1997).

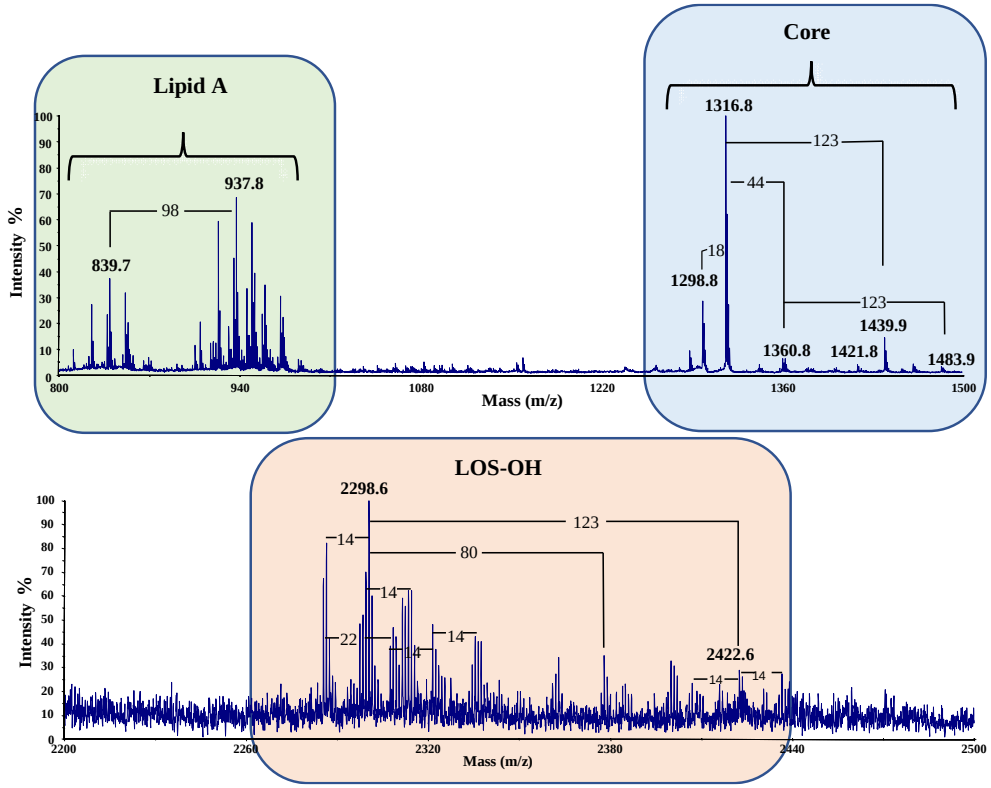

Figure 3.2 Negative ions MALDI-TOF mass spectrum in reflector mode of the LOS-OH from *S vesiculosa* HM13 grown at 4 °C. The notation 14 Da indicates differences of single CH_2 in the fatty acid chains. 18, 44, 80, 98 and 123 Da indicates the loss of water, CO_2, phosphate group, phosphate plus water and phosphoethanolamine group, respectively.

3.3 NMR analysis of the fully deacylated LOS

The core oligosaccharide, named OS, was obtained from the LPS-OH by de-*N*-acylation with strong alkaline hydrolysis. Then the OS was submitted to a complete 1D and 2D NMR analysis (^{1}H,^{1}H DQF-COSY, ^{1}H,^{1}H TOCSY, ^{1}H,^{1}H ROESY, ^{1}H,^{13}C DEPT-HSQC, and ^{1}H,^{13}C HMBC), that allowed to assign all the proton and carbon resonances of the oligosaccharide (Table 3.1) and to establish its structure. The experiments indicated for all the residues the occurrence of pyranose rings. Anomeric configurations were assigned by both chemical shift values of anomeric protons and

carbons and by the $^{1}J_{C1,H1}$ values obtained from the coupled ^{1}H, ^{13}C DEPT-HSQC experiment.

Table 3.1 ^{1}H and ^{13}C chemical shifts of OS of the LOS from *S. vesiculosa* HM13. The values are referred to sodium 3-trimethylsilyl-(2,2,3,3-$^{2}H_4$)-propanoate (TSP, δ_H 0.00) and 1,4-dioxane in D_2O (δ_C 67.40) as external standards. Spectra were recorded at 298 K at 600 MHz.

Residue	H1 C1 $^{1}J_{C,H}$	H2 C2	H3 C3	H4 C4	H5 C5	H6a,H6b C6	H7a,H7b C7	H8a,H8b C8
A α-GlcN*p1P*	5.65 92.0 179	3.36 55.8	3.91 71.2	3.46 71.4	4.20 73.5	3.91, 4.32 70.9		
B α-*t*-Glc*p*	5.40 99.1 182	3.58 72.5	3.76 74.0	3.49 70.7	4.04 73.5	3.76 61.9		
C α-2-L,D-Hep*p*	5.37 98.8 184	3.91 82.1	4.05 71.7	3.83 68.7	3.91 75.2	4.07 70.3	3.78,3.75 64.7	
D α-2,6,7-D,D-Hep*p*	5.17 101.9 170	4.08 79.4	4.15 71.7	3.79 68.7	4.06 74.4	4.34 78.2	4.02,4.13 70.8	
E α-*t*- L,D-Hep*p*	5.12 103.5 173	4.07 70.5	3.83 72.0	3.86 67.6	3.66 73.8	4.06 70.5	3.84,3.72 63.5	
F α-*t*-Glc*p*	5.05 102.3 170	3.59 73.1	3.72 74.2	3.49 70.8	4.04 73.0	3.81 61.8		
G β-6-GlcN*p4P*	4.95 100.8 164	3.11 56.9	3.80 73.6	3.85 74.5	3.75 75.4	3.51,3.73 63.4		
H β-2-Glc*p*	4.65 105.0 164	3.47 77.1	3.57 75.9	3.42 71.4	3.44 78.5	3.73,3.93 62.3		
I α-5-Kdo8N*p4P*	n.d.	101.2	2.01,2.25 35.8	4.58 71.3	4.34 76.3	3.92 74.6	4.02 67.0	3.20,3.50 44.4

The ^{1}H NMR spectrum of OS revealed the occurrence of eight main anomeric signals, confirmed by ^{1}H, ^{13}C DEPT-HSQC spectrum (Figure 3.4), indicating an equivalent number of monosaccharides (Figure 3.3, residues **A**-**H**). In addition, the proton signals at δ 2.01 and 2.25 ppm suggested the presence of a deoxy sugar (residue **I**).

The residue **A** with H-1 at 5.65 ppm was recognized as *gluco*-configured, due to the typical $^{3}J_{H,H}$ vicinal coupling constant values observed in the COSY and TOCSY spectra. This residue was identified as the phosphorylated proximal glucosamine residue (α-GlcNI), due to the typical multiplicity of a phosphorylated anomeric signal

(doublet of doublets, $^{3}J_{H1,H2}$ = 3.6 Hz and $^{3}J_{H1,P}$ = 7.0 Hz), and to the chemical shift value of its C-2 at δ 55.8 ppm typical of a nitrogen-bearing carbon.

The residue **G** was identified as the distal glucosamine (β-GlcNII) of lipid A portion. In fact, the ROESY and HMBC experiments indicated that residues **G** and **A** were linked through a linkage (1→6). Phosphorylation of **G** at position O-4 was suggested by the H-4 and C-4 downfield shifts (3.85 ppm and 74.5 ppm, respectively) and by the correlation in the $^{1}H,^{31}P$ HSQC spectrum between H-4 of **G** and ^{31}P signal at δ -0.2 ppm (Figure 3.5).

Residues **C**, **D** and **E** were recognized as *manno*-configured due to the occurrence of the connectivities between only H-1 and H-2 in the TOCSY experiment, indicating small values for the $^{3}J_{H1,H2}$ and $^{3}J_{H2,H3}$. Indeed, these residues were identified as α-heptoses, based on their spin-system connectivities in TOCSY and ROESY spectra.

C was 2-substituted due to downfield shift of its C-2 chemical shift at 82.1 ppm (reference value for an unsubstituted residue 71.9 ppm) (Pieretti, G. et al. 2012).

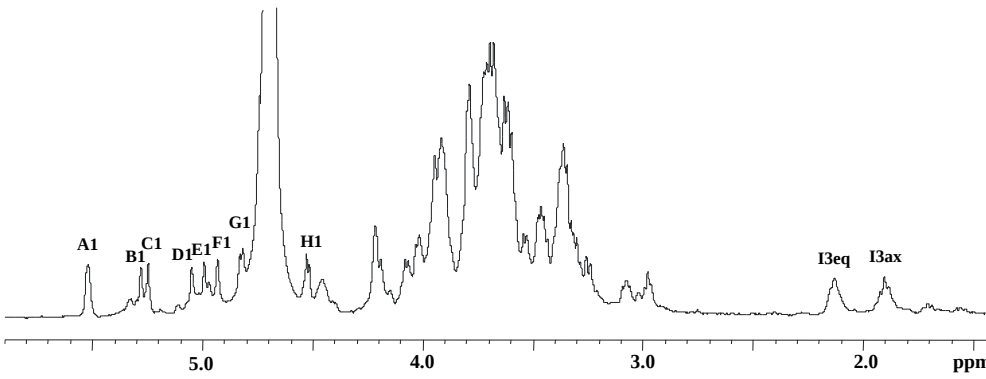

Figure 3.3. ^{1}H NMR spectrum of the oligosaccharide obtained by strong alkaline hydrolysis of the LOS-OH. The spectrum was recorded in D_2O at 298 K at 600 MHz.

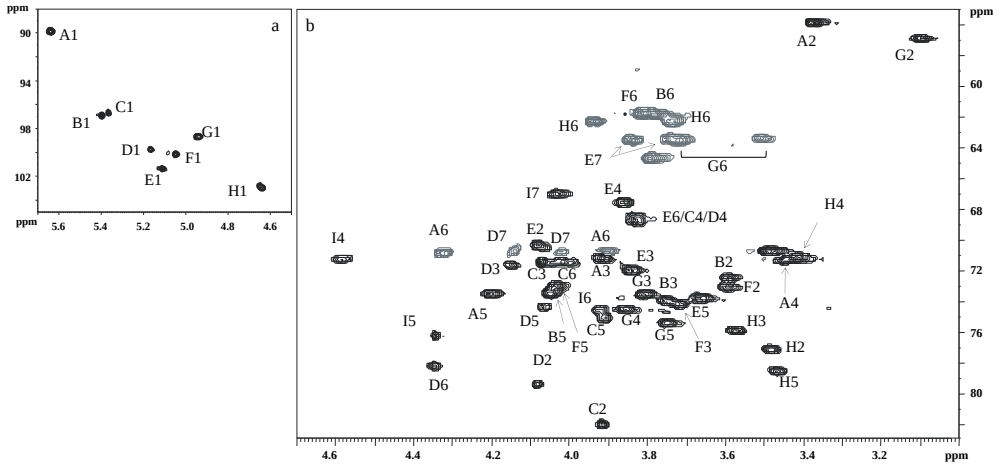

Figure 3.4 a) Anomeric and b) carbinolic regions of ^{1}H-^{13}C DEPT-HSQC spectrum of OS of *Shewanella vesiculosa* HM13. The spectrum was recorded in D_2O at 298 K at 600 MHz.

The residue **D** was identified as a 2,6,7-trisubstituted heptose, since its C-2, C-6, and C-7 carbon chemical shifts occurred at 79.4, 78.2, and 70.8 ppm, respectively. The D,D-configuration of **D** was suggested from its presence in other LOSs from *Shewanella* species, and based on the strong similarity of proton and carbon chemical shifts of this residue with those already reported (Vinogradov E. et al., 2004). Residue **E** did not show any downfield chemical shifts, and therefore was assigned to a terminal non-reducing α-heptose.

Residues **B**, **F** and **H** was deduced to be *gluco*-configured based on the typical $^{3}J_{H,H}$ vicinal coupling constant values. Comparing the ^{13}C chemical shifts of an unsubstituted residues (Lipkind G.M. et al., 1988), only one signal with a downfield shift was identified for C-2 of **H**, indicating that **B** and **F** were terminal non-reducing glucose units.

Finally, **I** was identified as a Kdo8N residue based on the diagnostic diastereotopic proton signals at δ 2.01 and 2.25 ppm and from the high-field chemical shift of its C-8 signal at δ 44.8 ppm. The α configuration for **I** was suggested from the coupling constant values of $^{3}J_{H7,H8a}$ (8 Hz) and $^{3}J_{H7,\ H8b}$ (3.2 Hz) (Birnbaum G. I. et al., 1987). The ROE contact between H-5 of residue **D** and H-3_{ax} of **I** indicated that Kdo8N is D

configured (Bock K. et al., 1994). The ^{1}H-^{31}P HSQC experiment of the OS revealed the following three-bond correlations of the phosphorus signals with ^{1}H signals: H-1 and H-2 of residue **A** with ^{31}P signal at δ -2.1 ppm; H4 of **G** with ^{31}P signal at δ -0.2 ppm and H4 of **I** with ^{31}P signal at δ 0.3 ppm (Figure 3.5).

Therefore, based on these results and in agreement with the OS structures from other *Shewanella* species (Vinogradov E. et al., 2003; Silipo A. et al., 2005), it was possible to hypothesize that the additional phosphoethanolamine is linked by a phosphoanhydride bond to the phosphate group at the O-4 of the Kdo8N.

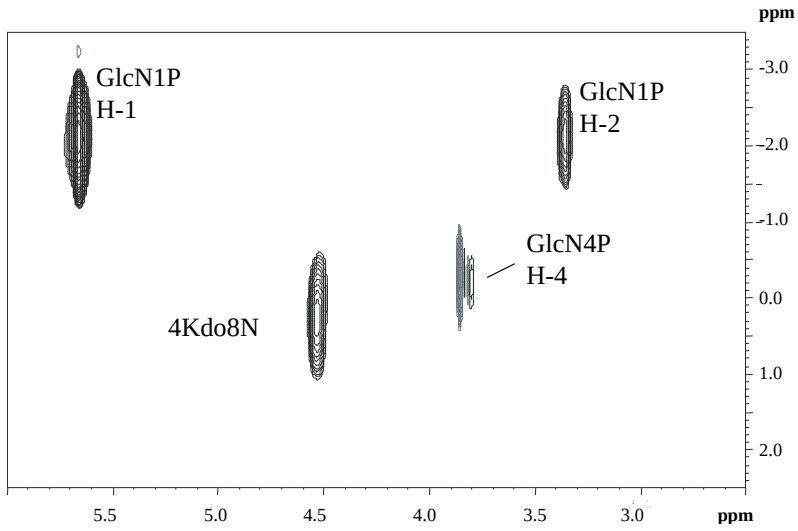

Figure 3.5 Zoom of ^{1}H-^{31}P HSQC spectrum of the OS of the LOS from *S. vesiculosa* HM13. The spectrum was recorded in D_2O at 298 K at 400 MHz.

ROESY and HMBC experiments allowed to obtain the monosaccharides sequence and the linkage positions. The ROESY experiment revealed the following *inter*-residue correlations: H-1 of **D** with H-5 of **I**, H-1 of **C** with H-6 of **D**, H-1 of **H** with both H-7 of **D**, H-1 of **E** with H-2 of **D**, H-1 of **B** with H-2 of **H**, and H-1 of **F** with H-2 of **C**. The HMBC spectrum (Figure 3.6) confirmed the identified sequence by the following long range contacts: H-1 of **G** with C-6 of **A**, H-1 of **D** with C-5 of **I**, H-1 of **C** with C-6 of **D**, H-1 of **E** with C-2 of **D**, H-1 of **H** with C-7 of **D**, H-1 of **F** with C-2 of **C**, H-1 of **B** with C-2 of **H**.

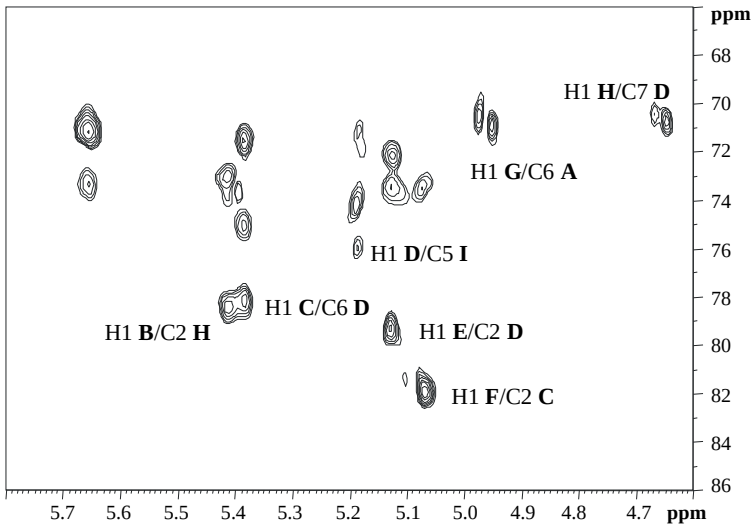

Figure 3.6 Anomeric region of the $^{1}H,^{13}C$ HMBC spectrum of the **OS** oligosaccharide. The spectrum was recorded in D_2O at 298 K at 600 MHz.

Based on these data, the structure of the oligosaccharide (OS) moiety of LOS isolated from *S. vesiculosa* HM13is that reported in Figure 3.7.

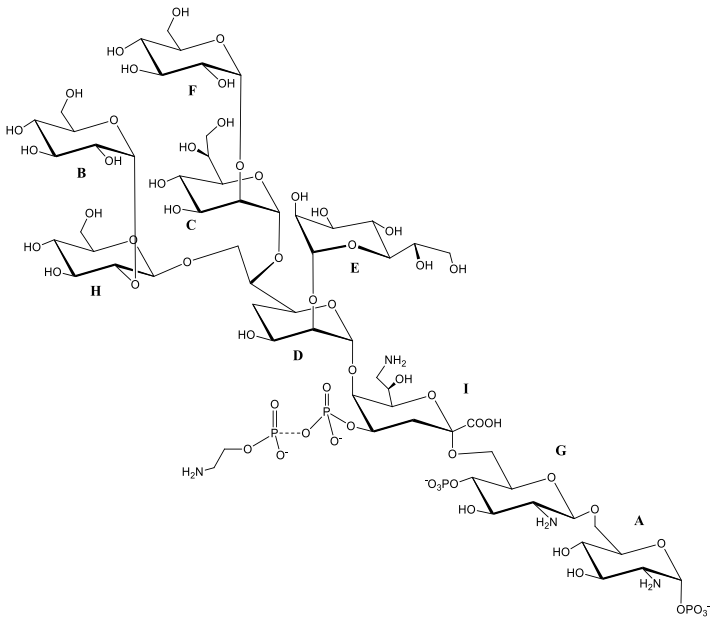

Figure 3.7 OS structure of the LOS from *S. vesiculosa* HM13, grown at 4 °C.

3.4 Discussion

The LOS of the cold-adapted bacterium *S. vesiculosa* sp. HM13, grown at 4 °C, was isolated and the complete structure of its saccharidic backbone was reported. The structure, obtained by chemical analysis, MALDI-TOF mass spectrometry and NMR spectroscopy, revealed some structural features of LPS isolated from other *Shewanella* species. The presence of the Kdo8N, already reported for the species *oneidensis* (Vinogradov E. et al., 2003), *algae* (Vinogradov E. et al., 2004), *pacifica* (Silipo A. et al., 2004), *putrefaciens*, (Moule A. L et al.., 2004), and *Shewanella* spp. MR-4 (Vinogradov E. et al., 2008), is a hallmark of *Shewanella* species. In addition, the D,D- heptose possess a central position in the oligosaccharide structure, as well as for all the other characterized LOS structures (Vinogradov E. et al., 2008; Vinogradov E. et al., 2003; Vinogradov E. et al., 2004; Moule A. L. et al., 2004). The rough nature of the LPS from *S. vesiculosa* HM13 is not surprising, since it has also been reported for other *Shewanella* species (Vinogradov E. et al., 2008; Vinogradov E. et al., 2003, Vinogradov E. et al., 2004; Moule A. L. et al., 2004). However, this feature is common among the LPSs isolated from cold-adapted Gram-negative bacteria (Casillo A. et al., 2019). A possible explanation lies in the enhanced flexibility and stability of the outer membrane when the O-polysaccharide chain is absent (Corsaro M. M. et al., 2017). Due to the low amount of the EMVs biomass produced from this bacterium at 4 °C it was not possible to characterize the LPS from the vesicles, and therefore the bacterium was grown at 18 °C (its optimal growth temperature).

Chapter IV: *Shewanella vesiculosa* HM13 Rif^r grown at 18°C

4.1 LPS isolation and characterization from cells and EMVs

4.1.1 Isolation and chemical analyses of the LPS

S. vesiculosa HM13 Rif^r (rifampin-resistant mutant) was used as parental strain for the mechanistic studies on the of P49 transport to EMVs, in which LPS and CPS were presumably involved.

LPSs were extracted from the dried cells and EMVs using the phenol/chloroform/light petroleum (PCP) method (Galanos C. et al., 1969). The LPS yields for the cells and the EMVs after precipitation were 3% and 19%, respectively. The LPS precipitates were analysed by sodium deoxycholate polyacrylamide gel electrophoresis (DOC-PAGE, Figure 4.1). After silver nitrate staining the gel showed, for both samples, the presence of bands at low molecular masses, confirming the rough nature of the LPS as previously described for *S. vesiculosa* HM13 grown at 4 °C (see paragraph 3.1).

Figure 4.1 Analysis of the PCP precipitates from *S. vesiculosa* HM13 Rif^r cells (Lane B) and its EMVs (Lane C) by 14% DOC-PAGE. The LOSs were compared with a smooth-LPS from *E. coli* O127: B8 (Lane A).

The glycosyl composition for both LOSs was achieved by GC-MS analysis of the acetylated methyl glycosides (AMGs). The chromatograms showed the same sugar composition already found for *S. vesiculosa* HM13 cells grown at 4 °C (see paragraph 3.1): D-glucose (D-Glc), 2-amino-2-deoxy-D-glucose (D-GlcN), D,D-

and L-*glycero*-D-*manno*-heptoses (D,D-Hep and L,D-Hep, respectively) (Figure 4.2a, and Table 4.1). In addition, the fatty acids analysis indicated for both the cells and the EMVs the presence of C12:0(3OH) and the C13:0(3OH), as the major 3-hydroxylated components, and a little amount of C14:0(3OH) (Figures 4.2b and Table 4.2). Non-hydroxylated fatty acid residues were also found: C12:0, C13:0, C14:0, and C15:0.

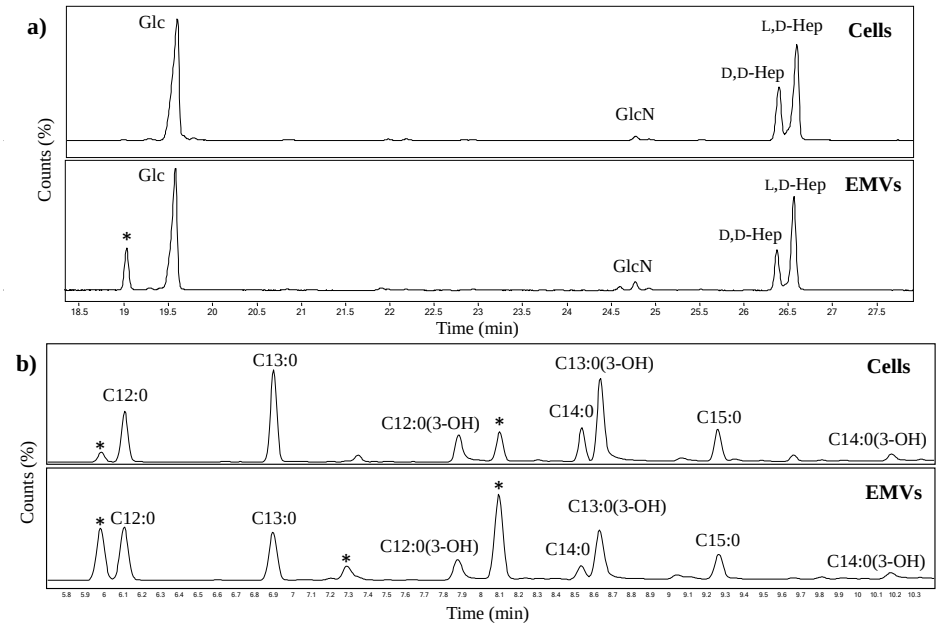

Figure 4.2 a**)** GC-MS chromatograms of AMGs of the LOSs from *S. vesiculosa* HM13 cells and EMVs. b) GC-MS chromatograms of the FAMEs of the LOS samples from *S. vesiculosa* HM13 cells and EMVs. Asterisks "*" indicate contaminants.

Table 4.1. Molar ratio percentage of monosaccharide residues of the LOS from *S. vesiculosa* HM13, grown at 18 °C.

	Glc	**GlcN**	**D,D-Hep**	**L,D-Hep**
Cells	49.9%	1.1%	16%	33%
EMVs	55.7%	1.9%	12.1%	30.3%

Table 4.2. Molar ratio percentage of fatty acids of the LOSs from *S. vesiculosa* HM13, grown at 18 °C.

	C12:0	C13:0	C12:3OH	C14:0	C13:3OH	C15:0	C14:3OH
Cells	22.8%	24%	10.2%	8%	23%	9%	3%
EMVs	23.6%	21%	10.8%	6%	23.6%	11.3%	3.7%

4.1.2 Mass spectrometric analysis of the LOSs

The LOSs isolated from the cells and the EMVs were analysed by negative ions MALDI-TOF analysis. The mass spectra (Figure 4.3) indicated for both LOSs an identical composition, as suggested by the ions at *m/z* 3103.05 (Calculated $[M-H]^-$ 3103.56 Da). In addition, signals attributable to the lipid A and to the core oligosaccharide (OS) fragments, arising from the in-source cleavage of the linkage between the lipid A and the 8-amino-Kdo8N residue, were detected (Di Guida R. et al., 2019) (Figure 4.3). The signals attributable to the core fragments were the same as those observed at 4 °C (Casillo A. et al., 2019). In particular, signals at *m/z* 1360.63 and 1483.66 can be attributed to the fragments $Hex_3Hep_3Kdo8NP$ and $Hex_3Hep_3Kdo8NPPEtN$, respectively (Calculated $[M-H]^-$ 1360.38 and 1483.39 Da, respectively).

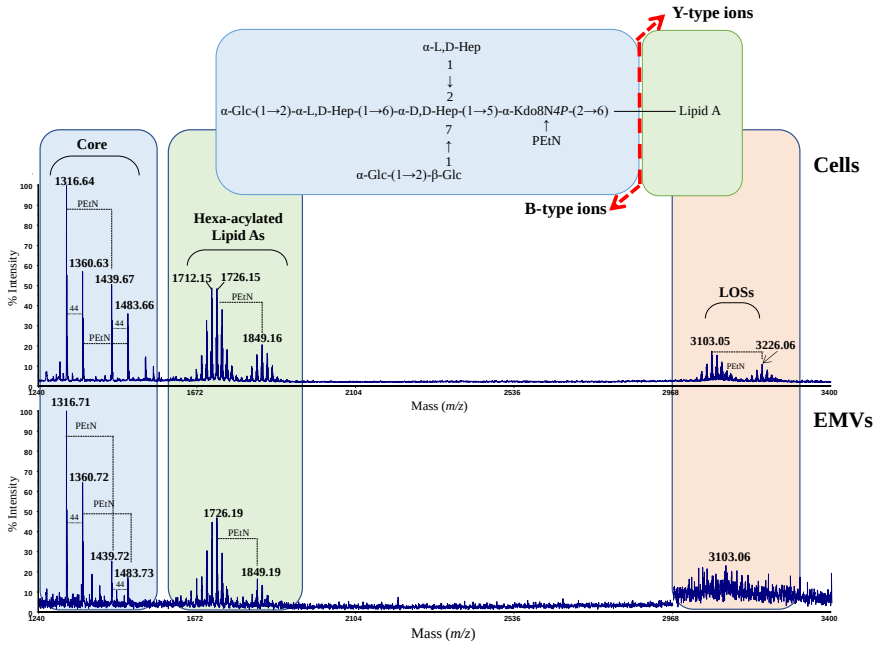

Figure 4.3. Negative ions MALDI-TOF spectra of whole LOSs from the *S. vesiculosa* HM13 Rif^r cells and EMVs. The insert shows the fragment ions.

4.1.3 NMR analysis of LOS oligosaccharide moiety

To establish the chemical structure of the saccharidic region of LOS from the EMVs, a full de-acylation was performed. Thus, the LOS isolated from the EMVs was de-*O*-acylated by mild hydrazinolysis and then de-*N*-acylated by strong alkaline hydrolysis (Di Guida et al., 2019). The mixture was desalted on a Sephadex resin, yielding a fraction containing the core oligosaccharide attached to the lipid A glucosamine disaccharide. To characterize this oligosaccharide homo- and heteronuclear 1D and 2D NMR experiments were performed (^{1}H, ^{1}H DQF-COSY, ^{1}H, ^{1}H TOCSY, ^{1}H, ^{1}H ROESY, ^{1}H, ^{13}C DEPT-HSQC, ^{1}H, ^{13}C HMBC and ^{1}H, ^{31}P HMBC). The ^{1}H NMR spectrum displayed the same eight anomeric signals (residues **A**-**H**, Table 4.4) already found for the oligosaccharide from the cells grown at 4 °C (see paragraph 4.4), despite the small differences in

the chemical shift values. The 2D-NMR spectra allowed to assign all the spin systems of the monosaccharide residues of the OS (Table 4.3). Among these, the anomeric region of the HMBC spectrum is reported in Figure 6. This experiment indicated that the sequence of the oligosaccharide structure from the EMVs was the same as that already found for LOS isolated from *S. vesiculosa* HM13 cells grown at 4 °C (Casillo A. et al., 2019).

Table 4.3 ^{1}H and ^{13}C assignments of the fully deacylated oligosaccharide from the EMVs of *S. vesiculosa* HM13. All the values are referred to sodium 3-trimethylsilyl-(2,2,3,3-$^{2}H_4$)-propanoate (TSP, δ_H 0.00, internal standard) and 1,4-dioxane in D_2O (δ_C 67.40, external standard). Spectra were recorded at 298 K at 600 MHz.

Residue	H1 C1	H2 C2	H3 C3	H4 C4	H5 C5	H6a,b C6	H7a,b C7	H8a,b C8
A	5.65	3.35	3.91	3.46	4.21	3.93-4.36		
α-GlcN*p1P*	92.0	55.9	71.5	71.2	73.3	70.3		
	1.73							
B	5.43	3.60	3.77	3.50	4.05	3.77		
α-Glc*p*	98.9	72.7	73.8	70.6	73.1	72.3		
C	5.37	3.90	4.11	3.82	3.91	4.07	3.80-3.75	
α-L,D-Hep*p*	98.6	82.3	70.5	68.5	75.2	70.5	64.3	
D	5.23	4.09	4.17	3.84	4.07	4.35	4.03	
α-D,D-Hep*p*	101.6	79.6	71.7	68.4	74.6	78.1	71.0	
E	5.12	4.08	3.85	3.87	3.69	4.06	3.82-3.69	
α-L,D-Hep*p*	103.5	71.3	72.0	67.7	73.9	70.5	64.6	
F	5.08	3.62	3.74	3.50	4.04	3.82		
α-Glc*p*	102.1	73.1	74.2	70.8	73.2	62.1		
G	4.89	3.07	3.80	3.85	3.76	3.53		
β-GlcN*p4P*	100.8	57.0	73.6	74.2	75.5	63.5		
				3.47				
H	4.66	3.50	3.59	3.44	3.50	3.76		
β-Glc*p*	105.1	77.3	75.9	71.1	78.4	62.3		
I		-	2.03-2.28	4.54	4.36	3.93	4.05	3.21-3.54
α-Kdo8N*p4P*	n.d.	101.2	6.4	70.6	76.3	75.0	67.1	44.4
			3.77					

Signals in italic refer to the ^{31}P chemical shifts, measured in D_2O at 298 K at 160 MHz.

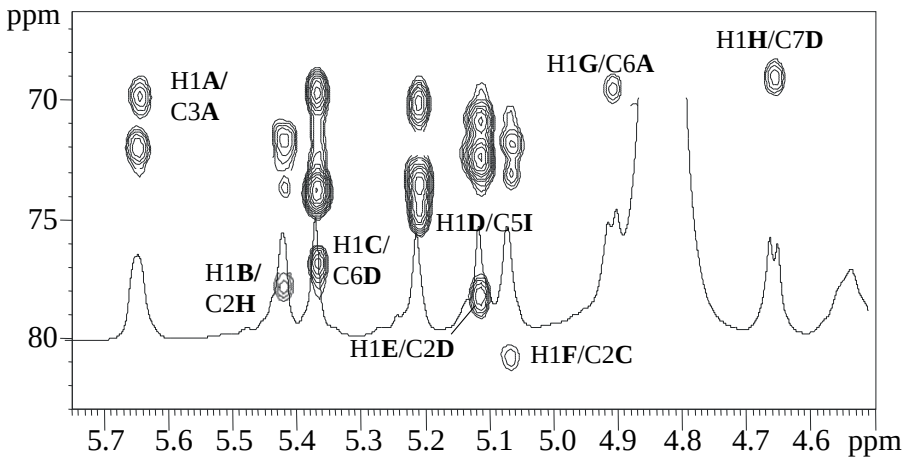

Figure 4.4. ^{1}H, ^{13}C HMBC anomeric region of the oligosaccharide obtained after de-acylation of the LOS from *S. vesiculosa* HM13 EMVs. The spectrum was recorded in D_2O at 298 K at 600 MHz.

The ^{1}H-^{31}P HSQC spectra of the OS from the EMVs indicated correlations between the ^{31}P and ^{1}H signals as follows: H-1 and H-2 of GlcNI with ^{31}P signal at δ 1.73 ppm; H4 of GlcNII with ^{31}P signal at δ 3.47 ppm; H-4 of Kdo8N with ^{31}P signal at δ 3.77 ppm (Figure 4.5). Finally, the correlations of the ^{31}P at δ 3.86 ppm with the ^{1}H signals at δ 4.00 and 3.24 ppm were attributed to free PEtN molecules (Wishart D.S. et al., 2009).

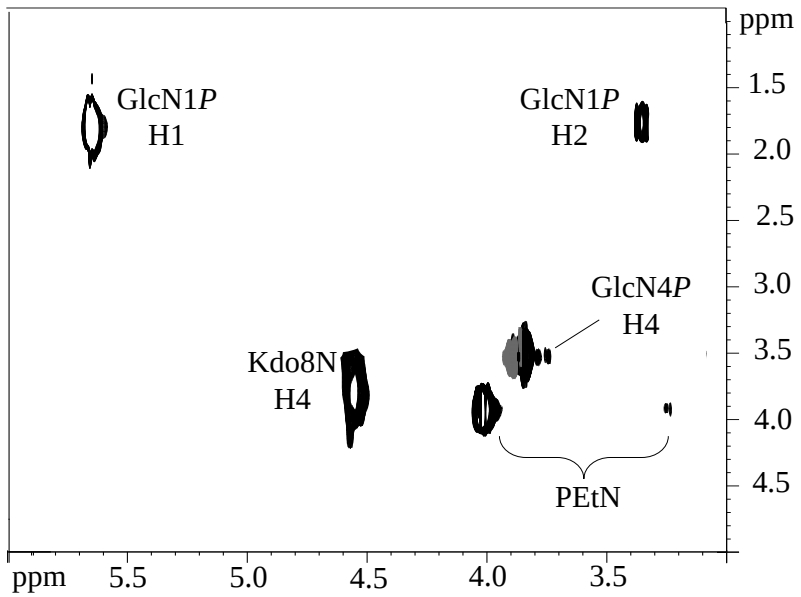

Figure 4.5. Zoom of ^{1}H-^{31}P HSQC spectrum of the OS from LOS of *S. vesiculosa* EMVs. The spectrum was recorded in D_2O at 298 K and at 400 MHz.

Based on the above results it was possible to define the complete structure of the LOS molecule from EMV of *S.vesiculosa* HM13 (Scheme 4.1).

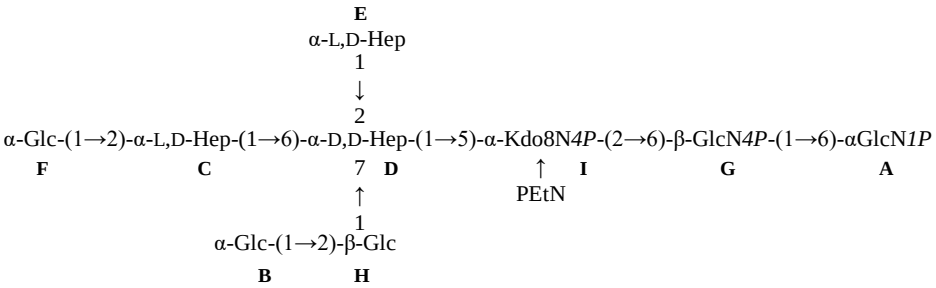

Scheme 4.1 Structure of OS moiety of the LOS from EMV of *S.vesiculosa* HM13

4.1.4 Structural characterization of the lipid A from cells and EMVs

To establish the chemical structure of the lipid A moiety of the LOSs from cells and EMVs, a mild acid hydrolysis was performed. This reaction yielded the lipid

A domain as a precipitate. To determine the acyl chains distribution on the glucosamine backbone, negative ions MALDI-TOF spectra of the lipid A samples were performed (Figure 4.6). The experiments indicated **M1** and **M2** as the major signal clusters, corresponding to glycoforms with different acylation patterns (Figure 4.6, Scheme 1a). Both glycoforms were hexa-acylated, with a difference between the two clusters of 80 Da, corresponding to a phosphate group. Differences of 14 Da within each cluster are responsible for the variations of fatty acids length. In particular, to the ion at *m/z* 1726.15, the following composition was assigned $GlcN_2P_2[C13:0(3\text{-}OH)]_3[C12:0(3\text{-}OH)][C13:0]_2$ (Calculated $[M\text{-}H]^-$ 1726.15 Da).

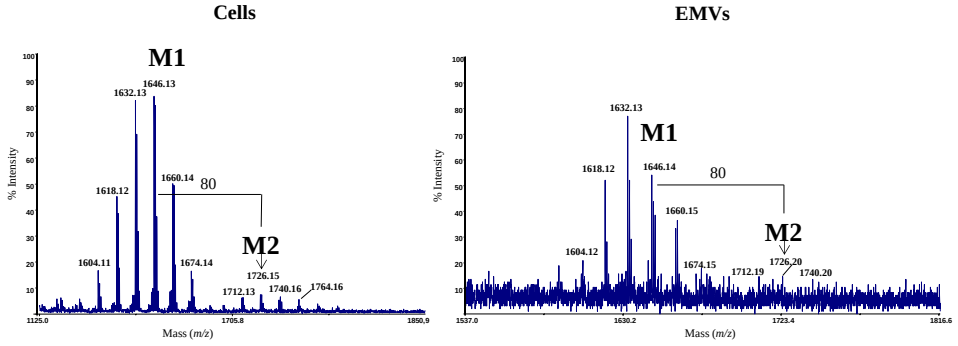

Figure 4.6. Negative ions MALDI-TOF spectra of the lipid As from the *S. vesiculosa* HM13 cells and EMVs.

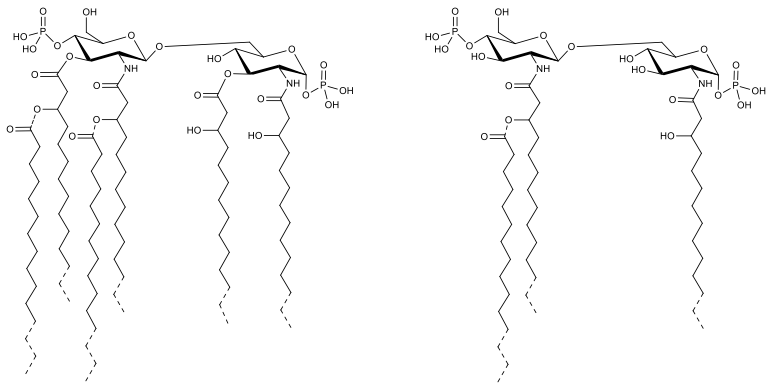

a **b**

Scheme 4.2 Structures of the **a**) lipid A and **b**) lipid A after NH_4OH treatment from *S. vesiculosa* HM13.

In addition, lipid A in both structures is substituted by a phosphoethanolamine group, as revealed from the mass spectra of the entire LOSs (Figure 4.7).

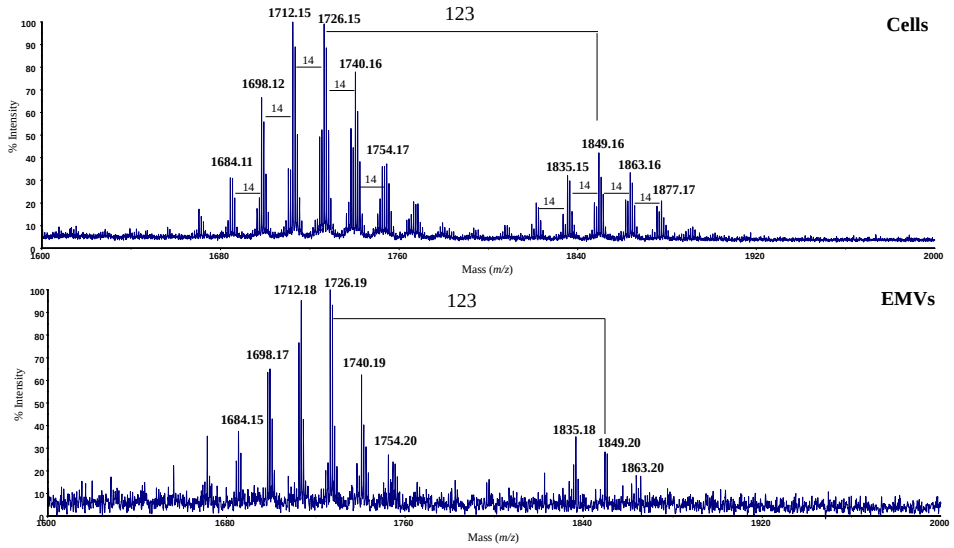

Figure 4.7. Selected region (*m/z* 1,600-2,000), indicating the lipid A signals, of the negative ions MALDI-TOF MS spectra of intact LOSs from the *S. vesiculosa* HM13 cells and EMVs.

In order to detect the position of the secondary fatty acids, an alkaline hydrolysis with NH_4OH was performed. This treatment hydrolyses acyl and acyloxacyl esters and leaves intact acyl and acyloxacyl amides. The negative ions MALDI-TOF spectra of the NH_4OH products (Figure 4.8, Scheme 1b) indicated a signal at *m/z* = 1119.65 attributable to a tri-acylated bis-phosphorylated lipid A species with two amide-linked C13:0(3-OH) residues, one of which is substituted at O-3 by a secondary 13:0 acyl chain (Calculated $[M-H]^-$ 1119.62 Da). The additional 14 Da can be attributed to a combination of two C13:0(3-OH) residues and one C14:0, as well as a C14:0(3-OH) instead of a C13:0(3-OH) as a primary fatty acid residue. Similarly, differences of 14 Da less can be due to a C12:0 as secondary fatty acid as well as to a C12:0(3-OH) instead of a C13:0(3-OH) as primary fatty acid residues.

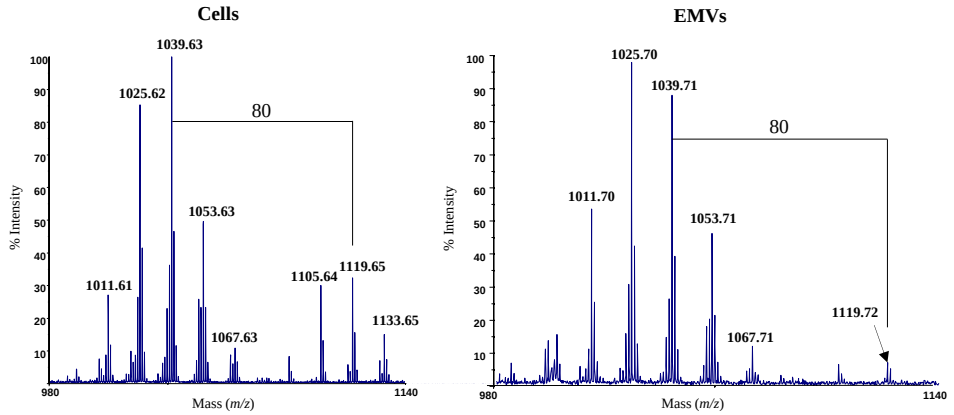

Figure 4.8. Negative ions MALDI-TOF spectra of NH_4OH treated lipid As from *S. vesiculosa* HM13 cells and EMVs.

The low amounts of bis-phosphorylated species compared to the monophosphorylated ones in both lipid A spectra can be attributed to a partial hydrolysis of the phosphate group during the mild acid treatment. Indeed, no differences were found in the relative amount of the intact lipid A species (Figure 4.2 and 4.7).

Finally, all these results together with those already reported for *Shewanella pacifica* (Silipo A. et al., 2005) have suggested that the lipid A structures were the same between the cells and EMVs with regard to the acyl substitution pattern. It is worth mentioning that the presence of a phosphoethanolamine group that substitutes the lipid A in *Shewanella* species has never been previously described.

4.1.5 Discussion

In this study, the whole LOSs isolated from both the cells and EMVs of *S. vesiculosa* HM13 Rif^r have been fully characterized. The characterization shown the same structure for the cells and EMVs. This result confirmed the vesicles biogenesis mechanism consisting in the budding and pinching off of the EMVs from the bacterial outer membrane (Chen C. et al., 2020). In addition, no differences were found with respect to the LOS between the cells grown at 4 °C and 18 °C.

In literature, few studies are present about the EMVs produced by cold-adapted bacteria and their LPSs content (Nevot M. et al., 2006). In particular, this is the first study about the complete characterization of an LPS isolated from EMVs. In *Pseudomonas aeruginosa*, two different LPSs have been identified, and one of them is enriched in the EMVs relatively to the cells (Li Z. et al., 1996). It has been reported that in *Bacteroides fragilis* the comparison of cellular lipid A and EMVs revealed that they were identical (Elhenawy W. et al., 2014). Finally, in *Porphyromonas gingivalis* the lipid A is less acylated in EMVs compared with cells (Haurat M. F. et al., 2011).

4.2 CPS isolation and characterization

4.2.1 Extraction and purification of CPS

After LOSs precipitation (see paragraph 4.1.1, Casillo A. et al. 2019), the phenolic phases from PCP extraction of the cells and EMVs were dialyzed against water. The 14 % DOC-PAGE analysis of the two phenolic phases after Alcian blue and silver staining suggested the presence of additional bands at high molecular weight attributable to a capsular polysaccharide (Figure 4.9).

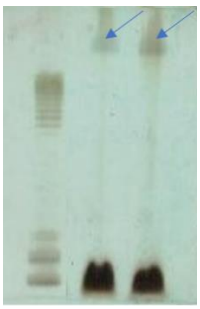

Figure 4.9 14% DOC-PAGE analysis of dialyzed phenolic phase from cells (lane B) and the EMVs (lane C) obtained after PCP extraction. In the lane A, the smooth LPS of *E. coli* O127:B8 used as standard is visible. The blue arrows indicated bands at high molecular masses attributed to the CPS.

To separate the polysaccharide from the LOS, the dialyzed phenolic phases were hydrolysed under mild acidic conditions, and the supernatant fractionated on Biogel P-10 resin. The monosaccharide composition of the CPS samples was achieved by GC-MS analysis of AMGs. The chromatograms revealed the presence of glucose (Glc), 2-amino-2-deoxy-glucose (GlcN) and rhamnose (Rha). In addition, the GC-MS analysis of the acetylated (*R*)-2-octyl glycosides indicated that the absolute configurations were D for both Glc and GlcN and L for Rha. However, this sugar analysis was not compatible with the presence of so many signals of carbons bearing nitrogen in the $^{1}H,^{13}C$-DEPT-HSQC NMR spectrum (Figure 4.10).

4.2.2 NMR analysis of purified CPS

All the ^{1}H and ^{13}C NMR resonances (Table 4.4) of the CPS were assigned by the study of all the one and two-dimensional NMR experiments (^{1}H, ^{1}H COSY, TOCSY, NOESY, ^{1}H, ^{13}C DEPT-HSQC, and ^{1}H, ^{13}C HMBC) acquired at 308 K and pD 2. The ^{1}H, ^{13}C DEPT-HSQC spectrum (figure 4.10) showed the presence of five proton signals (**A**-**E**) correlated to anomeric carbons in the anomeric region. The same number of signals were also found in the *N*- and *O*-acetyls region at δ 2.18, 2.14, 2.09, 2.03, 1.99, 1.97 and 1.91 ppm. At high fields, the presence of signals at δ 1.12 and 1.38 ppm confirmed the presence of deoxy sugars. The anomeric configuration of the residues **A**, **C** and **D** was deduced to be α, and β for **B** and **E**, by the values of the $^{1}J_{C1,H1}$ coupling constants obtained from the 2D F2-coupled HSQC experiment (Table 4.4).

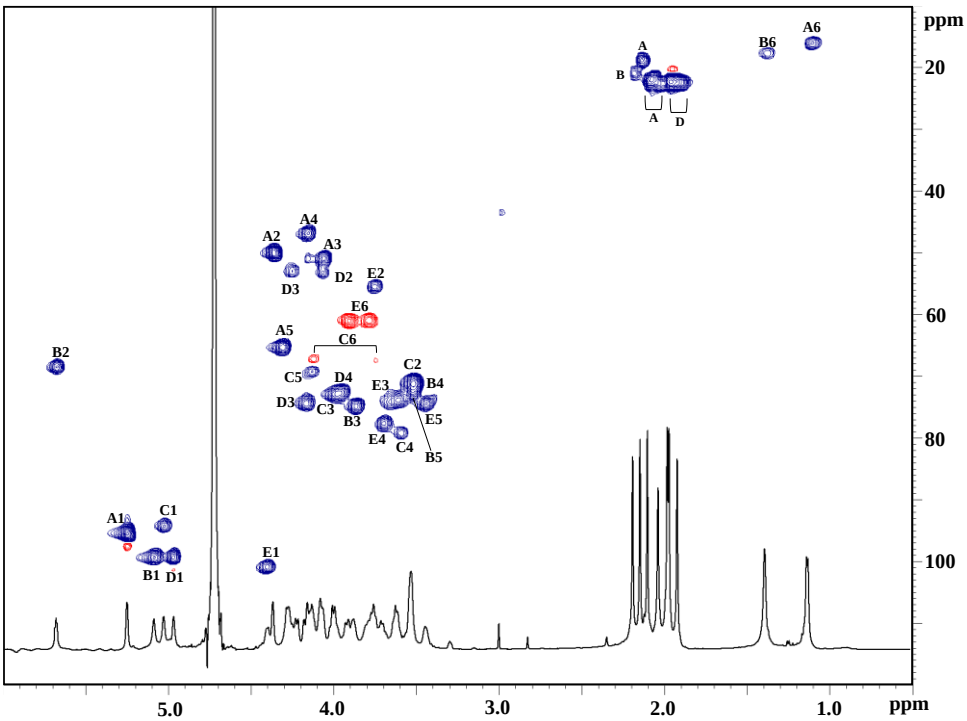

Figure 4.10. ^{1}H NMR and ^{1}H, ^{13}C DEPT-HSQC spectra of the CPS isolated from the cells of *S. vesiculosa* HM13 Rif^{r}, grown at 18 °C. The spectra are record at pD 2 and 308K at 600 MHz.

Residue **A** with H-1 at δ 5.25 ppm showed in the TOCSY spectrum correlations up to H-4, a pattern diagnostic of a *galacto*-configured residue. The analysis of both TOCSY and COSY spectra led to the assignment of all the protons chemical shifts of this spin system. The H-2, H-3 and H-4 correlated in the ^{1}H, ^{13}C HSQC spectrum with nitrogen bearing carbons at δ 46.7, 50.6, 49.7 ppm, respectively. Long-range scalar contacts among H-2 and H-4 and carbonyl groups at δ 173.9 and 175.6 ppm, respectively, suggested the *N*-acetyl substitution at these two positions. Moreover, the H-3 showed a long-range scalar correlation with the signal at δ 166.0 ppm, characteristic of an *N*-acetamidinoyl group (Shashkov S. et al., 2002; Kilcoyne M. et al., 2002; Kilcoyne M. et al., 2005). Finally, the COSY spectrum revealed a correlation between the H-5 at δ 4.27 ppm and the H-6 protons at δ 1.12 ppm. Thus, residue **A** was suggested to be a terminal α-3-acetimidoylamino-2,4-diacetamido-2,3,4,6-tetradeoxy-*galacto*-pyranose (named shewanosamine, ShewN). The D configuration of this novel monosaccharide was suggested by the optical rotation measurement of the isolated monosaccharide compared with that obtained from the synthetic one.

Residue **B** with H-1 at δ 5.08 ppm showed in the COSY experiment a correlation with H2 at δ 5.69 ppm, which was in turn correlated in the HSQC spectrum with a carbon at δ 68.1 ppm attributable to a carbon substituted with an *O*-acetyl group. The *O*-acetyl substitution at position 2 was also demonstrated by the ^{1}H, ^{13}C HMBC spectrum, where the methyl signal at δ 2.18 ppm showed a long-range scalar connectivity with the carbonyl group at δ 173.4 ppm (Figure 4.11), which in turn displayed a long-range scalar connectivity with the H-2 of this residue. The correlations found in the TOCSY and COSY spectra together with the NOE contact between H-5 at δ 3.53 ppm and a methyl signal at 1.38 ppm allowed to identify the residue **B** as a rhamnose. The β-configuration, indicated by the $^{1}J_{C1,H1}$ value of 166 Hz, was also confirmed by the strong *intra*-residue NOE contact between H-1 and both H-3 and H-5. Finally, the observed downfield shift of the

C-3 carbon resonance at δ 74.3 ppm was indicative of a substitution at this position (Bock K. and Pedersen C. J., 1983).

The spin system **C** with H-1 at δ 5.03 ppm was identified as an α-glucose, due to the strong scalar correlations in both COSY and TOCSY experiments and the correlation of its H-2 at 3.53 ppm with a carbon resonance at δ 70.8 ppm in the DEPT-HSQC spectrum. The α-configuration was deduced from the $^{1}J_{C1,H1}$ value (174 Hz). Finally, this residue was identified as a 4,6-substituted glucose (α-4,6-Glc), based on the downfield shift of its C-4 and C-6 carbon at δ 79.1 and 66.8 ppm, respectively (Bock K. and Pedersen C. J., 1974).

Residue **D** with H-1 at δ 4.97 ppm was identified as α-2,3-diacetamido-2,3-dideoxyglucuronic acid. TOCSY experiment revealed a correlation of H-1 signal with H-2 at δ 4.07 ppm and H-3 at δ 4.25 ppm, both correlated with carbon signals indicating the linkage with nitrogen atoms at δ 52.6 and 52.5 ppm, respectively. The *N*-acetyl substitution of these two carbons was suggested by the long-range scalar connectivity with the carbonyl signals at δ 173.9 and 174.1 ppm, in turn correlated to signals at δ 1.97 and 1.91 ppm, respectively. Moreover, the HMBC spectrum revealed a long-scalar range correlation between its H-5 at δ 4.24 ppm and a carbonyl group at δ 174.4 ppm. (Perepelov A. V. et al. 2000; Vinogradov E. et al 2018; Zdorovenko E. L. et al. 2020). The α-configuration for this residue was deduced from the $^{1}J_{C1,H1}$ value (174 Hz).

Based on glycosylation effect of ^{13}C chemical shifts (Lipkind G. M. et al., 1988) the absolute D configuration of this residue was achieved. Taking into account the disaccharide α-GlcNAc3NAcA-(1→4)-α-Glc (P'→P) were calculated the values of the C4 chemical shift of the glycosylated (P) residue and of the C1 of glycosylating residue (P') for both D-L and D-D configurations couples. In particular, for the D-L configurations, the C4 of residue P should be at 78.4 ppm (+7.5), while the C1 of residue P' 98.1 ppm (+6.4). On the contrary, for the D-D configurations, the value of the C4 chemical shift of the glycosylated residue should be at 78.3 ppm (residue P, +7.4), while the value of C1 of glycosylating

residue (Tomshich S. V. et al., 2016) should be at 99.2 ppm (residue P', +7.6). The calculated chemical shifts for the couple D-D were much more in agreement with the real values than those of the D-L couple.

A *gluco*-configuration was also found for residue **E**. The H-1 of this residue at δ 4.39 ppm showed a correlation in the COSY experiment between its anomeric proton and H-2 at 3.75 ppm, which was in turn correlated to a nitrogen bearing carbon at δ 55.3 ppm. The HMBC spectrum revealed a long-range scalar connectivity between the δ H-2 at 3.75 ppm and the carbonyl at δ 174.3 ppm, correlated to a methyl signal at δ 2.03 ppm. This confirmed the *N*-acetyl substitution at position 2 of residue **E**. The β-configuration of this residue was suggested by the value of 163.3 Hz for the $^{1}J_{C1,H1}$, and confirmed by the strong *intra*-residue NOE contact between H-1 and both H-3 and H-5. Finally, due to the downfield shift of the C-4 at δ 77.4 ppm (Bock K. and Pedersen C. J., 1974) this residue was identified as a 4-substituted GlcNAc (β-4-GlcNAc).

Table 4.4 ^{1}H and ^{13}C NMR chemical shifts of the CPS from the cells of *Shewanella vesiculosa* HM13, grown at 18 °C, at pD2 and 308 K (600 MHz).

Residue	**H1** **C1** **$^{1}J_{C1,H1}$**	**H2** **C2**	**H3** **C3**	**H4** **C4**	**H5** **C5**	**H6** **H6a,H6b** **C6**	**NAc/(OAc)** **[Am]**	**NH (C)**
α-2,3,4-ShewN	5.25	4.16	4.06	4.36	4.27	1.12	1.99/173.9(C2)	9.02 (C2)
A	95.4	46.7	50.6	49.7	65.0	15.6	2.14/166(C3)	8.17 (C3)
	178 Hz						2.09/175.6(C4)	8.44(C4)
β-2-OAc-3-Rha	5.08	5.69	3.88	3.52	3.53	1.38	(2.18/173.4)	
B	99.0	68.1	74.3	70.8	72.3	17.0		
	166 Hz							
α-4,6-Glc	5.03	3.53	4.00	3.60	4.13	4.12,3.77		
C	93.9	70.8	72.6	79.1	68.8	66.8		
	174 Hz							
α-4-GlcNAc3NAcA	4.97	4.07	4.25	3.95	4.22	-	1.97/173.9	
D	99.1	52.6	52.5	72.6	73.8	174.4	1.91/174.1	
	174 Hz							
β-4-GlcNAc	4.39	3.75	3.62	3.71	3.44	3.79,3.91	2.03/174.3	
E	100.6	55.3	73.3	77.4	74.0	60.6		
	163 Hz							

The sequence of the repeating unit of the CPS (Figure 4.12) was obtained by the glycosylation effect, the long-range correlations found in HMBC spectrum, and

the *inter*-residue NOE connectivities (Figure 4.11). In particular, the HMBC spectrum confirmed the sugar sequence based on the following correlations: H-1 of **A** with C-4 of **D**, H-1 of **B** with C-4 of **E**, H-1 of **D** with C-4 of **C**; H-1 of **E** with C-6 of **C**, H-1 of **C** with C-3 of **B** (Figure 4.11b). Moreover, the NOESY spectrum revealed *inter*-residues contacts assigned to H-1 of **A** with H-4 of **D**, H-1 of **D** and H-4 of **C**, H-1 **C** of with H-3 of **B**, H-1 of **B** with H-4 of **E**, H-1 of **E** with H-6 of **C** (Figure 4.11 c and d).

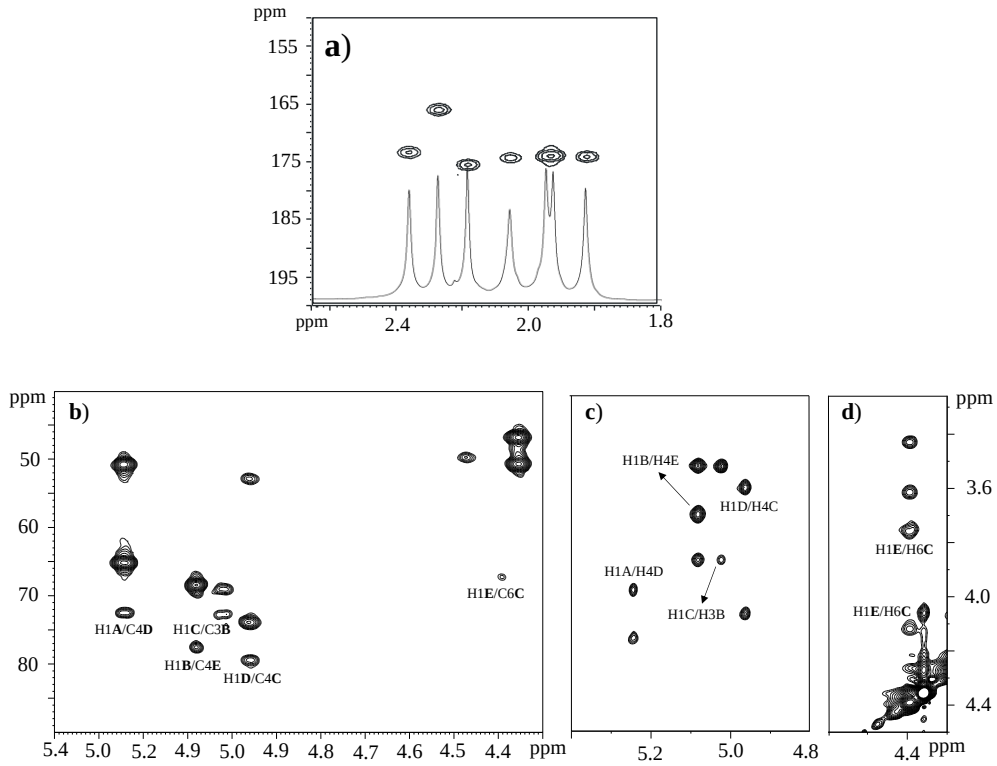

Figure 4.11 a) Acetyl groups region, **b)** long-range scalar connectivities in the $^{1}H,^{13}C$ HMBC spectrum, **c)** and **d)** *inter*-residue correlations in the NOESY spectrum of the CPS from *S. vesiculosa* sp. HM13. The spectra were recorded in D_2O (pD 2) at 308 K and at 600 MHz.

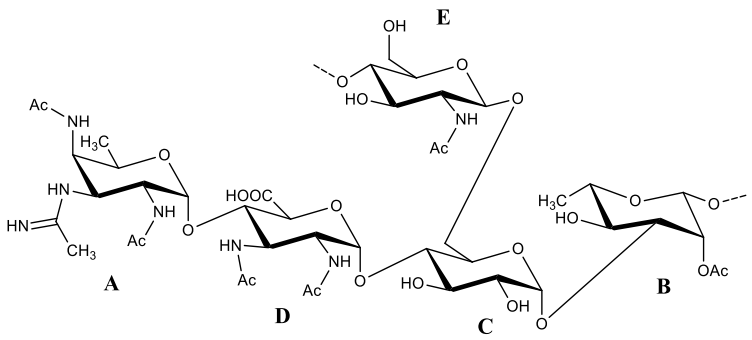

Figure 4.12 Structure of the repeating unit of the CPS from *S. vesiculosa* HM13 Rif^r cells, grown at 18 °C.

Finally, all the NMR spectra (Figure 4.13) acquired for the CPS isolated from both cells and EMVs together with chemical analysis indicated that the two CPSs possess the same structure.

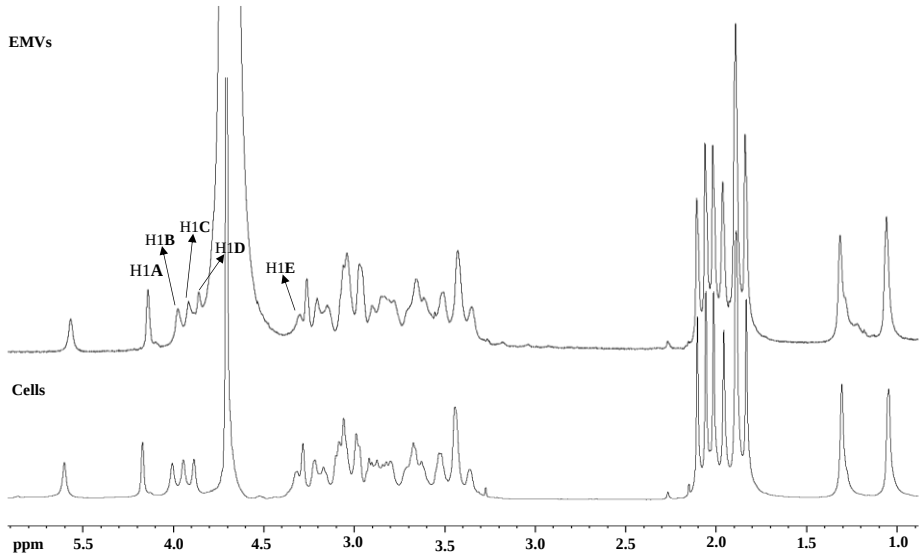

Figure 4.13 ^{1}H NMR spectra of the CPSs isolated from the cells and the EMVs of *S. vesiculosa* HM13 Rif^r, grown at 18 °C. The spectra were recorded in D_2O (pD 2) at 308 K and 600 MHz.

4.2.3 Isolation of the novel monosaccharide (ShewN)

The whole CPS isolated from the cells was subjected to a treatment with aqueous ammonia (Kilcoyne M. et al., 2005), this allowed to convert the *N*-acetamidoyl group into an *N*-acetyl group, and to eliminate the *O*-acetyl group. Then the product was fully hydrolysed with triflic acid under anhydrous conditions (Perepelov A. V. et al., 2000, Kocharova N. A. et al., 2001). The reaction mixture was neutralized with aq. NH_3, desalted on a Biogel P-2 resin, and purified on a reverse phase HPLC column. Starting from the ^{1}H NMR analysis of the all fractions was selected the fraction, which was further investigated by 1-D and 2-D NMR experiments.

4.2.4 NMR analysis of ShewN

The analysis of the acquired spectra (^{1}H, ^{1}H COSY, TOCSY, NOESY, ROESY, ^{1}H,^{13}C DEPT-HSQC, and HMBC) allowed to assign all the ^{1}H and ^{13}C NMR resonances of the isolated monosaccharide (Table 4.5). The analysis of both ^{1}H (Figure 4.14) and ^{1}H,^{13}C DEPT-HSQC spectra allowed to identify the anomeric signals at δ 5.14/90.4 ppm and δ 4.65/96.4 ppm assignable to the α- and β-residues, respectively.

Table 4.5 ^{1}H and ^{13}C NMR chemical shifts (δ), visible **multiplicities** and coupling constants (Hz) of the isolated monosaccharide, at pD 6 and 298 K (600 MHz).

	Anomers	
	β-2,3,4,6-tetradeoxy-2,3,4-triacetamido-galactopyranose	α-2,3,4,6-tetradeoxy-2,3,4-triacetamido-galactopyranose
H1	4.67 **d**	5.14 **d**
C1	96.0	90.4
($^{1}J_{C1,H1}$)	(166 Hz) 8.4	(176 Hz) 3.4
$J_{H1,H2}$		
H2	3.70 **dd**	3.99 **dd**
C2	51.0	47.6
$J_{H2,H3}$	11.8	12.2
H3	4.07 **dd**	4.25 **dd**
C3	51.8	47.6
$J_{H3,H4}$	3.9	3.3
H4	4.13 **s**	4.18 **s**
C4	51.1	51.3
H5	3.93 **q**	4.37 **q**
C5	70.8	64.8
H6	1.08 **d**	1.03 **d**
C6	15.7	15.7
NAc	1.91/22.0/174.8(C2) 1.83/21.8/174.3(C3) 2.03/22.0/175.3(C4)	1.91/22.0/174.6 (C2) 1.83/21.8/174.4(C3) 2.02/21.8/175.4 (C4)

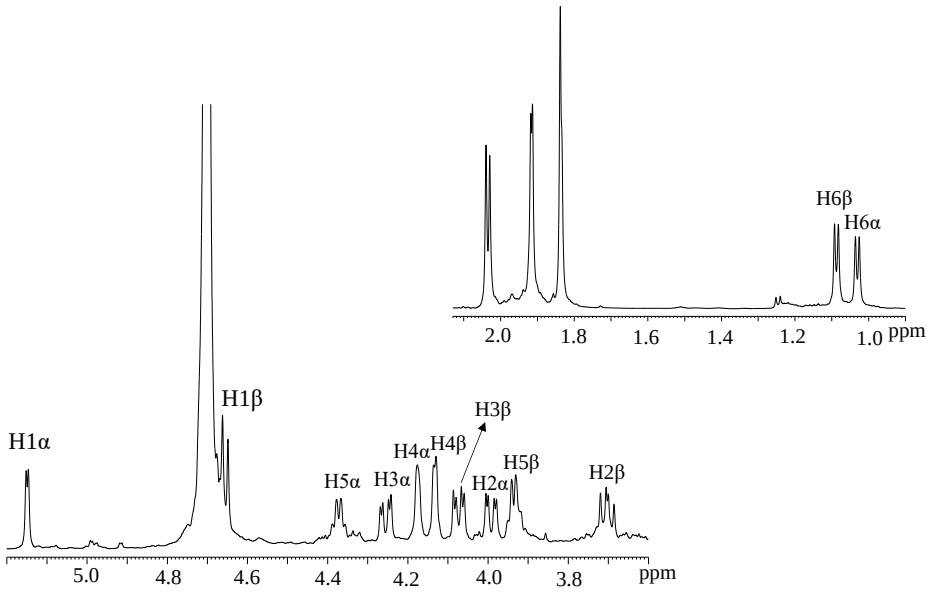

Figure 4.14. Zooms of the ^{1}H NMR spectrum of the isolated monosaccharide. The spectrum was performed at 298 K and recorded in D_2O at 600 MHz.

The COSY spectrum showed for the α-anomer the correlation of its H-1 at δ 5.14 ppm with the H-2 at δ 3.99 ppm, in turn correlated to a carbon linked to a nitrogen at 47.6 ppm. Also, the H-3 and H-4 were correlated to carbons linked to nitrogen at δ 47.6 and 51.3 ppm, respectively. The *N*-acetyl substitution of these three positions was confirmed by the long scalar range connectivity between H-2, H-3 and H-4 with carbonyl signals at δ 174.6, 174.4 and 175.4 ppm, respectively. Furthermore, the TOCSY spectrum revealed the correlation between H-5 and methyl protons at 1.03 ppm, the last correlated to a carbon at δ 15.7 ppm. The same procedure allowed to assign all the resonances for the β-anomer (Table 4.5). The small values of the $^{3}J_{H,H}$ coupling constants (Table 4.5) and NOE contacts between H-3 and H-5 found in the ROESY spectrum suggested the occurrence of a *galacto* configuration.

All these data allowed to establish the structure of the isolated shewanosamine, as reported in the following scheme:

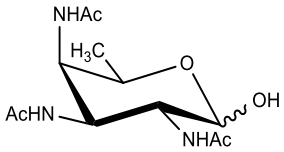

Scheme 1. Structure of D-shewanosamine (D-ShewN).

The skeleton of the ShewN, which contains three carbons substituted with nitrogens, was also confirmed by its EI mass spectrum as alditol acetate (Figure 4.15). The mass spectrum revealed an extensive secondary fragmentation, as reported in the scheme inserted in figure below.

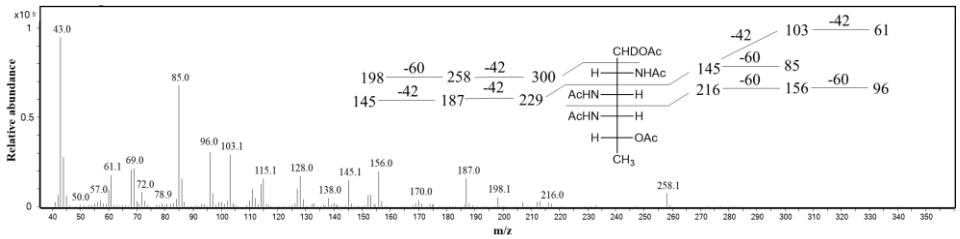

Figure 4.15 EI mass spectrum of the ShewN as acetylated alditol and its fragmentation scheme.

4.2.5 Ice recrystallization inhibition assay

To evaluate a possible cryoprotective effect of the CPS isolated from *S. vesiculosa* HM13 Rif^r, grown at 18°C, ice recrystalization inhibition (IRI) activity was measured in collaboration with Prof. Matthew Gibson's research group, at University of Warwick.

As reported in Figure 4.16, this polysaccharide showed a very weak ice recrystallization inhibition activity at a concentration of 10 mg/mL, which rapidly decreases as the concentration of the sample is lowered.

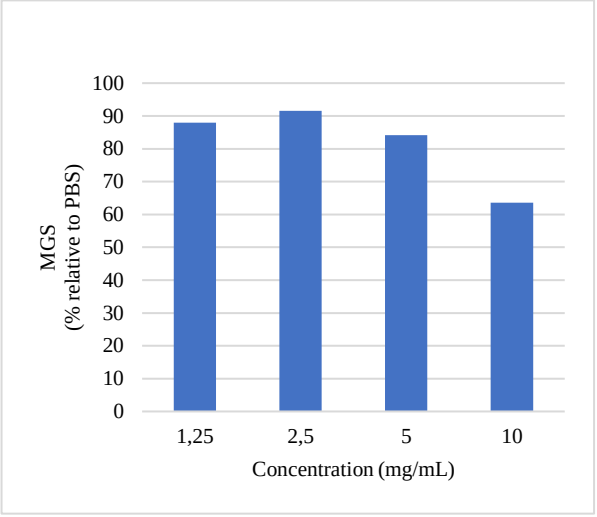

Figure 4.16. Ice Recrystalization Inhibition (IRI) activity of the CPS isolated from *S. vesiculosa* HM13 Rif^r, grown at 18 °C, measured as mean grain size (MGS) of the ice crystals. The MGS is expressed as a percentage of PBS buffer. High MGS value indicates decreased IRI activity.

4.2.6 Physicochemical properties of the CPS

All the following physicochemical measurements were performed in collaboration with Prof. Luigi Paduano's group, at the University of Naples Federico II. In particular, all the physicochemical characteristics of the CPS were determined by using Static and Dynamic Light Scattering.

4.2.6.1 Molecular mass

From Dynamic Light Scattering measurements, performed with a 5.0 mg/mL water solution of the CPS, the hydrodynamic radius of the polysaccharide was found to be 5.2 ± 0.2 nm (Figure 4.17).

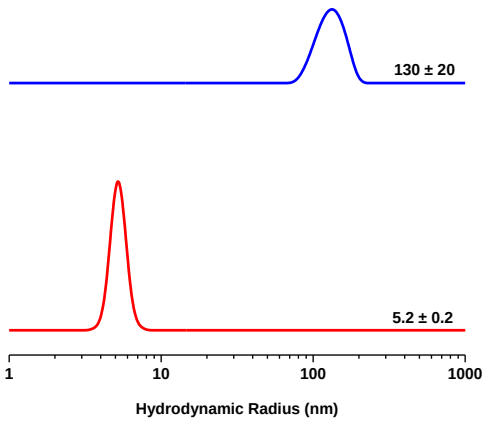

Figure 4.17 Hydrodynamic radius distribution measured by DLS of the CPS from *S. vesiculosa* HM13 cells, grown at 18 °C.

Then by Static Light Scattering (SLS) of the single molecules in non-aggregated state was determined the molecular weight of the polymer. However, it is important to note that, in solution, the single chains tend to aggregate, forming a large aggregate of approximately 130 nm radius after 4 weeks. The mass-average molecular weight for CPS was found to be 40000 ± 3000 g/mol. In this condition

it was also performed zeta potential measurement and for the aqueous solution of the CPS and the value of zeta potential was found to be -11.2 ± 0.9 mV.

4.2.6.2 Adhesion assays of the CPS

To determine the adhesion ability of the CPS to a solution of extremely monodisperse polystyrene nanoparticles, with a radius of 50 nm, was added an increasing volume of a stock solution of polysaccharide and after each addition a DLS measurement was performed.

The calculated hydrodynamic radius (Figure 4.18) revealed that the size of polystyrene nanoparticles increases with the concentration of CPS, suggesting the formation of a CPS corona around the nanoparticles. The thickness of this corona can be estimated to be about 10 nm and, considering the size of the polysaccharide, the CPS corona is formed by several layers.

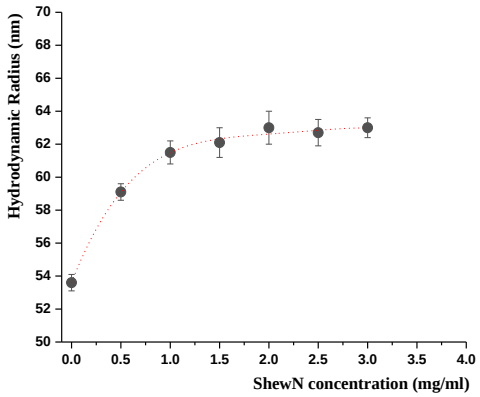

Figure 4.18 Increasing of the hydrodynamic radius of polystyrene nanoparticles upon CPS adhesion.

The CPS adhesion was also evaluated on mimic vesicles of bacteria (POPE/POPG 7/3 mol/mol) in absence and in presence of the LOS at 20% in mole, in order to shed light on the LPS role in ruling the interaction to the membrane. The polymer was added to a solution with a concentration of 0.2 mM

of mimic vesicles. Also, in this case was noted a decrease of the diffusion coefficient attributable to the adhesion of the polymer to the surface of the vesicles. It is important to note that after 24h the value of the hydrodynamic radius of the vesicle increased indicating that the adhesion of the polymer continues over time (Figure 4.19).

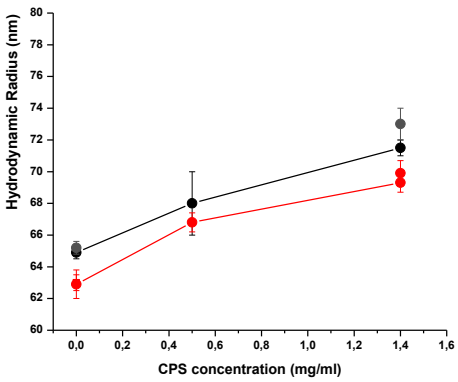

Figure 4.19 Hydrodynamic vesicle radii at increasing CPS concentration, POPE/POPG 7/3 mol/mol(black), (red)POPE/POPG 7/3 mol/mol - LPS 20% mol. In transparency the values after 24h

4.2.7 Discussion

Shewanella vesiculosa HM13 Rif^{r} grown at 18 °C is able to produce a capsular polysaccharide, which was isolated from both cells and vesicles. All the analyses performed have revealed that the two polysaccharides share the same structure. In particular, the repeating unit is a branched pentasaccharide with a high degree of acetylation. This feature is also due to the presence of a residue, here named shewanosamine, not previously found in nature.

To evaluate a possible involvement of this CPS in cold survival by conferring cryoprotection to the cells, Ice Recrystallization Inhibition (IRI) assays were performed. The polysaccharide was found to have very weak IRI activity at the highest concentration tested, and this activity is rapidly depleted as the concentration of the sample is lowered. These results suggested that the CPS should be considered to exhibit no IRI activity (Caroline I. Biggs et al. 2019).

In addition, the adhesion assays of CPS on polystyrene nanoparticles and bacterial mimic vesicles by DLS measurement together with zeta potential measurements indicated the ability of the polysaccharide to form a corona around the vesicles, and that the driving force of this process is suggested to be hydrophobic instead of electrostatic, since the CPS and the vesicles possess both a negative charge.

Chapter V: *Shewanella vesiculosa* HM13 Rif^r *wzx*-mutant grown at 18 °C

5.1 LPS isolation and characterization from cells and from EMVs

5.1.1 Isolation and chemical analyses of the LOS

The LPS from the lyophilized cells and EMVs of *S. vesiculosa* Rif^r *wzx*-mutant (*hm3343*::pKNOCK) (Kamasaka K. et al., 2020) grown at 18 °C, were isolated by the phenol/chloroform/light petroleum (PCP) extraction (Galanos C. et al., 1969). The LPSs were obtained as precipitates with a yield of 2.1% and 24%, respectively. Then the LPS samples were analysed by 14 % DOC-PAGE. After silver nitrate staining the gel confirmed, for both samples, the rough nature of the LPS (Figure 5.1) as already observed for the wild-type strain (see paragraph 4.1.1).

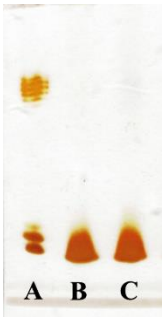

Figure 5.1 Analysis of the PCP precipitates from *wzx*-mutant cells (Lane **B**) and EMVs (Lane **C**) by 14% DOC-PAGE. The LOSs were compared with the smooth-LPS from *E. coli* O127: B8 (Lane **A**).

The GC-MS analysis of the monosaccharide as AMGs revealed the presence of the same sugars observed for the cells of *S. vesiculosa* HM13 grown at 4 °C (see paragraph 3.1) and for the cells and EMVs of *S. vesiculosa* HM13 Rif^r grown ate 18 °C (see paragraph 4.1.1). In particular, the analysis confirmed the presence of D-glucose (D-Glc), 2-amino-2-deoxy-D-glucose (D-GlcN), and both D,D- and L-*glycero*-D-*manno*-heptoses (D,D-Hep and L,D-Hep, respectively) (Table 5.1).

The fatty acids analysis for both *wzx*-cells and *wzx*-EMVs also confirmed the presence of the C12:0(3OH) and the C13:0(3OH) as the major 3-hydroxylated components (Figures 5.2, and Table 5.2). Non-hydroxylated fatty acid residues were found to be C12:0, C13:0, C14:0, and C15:0.

Table 5.1 Molar ratio percentage of monosaccharide residues of the LOSs from *S. vesiculosa* HM13 Rif^r *wzx*- mutant cells and EMVs.

	Glc	**GlcN**	**D,D-Hep**	**L,D-Hep**
Cells	47.7%	1.3%	17.8%	33.0%
EMVs	49.4%	0.9%	18.9%	30.8%

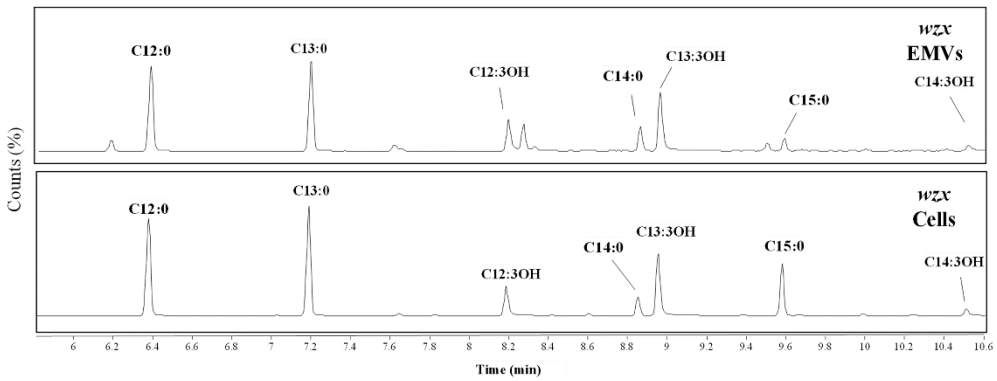

Figure 5.2. GC-MS chromatograms of the FAMEs of the LOS samples from *S. vesiculosa* HM13 Rif^r *wzx*-mutant cells and EMVs.

Table 5.2 Molar ratio percentage of fatty acids of the LOSs from *S. vesiculosa* HM13 Rif^r *wzx*- mutant cells and EMVs.

	C12:0	**C13:0**	**C12:3OH**	**C14:0**	**C13:3OH**	**C15:0**	**C14:3OH**
***wzx* Cells**	27.51%	28.70%	10.57%	6.96%	20.33%	3.46%	2.45%
***wzx* EMVs**	26.56 %	28.80%	8.41%	4.71%	17.09%	2.27%	2.16%

5.1.2 Mass spectrometric analysis of the *O*-deacylated LOS

The LOS samples from both *wzx*-cells and *wzx*-EMVs were subjected to an alkaline degradation with hydrazine, in order to obtain the de-*O*-acylated LOSs (LOS-OHs). Then, the products were analyzed by negative ions MALDI-TOF in reflector mode (Figure 5.3). In both mass spectra are visible several cluster of ions. At low molecular masses, signals attributable to core and lipid A fragments were detected. The intense signals at *m/z* 1119.79, in both spectra, were assigned to a lipid A fragment with the following composition $GlcN_2P_2[C13:(3OH)]_2(C13:0)$ (Calculated $[M-H]^-$ = 1119.62 Da). Less intense are the signals at *m/z* 923.59, also attributed to a lipid A fragment ion without a C13:0 group. The clusters of signals attributed to the core fragments showed the same pattern of species found in those of the LOS-OH from cells at 4 °C (see paragraph 3.2) and the LOSs from both wild-type cells and EMVs at18 °C (see paragraph 4.1.2).

Finally, at high molecular masses in both spectra there is a signal at *m/z* 2481.28, which was assigned the entire LOS-OH molecule with following composition: $Hex_3Hep_3Kdo8NGlcN_2P_3[C13:0(3OH)]_2(C13:0)$ (calculated $[M-H]^-$ = 2481.00 Da) (data not showed).

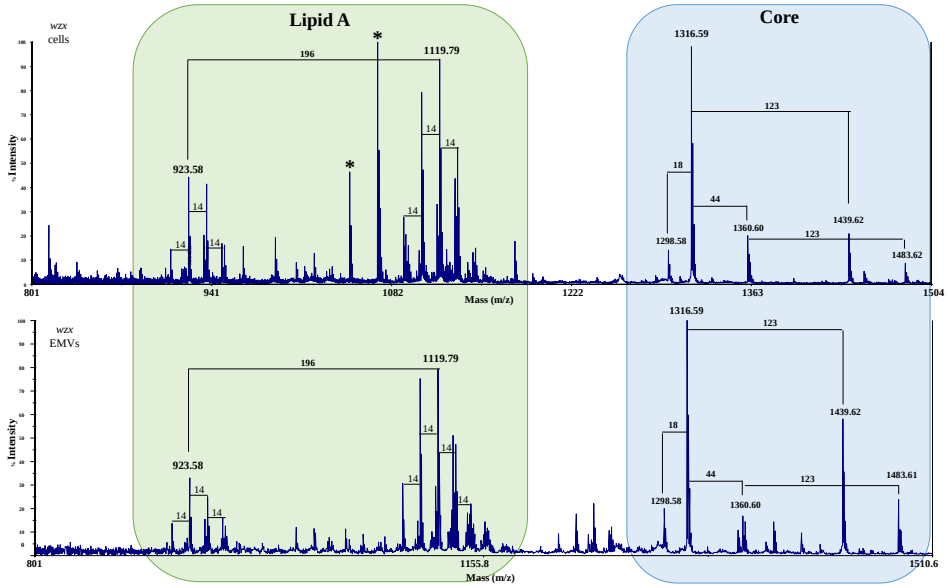

Figure 5.3. Negative ions MALDI-TOF mass spectra of the LOS-OHs from the *S. vesiculosa* HM13Rif^{r} *wzx*-mutant cells and EMVs. The notation '*'indicate contaminats.

5.1.3 NMR analysis of the fully deacylated LOS

To obtain the oligosaccharide structure of the isolated LOSs, both LOS-OH molecules were de-*N*-acylated by strong alkaline hydrolysis. The obtained OSs were analysed by 1D and 2D NMR spectroscopy, that allowed to assign all the ^{1}H and ^{13}C resonances.

In both ^{1}H NMR spectra (Figure 5.4) are visible the eight anomeric signals and the two diastereotopic protons of the Kdo8N, as confirmed by $^{1}H,^{13}C$ DEPT-HSQC experiments (Figure 5.5 and 5.6), already found for wild-type cells and EMVs at 18 °C (see paragraph 4.1.3). Based on the comparison of all the NMR spectra performed (^{1}H, ^{1}H DQF-COSY, ^{1}H, ^{1}H TOCSY, ^{1}H, ^{1}H ROESY, ^{1}H, ^{13}C DEPT-HSQC, ^{1}H, ^{13}C HMBC) the isolated LOSs from both cells and EMVs of *S. vesiculosa* HM13 Rif^{r} *wzx*-mutant possess the same oligosaccharide moiety already found for wild-type cells and EMVs at 18 °C (see paragraph 4.1.3).

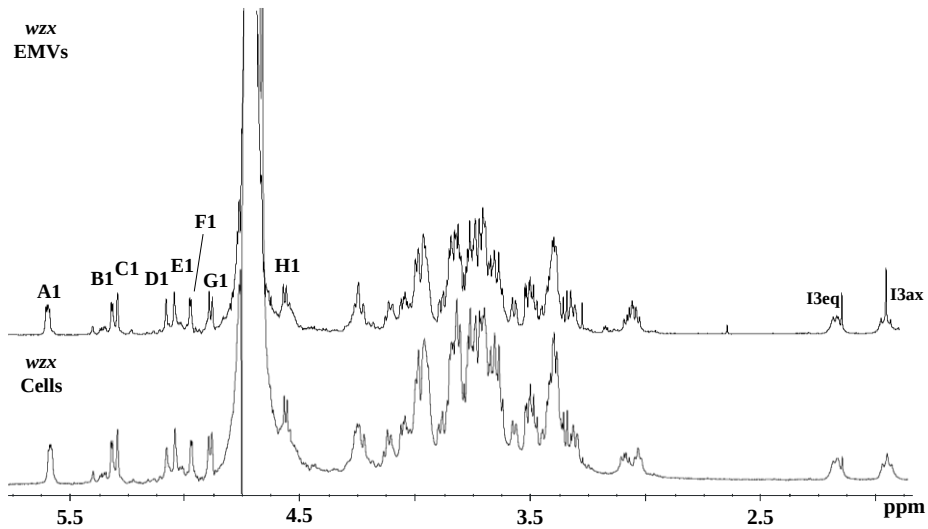

Figure 5.4.^{1}H NMR spectrum of the OSs from the cells and EMVs of *S. vesiculosa* sp. HM13 Rif^{r} *wzx*-mutant, grown at 18 °C. The spectrum was performed at 298 K and recorded in D_2O at 600 MHz.

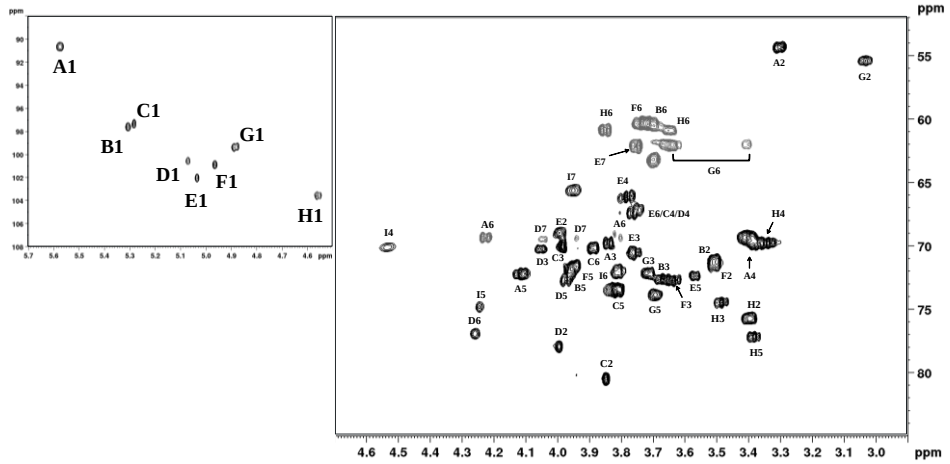

Figure 5.5 Anomeric and carbinolic regions of the ^{1}H, ^{13}C DEPT-HSQC spectrum of the OS from the EMVs of *S. vesiculosa* HM13 Rif^{r} *wzx*-mutant.

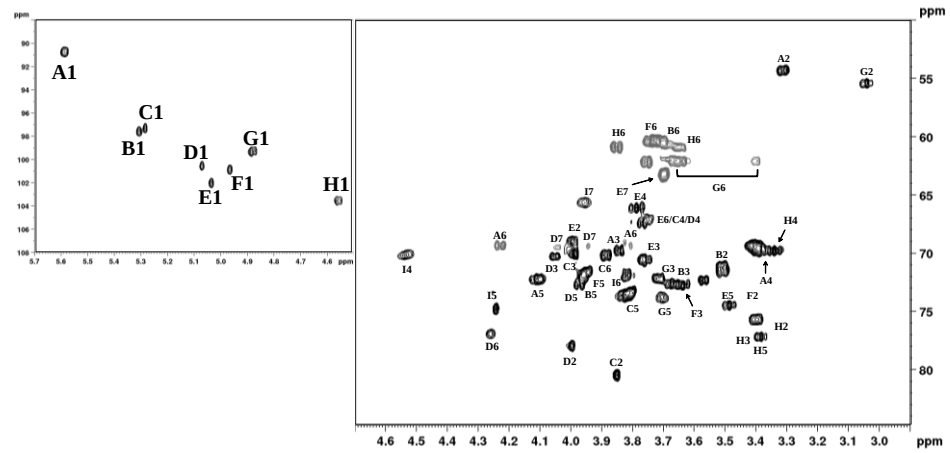

Figure 5.6. Anomeric and carbinolic regions of the ^{1}H, ^{13}C DEPT-HSQC spectrum of the OS from the cells of *S. vesiculosa* HM13 Rif^{r} *wzx*-mutant.

5.1.4 Discussion

In this study, the structure of the LOSs isolated from cells and EMVs of a *S. vesiculosa* HM13 mutant was determined. The mutant defects in a gene (HM3343) encoding a protein with homology to Wzx. This protein is a flippase involved in the translocation of the repeating units of the LPS or the CPS, across the inner membrane from the cytoplasmic to periplasmic side. The disruption of HM3343 gene resulted in the disappearance of P49 from EMVs and in the decrease of cellular P49 level (Kamasaka K. et al., 2020). These results suggested that the protein encoding by this gene is necessary for the P49 association to EMVs after its translocation and also for the P49 tethering to the cells.

The cells and EMVs extraction confirmed the rough nature of the LPS (LOS). In addition, the chemical analysis, the MALDI-TOF and the NMR experiments suggested that the LOSs isolated from the cells and EMVs of this mutant and the wild-type are identical. Therefore, the HM3343 gene is not involved in the LPS biosynthesis of *S. vesiculosa* HM13.

5.2 CPS isolation and characterization from cells and vesicles

5.2.1 Extraction and purification of CPS

The dialyzed phenolic phases obtained from the extraction of the *S. vesiculosa* Rif^r *wzx*-mutant cells and EMVs, after LOSs precipitation (see paragraph 5.1.1), were analyzed by 14% DOC-PAGE. Alcian blue and silver nitrate staining of the gel indicated for both samples the presence of bands at low molecular masses of the LOS and at high molecular weight of the CPS. However, comparing on the same 14% DOC-PAGE the dialyzed phenolic phases from the cells and EMVs of the wild-type and the *wzx*-mutant was possible to note a smaller amount of CPSs for samples of the *wzx*-mutant (Figure 5.7).

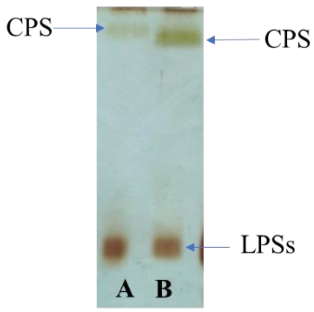

Figure 5.7. 14% DOC-PAGE analysis of the dialyzed phenolic phase from wild-type EMVs (lane **B**) and *wzx*-mutant EMVs (lane **A**), both produced at 18 °C.

In order to isolate the CPS, the dialyzed phenolic phases were hydrolysed under mild acidic conditions. After centrifugation, the supernatant mixtures were fractionated on a Biogel P-10 column, using water as eluent. The ^{1}H NMR analysis of all the fractions revealed that the first one, eluted in the void volume, contains the pure capsular polysaccharide. The GC-MS analysis of the monosaccharide confirmed the composition observed for those isolated from wild-type cells and EMVs (see paragraph 4.2.1).

Finally, the amount of CPS present in both phenolic phases from the wild-type and *wzx*-mutant (Table 5.3), by measuring the quantity of rhamnose, was

evaluated. This experiment confirmed that the *wzx*-mutant secreted a minor amount of CPS with respect to the wild-type.

Table 5.3 Amount of rhamnose in each phenolic phases obtained from the calibration method of internal standard.

	0.5 mg Cells Rif^r	**0.5 mg *wzx*- Cells**	**0.5 mg EMVs Rif^r**	**0.5 mg *wzx*-EMVs**
Rha µg	6,41	5,02	26,49	18,25

5.2.2 NMR analysis of purified CPS

The ^{1}H NMR spectra (Figure 5.8) of both CPSs isolated suggested that they share the same structure observed for those isolated from wild-type cells and EMVs (see paragraph 4.2.2).

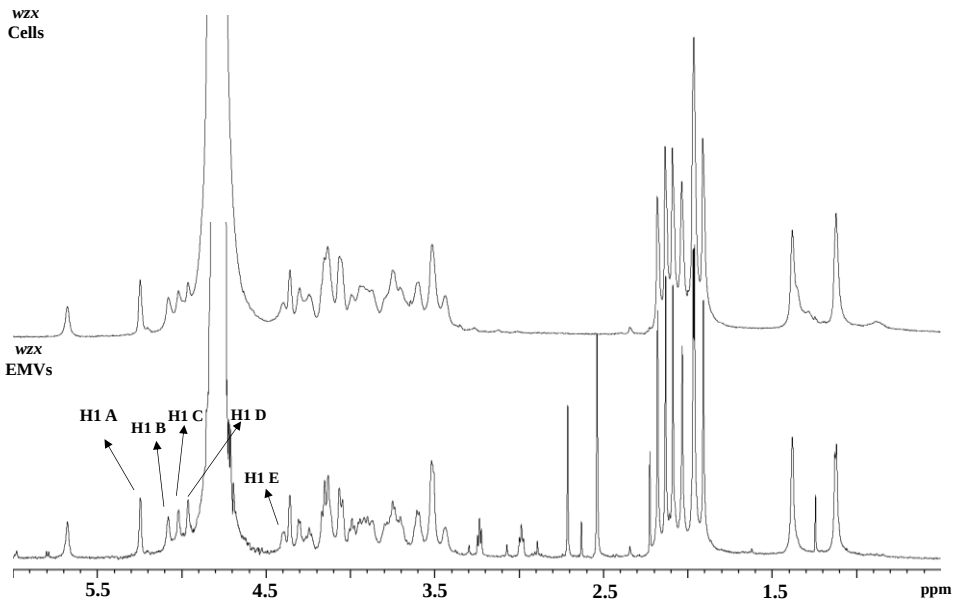

Figure 5.8 ^{1}H NMR spectra of the CPSs isolated from the cells and the EMVs of *S. vesiculosa* HM13 Rif^r *wzx*-mutant, grown at 18°C. The spectra are recorded at pD 2 and 308K at 600 MHz.

5.2.3 Discussion

In conclusion, *S. vesiculosa* HM13 Rif^r *wzx*-mutant secretes a capsular polysaccharide, which was isolated from both cells and EMVs. The experiments suggested that these two CPSs share the same structure with those already observed for wild-type cells and EMVs. The only difference that has been found is the lower amount of CPS for both cells and vesicles compared to those of the wild-type. This result could suggest that the protein encoding by the HM3343 gene is involved in the membrane translocation of the repeating units of this polysaccharide, which in turn is implicated in the P49 association to cells and vesicles.

Conclusion

The *Shewanella vesiculosa* HM13 is a psychrotolerant bacterium, isolated from the intestine of a horse mackerel (*Trachurus japonicus*) (HM13 Horse Mackerel strain no. 13) (Chen C. et al., 2020). Chen and colleagues have selected *S. vesiculosa* HM13 as a novel cold-adapted bacterium for secretory production of foreign proteins at low temperature (Chen C. et al., 2020). This strain is able to secrete abundant amount of EMVs which contain a single major cargo protein (named P49) with an unknown function. This protein was found also in the outer membrane and in the culture supernatant. In these chapters were isolated and characterized the LOS and capsular polysaccharide from the cells and the EMVs of this bacterium.

To identify possible variations in the LPS structure produced by *S. vesiculosa* HM13 due to temperature change, the bacterium was grown at two different temperatures (4 ° C and 18 °C). From the PCP extraction of the cells at 4 °C and 18 °C, the LPSs were isolated with a yield of 2.4% and 3%, respectively. The lower amount of LPSs isolated at 4 °C could be attributable to the fact that 4 °C is not the optimal growth condition for this bacterium. The DOC-PAGE analysis revealed that the isolated LPSs are Rough (LOS) at both the temperatures investigated. Sugar, MALDI-TOF, and NMR analysis have demonstrated that the LOSs share the same sugar moiety. Also, the GC-MS analysis of fatty acids and MALDI-TOF experiments suggested that no changes in the lipid A composition were observed with the temperature. It is important to note that the isolated LOSs share some structural features with other LPS from *Shewanella* species, such as the rough nature of the LPS and the presence of both Kdo8N and D,D-heptose (Vinogradov, E. et al., 2008, Vinogradov E. et al., 2003, Vinogradov, E. et al., 2004; Moule A. L. et al., 2004).

The rough nature of the LPS is common among the few LPS structures from cold-adapted bacteria up to now analysed (Casillo A. et al. 2019). This feature could enhance the outer membrane flexibility and stability at low temperatures (Corsaro M. M. et al., 2017). In addition, lipid A structure displayed another structural element

associated to the survival at low temperature, the presence of fatty acids with short acyl chains (Casillo A. et al., 2019). In fact, it was observed the occurrence of fatty acids ranging from 10 to maximum 15 carbon atoms in length. This feature allows to maintain the correct fluidity of the membrane leading to a good solute exchange rate. However, contrary to the expectations, a significant increase of amount of C15:0 at 4 °C with respect to that observed at 18 °C was found. This finding could be attributable to a LPS sample contaminated by membrane phospholipids, as suggested by the presence of both glycerol in the fatty acid chromatogram and by the fact that the C15:0 as one of major fatty acids in the phospholipid extracts of *S. vesiculosa* HM13 cells (Chen C. et al., 2020).

Unfortunately, due to the low amount of vesicles biomass secreted at 4 °C was not possible to obtain the structure of the LOS from the EMVs at this temperature. However, the analysis performed on the LOS isolated from the vesicles at 18 °C revealed the same structure for the cells and vesicles. This result is in agreement with the budding biogenesis of the EMVs from the outer membrane (Kamasaka K. et al., 2020).

In this study it was also demonstrated that *S. vesiculosa* HM13 produces a capsular polysaccharide, which was isolated from both cells and EMVs. This capsule is composed of a branched pentasaccharide repeating unit with a high hydrophobic character and contains a monosaccharide (ShewN) not previously reported in the literature. To confirm the structural hypothesis the novel monosaccharide was isolate and characterized by mass spectrometry and NMR spectroscopy.

It is important to underline that the presence of a high number *N*-acetyl groups, that give hydrophobicity to this polysaccharide, is a feature already found in other capsular polysaccharides from Gram-negative bacteria (Fiebig T. et al., 2014; Micoli F. et al., 2018; Wang X. et al., 2004).

To evaluate a possible involvement of the CPS in cold-survival by conferring cryoprotection to the cells Ice Recrystallization Inhibition (IRI) assays were performed. The results have demonstrated that the CPS possesses a very weak IRI

activity at highest concentration tested (Biggs C. I. et al., 2019). In addition, adhesion assays of CPS on polystyrene nanoparticles and bacterial mimic vesicles by DLS measurement together with zeta potential measurements showed its ability to aggregate, forming a corona around the particles with a driving force attributable to hydrophobic interactions. This result could suggest a key role of this hydrophobic polysaccharide in the aggregate formation and attachment to surfaces by biofilms formation. For this property, the polysaccharide could be a promising molecule for the development of adhesive materials from biological resources to avoid environmental and health hazardous chemicals as well as dependence on petroleum resources. In fact, components of the majority of commercial adhesives are based on non-renewable and depleting petrochemical resources.

Finally, the surface components of the cells and EMVs of a *S. vesiculosa* HM13 mutant, that defects in the gene HM3343, were isolated and characterized to shed light into the mechanism of cargo transport on EMVs of this bacterium. HM3343 gene encodes a protein with homology to a flippase (Wzx) involved in membrane translocation of the repeating units constituting the O-chain of a Smooth-LPS or CPS. Kamasaka and colleagues have demonstrated that the disruption of HM3343 gene leads to no P49 loading to the EMVs and to its release into the extracellular medium (Kamasaka K. et al., 2020). All the analysis performed have suggested that the LOSs isolated from cells and EMVs of the *wzx*-mutant have the same structure already reported for the wild-type (Di Guida R. et al., 2020). Therefore, the HM3343 is not involved in the LOS biosynthesis. However, it has been found that the mutant secreted a lower amount of CPS of compared to the wild-type. This result could suggest that the protein encoding by the HM3343 gene is involved in the membrane translocation of the repeating units of this polysaccharide, which in turn is implicated in the P49 association to cells and vesicles.

The CPS still synthesized in the HM3343 mutant, could be due to the occurrence of an HM3343-independent CPS-synthesizing pathway in the bacterium. In fact, our co-workers observed the presence of a protein, named HM3315, that shows weak

sequence similarity to HM3343 and therefore could be involved in a HM3343-independent pathway.

Chapter VI: *Pseudoalteromonas nigrifaciens* Sq02

Pseudoalteromonas species are Gram-negative bacteria originally characterized as members of *Alteromonas* genus. However, in the 1995 G. Gauthier and co-workers proposed for these species a new genus named *Pseudoalteromonas* (from the Greek pseudo, that means "false or similar"), also belonging to the class of *Gammaproteobacteria.* This genus contains bacteria exclusively isolated from deep-sea and sea-water, sediments, marine invertebrates, fish, and algae from marine environments (Skovhus T. L. et al., 2007). Their presence in a wide range of habitats suggests that the adaptive and survival strategies of *Pseudoalteromonas* species are efficient and of great interest for both basic and applied research. In addition, this genus has attracted considerable interest due to the ability of some *Pseudoalteromonas* species to produce a variety of compounds with numerous pharmaceutical relevant activities, such as antimicrobial, antifouling, and algicidal (Holmström C. and Kjelleberg S., 1999). Among these, it was demonstrated that EPSs production improve the survival chances for other organisms in marine habitats and can serve as anti-bacterial components (Gauthier M. J., 1989), control bacterial attachment (Fletcher, M. and Floodgate, G. D., 1973; Wrangstadh M. et al., 1986) and can be beneficial for the survival of both the host and other organisms that live neighbourhood of the producer strain (Szewzyk, U. et al., 1991).

EPSs isolated from some cold-adapted *Pseudoalteromonas* species, such as *P. arctica* KOPRI 21653, *P. elyakovii* Arcpo 15, *Pseudoalteromonas* sp. MER144, and *Pseudoalteromonas* spp. CAM025, have been found to display cryoprotection ability (Parrilli E. et al., 2021). In addition, EPSs from marine bacteria also play a key role in the attachment to surfaces, through the biofilms formation that can be influenced by the polysaccharide structure. The EPSs form a matrix together with secreted proteins, which are directly involved in hydrophobic interactions. Recently, it was also found that the acetyl-rich EPS of *Pseudoalteromonas* sp. SM9913 (Qin G. et al.,

2007) showed a high ability to adhere to suspended kaolin clay particles (Li W. W. et al., 2008).

Pseudoalteromonas nigrifaciens Sq02 is a psychrotrophic Gram-negative bacterium isolated from the intestine of a *Seriola quinqueradiata* (yellowtail). This strain possesses a high-protein-secretion capacity at low temperatures (unpublished data), secreting a large quantity of a protein named P320 into the culture supernatant. The deletion of the P320 gene revealed its functions as adhesion factor in the biofilm formation. In this chapter, the LOS and the capsular polysaccharide produced by this bacterium were isolated and fully characterized by chemical analyses, mass spectrometry and NMR spectroscopy. Furthermore, the biological activities of these two isolated carbohydrate-based molecules were evaluated.

6.1 LPS isolation and characterization

6.1.1 Isolation and chemical analyses of the LOS

The LPS was extracted from dried cells of a spontaneous rifampicin-resistant mutant (Rif^r) of *Pseudoalteromonas nigrifaciens* Sq02, grown at 18°C, by the PCP procedure (Galanos C. et al., 1969). Since no precipitation was observed, the phenol extract was dialyzed against water, freeze-dried, and lyophilized. The nature of the LPS was identified by 14% DOC-PAGE electrophoresis visualized after silver staining. This experiment showed (Lane B, Figure 6.1) the presence of bands only at low molecular masses that suggest the rough nature of LPS (LOS).

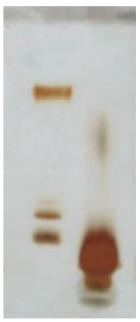

A B

Figure 6.1 14% DOC-PAGE analysis of the PCP extract. The gel, stained with silver nitrate, displays in lane **A** a smooth-LPS from *E. coli* O127: B8, used as a standard; lane **B** the dialyzed phenolic phase (LOS) of the PCP extraction.

The glycosyl composition of the LOS was obtained through GC-MS analysis that revealed the presence of D-galactose (D-Gal), D-glucosamine (D-GlcN), D-mannosamine (D-ManN), and a L-*glycero*-D-*manno*-heptose (L,D-Hep). The sugar analysis performed after HF treatment revealed the additional presence of a 3-deoxy-D-*manno*-oct-2-ulosonic acid (Kdo), thus suggesting its phosphorylation (Corsaro M. M. et al., 2008).

The GC-MS analysis of the fatty acids as methyl esters revealed mainly the presence of 3-hydroxydodecanoic C12:0(3-OH) and dodecanoic (C12:0). 3-hydroxydecanoic C10:0(3-OH), 3-hydroxyundecanoic C11:0(3-OH), tridecenoic (C13:1), 3-hydroxytridecanoic C13:0(3-OH), tetradecenoic (C14:1), tetradecanoic (C14:0), and pentadecanoic acids (C15:0) were detected in minor amount. In addition, the GC-MS analysis on the sugars as partially methylated alditol acetates (PMAAs) revealed the following points of attachment: 3-substituted Hex, 4-substituted Hep, terminal non reducing HexN, and a 6-substituted HexN. These results remind those reported for the LOS of *Pseudoalteromonas haloplanktis* TAC 125, a cold-adapted bacterium isolated from the Antarctic Ocean (Corsaro M. M. et al., 2001).

6.1.2 Mass spectrometric analysis of the LOS

The whole LOS molecule was analysed by negative ions MALDI-TOF in reflector mode. At higher *m/z* value, the mass spectrum showed the presence of a signal at *m/z* 2330.84, that was attributed to a penta-acylated di-phosphorylated LOS molecule with the following composition: $HexHexNAcHepKdoPGlcN_2P_2[C12:0(3OH)]_4(C12:0)$ (calculated $[M-H]^-$ = 2331.12 Da) (Figure 8.2). The spectrum also displayed a signal at *m/z* 2132.71, attributable to a tetra-acylated di-phosphorylated LOS species (calculated $[M-H]^-$ = 2132.96 Da), differing from the previous one for the lack of a C12:0(3OH) unit (Figure 8.2). Both species were also observed in the ESI-MS spectrum of the LOS from *Pseudoalteromonas haloplanktis* TAC 125, even if in this case the tetra-acylated species was the main one observed (Corsaro M. M. et al., 2001).
At lower molecular masses, signals attributable to lipid A and core fragments were also detected. These latter are due to an in-source breaking of the glycosidic bond between the Kdo and the lipid A. The signals at *m/z* 1473.72 and 1275.58 (calculated $[M-H]^-$ = 1473.90 and 1275.74 Da, respectively) were both assigned to lipid A fragments with a composition that differs of a C12:0(3OH) (Figure

6.2). These two fragments were also observed for the lipid A of *P. haloplanktis* TAC 125 (Corsaro M. M. et al., 2002). Moreover, the signals at *m/z* 856.12 and 812.13 were attributed to the oligosaccharide core, which differs of 44 Da due to loss of a CO_2 molecule from the Kdo residue (calculated $[M-H]^-$ = 856.21 and 812.22 Da, respectively).

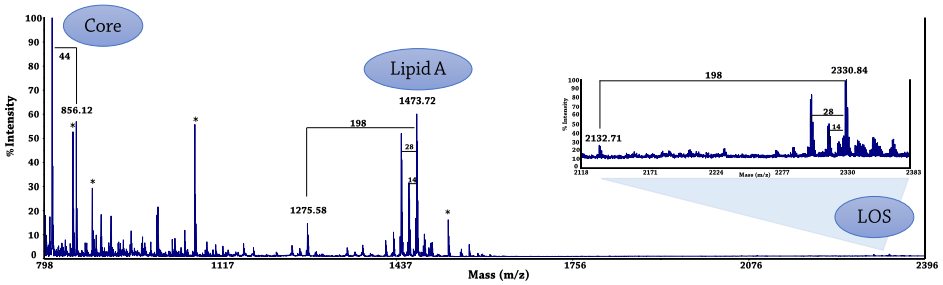

Figure 6.2 Negative ions MALDI-TOF mass spectrum recorded in reflector mode of the LOS from *P. nigrifaciens* Sq02-Rif^r. Mass range 798-2396 m/z. The notation '14 Da' and '28 Da' indicate differences of one or two units of CH_2 in the fatty acid chains, respectively. '198 Da' and '44 Da' indicates differences of a C12:0(3OH) or CO_2 molecule, respectively.

6.1.3 Mass spectrometric analysis of lipid A

The lipid A sample was obtained as a precipitate after treatment of the LOS with 1% acetic acid solution. The negative ions MALDI-TOF spectrum acquired in reflector mode of the lipid A sample revealed three main clusters of signals corresponding to glycoforms with different acyl substitutions (Figure 6.3). The signals at *m/z* 1473.29 and 1275.21 correspond to penta- and tetra-acylated di-phosphorylated glycoforms, respectively. The difference between the two signals corresponds to a C12:0(3OH) unit. To the ion at *m/z* 1473.29 the following composition was attributed: $GlcN_2P_2[C12:0(3\text{-}OH)]_4(C12:0)$ (Calculated $[M - H]^-$ = 1473.91 Da). Less intense is the cluster assigned to tri-acylated di-phosphorylated species at *m/z* 1093.12, carrying three C12:0(3-OH) chains (Calculated $[M - H]^-$ = 1093.57 Da). Within each cluster the mass differences of 14 and 28 u indicate the variations of fatty acid chain length.

These results suggested a high heterogeneity of the lipid A moiety, as already reported for other cold-adapted bacteria belonging to the genus *Pseudoalteromonas* (Corsaro M. M. et al., 2002; Krasikova I. N. et al., 2003; Volk A. S. et al., 2007; Carillo S. et al., 2011).

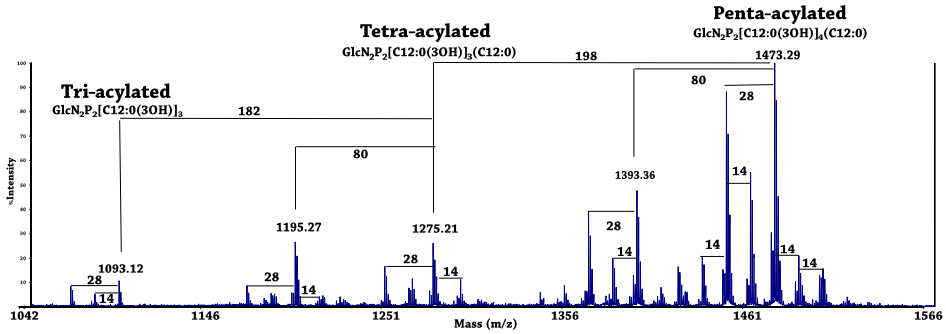

Figure 6.3 Negative ions MALDI-TOF mass spectrum recorded in reflector mode of the *P. nigrifaciens* Sq02-Rif^r lipid A. Mass range 1042-1566 *m/z*. The notation '14' and '28' u indicates differences of one or two units of CH_2 in the fatty acid chains, respectively. '198' and '80' u indicate differences of a C12:0(3OH) and a phosphate group, respectively.

An alkaline hydrolysis of the lipid A with NH_4OH allowed to identify the position of secondary fatty acids (Silipo A. et al., 2002), since this procedure leads to a lipid A devoid only of acyl and acyloxacyl esters. The negative ions MALDI-TOF spectrum of the product (Figure 6.4) showed the presence of a signal at *m/z* 1077.77 attributed to a tri-acylated di-phosphorylated lipid A species with two 12:0(3-OH) fatty acid residues linked as amides, one of which substituted at O-3 position by a secondary 12:0 acyl chain (Calculated $[M - H]^-$ = 1077.58 Da). This ion was already detected for the NH_4OH treated lipid A isolated from *Pseudoalteromonas haloplanktis* TAB 23 and *Pseudoalteromonas issachenkonii* KMM 3549^T (Carillo S. et al., 2011; Silipo A. et al., 2004).

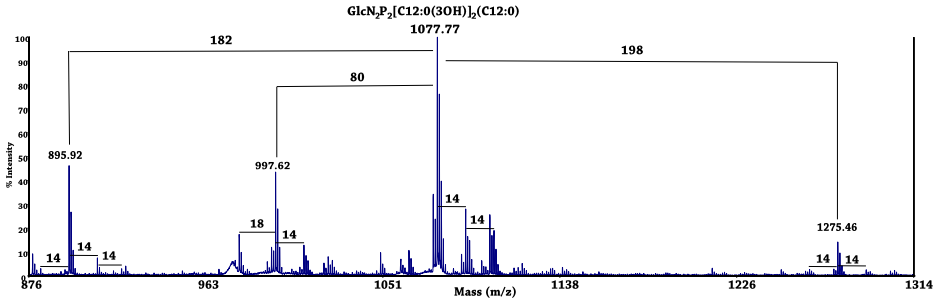

Figure 6.4. Negative ions MALDI-TOF mass spectrum recorded in reflector mode of the NH_4OH treated Lipid A from *P. nigrifaciens Sq02*-Rif^r. Mass range 876-1314 *m/z*. The notation '14' u indicates a difference of one unit of CH_2 in the fatty acid chains. '198' and '182' u indicate differences of a C12:0(3OH) and C12:0, respectively.

To establish which of the two GlcN units carries the C12:0 as secondary fatty acid a tandem mass experiment on the intact lipid A was performed. The negative ions MS/MS spectrum of the precursor ion at *m/z* 1473.29 showed the presence of several signals (Table 6.1). The last were attributable either to the loss of a phosphate and acyl substituents or to inter-residue fragmentations. At *m/z* 654.66 and 818.88 the Y_1 and B_1 fragments (Domon B. and Costello C. E. 1988), respectively, have suggested that the non-reducing GlcN unit bears the C12:0.

Table 6.1 Main signals observed in the negative ions MALDI-TOF MS/MS spectrum, acquired in reflector mode, of the precursor ion ($[M-H]^-$) at *m/z* 1473.29.

$[M-H]^-$ - C12:0(3-OH)-H_2O	1258.38
$[M-H]^-$ - C12:0(3-OH)-H_2O-P	1178.34
$[M-H]^-$ - [C12:0(3-OH)]$_2$-H_2O-P	980.01
B_1	818.88
Y_1	654.65

Therefore, all the above MS experiments indicated that the main species of the lipid A of the LOS isolated from *P. nigrifaciens* Sq02-Rif^r is a penta-acylated di-phosphorylated glycofrom, with the secondary fatty acid as acyloxamide on the non-reducing GlcN residue. This distribution is identical to that already found for the lipid A of the cold-adapted bacteria *Pseudoalteromonas haloplanktis*

TAB 23 and *Pseudoalteromonas nigrifaciens* IAM 13010T (Carillo et al., 2011; Volk A. S. et al., 2007).

6.1.4 NMR analysis of the fully deacylated LOS

To confirm the structure of the core-lipid A carbohydrate backbone the LOS was completely de-acylated. Therefore, a LOS sample was de-*O*-acylated by mild hydrazinolysis and then de-*N*-acylated by strong alkaline hydrolysis. After fractionation of the resulting mixture using a Sephadex column, the obtained oligosaccharide fraction was analysed by NMR experiments.

All the ^{1}H and ^{13}C chemical shifts (Table 6.2) of oligosaccharide were obtained by 2D NMR experiments (^{1}H-^{1}H COSY, ^{1}H-^{1}H TOCSY, ^{1}H-^{1}H ROESY, ^{1}H-^{13}C DEPT-HSQC, ^{1}H-^{13}C HMBC). The ^{1}H-^{13}C HSQC overlapped to the ^{1}H NMR spectrum (Figure 8.5), showed five anomeric signals and, at low chemical shifts, two signals diagnostic of the axial and equatorial H-3 diastereotopic protons of the Kdo (2.23 and 2.01 ppm, respectively). The anomeric configurations were deduced from the $^{1}J_{C1,H1}$ coupling constant values observed in the 2D F*2*-coupled HSQC spectrum. Residues **A**-**C** were identified as α-configured (185, 176 and 179 Hz, respectively), while **D** and **E** were β-configured (171 and 165 Hz, respectively).

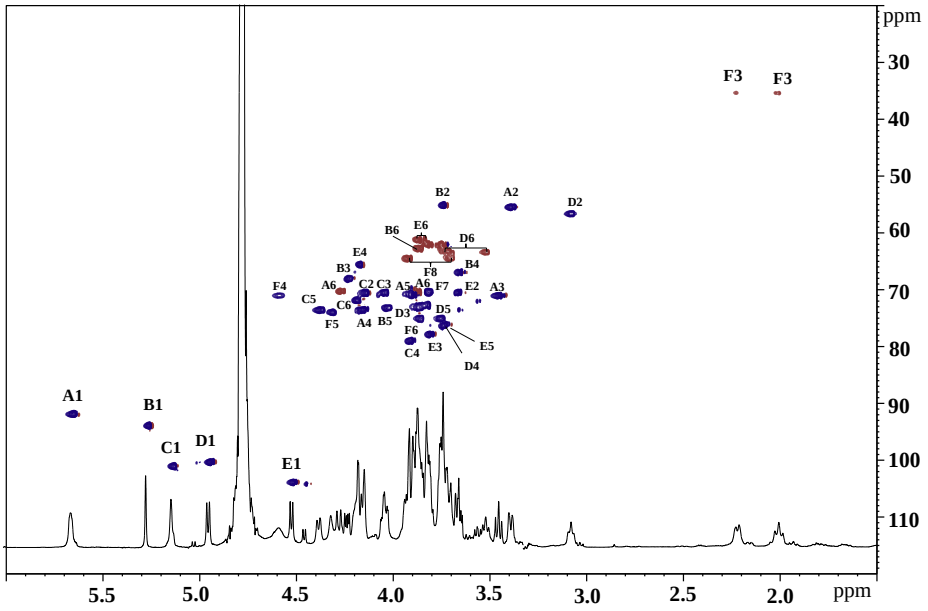

Figure 6.5 ^{1}H and $^{1}H,^{13}C$ DEPT-HSQC overlapped spectra of the OS from the LOS of *P. nigrifaciens* Sq02-Rif^{r}. The spectra were performed at 298 K and recorded in D_2O at 600 MHz.

Residues **A** and **D** were recognized as the two GlcN units of the lipid A backbone. In particular, the spin system **A** with H-1/C-1 at δ 5.65/91.9 ppm was identified as the proximal GlcN, based on the multiplicity of the anomeric proton signal due to its phosphorylation and on the chemical shift of its C-2 at δ 55.5 ppm, indicating a nitrogen-bearing carbon atom. Moreover, the glycosylation shift of its C-6 at δ 70.3 ppm suggested the C-6 linkage position of this residue. Spin system **D** with H-1/C-1 signals at δ 4.94/100.4 ppm was assigned to the distal GlcN, because of its C-2 chemical shift at δ 56.7 ppm and a long-range scalar correlation between 1-H of **D** and C-6 of **A** in the HMBC spectrum. In addition, the downfield shifts of both H-4 and C-4 are diagnostic of a phosphate group linked at O-4 (Holst O. et al., 1993). The β-anomeric configuration of this residue was confirmed by the *intra*-residue NOE correlations observed between H-1and both H-3 and H-5 in the ROESY spectrum.

Since in the TOCSY experiment the H-1 signal of residue **B** at δ 5.26 ppm showed a correlation only with H-2, **B** was recognized as *manno*-configured. In addition, the H-2 is correlated with a carbon linked to a nitrogen at δ 55.2 ppm. This residue was identified as a terminal mannosamine (t-ManN) since no glycosylation shift of its carbons was observed (Bock K. and Pedersen C. J., 1974).

The residue **C**, with H-1/C-1 at δ 5.12/101.1 ppm, was identified as a heptose due to the presence in the TOCSY experiment only of the correlation between H-1 and H-2, suggesting a *manno*-configuration. The downshifted of its C-4 chemical shift, compared to the reference value for an unsubstituted residue (Carillo S. et al., 2011), was found to be 4-substituted, (4-Hep).

The spin system **E** was attributed to a *galacto*-configured residue based on the correlation of its H-1 with only four protons in the TOCSY experiment. The β anomeric configuration of **E** was indicated by both *intra*-residue NOE correlations between H-1/H-3 and H-1/H-5, and the value of $^{1}J_{C,H}$ =165 Hz. Since the chemical shift of its C-3 is downshifted, with respect to that of an unsubstituted galactose residue (Bock K. and Pedersen C. J., 1983), **E** was assigned to a 3-substitued galactose (3-Gal).

Finally, the residue **F** was identified as a Kdo unit based on the two diastereotopic protons of the C-3 at δ 2.23 and 2.01 ppm. In the TOCSY spectrum these two protons are correlated to signals at δ 4.59 and 4.31 ppm, assigned to H-4 and H-5, respectively. The downfield shift of the C-5 signal compared to the value for the unsubstituted monosaccharide (Brade H. and Rietschel E.T., 1984), at δ 74.0 ppm suggested the glycosylation at the O-5 position. Furthermore, the H-4 and C-4 chemical shifts, downfield shifted at δ 4.59 and 71.7 ppm, respectively, are an index for the Kdo phosphorylation at this position (Müller-Loennies S. et al., 2002). The α-configuration of this residue was suggested by the difference (Δ= 0.22) between H-3_{ax} and H-3_{eq} chemical shifts (Agrawal P. K. et al., 1994).

Table 6.2 ^{1}H and ^{13}C NMR assignments of OS from the LOS of *Pseudoalteromonas nigrifaciens* Sq02-Rif^{r} grown at 18 °C. Spectra were recorded in D_2O at 298 K at 600 MHz, using acetone as internal standard (δ_H/δ_C 2.225/31.45 ppm).

Sugar residue	Chemical shift (ppm)							
	H1 **C1** $^{1}J_{C,H}$	**H2** **C2**	**H3** **C3**	**H4** **C4**	**H5** **C5**	**H6a,H6b** **C6**	**H7** **C7**	**H8a,H8b** **C8**
A α-6-D-GlcN*p*1P	5.65 91.9 185 Hz	3.39 55.5	3.45 71.1	4.16 73.6	3.89 70.9	4.26,387 70.3		
B α-t-D-Man*p*N	5.26 93.9 176 Hz	3.74 55.2	4.23 68.2	3.65 66.9	4.03 73.2	3.86 62.8		
C α-4-L,D-Hep*p*	5.12 101.1 179 Hz	4.14 70.6	4.04 70.5	3.91 78.9	4.37 73.6	4.19 71.9	3.74 62.2	
D β-6-D-Glc*p*4P	4.94 100.4 171 Hz	3.08 56.7	3.86 72.9	3.74 76.5	3.75 75.1	3.52, 3.71 63.4		
E β-3-D-Gal*p*	4.51 103.9 165 Hz	3.66 70.5	3.80 77.9	4.16 65.6	3.73 76.2	3.83, 3.87 61.3		
F α-5-D-Kdo*p*4P	- 175.7	- 100.7	2.23,2.01 35.5	4.59 71.7	4.31 74.0	3.86 75.0	3.81 70.5	3.92,3.71 64.6

The sequence of the monosaccharides was deduced by using the ROESY experiment, which revealed typical NOE *inter*-residue correlations between the anomeric and linkage protons (Figure 6.6a, Table 6.3), and the HMBC experiment which revealed long-range scalar connectivities between the anomeric protons and linkage carbons (Figure 6.6b, Table 6.3) and vice versa.

Table 6.3 NOE *inter*-residues correlations and long-range scalar contacts obtained by ^{1}H, ^{1}H ROESY and ^{1}H, ^{13}C HMBC experiments recorded at 298 K and 600 MHz.

Anomeric proton	**NOE *inter*-residues correlations**	**Long-range scalar connectivities**
H-1 **B**	H-3 **E**	C-3 **E**
H-1 **E**	H-4 **C**	C-4 **C**
H-1 **C**	H-5 **F**	C-5 **F**
H-1 **D**	H-6 **A**	C-6 **A**
H-1 **E**	H-6 **C**	C-6 **C**

In addition, the C-2 of the Kdo at δ 100.7 ppm showed a long-range correlation with H-6 of residue **D** at δ 3.52 ppm, confirming its linkage to the lipid A backbone. These data agreed with the glycosylation effect observed for ^{13}C chemical shift from the ^{1}H-^{13}C DEPT-HSQC spectrum and the linkage position obtained by GC-MS analysis of PMAAs.

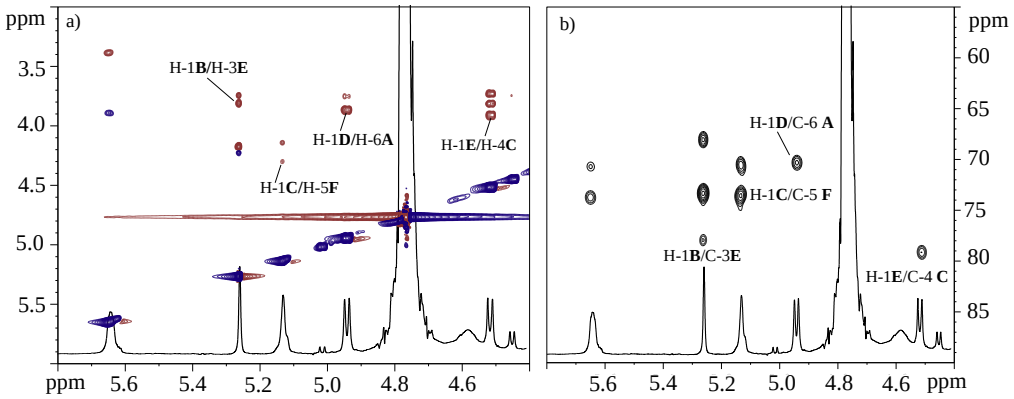

Figure 6.6 a) *Inter*-residue correlations of ROESY spectrum and **b)** long-range scalar connectivities of HMBC spectrum of the OS from the LOS of *P. nigrifaciens* Sq02-Rif^r. The spectra were performed at 298 K and recorded in D_2O at 600 MHz.

Based on the MALDI-TOF and NMR results, the LOS from *Pseudoalteromonas nigrifaciens* Sq02-Rif^r has the following structure:

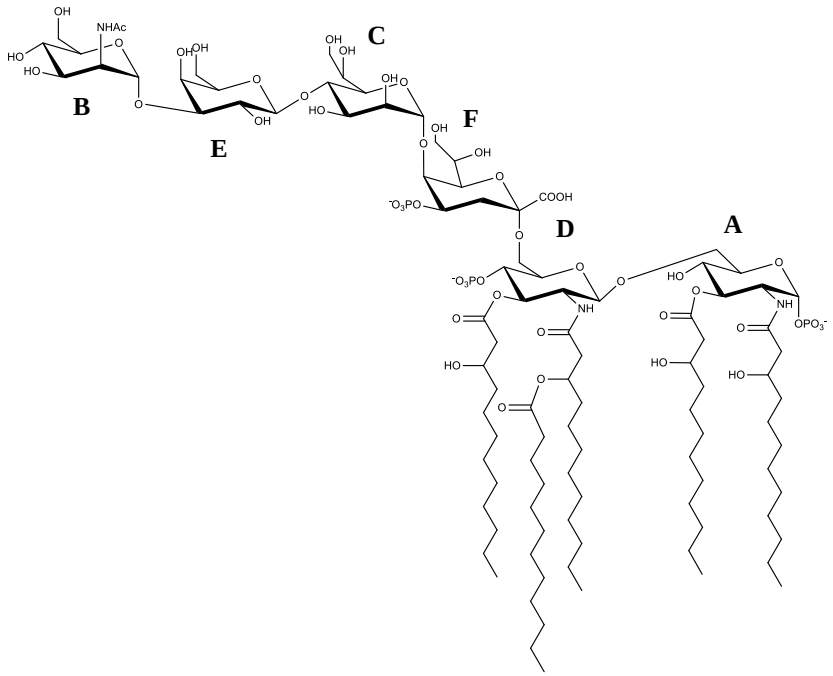

Figure 6.7 Structure of the whole LOS isolated from *P. nigrifaciens* Sq02-Rif^r.

6.1.5 Biological assays

Biological assays were performed in collaboration with Prof. Chiara Schiraldi, from the University Luigi Vanvitelli of Naples.

In mammals the LPS molecules are able to stimulate the innate immune system, leading to the overexpression of a wide range of proinflammatory cytokines, such as TNF (tumor necrosis factor), IL-1 (interleukin-1) and IL-6 (interleukin-6) by macrophages (Miyake K. 2004).
LPS-binding protein (LBP) is a serum glycoprotein that binds to the lipid A portion of LPS and catalyses the transfer of bacterial membrane LPS from the OM to CD14. CD14 is a glycoprotein, which is either expressed on the surface of myelomonocytic cells as a glycosylphosphatidylinositol-anchored molecule (membrane CD14, mCD14) or it is present in the circulation as a soluble molecule (sCD14). CD14 then transfers LPS to Toll-like receptor 4 (TLR4), which is a transmembrane protein expressed on the cell surface of both immune and other body cells (El-Zayat S. R. et al 2019), and its associated factor MD-2 (myeloid differentiation protein 2). LPS-binding promotes TLR4/MD-2 dimerization, which triggers two distinct signalling pathways MyD88 (Myeloid differentiation primary-response protein 88)-dependent and TRIF (TIR-domain-containing adaptor protein)-dependent responses leading to the transcription of immune system genes including cytokines and chemokines.
Excessive TLR4 activation by LPS and the consequent cytokine overproduction underlie the endotoxic shock or sepsis, a leading cause of death in patients with bacterial infections.

6.1.5.1 TLR-4 activation and IL-6 mRNA expression

To investigate the effect of the LOS and lipid A from *P. nigrifaciens* Sq02-Rif^r on the inflammatory cascade was analyzed at transcriptional level the TLR-4 and IL-6 mRNA expression in differentiated CaCo-2 cells. As reported in Figure 6.8, both TLR-4 and IL-6 were up-regulated in presence of commercial LPSs (from *E. coli* O55:B5 and *Salmonella minnesota*) and of *P. nigrifaciens* Sq02-Rif^r LOS and lipid A. In particular, both commercial LPSs increased expression of TLR-4 of about 2 fold respect to untreated cells (CTR), whereas the LOS and the lipid A isolated from *P. nigrifaciens* Sq02-Rif^r increased the TLR-4 expression of about 10 and 15 fold, respectively, compared to the control. In fact, as expected considering the TLR-4 activation, a significant up regulation of IL-6 was found for all the samples analyzed at concentration of 20 μg/mL. Therefore, a significant increase of IL-6 mRNA expression was observed for all samples analyzed. In particular, for commercial and isolated LPSs the expression of IL-6 was about 30-45 fold higher compared to control. Interestingly, the lipid A from *P. nigrifaciens* Sq02-Rif^r increased IL-6 expression of about 80 fold respect to the control.

Arbizu and colleagues (Arbizu S. et al., 2020) described an increase of TLR-4 mRNA expression of about 2.5 fold respect to control in HT-29 colon cancer cells treated with LPS of *E. coli* at 4 μg/mL concentration (Arbizu S. et al., 2020). This difference of gene expression compared with the results obtained may be ascribed to the different concentrations of LPSs tested.

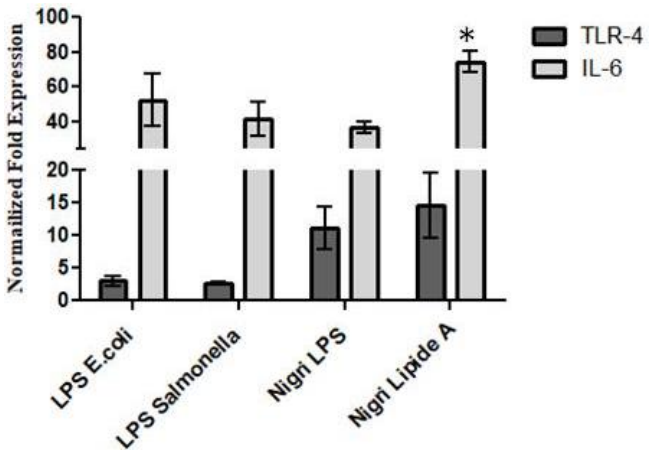

Figure 6.8 Gene expression analyses: the results are expressed as fold change of LPS treated cells respect to untreated cells (CTR) for TLR-4 and IL-6 in differentiated CaCo-2 cells. Data showed as the average±SD.*$p<0.01$ vs CTR and vs commercial LPS ones.

6.1.5.2 NF-κB up-regulates protein expression in response to TLR-4 activation

To identify and confirm the underlying signaling pathways the protein expression of TLR-4 and NF-kB were evaluated by western blotting experiments. As showed in Figure 6.9, an increase of TLR-4 expression was observed for all the samples analyzed compared to the control. Consistent with this result the NF-κB was also increased compared to the untreated cells.

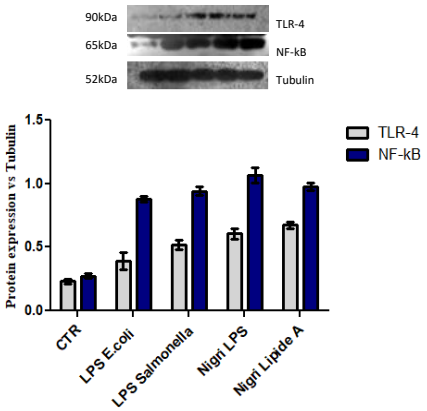

Figure 6.9 Western blotting for expression of TLR-4 and NF-κB protein signal normalized to tubulin in the densitometry reported as average, and SD.

6.1.5.3 Quanti- THP-1 Blue assay

The NF-kB activation was also observed with a recently available tool for the detection in monocytes to quickly highlight the activation of the inflammation pathway (by THP1-Blue™ cells). Co-culture of CaCo-2 and THP1-Blue™ NF-κB reporter cells allowed to compare the inflammatory modulation via-NF-κB pathway of LPS- and lipid A-treated cells and untreated cells, by spectrophotometric analyses. In particular, the LPS isolated from *P. nigrifaciens* Sq02-Rif^r possesses a similar NF-κB up-regulation (Figure 6.10), with respect to the LPS from *Salmonella,* that is slightly but not significantly lower.

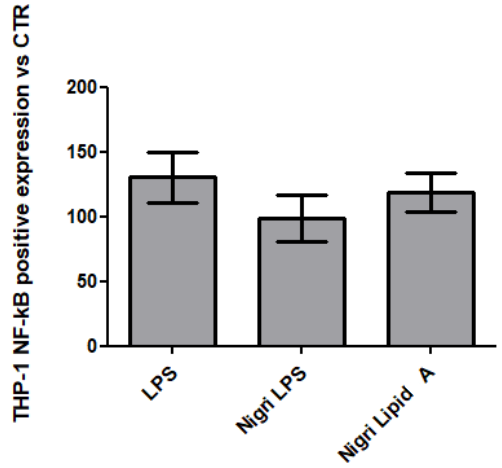

Figure 6.10 Spectrophotometric quantification of NF-kB by QUANTI-Blue™ assay in cells that were untreated (CTR) or exposed to commercial LPS from *Salmonella minnesota* and LOS and lipid A fractions isolated from *P. nigrifaciens* Sq02-Rif^r.

6.1.6 Conclusion

In this study, it was demonstrated that the LOS isolated from *Pseudoalteromonas nigrifaciens* Sq02-Rif^r shares the same oligosaccharide structure found for another cold-adapted bacterium belonging to the same genus, *Pseudoalteromonas haloplanktis* TAC125 (Corsaro M. M. et al., 2001). Confirmation of this result was achieved by 2D NMR spectra of the fully deacylated LOS (OS) and by comparison with those reported for the dephosphorylated and reduced LOS from *Pseudoalteromonas haloplanktis* TAC125 (Corsaro M. M. et al., 2001). Moreover, the lipid A possesses the same fatty acids composition and heterogeneity already found for other *Pseudoalteromonas* species (Corsaro M. M. et al., 2002, Krasikova I. N. et al., 2003, Silipo A. et al., 2004, Volk A. S. et al., 2007, Carillo S. et al., 2011). The main lipid A species possess a di-phosphorylated disaccharide GlcN backbone substituted by four C12:0(3-OH) and a C12:0 residue. The MS analysis of the lipid A from *P. nigrifaciens* Sq02-Rif^r revealed that the C12:0 is the substituent of the N-linked primary fatty acid of the non-reducing GlcN, as already found for *P. haloplanktis* TAB 23 and *P. nigrifaciens* IAM 13010T (Carillo et al., 2011, Volk A. S. et al., 2007). The rough nature of the LPS isolated and the presence of mainly fatty acids with a short chain confirm the trend commonly found in cold-adapted bacteria.
LPS is also known as microbe- or pathogen-associated molecular pattern (MAMP or PAMP) that can be recognized by several receptors, such as the TLR4/MD-2 complex. TLR4 is expressed on the surface of a wide number of different (immune and non-immune) cells. TLR4-stimulating activity of LPS depends on the primary structure of lipid A, i.e. on its phosphorylation and acylation pattern (number, length and position of lipid chains), and can vary from highly endotoxic (TLR4 agonist) to anti-inflammatory (TLR4 antagonist). This strongly supports the importance of the detailed structure characterization of lipid A beside the assessment of its immunological properties. In 1898 Coley observed that infection, produced by injections of a mixture of bacterial toxins, may mediate antitumor effects. It was later discovered by Shear and co-workers that LPS was the component of Coley's toxin

that accounts for its anticancer effects (Pance A. et al., 2002). Since LPS is the ligand for TLR4, these observations indicate that Coley's toxin can activate TLR4. The anti-tumor effect of TLR4 agonist is related to stimulation of the immune response which leads to the synthesis and/or secretion of several cytokines.

For this reason, it was also investigated the immunomodulatory effect of the LPS and the lipid A from this bacterium through the most common mechanism underlying the LPS immunomodulatory pathway. On differentiated CaCo-2 cells, the results showed a similar action to the commercial LPS from *E. coli* and *S. minnesota*. In fact, differentiated CaCo-2 cells increased TLR-4 expression at both mRNA and protein levels after LPS and lipid A treatments. Then, NF-κB pathway was activated towards cytokines production (Kaszowska M. et al., 2017; Nyati K. K. et al., 2017). To confirm the role of NF-κB spectrophotometric analyses were performed. In particular, the THP-1 blue NF-κB reporter assay gave a further indication of the inflammation cascade induction in response to the LPSs/LipidA binding, confirming the RT-PCR results.

Preliminary *in vitro* tests to develop the THP-1 NF-kB reporter assay were performed at different concentrations of LPS, indicating the concentration of 20 μg/ml as the most effective in the pro-inflammatory response of the LPS itself. Therefore, in this study this concentration of LPSs or Lipid A was evaluated.

The lipid A from *P. nigrifaciens* and *P. haloplanktis* TAB 23 share an identical primary structure, but they show a different immunostimulant effect on the treated cells. While *P. nigrifaciens* lipid A showed a promising stimulant activity on enterocytes cells, *P.haloplanktis* TAB 23 lipid A does not provide the same effect on the THP-1 (human monocytic)cell line (Carillo S. et al. 2017). Therefore, the biological activity may be influenced not only by the three-dimensional structure of the lipid A but also by the type of cell lines used as target.

6.2 CPS isolation and characterization

6.2.1 Isolation and purification of CPS

The residual pellet of *Pseudoalteromonas nigrifaciens* Sq02-Rif^r cells, previously extracted by the PCP procedure (see paragraph 8.1.1), was also subjected to the phenol/water method (Westphal O. and Jann K., 1965). The aqueous phase was dialyzed against water, and subjected to a digestion with DNAse, RNAse and protease to remove the contaminants.

The 14% DOC-PAGE analysis of the purified extract (Figure 1, lane C) after both silver nitrate and Alcian blue staining, indicated the absence of contaminants and the presence of a band at low molecular weight attributable to the Rough-LPS (see paragraph 8.1.1). An additional band at high molecular masses attributable to a capsular polysaccharide (CPS), was clearly visible after Alcian blue (Figure 6.11b, lane C) and double staining (Figure 6.11c, lane C).

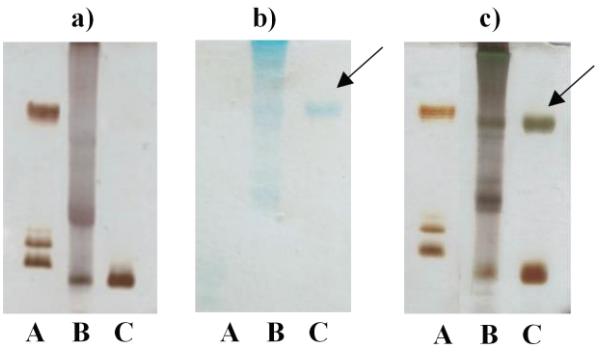

Figure 6.11 14% DOC-PAGE analysis of the Smooth-LPS of *E. coli* (**A**) aqueous phase before (**B**) and after (**C**) enzymatic digestion stained with a) silver nitrate, b) Alcian blue, and c) Alcian blue followed by silver nitrate. Arrows indicate the bands of the CPS.

The CPS was isolated from the LOS by subjecting the extract to a mild acidic hydrolysis with 1% acetic acid (Carillo S. et al., 2015). After centrifugation, the supernatant mixture was fractionated on a Bio-gel P10 column, using water as eluent. The CPS fraction was further purified with the same column providing a fraction containing a pure polysaccharide. The absence of proteins in the CPS sample was confirmed by both DOC-PAGE analysis stained by Coomassie Blue and Bradford assay.

The GC-MS analysis of the monosaccharides derivatized as acetylated methyl glycosides (AMGs) provided the glycosyl composition of the pure CPS. This analysis revealed the presence of glucosamine (GlcN), mannosamine (ManN), and 2-amino-2-deoxymannuronic acid (ManNA). The presence of both ManN and GlcN was also confirmed by the preparation of the corresponding alditol acetates. The D-configuration of these two latter monosaccharides was achieved by the GC–MS analysis of the corresponding acetylated 2-octyl glycosides (Leontein K. et al., 1978), by comparison with original standards, while the D-configuration of the ManNA was established by ^{13}C glycosylation shifts analysis (see paragraph 8.2.2) (Lipkind, G. M. et al., 1988).

6.2.2 NMR analysis of the purified CPS

The ^{13}C NMR spectrum of the pure CPS (Figure 6.12), performed at pD 6 and 298 K, showed four signals in the anomeric region at δ 103.1, 102.1, 100.2, and 98.3 ppm, four signals for carbons linked to nitrogen at δ 56.4, 54.8, 54.6, and 54.2 ppm, four N-acetyl groups at δ 23.3, 23.1, 23.0, and 22.9 ppm, and five carbonyl groups at δ 176.5, 175.9, 175.6, 175.4, and 175.3 ppm.

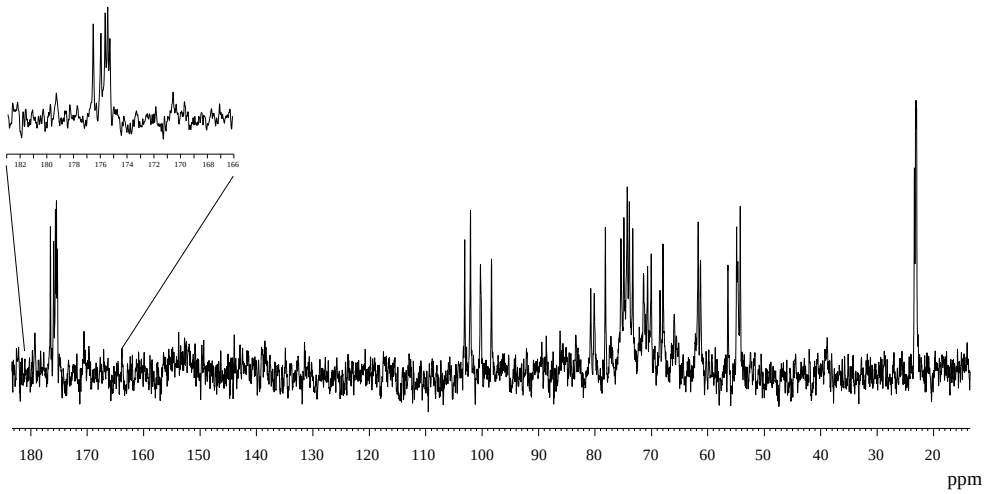

Figure 6.12 ^{13}C NMR spectrum of the CPS from *Pseudoalteromonas nigrifaciens* Sq02 performed at 298 K and pD 6. The spectrum was recorded in D_2O at 400 MHz.

Starting from the 2D NMR spectra acquired at pD 6 and 298 K it was not possible to assign all the resonances. Therefore, it was necessary to record all NMR experiments at a different pD value. Thus, the complete assignment of ^{1}H and ^{13}C resonances of the capsular polysaccharide was obtained at pD 2 and 298 K, as reported in Table 6.4. The ^{1}H NMR spectrum revealed in the anomeric region (δ 4.4-5.5 ppm) five signals, but only four (**A**-**D**) were correlated with anomeric carbons, as showed in the $^{1}H,^{13}C$ DEPT-HSQC spectrum (Figure 6.13a). The 2D F*2*-coupled HSQC experiment allowed to measure the $^{1}J_{C1,H1}$ coupling constant values (Figure 6.13b), indicating that

the residues **A** and **C** were α-configured (181 and 185 Hz for **A** and **C**, respectively) while **B** and **D** were β-configured (170 and 165 Hz for **B** and **D**, respectively) (Bock K. and Pedersen C. J., 1974).

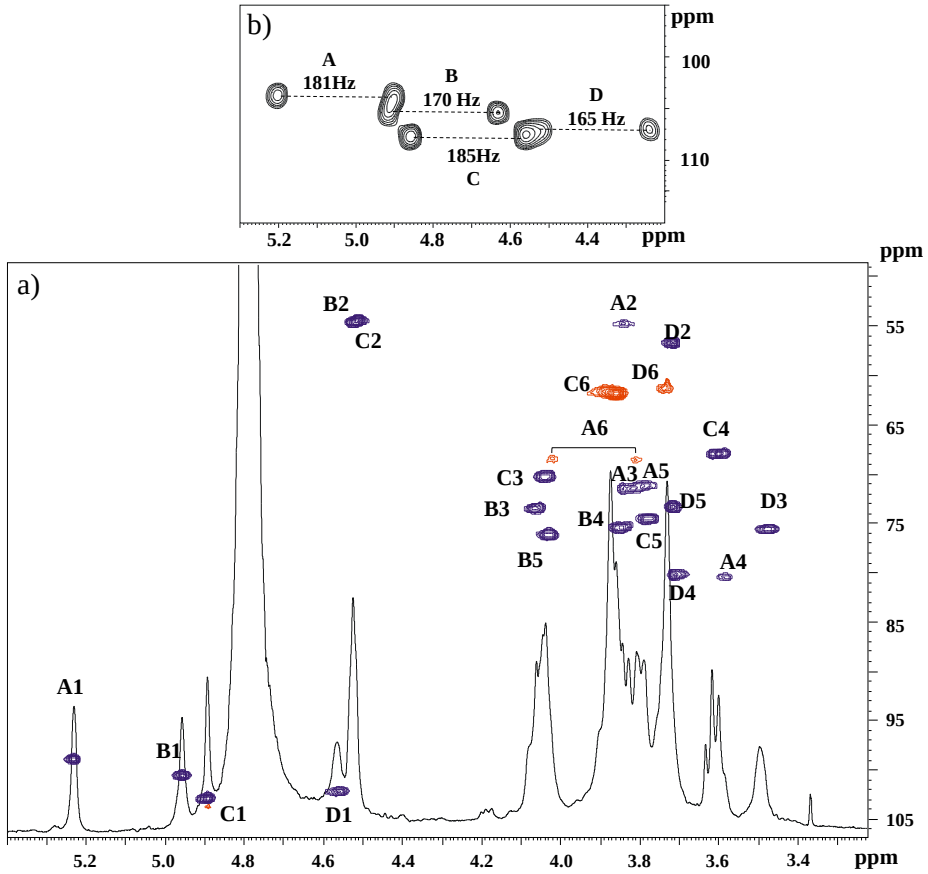

Figure 6.13 a) Anomeric and carbinolic regions of overlapped ^{1}H and $^{1}H,^{13}C$ DEPT-HSQC spectra of the CPS from *P. nigrifaciens* Sq02. b) Anomeric section of the 2D F*2*-coupled HSQC experiment. The spectra were performed at 298 K and pD 2 and recorded in D_2O at 600 MHz.

The spin systems **A** and **D**, at δ 5.23 and 4.56 ppm respectively, were identified as 2-acetamido-2-deoxy-glucose (GlcNAc) units. In fact, the H-2 of both **A** and **D** is correlated with two nitrogen-bearing carbon atoms at δ 54.7 and 56.6 ppm, respectively. Residue **A**, with H-1/C-1 signals at δ 5.23/98.9 ppm, was recognized as

a 4,6-disubstituted GlcNAc residue (4,6-GlcNAc) thanks to the downfield shift of both C-4 and C-6 carbon resonances at δ 80.3 and 68.5 ppm, respectively (Bock K. and Pedersen C. J., 1983). Finally, H-2 deshielded at δ 3.84 ppm together with the presence of acetyl signals in the range of 2.00-2.10 ppm indicated the *N*-acetylation for residue **A**.

Residue **D**, with H-1/C-1 signals at δ 4.56/102.1 ppm was recognized as a 4-substituted GlcNAc residue (4-GlcNAc) since it showed a C-4 downfield shifted signal at δ 80.2 ppm (Bock K. and Pedersen C. J., 1983). The *intra*-residue NOE contacts of H-1 with H-3 and H-5 for residue **D** confirmed the β-configuration.

The **B** residue, with H-1/C-1 at δ 4.96 /100.5 ppm, was identified as a 2-acetamido-2-deoxy-mannuronic acid (ManNAcA). This result was obtained based on the correlations found only from H-1 to H-2 in the TOCSY spectrum, the correlation of H-2 signal with a carbon linked to a nitrogen at δ 54.4 ppm in the ^{1}H, ^{13}C DEPT-HSQC experiment, and the correlation of H-5 to a carbonyl group at δ 173.7 ppm in the HMBC spectrum. In addition, **B** was identified as a 4-substituded (4-ManNAcA) since its C-4 was downfield shifted at δ 75.4 ppm (Branefors-Helander, P. et al., 1981; Lugowski, C. et al., 1983).

Finally, residue **C** with H-1/C-1 at δ 4.89/102.9 ppm, was identified as a 2-acetamido-2-deoxy-mannose (ManNAc). The *manno*-configuration was suggested by the TOCSY experiment that showed a correlation of H-1 signal only with H-2, in turn correlated with a carbon linked to a nitrogen atom at δ 54.4 ppm. This residue was recognized as terminal since none of its carbons was shifted by glycosylation (Agrawal P. K., 1992).

Table 6.4 ^{1}H and ^{13}C NMR assignments of CPS from *P. nigrifaciens* Sq02 Rif^{r} grown at 18 °C. Spectra were recorded in D_2O at 298 K and pD 2 at 600 MHz, using acetone as internal standard (δ_H/δ_C 2.22/31.45 ppm).

Residue	Chemical shift (ppm)					
	H1 **C1** $^{1}J_{CH}$	**H2** **C2**	**H3** **C3**	**H4** **C4**	**H5** **C5**	**H6a,H6b** **C6**
A α-3,6-D-GlcNAc	5.23 98.9 181 Hz	3.84 54.7	3.84 71.5	3.59 80.3	3.78 71.1	3.81,4.04 68.5
B β-4-D-ManNAcA	4.96 100.5 170 Hz	4.52 54.4	4.07 73.4	3.84 75.4	4.04 76.1	- 173.7
C α-*t*-D-ManNAc	4.89 102.9 185 Hz	4.51 54.4	4.04 70.2	3.60 67.8	3.78 74.5	3.78 61.6
D β-4-D-GlcNAc	4.56 102.1 165 Hz	3.72 56.6	3.47 75.6	3.70 80.2	3.72 73.3	3.73 61.0

Acetyl groups: $C\underline{H}_3$ 2.03, 2.07. $\underline{C}H_3$ 23.3, 23.4. $\underline{C}$=O 175.5, 176.6.

The D-configuration of ManNAcA was established based on the values of ^{13}C chemical shifts (Lipkind G. M. et al., 1988). Considering the disaccharide unit α-GlcNAc-(1→4)-ManNAcA with D-D configurations, the value of the C-4 chemical shift of the glycosylated residue should be 76.6 ppm (residue P, +7.3), while the value of C-1 of the glycosylating residue at 99.1 ppm (residue P', +7.0). In contrast, for the disaccharide unit with D-L configurations, the C-4 of P should be at 78.3 ppm (+9.0), while the C-1 of P' at 99.4 ppm (+7.3). Based on the higher closeness to the chemical shift values reported in the Table, the disaccharide 2 α-GlcNAc-(1→4)-ManNAcA possess the D-D configurations.

Finally, NOE *inter*-residues correlations and long-range scalar connectivities allowed to deduce the sequence of the monosaccharide residues (Figure 6.14). In particular, the NOESY spectrum showed the following *inter*-residues contacts: H-1of **C** with H-4 of **A**, H-1 of **A** and H-4 of **B**, H-1of **B** with H-4 of **D**, H-1 of **D** with H-6 of **A** (Figure 4a). The HMBC spectrum confirmed these correlations showing the following long-

range scalar contacts: H-1 of **C** with C-4 of **A**; H-1 of **A** with C-4 of **B**, H-1 of **B** with C-4 of **D** and H-6 of **A** with C-1 of **D** (Figure 4a). These data agree with the glycosylation pattern revealed by the $^{1}H,^{13}C$ DEPT-HSQC chemical shift.

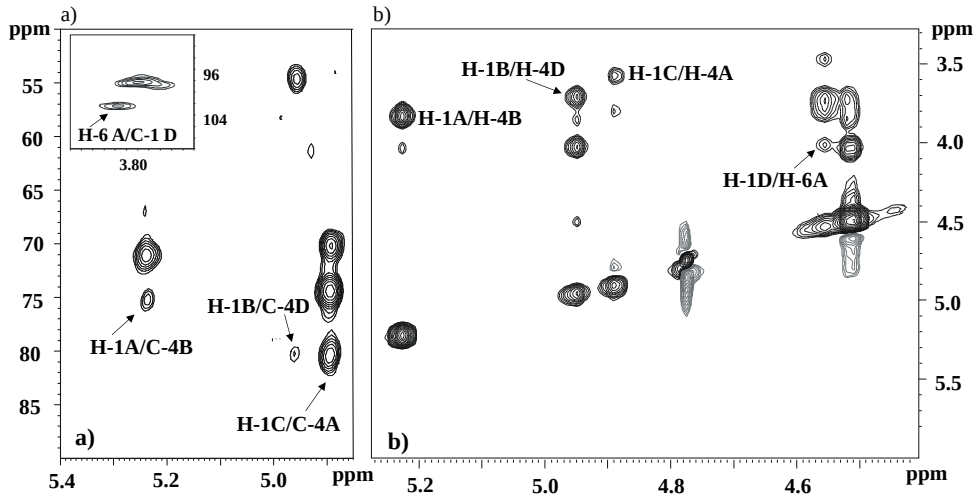

Figure 6.14 a) Long-range scalar connectivities in the $^{1}H,^{13}C$ HMBC spectrum and b) *inter*-residue correlations in the NOESY spectrum of the CPS from *P. nigrifaciens* Sq02-Rif^{r}. The spectra were acquired at 298 K and recorded in D_2O (pD 2) at 600 MHz.

Therefore, the repeating unit of the CPS isolated from *Pseudoalteromonas nigrifaciens* Sq02-Rif^{r} has the following structure (Figure 6.15):

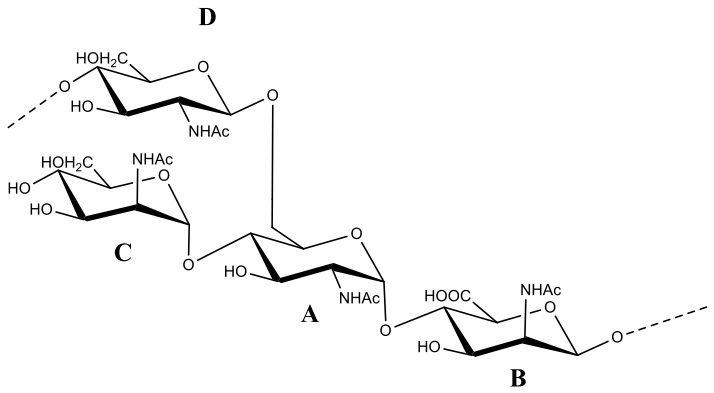

Figure 6.15 Repeating unit of the CPS from *P. nigrifaciens* Sq02-Rif^{r}.

6.2.3 Molecular weight determination

In collaboration with Prof. Schiraldi group, from the University Luigi Vanvitelli, the molecular weight (M_w) of this polysaccharide was established. In particular, the average M_W of the purified CPS was found to be 8.7 kDa (table 6.5). The hydrodynamic characterization was reported in terms of retention volume (Ret.Vol.), average molecular weight (M_w), number average molecular weight (M_n), polydispersity index (M_w/M_n), intrinsic viscosity (IV), hydrodynamic radius (Rh), and recovery percentage. The 76.5% recovery was found consistent with a relative humidity of the samples above 20%, potentially present in lab scale purified samples.

Table 6.5 Hydrodynamic characterization performed by SEC-TDA of CPS from *P. nigrifaciens* Sq02

Ret.Vol. (mL)	M_w (kDa)	M_n (kDa)	M_w/M_n	[IV] (dL/g)	Rh (nm)	Recovery (%)
15.676	8.676	7.543	1.164	0.115	2.450	76.491

6.2.4 Biological assays

Biological assays were performed in collaboration with Prof. Chiara Schiraldi.

6.2.4.1 Cell viability assays

The *in vitro* anti-cancer activity of this capsular polysaccharide against two colon cancer cell lines (CaCo-2 and HCT-116) was determined. In particular, the anti-proliferation/cell growth effects were primarily evaluated.

As shown in Figure 6.16, for CaCo-2 cells no cytotoxicity was found for the two CPS concentrations tested. Cell viability was higher 70% of the untreated cells (CTR), according to ISO 10993-5 (Srivastava G. K. et al. 2018) and above the reference threshold. Among the amounts of CPS tested only CPS tested at 200 μg/mL slightly increased cell proliferation (about 136%) with respect to CTR (Figure 6.16A).

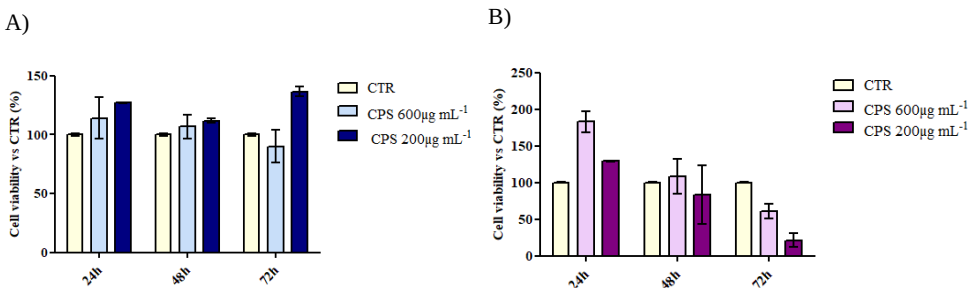

Figure. 6.16 Quantification of cell viability was performed using CCK8 staining for both CaCo-2 (A) and HCT-116 cells (B).

All the CPS samples tested showed the same effect on HCT-116 cells up to 48h. On the contrary at 72h, *P. nigrifaciens* CPS at 600 µg/mL showed viability reduction at around 60% of the control while at 200 µg/mL, a lower cell viability than the threshold for toxicity was found (i.e. 20% with respect to CTR) (Figure 6.16B).

6.2.4.2 Mechanism evaluation

To shed light on the mechanism of action of the CPS against the two cancer cell lines, four specific markers of the apoptosis pathway (Bax, Bcl-2, Caspase 3, and Caspase 9) were targeted.

Gene expression analyses indicated that on CaCo-2 cells Caspase 3 was expressed with a 10-fold increase respect to CTR at 600 µg/mL while at 200 µg/mL the fold increase was about 5 times the control (Figure 6.17A). Furthermore, Caspase 9 was up-regulated for both concentrations tested. At 600 µg mL^{-1} Caspase 9 is up-regulated of 18-fold while at 200 µg/mL of about 6-fold compared to CTR (Figure 6A). On HCT-116 cells, after CPS treatment the expression of Caspase 3 increase of about 10- and 5-fold with respect to the CTR at both concentrations tested. While an increment of about 4- and 14-fold for Caspase 9, were observed for the concentrations tested, compared to CTR (Figure 6.17B).

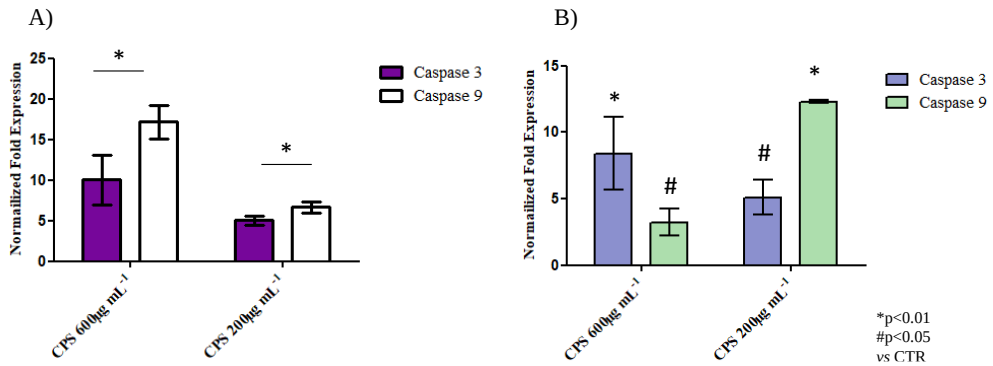

Fig. 6.17 Gene expression analyses normalized with respect to untreated cells (CTR) for Caspase 3 and 9 on A) CaCo-2 and B) HCT- 116 cells. Data shows the averages ± S.D. Significant differences are indicated as *p<0.01 and #p<0.05 *vs* CTR.

To confirm these data the expression of these two proteins was also evaluated by western blotting analyses (Figure 6.18).

On CaCo-2 cells, Caspase-9 was slightly activated at 600 µg/mL while Caspase-3 significantly increased at both concentrations tested (Figure 6.18A). In contrast, a similar trend with respect to CTR was found for HCT-116 cells (Figure 6.18B). However, a significative reduction of viability was found (see paragraph 6.2.4.1).

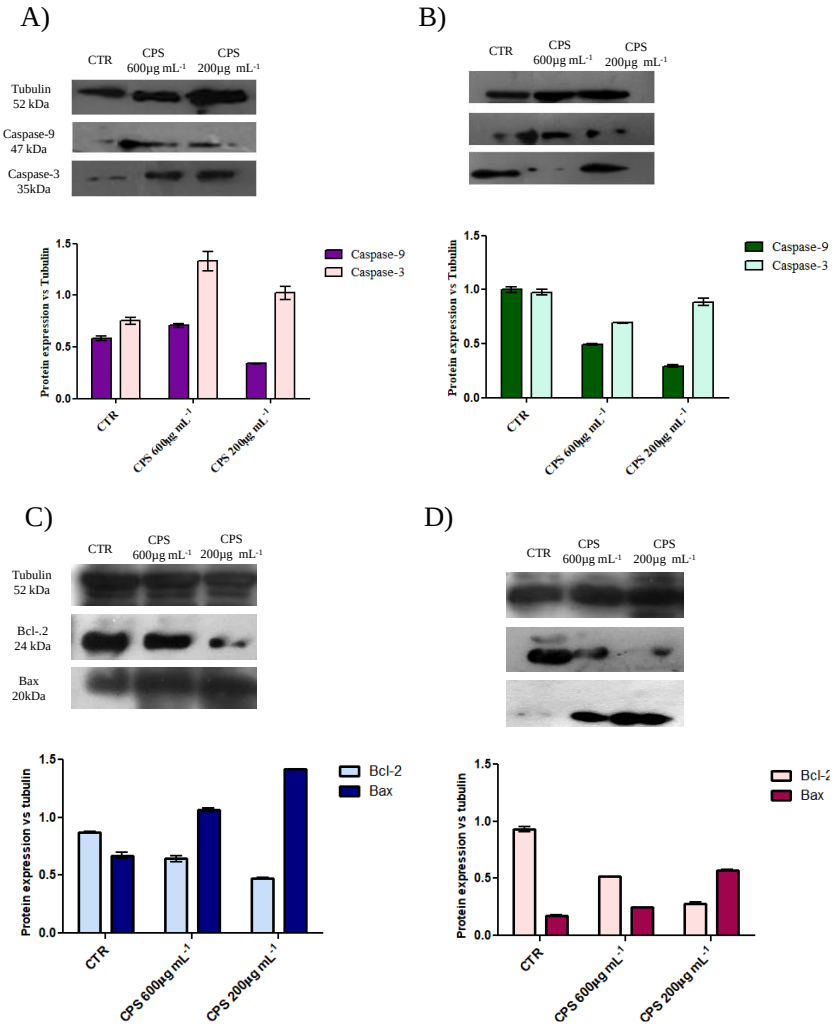

Figure 6.18 Analysis of Caspase-3, Caspase-9, Bax, and Bcl-2 by western blotting on CaCo-2 (A and C) and on HCT-116 cells (B and D) treated with *P. nigrifaciens* Sq02-Rif^r CPS at 600 and 200 µg mL-^{1} in comparison to untreated cells (CTR) at 48h of incubation. The expression of each protein was normalized with respect to tubulin housekeeping protein.

In addition, Bax and Bcl-2 were also investigated as apoptosis markers on CaCo-2 and HCT-116 cells after treatments with CPSs of *P. nigrifaciens* Sq02-Rif^r (Figure 6.18C and D). The results revealed an increase of Bax and a decrease of Bcl-2 for both cell lines, in agreement with the antagonist role of Bcl-2 that binds Bax inhibiting its translocation to the mitochondrial membrane.

Indeed, during the apoptosis mechanism, Bax protein reaches the mitochondrial outer membrane, permeabilizing it and leading to the release of cytochrome C (Larsen B. D. and Sørensen, C. S., 2017; Tukenmez U. et al., 2019). Furthermore, Bax has a key role in cellular mitochondrial stress activating Caspase-9 and therefore in the apoptosis route (Larsen B. D. and Sørensen, C. S., 2017; Sharpe J. C. et al., 2004). Finally, Western blotting analyses showed that CPS at 200 µg/mL, after 48h of incubation, was indeed able to activate apoptosis in both cancer cell lines investigated.

6.2.5 Ice recrystallization inhibition assay

To assess cryoprotective activity of the CPS isolated from *P. nigrifaciens* Sq02-Rif^r ice recrystallization inhibition (IRI) assays, in collaboration with Prof. Matthew Gibson (University of Warwick) were performed. The assays indicated that this polysaccharide does not display IRI activity in the concentration range of 1.25–10 mg·mL^{-1} (Figure 6.19).

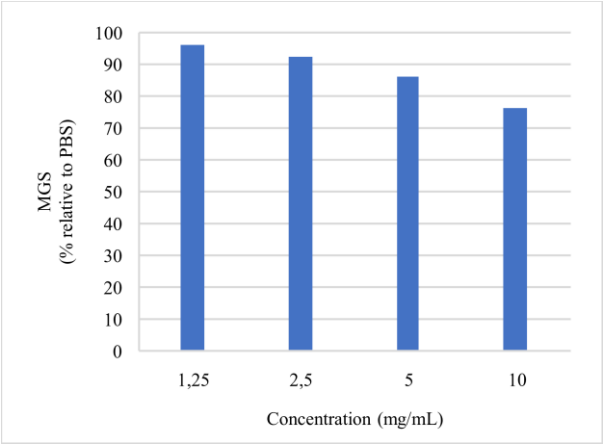

Figure 6.19 Ice Recrystallization Inhibition (IRI) activity of the CPS isolated from *P. nigrifaciens* Sq02-Rif^r, measured as mean grain size (MGS) of the ice crystals. The MGS is expressed as a percentage of PBS buffer. High MGS value indicates decreased IRI activity.

6.2.6 Conclusion

The psychrotrophic bacterium *P. nigrifaciens* Sq02-Rif^r produces a capsular polysaccharide, which was isolated and fully characterized by chemical analyses and NMR spectroscopy. The CPS consists of a branched tetrasaccharidic repeating unit containing all *N*-acetylated aminosugars. This structural feature was already found in the capsular polysaccharide from *S. vesiculosa* HM13 (see paragraph 4.4.2), and for other Gram-negative bacteria (Fiebig T. et al., 2014; Micoli F. et al., 2018; Wang P. et al., 2004). The high degree of acylation could be related to the capacity of the bacterium to adhere to surfaces, since this strain is able to produce biofilm (unpublished data).

In literature, several studies have demonstrated that polysaccharides produced by extremophilic bacteria exhibit a wide range of biological activities, such as anti-cancer, antioxidant, and immunomodulatory (Wang J. et al., 2019; Chaisuwan W. et al., 2020). These properties together with their biodegradability, biocompatibility and low toxicity make them suitable for biomedical applications. Although the anti-cancer activity (with low side effects) of polysaccharides has been documented for a long time, the mechanisms underlying the action of these polymers still awaits to be clarified. Among the identified mechanisms are reported examples of cancer-preventing activity, activation of the immune response, direct inhibition and killing of tumour cells, and angiogenesis inhibition of tumour tissues (Xie L. et al., 2020).

In Europe, cancer of colon and rectum (colorectal cancer, CRC), according to the World Health Organization, is the second most common cause of cancer death in both men and women. Currently, the conventional treatments for CRC are surgical resection, often in combination with radio- and chemotherapy. The well-known side effects deriving from chemotherapeutic agents lead to research alternative therapies. For this reason, a possible anti-cancer activity of the isolated capsular polysaccharide from *P. nigrifaciens* Sq02-Rif^r against two colon cancer cell lines (CaCo-2 and HTC-116) was preliminarily evaluated. The results suggested a significant reduction in cell viability especially on HCT-116 cells after 72h of treatment with *P. nigrifaciens*-Rif^r

CPS at 600 µg/mL. In addition, to identify the molecular mechanisms underlying the CPS activity four specific markers associated with the apoptosis pathway were targeted. Gene and proteins expression analyses showed that the CPS induces the apoptosis by up-regulation of Bax, Caspase 3 and Caspase 9 and down-regulation of Bcl-2.

However, further studies are necessary to confirm and better identify the molecular mechanisms of the CPS action and to evaluate the potential interactions between this bacterial polysaccharide and the immune system cells to better ensure its efficacy and safety in the prevention or as support/integration in the treatment of colon cancer.

Pseudomonas ANT_J38B

The genus *Pseudomonas* belonging to the family *Pseudomonadaceae* was already described in 1984. It comprises bacteria inhabiting many niches and habitats, thus representing one of the most diverse and ubiquitous genera. *Pseudomonas* species were isolated from a wide range of environments, from the Antarctica to the Tropics, from sediments, clinical samples, plants, fungi and diseased animal specimens, water, soil, plant rhizosphere, sea, and deserts (Peix A. et al., 2009). This widespread distribution suggests an extraordinary adaptability, both physiological and genetic. In humans, some *Pseudomonas* species are recognized as opportunistic pathogens, found in lungs of cystic fibrosis (CF) patients, in people with eye infections, in burn victims, and in AIDS patients. This pathogenicity is due to the secretion of many toxins, which can promote the adherence to host cells, damage host tissues, cause inflammation, and elude defence mechanisms.

Pseudomonas sp. ANT_J38B is a psychrotrophic Gram-negative bacterium isolated from a sample soil collected at the Jardine Peak (King George Island, Antarctica), at a depth of 15–20 cm (Romaniuk K. et al., 2018). In this chapter the isolation of the LPS from *Pseudomonas* sp. ANT_J38B grown at 4 °C was described, and the structural characterization, by chemical analyses and NMR spectroscopy, of the O-chain repeating unit.

Chapter VII: *Pseudomonas* ANT_J38B

7.1 LPS isolation from cells and characterization

7.1.1 Isolation and chemical analyses of the LPS

The dried cells of *Pseudomonas* sp. ANT_J38B, grown at 4 °C in LB (Luria Bertani) medium, were extracted in sequence by the PCP method (Galanos C. et al., 1969), and then by the phenol/water extraction (Westphal O. and Jann K., 1965). The PCP extract was analysed by 14% DOC-PAGE electrophoresis and visualized after silver staining, allowing to establish the smooth nature of LPS due to the presence of the typical "ladder-like" pattern (Figure 7.1). Since the aqueous extract only showed a very low amount of S-LPS as revealed by DOC-PAGE analysis, all the following analyses were performed on the LPS isolated from the PCP extraction.

Figure 7.1 14% DOC-PAGE analysis after silver nitrate staining of the PCP extract (lane A) from *Pseudomonas sp*. ANT_J38B, and LPS from *Escherichia coli* 055:B5 (lane B), used as standard.

The GC-MS analysis of the monosaccharide derivatised as acetylated methyl glycosides (AMGs) suggested the presence of quinovosamine (Qui2N), mannose (Man), glucose (Glc), gulosaminuronic acid (GulNA), glucosamine (GlcN), and 3-deoxy-D-*manno*-oct-2-ulosonic acid (Kdo). This analysis was repeated after

48 % HF treatment showing the additional presence of a heptose, thus suggesting its phosphorylation (Carillo S. et al., 2013).

Moreover, the analysis of the fatty acids derivatized as fatty acids methyl esters (FAMEs), revealed the presence of 3-hydroxydecanoic [C10:0(3-OH)], 2-hydroxydodecanoic [C12:0(2-OH)], 3-hydroxydodecanoic [C12:0(3-OH)], dodecanoic (C12:0), tetra-decanoic (C14:0), and pentadecanoic acids (C15:0).

7.1.2 Mild acid hydrolysis of the LPS

A mild acid treatment of the LPS allowed to hydrolyse the glycosidic linkage between the Kdo and the GlcNII of the lipid A portion. The supernatant containing the saccharide moiety was separated from the lipid A by centrifugation. The obtained supernatant was purified through a gel filtration chromatography, using water as eluent. The fraction containing the O-chain, named OPS, was characterized by chemical analysis and 1D and 2D NMR spectroscopy. The GC-MS of the AMGs of OPS revealed that only the Qui2N and the GulNA were attributable to the O-chain. The GC-MS analysis of acetylated (R)-2-octyl glycosides suggested a D absolute configuration for Qui2N and L for the GulNA.

7.1.3 NMR spectroscopic analysis of the O-chain

The 1D and 2D NMR experiments revealed the presence of two spin systems. The ^{1}H NMR spectrum showed in the anomeric region (4.4–5.5 ppm) four signals (Figure 7.2), although the ^{1}H,^{13}C DEPT-HSQC spectrum (Figure 7.2) revealed that only two proton signals at δ 5.07 and 4.49 ppm are correlated with anomeric carbon signals at δ 97.0 and 102.1 ppm, respectively. Moreover, at up-field the ^{1}H spectrum showed signals attributable to *N*- and *O*-acetyl groups in the range 1.8–2.2 ppm, and a signal at δ 1.29 ppm attributable to the methyl group of the Qui2N residue.

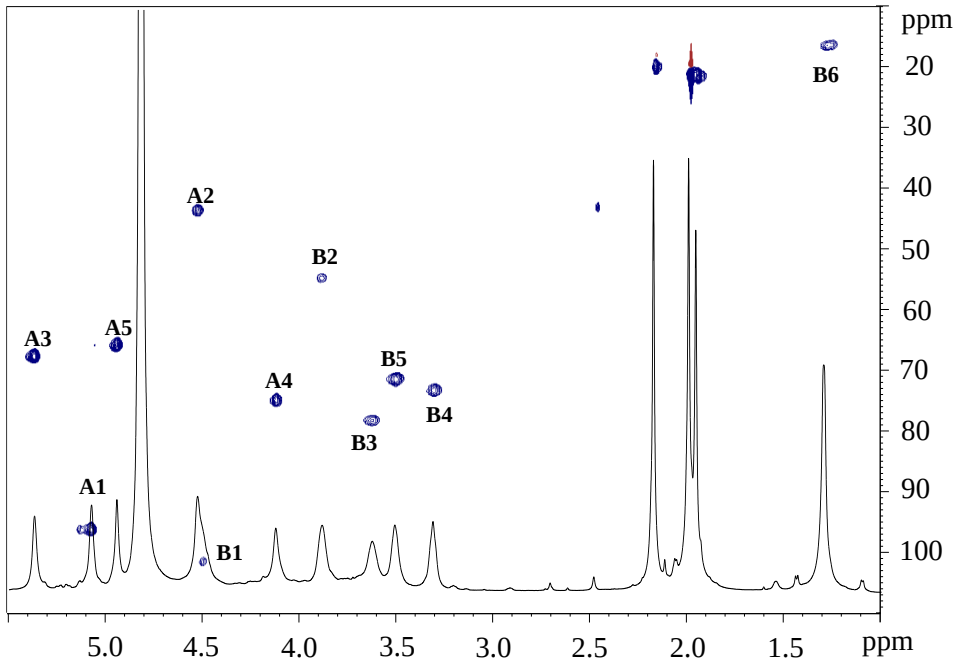

Figure 7.2. $^{1}H,^{13}C$ DEPT-HSQC and ^{1}H NMR spectra of the O-chain from *Pseudomonas* ANT_J38B.

Residue **A** at H-1 at δ 5.07 ppm was recognized as a 2-acetamido-2-deoxy-3-O-acetylgulopyranuronamide (Gul*p*NAc3OAcAN). In the COSY spectrum starting from the H-1, the H-2 proton at δ 4.52 ppm was observed, which was correlated in the DEPT-HSQC experiment with a C-2 occurring at δ 44.6 ppm. The last value indicates the *gulo* configuration as already reported (Kondakova A. N. et al., 2012). Based on the COSY experiment, all the protons of this spin system were identified. In particular, the H-2 proton signal showed a correlated to the proton at δ 5.37 ppm (H-3), that is in turn correlated with the carbon signal at δ 68.7 ppm indicative of a carbon substituted with an *O*-acetyl group. Successively, from the H-3 the correlations with the proton H-4 at δ 4.12 ppm and the H-5 at δ 4.94 ppm were observed. Finally, the HMBC spectrum showed a long-range scalar connectivity between the H-5 proton signal at δ 4.94 ppm, and the C-6

signal at δ 173.9 ppm, confirming the occurrence of a uronic acid residue. The *gulo* configuration was definitively confirmed by the values of the ^{13}C chemical shifts (Table 1) (Kondakova A.N. et al., 2012). In addition, the downfield shift signal of C-4 at δ 76.0 ppm together with an upfield shift of both C-3 and C-5 values were indicative of a C-4 substitution, as demonstrated by comparison with those of the α-GulpNAc (Michon F. et al., 1985). Finally, the chemical shift value of the C-6 signal suggested the occurrence of an amide. To confirm this hypothesis the proton and $^{1}H,^{13}C$ HMBC experiments were performed at two different pD values, namely at pD 2 and pD 7. Since no differences were observed for ^{1}H and ^{13}C chemical shifts at these two pD values, it was possible to confirm the amidation at the carboxyl group of the GulNAcA (Molinaro A. et al., 2003).

Residue **B** with H-1 at δ 4.49 ppm was identified as a β-*N*-acetylquinovosamine (β-Qui2NAc). In particular, the correlations in COSY and TOCSY spectra suggested its *gluco*-configuration. The $^{1}H,^{13}C$ DEPT-HSQC experiment correlated the correlation of its H-2 at δ 3.88 ppm with a nitrogen bearing carbon at δ 55.8 ppm. All the ^{13}C chemical shift values assigned to each carbon of this monosaccharide were comparable to those already reported (Corsaro M. M. et al., 2006). Moreover, the C-3 at δ 79.1 ppm was shifted downfield with respect to that of an unsubstituted Qui2N residue (Knirel Y. A. et al., 1987), suggesting a substitution at this position. The occurring of a β configuration was confirmed by the presence of H-1, H-3 and H-1, H-5 NOE *intra*-residue correlations in the NOESY experiment.

Table 7.1 ^{1}H and ^{13}C NMR chemical shift (δ, ppm) assignments of the repeating unit of the OPS from *Pseudomonas* ANT_J38B. Internal standard sodium 3-trimethylsilylpropanoate-2,2,3,3-d4 (δ_H 0.0 ppm) and external standard acetone (δ_C 31.45 ppm) were used.

Chemical shift (ppm)	Residues	
	α-L-4-GulNAc3OAcAN	**β-D-3-Qui2NAc**
	A	**B**
H1	5.07	4.49
C1	97.0	102.1
H2	4.52	3.88
C2	44.6	55.8
H3	5.37	3.62
C3	68.7	79.1
H4	4.12	3.31
C4	76.0	74.5
H5	4.94	3.51
C5	66.7	72.4
H6	-	1.29
C6	173.9	17.8
CH_3CO (N-2)	1.99	1.96
	22.4	22.4
CH_3CO (N-2)	-	-
	174.0	174.4
CH_3CO (O-3)	2.17	
	20.8	
CH_3CO (O-3)	-	
	173.9	

The *N*-acetyl substitution at C-2 position of both residues was evidenced by the ROESY experiment. The methyl signal at δ 1.97 ppm showed a ROE contact with H-2 at δ 4.52 ppm of residue **A**. In addition, a ROE contact between H-2 of **B** at δ 3.88 ppm and the methyl signal at δ 1.95 ppm was also visible. Finally, the *O*-acetyl substitution at C-3 position of residue **A** was confirmed by the HMBC spectrum, since the methyl signal at δ 2.17 ppm showed a long-range scalar connectivity with the carbonyl group at δ 173.9 ppm (Figure 7.3b), in turn correlated with the H-3 of **A** at δ 5.37 ppm.

Finally, the sequence of the disaccharide repeating unit of the OPS was deduced by the following *inter*-residues NOE correlations: H-1 of **A** with H-3 of **B**, and H-1 of **B** with H-4 of **A**.

Based on these data, the structure of the repeating unit of the O-chain from *Pseudomonas* sp. ANT_J38B was identified as reported in the Figure 7.3a:

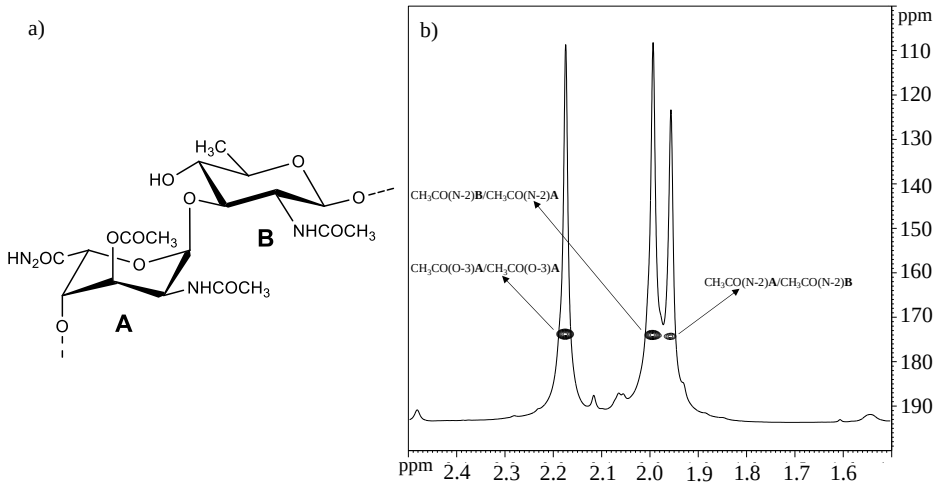

Figure 7.3 a) Structure and b) $^{1}H,^{13}C$ HMBC section of the OPS from *Pseudomonas* ANT_J38B.

7.1.4 Conclusion

In this chapter, the structure of the O-chain from the LPS extracted from the psychrotolerant Gram-negative bacterium *Pseudomonas* sp. ANT_J38B, isolated from an Antarctic Island, is described. The repeating unit is a disaccharide composed of 2-acetamido-2,6-di-deoxyglucopyranose (β-D-3-QuipNAc) and 2-acetamido-2-deoxy-gulopyranuronamide acetylated at O-3 position (α-L-4-GulpNAc3OAcAN). The presence of a high number of acetyl substituent, conferring a high hydrophobic character to the molecule, may explain the unusual recovery of a smooth LPS from the PCP extraction. The described O-chain has already been found for the LPS isolated from the mushroom's pathogenic bacterium *Pseudomonas tolasii*, where an uncomplete acetylation at O-3 of GulNAcAN residue was observed (Molinaro A. et al., 2003). The finding of the O-chain in the LPS of psychrophiles is not common, since up to now the majority of the LPSs from cold-adapted bacteria grown at low temperatures characterised were rough (Casillo A. et al., 2019). To date smooth-LPSs have been isolated exclusively for cold-adapted bacteria grown at temperatures above 20 °C. A common feature of O-chain from psychrophilic bacteria is the presence of both uronic acids and amino sugars (Kilcoyne M. et al., 2004; Hoffman J. et al., 2012) and of acyl substituents. The presence of hydrophobic residues may suggest the ability to counteract the ice crystal formation around the cell, as demonstrated for some capsular and extracellular polysaccharides (Carillo S. et al., 2015; Casillo A. et al., 2017).

Based on studies reported in the literature the LPS structure seems to be essential for bacterial adaptation at low temperatures, but it is not possible to assign a role to the O-chain in this context. A possible correlation between the O-chain expression and cold adaptation could be achieved through molecular biology experiments that allow to obtain, starting from bacteria with a smooth-LPS, rough-LPS mutants. The genome of *Pseudomonas* sp. ANT_J38B is not sequenced, therefore, it was not possible to perform molecular biology

experiments in order to obtain a rough mutant and evaluate its ability to grow at lower temperatures. For this reason, the psychrotolerant bacterium *Idiomarina zobellii* KMM 231^{T} able to produce a S-LPS was bought.

Idiomarina zobellii KMM 231^T

The *Idiomarina* genus belongs to the *Idiomarinaceae* family, member of the *Gammaproteobacteria* class. It comprises Gram-negative marine bacteria, isolated from open and deep-sea water, with a temperature range of 4–30 °C, with optimal growth temperature between 20 °C and 22 °C. For this reason, *Idiomarina* are recognized as cold-adapted species. In addition, the members of this genus have been isolated from saline environments (Ivanova E. P. et al., 2004; Taborda M. et al., 2009). *Idiomarina zobellii* KMM 231^T is a psychrotolerant and halophilic bacterium isolated from a seawater sample taken at a depth of 4000–5000 m (salinity, 34%; temperature, 2 °C) in the north-western area of the Pacific Ocean during July 1985 (Ivanova E. P. et al., 2000). This bacterium is strictly aerobic, rod-shaped, with a single polar flagellum and a scarcely visible long fimbria originating at one pole, near the flagellum. Michelle Kilcoyne and colleagues (Kilcoyne M. et al., 2004) isolated the LPS produced by this bacterium and characterized the chemical structure of the O-polysaccharide moiety (Figure 8.1). The latter is composed of a linear pentasaccharidic repeating unit containing unusual monosaccharides, such as 2-amino-2-deoxy-L-guluronic acid (L-GulNA) and 4-amino-4,6-dideoxy-D-glucose (D-Qui4N).

→3)-α-D-Qui*p*4N-(1→4)-α-D-Glc*p*A-(1→6)-α-D-Glc*p*NAc-(1→4)-α-L-Gul*p*NA-(1→3)-α-D-Fuc*p*NAc-(1→

Figure 8.1 Structure of the O-polysaccharide repeating unit from the LPS of *I. zobellii* KMM 231^T.

Idiomarina zobellii KMM 231^T represents one of the few examples of cold-adapted bacteria producing a smooth-LPS.

During the second year of my PhD, I spent six months in the research group of Prof. Susana Merino (University of Barcelona) where I had the opportunity to work on the identification and characterization of glycosyltransferases involved in the LPS

biosynthesis of two *Aeromonas* species. During that period, I acquired crucial skills for the manipulation of genes involved in the LPS biosynthesis.

These methodologies have been applied to the study of the relationship between the structure of LPSs and their involvement in cold adaptation mechanism. To evaluate the role the O-polysaccharide of the LPS from *Idiomarina zobellii* KMM 231^T in cold-adaptation, I tried to insert a deletion of *waaL* gene that encodes for a putative O-antigen ligase. This protein links the O-chain repeating unit to the core oligosaccharide (Figure 8.2).

In this thesis, the O-antigen ligase gene is named RS11405 and its sequence is reported in the Appendix (see page 183).

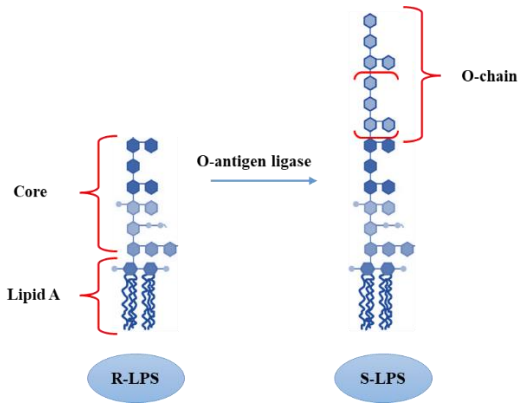

Figure 8.2 The O-antigen ligase converts Rough LPS (lipid A-core complex) into Smooth LPS, by attaching O-antigen.

Overview of the methodologies applied during the period at the University of Barcelona

Site specific mutagenesis by homologous recombination

To generate a gene deletion, reducing the polar effects that the mutation could produce in the expression of the other genes within the same cluster, a procedure known as crossover PCR can be used (Link A. J. et al., 1997). This method allows to create an in-frame deletion construct using two different PCR reactions. These latter amplify the **a** and **b** fragments (Figure 2.6), within the gene to delete, using the bacterial genomic DNA as template and specific oligonucleotide pairs (A–B and C–D, respectively). To create the **ab** construct the B and C primers can be designed to introduce an internal restriction site in order to link the **a** and **b** fragments (Giuliani M. et al., 2012). Also, the A and D primers possess restriction sites, since the obtained **ab** construct will be cloned in a non-replicating plasmid, also known as suicide plasmid, and transformed in the studied bacterium.

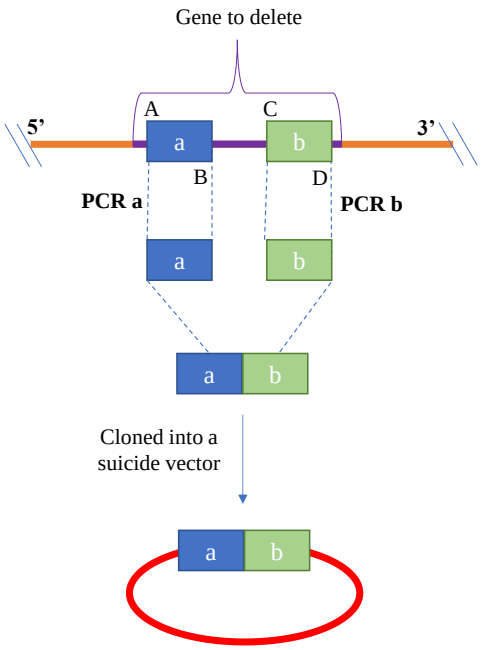

Figure 2.6 Generation of a deletion construct using crossover PCR.

The wild-type chromosomal gene with the obtained **ab** construct is replaced by homologous recombination, that is a mechanism of genetic material exchange between two DNA molecules containing large homologous regions. In bacteria, homologous recombination is one of the mechanism of DNA repair and a powerful genetic engineering tool used to introduce a mutation in a specific gene in order to investigate its function.

In particular, two crossing over events between the two chromosomal DNA segments with the synthetized **a** and **b** homologous fragments are necessary. The first recombination event allows the insertion of the entire plasmid on the genome, and for this reason this event is selected by imposing selection for the plasmid or a marker within the cloned sequences. Due to the presence of the **a** and **b** fragments, two different crossing over events can occurs, depending on which fragment undergoes recombination. The second recombination is an intramolecular crossing over event that can give the wild type gene, if the recombination is between the two **a** fragments

(Figure 2.6), or the mutated gene, if the recombination is between the two **b** fragments (Figure 2.7). In this case the mutant strain was selected for the loss of the integrated plasmid.

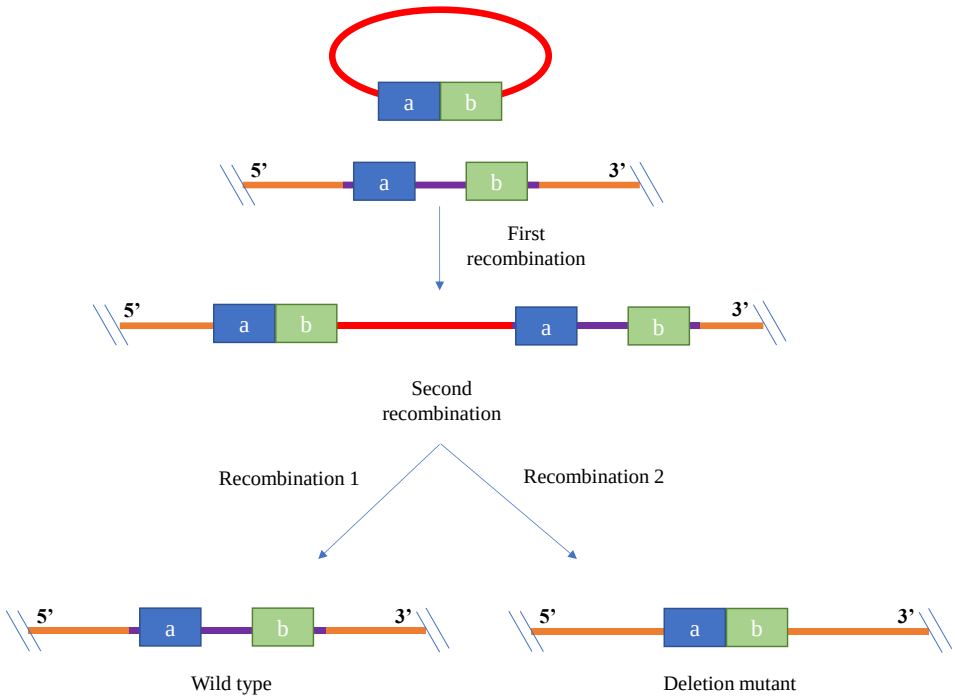

Figure 2.7 Schematic representation of the first and second homologous recombination events.

DNA transfer techniques

There are many approaches for the introduction of foreign DNA (transformation) into eukaryotes and prokaryotes, but the most commonly used are electroporation and conjugation.

1 Electroporation

Electroporation requires a brief, high intensity pulse in order to create transient pores in the cell membrane to facilitate the uptake of exogenous molecules, such as DNA and RNA. In literature is reported that exogenous DNA has been

successfully introduced with this technique into different kind of cells, such as plant cells, yeast cells animal cells and bacteria (Prasanna G. L. and T. Panda, 1997). In bacteria, can be applied to strains and species considered as untransformable so far and in some cases it is the only method of choice available for the transformation of intact cells.

During the first step of this method, cells are made competent to acquire exogenous material by several washings in cold, low ionic strength buffers. This allows to remove residual ions and substrates/metabolites from the growth medium, to stabilize cell membranes and to facilitate the DNA binding. Then, the cells are exposed to an electric field in the presence of the exogenous material, such as DNA. After the pulse, the mixture is incubated at the optimal temperature growth in an appropriate medium for bacterial repair. This incubation not allows the cell growth, because the cells are not incubated in the presence of the selective markers present in the acquired DNA. The efficiency of electroporation depends to the strain, but other factors can influence the experimental success, as pulse applied, growth conditions, and type of exogenous DNA.

2 Conjugation

Bacterial conjugation is the major horizontal gene transfer mechanism, where mobile elements as plasmids and transposons are transferred from a donor to a recipient bacterium by direct cell-to-cell contact. The bacterial conjugation machinery depends on the presence of a plasmid, known as conjugative or F-plasmid (F for fertility factor), containing an origin of transfer, also named oriT, and *tra* genes which encode all the proteins involved in conjugational transfer. The initiation of conjugation requires the expression of the *tra* genes, that form the type IV secretion system (T4SS) and the conjugative pilus. The latter is responsible of the recipient cell recruitment and mediates mating pair stabilization. Other Tra proteins of the complex, named relaxosome (TraI, TraM, and TraY), bind to the oriT and prepare the plasmid transfer by inducing the

nicking reaction by the TraI relaxase protein. When all the proteins necessary for conjugation are encoded by one individual plasmid, present in the donor strain, a biparental mating occurs. Otherwise, the complete conjugation machinery is encoded by more plasmids, thus involving a helper strain in addition to donor strain, and the process is defined as triparental mating. In particular, the helper plasmid encodes the transfer functions to move the mobilizable plasmid from the donor to the recipient strain. The main problem in the conjugation protocol is the selection of the donor strain from the recipient strain, known as transconjugant, after the mating. Up to now, many selection methods have been developed. A simple example is the selection of the conjugant cells of the cold-adapted bacterium *Pseudoalteromonas haloplanktis* TAC125 from *E. coli* donor cells by growing the conjugation mixture at 4°C, temperature not suitable for *E. coli* growth (Wang P. et al., 2015).

Chapter VIII: *Idiomarina zobellii* KMM 231^T

8.1 LPSs from *Idiomarina zobellii* KMM 231^T grown at different temperatures

Idiomarina zobellii KMM 231^T was grown in Marine Broth at three different temperatures (4, 15 and 25 °C). The results suggested that this bacterium was not able to grow at 4 °C and that the growth at 25 °C was faster than at 15 °C.

The LPSs from *I. zobellii* KMM 231^T cells grown at 15 °C and 25 °C were extracted by phenol/water method (Westphal O. and Jann K., 1965) and their smooth nature, at both temperatures, was confirmed by 14% DOC-PAGE analysis visualised after silver nitrate staining (Figure 8.3).

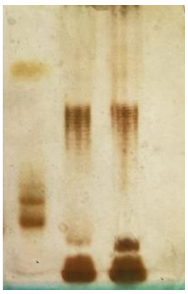

Figure 8.3 14% DOC-PAGE analysis. The gel stained with silver nitrate displays in lane **A** the smooth-LPS from *E. coli* O127: B8, used as a standard; lanes **B** and **C** the phenol/water extracts from *Idiomarina zobellii* KMM 231^T at 15 and 25 °C, respectively.

The sugar composition of the isolated LPS molecules was achieved by the GC-MS analysis of the correspondent AMGs. The experiments confirmed, at both temperatures, the presence of glucuronic acid (GlcA), 2-amino-2-deoxy-guluronic acid (GulNA), glucosamine (GlcN), 2-amino-2-deoxy-fucose (FucN) and 4-amino-4-deoxy-quinovose (Qui4N), as already found in literature (Kilcoyne M. et al., 2004).

8.2 Suicide plasmid construction

To select the suicide plasmid, MIC (Minimal Inhibitory Concentration) assays were performed. This strain was found to be resistant to ampicillin and susceptible to rifampicin, chloramphenicol, and kanamycin.

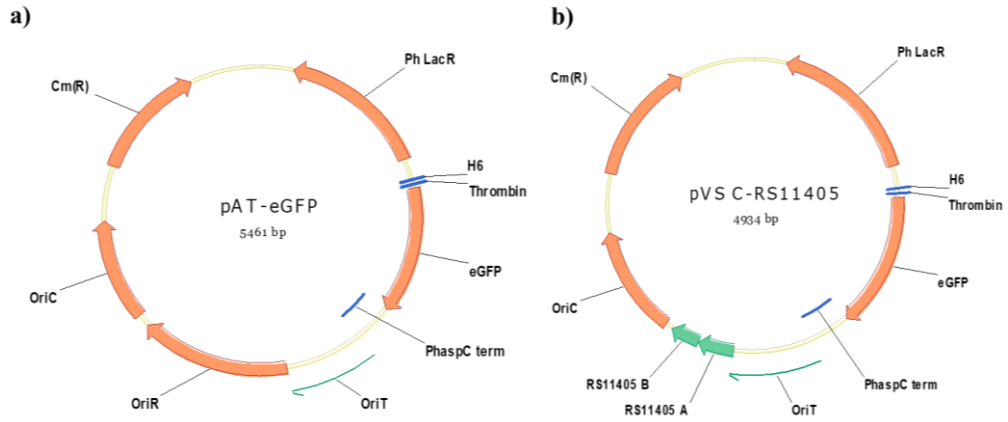

Figure 8.4 Maps of **a**) pAT-eGFP and **b**) pVS C-RS11405 vectors. The common elements to the two plasmids are the selection marker, which is a chloramphenicol acetyltransferase encoding sequence [cm(R)] and replication origin in *E. coli* (OriC).

Therefore, pAT-eGFP was selected due to the presence of *cm*(R) gene conferring resistance to chloramphenicol. Polymerase chain reaction (PCR) amplifications were used to produce two fragments, using as a template the chromosomal DNA extracted from *Idiomarina zobellii* KMM 231^{T}. One of two fragments contained 180 bp (A) of RS11405 gene was obtained by using primers RS11405-fw_A and RS11405-rv_A, whereas the other contained 153 bp (B) of RS11405 gene by using primers RS11405-fw_B and RS11405-rv_B (primers used for plasmid construction can be found in Table 9.10).

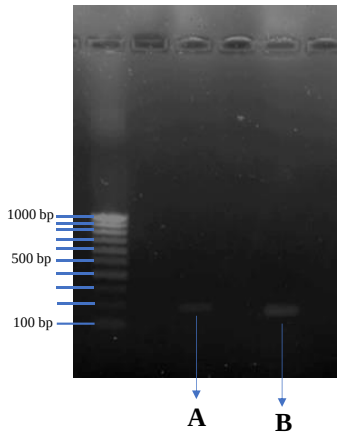

Figure 8.4 1.2% Agarose gel of the PCR amplifications of **A** (180 bp) and **B** (153 bp) fragment. As bp marker 1000 bp DNA ladder (Eurogentec) was used.

The **A** and **B** fragments (sequential and not adjacent in the gene) were amplified to provide a deletion in the RS11405 gene. The blend of the two fragments and the cloning into the suicide vector pAT-eGFP was performed by digestion with restriction enzymes to produce the construct pAT-eGFP ΔRS11405, named pVS-C RS11405 (Giuliani M. et al., 2012). The pVS-C RS11405 was transformed into a chemically competent *E. coli* strain (Top10), and the transformant colonies were selected on agar LB plate supplemented with Cm after incubation overnight at 37 °C. The presence of the insert was verified by both PCR and hydrolysis with restriction enzymes.

The recombinant plasmid was purified starting from a liquid culture of Top10 supplemented with Cm using the SmartPure Plasmid Kit (Eurogentec) according to manufacturer's protocol.

8.3 Transformation

Several marine strains belonging to different genera have been successfully transformed by electroporation, such as *Roseobacter*, *Vibrio*, *Pseudoalteromonas*, *Caulobacter*, *Cyanobacteria*, and *Halomonas* (Zeaiter Z. et al., 2018). In addition, conjugation protocol is a time-consuming procedure that also requires a specific step

to counter-select the donor from the transconjugant strains in the conjugation mixture. For these reasons, to insert the suicide vector pVS-C RS11405 into *Idiomarina zobellii* KMM231^T the electroporation method was selected.

Several electroporation experiments were performed to establish the optimal conditions. Different electroporation buffers (Table 9.11) were evaluated to made competent the cells to acquire the suicide vector.

In literature, it has been reported that the presence of high concentration of NaCl in the growth medium of marine bacteria is the main obstacle in the electroporation protocol (Zeaiter Z. et al., 2018). Therefore, to overcome this problem experiments with a different number of washings were performed to eliminate the remaining ions and the metabolites from the growth medium. Unfortunately, none of the experiments performed has been successful. Finally, *Idiomarina zobellii* KMM231^T was grown in LB to reduce the salt concentration, but also in this case the electroporation did not occur.

8.4 Conclusion

In conclusion, thanks to the skills acquired during my exchange period at the University of Barcelona, I tried to delete the *waaL* gene of *Idiomarina zobellii* KMM231^T. The lack of this gene determines the absence of the O-chain in the LPS molecule. The final goal was to assess that *waaL*-mutant of *Idiomarina zobellii* defected in the O-chain production could grow at lower temperature.

Currently, conjugation experiments are in progress to introduce the obtained suicide plasmid.

Concluding Remarks

The results obtained in the present thesis show structural characteristics commonly observed in psychrophilic bacteria, such as the rough nature of the LPS found for *Shewanella vesiculosa* HM13 and *Pseudoalteromonas nigrifaciens* Sq02. In addition, lipid A structures displayed fatty acids with short acyl chains ranging from 10 to maximum 15 carbon atoms in length. These two features allow to enhance the flexibility and to maintain the correct fluidity of the outer membrane leading to a good solute exchange rate at low temperatures.

S. vesiculosa HM13 was also grown at two different temperatures (4 ° C and 18 °C). The LPSs isolated in both conditions are rough (LOS) and share the same sugar moiety and fatty acids composition. Therefore, temperature variation seems to not implicate changes in the LPS structure. This result could be due to the fact that this bacterium is already cold adapted and then able to produce an LPS that possesses structural features allowing survival at low T.

S. vesiculosa HM13 was selected by our co-workers as host for the secretory production of foreign proteins at low temperature (Chen C. et al., 2020), due to its ability to secrete abundant amount of EMVs containing a single major cargo protein (P49) with an unknown function. The analysis of the P49 gene cluster revealed the presence of genes encoding homologs of surface glycolipid biosynthesis proteins. Among the latter HM3343 was found, a protein with homology with a flippase (Wzx) involved in membrane translocation of the repeating units constituting the O-chain of a S-LPS or CPS. When *hm3343* was disrupted, P49 was not loaded to the EMVs and released into the extracellular medium (Kamasaka K. et al., 2020). The analysis performed in this thesis on the LOS isolated from the vesicles at 18 °C revealed the same structure for the cells and vesicles. This result is in agreement with the budding biogenesis of the EMVs from the outer membrane (Kamasaka K. et al., 2020). In addition, it was demonstrated that the LOSs isolated from cells and EMVs of the *wzx*-mutant have the same structure already reported for the wild-type (Di Guida R. et al.,

2020). However, it has been found that the *wzx*-mutant secreted a lower amount of CPS of compared to the wild-type. This result could suggest that the protein encoding by *wzx* is involved in the membrane translocation of the repeating units of this polysaccharide, in turn implicated in the P49 association to cells and vesicles.

Shewanella vesiculosa HM13 and *Pseudoalteromonas nigrifaciens* Sq02 are also able to produce capsular polysaccharides, ability not observed for *Pseudomonas* ANT_J38B. The CPSs isolated are both made of branched repeating units containing all *N*-acetylated aminosugars. The capsular polysaccharide secreted by *S. vesiculosa* HM13 contains the α-3-acetimidoylamino-2,4-diacetamido-2,3,4,6-tetradeoxy-*galacto*-pyranose (named shewanosamine, ShewN), a monosaccharide not previously reported in the literature. This finding underlines how psychrophilic bacteria can be a valuable and promising resource of new molecules, still little explored compared to the mesophilic counterpart.

Common feature of the CPSs isolated is the high degree of acylation, which was already found in capsular polysaccharides from other Gram-negative bacteria (Fiebig T. et al., 2014; Micoli F. et al., 2018; Wang P. et al., 2004). This structural feature, that gives hydrophobicity to polysaccharides, could be related to the capacity of the bacterium to adhere to surfaces, since these two bacteria are able to produce biofilm. To confirm this hypothesis, adhesion assays of the CPS from *S. vesiculosa* HM13 on polystyrene nanoparticles and bacterial mimic vesicles were performed by DLS measurement. These experiments, together with zeta potential measurements, showed ability of the CPS to aggregate, forming a corona around the particles with a driving force attributable to hydrophobic interactions. This result could suggest a key role of this hydrophobic polysaccharide in the aggregate formation and attachment to surfaces by biofilms formation.

In addition, Ice Recrystallization Inhibition (IRI) assays were performed to evaluate a possible involvement of the isolated capsular polysaccharides in cold-survival through cellular cryoprotection. The results obtained have demonstrated that both CPS

do not possess a significative IRI activity at all the concentration tested (Biggs C. I. et al., 2019).

The finding of the O-chain is quite uncommon and to date S-LPSs have been isolated exclusively from cold-adapted bacteria grown above 20 °C. An exception is the S-LPS isolated in the present thesis from the Antarctic bacterium *Pseudomonas* ANT_J38B grown at 4 °C (Di Guida R. et al., 2020). The O-chain of this bacterium consists of a disaccharide repeating unit composed of 2-acetamido-2,6-di-deoxyglucopyranose and 2-acetamido-2-deoxy-gulopyranuronamide acetylated at O-3 position. Common feature of O-chain from psychrophilic bacteria is the presence of both uronic acids and amino sugars (Kilcoyne M. et al., 2004; Hoffman J. et al., 2012) and of acyl substituents. Acidic monosaccharides confer to the molecule an anionic character, increasing the ability to bind environmental cations (Ca^{2+} and Mg^{2+}) in order to overcome the electrostatic repulsion among them. In this way, the glycolipids can organize in a rigid net of cross-linkages through the metallic ions, providing higher resistance to physical stressors. In addition, the presence of hydrophobic residues may suggest the ability to counteract the ice crystal formation around the cell, as demonstrated for some capsular and extracellular polysaccharides.

To shed light on the role of the O-chain in the bacterial survival at low temperature molecular biology experiments has been performed. To date this kind of experiments performed using the cold-adapted bacteria, *Photobacterium profundum* SS9 (Lauro F. M. et al. 2008) and *Pseudomonas extremaustralis* (Benforte F. C. et al, 2018), showed that the LPS structure is essential for the cold adaptation, even if it is not possible to speculate about the O-chain role.

The genome of *Pseudomonas* sp. ANT_J38B is not sequenced, therefore, it was not possible to perform molecular biology experiments in order to obtain a rough mutant and evaluate its ability to grow at lower temperatures. For this reason, the psychrotolerant bacterium *Idiomarina zobellii* KMM 231^T able to produce a S-LPS was bought. During the last part of the PhD project, I tried to insert in the genome of this bacterium the deletion of the gene encoding for the O-antigen ligase, a protein

involved in the linkage between O-chain and core oligosaccharide-lipid A complex. All the electroporation experiments performed were unsuccessful, but conjugation experiments are currently in progress to introduce the obtained suicide plasmid.

Finally, the biological activities of the LPS and CPS isolated from *P. nigrifaciens* Sq02 were evaluated in order to find a possible application of these of biocompatible and biodegradable molecules. In particular, the immunostimulatory effect and the mechanism of action of the LPS and lipid A from *P. nigrifaciens* Sq02 were investigated on differentiated CaCo-2 cells. This cell line is considered the best *in vitro* model of human enterocytes and therefore is widely used for the study of the human intestinal barrier (Van De Walle, J. et al. 2010). The results showed a similar action to the commercial LPS from *E. coli* and *S. minnesota*. In fact, differentiated CaCo-2 cells increased TLR-4 expression at both mRNA and protein levels after LPS and lipid A treatments. Then, NF-κB pathway was activated towards cytokines production (Kaszowska M. et al., 2017; Nyati K. K. et al., 2017). Indication of the inflammation cascade induction in response to the LPSs/lipid A treatment have been obtained, validating the RT-PCR results. The CPS from *P. nigrifaciens* Sq02 possesses anti-cancer activity against two colon cancer cell lines (CaCo-2 and HTC-116). In particular, the results suggested a significant reduction in cell viability especially on HCT-116 cells after 72h of treatment with the CPS at 600 µg/mL. The molecular mechanism underlying the CPS activity was found to be the apoptosis, based on the gene and protein expression analyses of four specific markers associated with apoptosis (Bax, Caspase 3, Caspase 9 and Bcl-2). The high concentration of CPS tested in the present study was chosen in accordance with other studied reported in literature regarding the *in vitro* anti-cancer activity of bacterial polysaccharides (Li, W. et al. 2015; Liu, Z. et al. 2020). The results obtained *in vitro* appear to be promising, but it is essential that *in vivo* studies are performed to confirm those already reported. This together with the development of potential metabolic and genetic engineering strategies for enhanced yield of the capsular polysaccharide will be the subjects of future research.

Experimental Part

Chapter IX: Materials and methods

9.1 Bacterial growth

9.1.1 *Shewanella vesiculosa* HM13

Shewanella vesiculosa sp. HM13 growths were performed by Prof. Tatsuo Kurihara research group in Institute for Chemical Research of the Kyoto University.

9.1.1.1 Shewanella vesiculosa HM13 (4 °C)

S. vesiculosa HM13 was grown in 5 mL LB medium overnight at 18 °C. Five mL of the culture were inoculated into 1 L LB medium, and the cells were grown at 4 °C until the OD_{600} = 3.0-4.0. The cells were centrifuged at 6,800 × *g*, 4 °C for 10 min and the cellular pellet was freeze-dried.

9.1.1.2 Shewanella vesiculosa HM13 Rif^r (18 °C)

A spontaneous rifampin-resistant mutant of *S. vesiculosa* HM13 was grown aerobically in LB medium at 18 °C up to the stationary phase (OD_{600}= 2.5). The culture was centrifuged at 6,800 × g for 10-20 min at 4 °C to pellet the cells, which were washed with Dulbecco's phosphate buffered saline (DPBS: 0.2 g KCl, 0.2 g KH_2PO_4, 11.7 g NaCl, 1.2 g Na_2HPO_4, 0.1 g $MgCl_2 \cdot 6H_2O$, 0.1 g $CaCl_2$ in 1 L) and freeze-dried. Then the culture supernatant was centrifuged at 13,000 × g for 15 min at 4 °C. The supernatant thus obtained was filtrated with 0.45-µm membrane filter. The filtrate was concentrated with Minimate™ Tangential Flow Filtration system equipped with a 500K Minimate capsule with Omega membrane (Pall Corporation, Port Washington, NY, USA) at 4 °C. The concentrate was ultracentrifuged at 100,000 × g for 2 h at 4 °C to collect EMVs, which were freeze-dried.

9.1.1.3 *Shewanella vesiculosa* HM13 Rif^r *wzx*- mutant (18 °C)

S. vesiculosa HM13 *hm3343*::pKNOCK mutant (Kamasaka K. et al., 2020) was grown in 5 mL LB medium containing 50 μg/mL of rifampin at 18 °C until OD_{600} = 0.8-1.2. Five mL of the culture were inoculated into 1 L LB medium containing 50 μg/mL of rifampin, and the cells were grown at 18 °C until the OD_{600} = 2.0-3.0. The cells were centrifuged at 6,000 × *g*, 4 °C for 15 min and the cellular pellet was washed with Dulbecco's phosphate buffered saline (DPBS: 0.2 g KCl, 0.2 g KH2PO4, 11.7 g NaCl, 1.2 g Na2HPO4, 0.1 g MgCl2·6H2O, 0.1 g CaCl2 in 1 L) and freeze-dried. Then the culture supernatant was centrifuged at 15,000 × g for 15 min at 4 °C. The supernatant obtained was filtrated with 0.45-μm membrane filter. The filtrate was concentrated with MinimateTM Tangential Flow Filtration system equipped with a 500K Minimate capsule with Omega membrane (Pall Corporation, Port Washington, NY, USA) at 4 °C. The concentrate was ultracentrifuged at 100,000 × g for 2 h at 4 °C to collect EMVs, which were freeze-dried.

9.1.2 *Pseudoalteromonas nigrifaciens* Sq02

Pseudoalteromonas nigrifaciens Sq02 growth was performed by Prof. Tatsuo Kurihara research group in the Institute for Chemical Research of the Kyoto University.

A spontaneous rifampicin-resistant mutant of *Pseudoalteromonas nigrifaciens* Sq02, named *P. nigrifaciens* Sq02-Rif^r, was used in this study. A single colony of *P. nigrifaciens* Sq02-Rif^r was inoculated to 5 mL of LB with supplementation of NaCl to a final concentration of 3% (LB-NaCl: 10 g Bacto Tryptone [BD Difco, Detroit, MI], 5 g yeast extract [BD Difco], and 30 g NaCl in 1 L) and containing 50 μg mL^{-1} rifampicin. The cells were grown at 18 °C to OD_{600} = 1.0 - 1.5 and 5 mL of the culture were inoculated to 1 L of LB-NaCl. After overnight cultivation at 18 °C, the cells at OD_{600} = 2.0 - 2.5 were centrifugated at 6,800 × *g* for 20 min at 4 °C and suspended in 6 mL of Dulbecco's phosphate-buffered

saline (DPBS: 0.2 g KCl, 0.2 g KH_2PO_4, 11.7 g NaCl, 1.2 g Na_2HPO_4, 0.1 g $MgCl_2 \cdot 6H_2O$, 0.1 g $CaCl_2$ in 1 L). The suspension was centrifuged at 6,800 × *g* and 4 °C for 10 min, and the pelleted cells were washed two times with 4 mL of DPBS. The collected cells were lyophilized.

9.1.3 *Pseudomonas* ANT J_38B

Pseudomonas sp. ANT_J38B cells were grown at 4°C in LB medium until the stationary phase and separated from the culture supernatant by centrifugation at 8000 rpm for 15 min at 4°C.

9.1.4 *Idiomarina zobellii* KMM 231^T

Idiomarina zobellii KMM 231^T was purchased by Leibniz Institute DSMZ-(German Collection of Microorganisms and Cell Cultures).

A single colony of *Idiomarina zobellii* KMM 231^T was inoculated to 2 mL of MB medium for 48 h at 25 °C. Then the culture was inoculated to 10 mL of MB. The cells at the stationary phase (OD_{600} = 1.0 ~ 1.5) were centrifuged at 7000 rpm for 30 min at 4 °C, collected and lyophilized.

9.2 LPS and CPS isolation

9.2.1 LPS extraction

9.2.1.1 *Shewanella vesiculosa* HM13

Dried cells and EMVs were extracted by PCP method (Galanos C. et al., 1969). In particular, the cells and EMVs were extracted three times with a mixture of aqueous phenol 90%/chloroform/light petroleum ether (2:5:8 v/v/v, ~10ml/g of dried cells). After removal of the organic solvents under vacuum, the LPS was precipitated from phenol with some drops of water. Then the precipitate was washed three times with cold acetone and lyophilized. The yields obtained are summarized in the following Table 9.1.

Table 9.1 - Yields obtained after PCP extraction.

	Dried cells	**LPS_{PCP}**	**Dried EMVs**	**LPS_{PCP}**
S. vesiculosa HM13 4 °C	1.4 g	31.9 mg	-	-
S. vesiculosa HM13 Rif^r 18 °C	3.8 g	114.4 mg	202 mg	38.9 mg
S. vesiculosa HM13 Rif^r *wzx*-mutant 18 °C	2.1 g	44.9 mg	81 mg	19.3 mg

9.2.1.2 *Pseudoalteromonas nigrifaciens* Sq02

4.78 g of dried cells were extracted by PCP method (Galanos C. et al., 1969), as already described in the 10.2.1.1 paragraph. In this case, no precipitation of the LPS was observed. For this reason, the phenol was diluted with water, dialysed against water (cut-off 3500 Da) and lyophilized, giving 36.7 mg of LPS.

9.2.1.3 *Pseudomonas* ANT J_38B

5.4 g of dried cells were extracted by PCP method (Galanos C. et al., 1969), as already described in the 9.2.1.1 paragraph. The precipitate was freeze-dried obtaining 30 mg of crude LPS. The residual cells were also extracted by hot phenol/water method (Westphal O. and Jann K., 1965). The pellet was suspended in aqueous phenol 90%/water (1:1 v/v, ~10ml/g of pellet) at 68°C. After three extractions with hot water the supernatant (water phase) was collected, dialysed against water (cut-off 3500 Da) and lyophilized. The water phase was purified from proteins and nucleic acids with enzymatic digestion with DNase, RNase and protease K (Sigma-Aldrich) and then dialysed.

9.2.1.4 *Idiomarina zobellii* KMM 231^T

The dried cells were extracted by hot phenol/water method (Westphal O. and Jann K., 1965). The pellet was suspended in aqueous phenol 90%/water (1:1 v/v, ~10ml/g of pellet) at 68°C. After three extractions with hot water the supernatant

(water phase) was collected, dialysed against water (cut-off 3500 Da) and lyophilized.

Table 9.2 - Yields obtained after hot phenol/water extraction.

	Dried cells	**Dialyzed aqueous phase**
Idiomarina zobellii KMM 231^T 15 °C	78 mg	12 mg
Idiomarina zobellii KMM 231^T 25 °C	62 mg	12 mg

9.2.2 CPS isolation and purification

9.2.2.1 *Shewanella vesiculosa* HM13

The phenol supernatants obtained from the LPSs precipitation (see paragraph 9.2.1.1) were diluted with water, dialysed against water (cut-off 3500 Da) and lyophilized. The obtained samples were hydrolyzed with 1% CH_3COOH aq. (10mg/mL, 100 °C, 3 h). The resulting mixture was then centrifuged (7500 rpm, 30 min, 4 °C). The supernatant layers were combined, lyophilized and fractionated on a Biogel P-10 column (Biorad, 1.5 × 110 cm, flow rate 17 mL/h, fraction volume 2.5 mL), eluted with water obtaining a major fraction containing a pure capsular polysaccharide. The yields obtained are summarized in the following Table 9.2.

Table 9.3 Yields obtained after GPC purification.

	Phenol extract cells	**CPS**	**Phenol extract EMVs**	**CPS**
S. vesiculosa HM13 Rif^r18 °C	161 mg	16.4 mg	37.4 mg	9.9 mg
S. vesiculosa HM13 Rif^r *wzx*-mutant 18 °C	100 mg	3.3 mg	19.3 mg	1 mg

9.2.1.2 *Pseudoalteromonas nigrifaciens* Sq02

After PCP extraction (see paragraph 10.2.1.2) the residual cellular pellet was also extracted by hot water/phenol method, according to Westphal and Jann procedure (Westphal O. and Jann K., 1965) (see paragraph 9.2.1.3). The pellet was suspended in aqueous phenol 90%/water (1:1 v/v, ~10ml/g of pellet) at 68°C. After three extractions with hot water the supernatant (water phase) was collected, dialysed against water (cut-off 3500 Da) and lyophilized. The water phase was purified from proteins and nucleic acids with enzymatic digestion with DNase, RNase and protease K (Sigma-Aldrich) and then dialysed.

100 mg of the obtained water extract was hydrolyzed with 1% CH_3COOH aq. (10mg/mL, 100 °C, 3-5 h). The resulting suspension was then centrifuged (7500 rpm, 4 °C, 30 min). The pellet was washed twice with water, and the supernatant layers were combined and lyophilized. The supernatant portion was then fractionated on a Biogel P-10 column (Biorad, 1.5 × 110 cm, flow rate 17 mL/h, fraction volume 2.5 mL), eluted with water obtaining a pure capsule polysaccharide fraction (10.8 mg).

9.3 Electrophoretic analysis

PAGE experiments were performed using the Laemmli system (Laemmli U .K. et al., 1970) with sodium deoxycholate (DOC) as detergent. The separating gel was prepared in order to contain final concentrations of 14% acrylamide, 0.1% DOC, and 375 mM Tris/HCl (pH 8.8); while the stacking gel of 4% acrylamide, 0.1% DOC, and 125 mM tris/HCl (pH 6.8). Samples were prepared at a concentration of 0.05% in the sample buffer (2% DOC, 60 mM Tris/HCl [pH 6.8], 25% glycerol, 14.4 mM 2-mercaptoethanol, and 0.1% bromophenol blue). The electrode buffer contained SDS (1 g/L), glycine (14.4 g/L), and Tris (3.0 g/L).

The DOC-PAGE was performed at a constant amperage of 0.03 A. Gels were fixed in an aqueous solution of 40% ethanol and 5% acetic acid. Samples were visualized

by silver nitrate (Tsai C. M. and Frasch C. E., 1982) and Alcian blue staining (Al-Hakim A. and Linhardt R. J., 1990).

9.4 Chemical analysis

- Sugars and fatty acids composition: 0.5 mg of LPS or CPS samples were treated with 1 M HCl/MeOH (1 mL, 80°C, 20 h). The obtained mixtures were extracted three times with hexane and the methanol layer was dried and acetylated with Ac_2O (50 μL) and Py (50 μL) at 100°C for 30 min. When phosphorylated sugars were present the sample was previously treated with 48% HF. The hexane layer containing fatty acids, as methyl esters, was directly analysed by GC-MS.
  Monosaccharides were also analysed as acetylated alditols. Briefly, 1 mg of the sample was reduced with $NaBD_4$ and then acetylated with Ac_2O (50 μL) and Py (50 μL) at 100 °C for 30 min. The obtained alditol acetates were detected by using GC-MS.
- Absolute configuration: The absolute configuration of the sugars was determined by derivatization of the monosaccharide as acetylated (S)-2-octyl glycosides (Leontein K. et al., 1978) and analyzed by GC-MS.
- Linkage analysis: The linkage positions of the monosaccharides were determined by GC-MS analysis of the partially methylated alditol acetates (PMAAs). Briefly, the sample (2 mg) was methylated with CH_3I (100 μL) in anhydrous DMSO (300 μL) and NaOH powder at room temperature for 20 h (Ciucanu I. et al., 1984). The product was hydrolyzed with 100 μL of 2 M TFA (120°C, 2 h), reduced with $NaBD_4$ and finally acetylated using Ac_2O (50 μL) and Py (50 μL) (100°C, 30 min).
- Quantitative analysis: The amount of rhamnose was evaluated by construction of an Internal Standard Calibration Curve via GC-MS. The curve was obtained preparing seven standards with known amount of rhamnose and to each 50 μg of inositol as internal standards was added. The same amount of the internal

standard is added to the samples. Both standards and samples (0.5 mg) were derivatized as AMGs and injected to GC-MS.

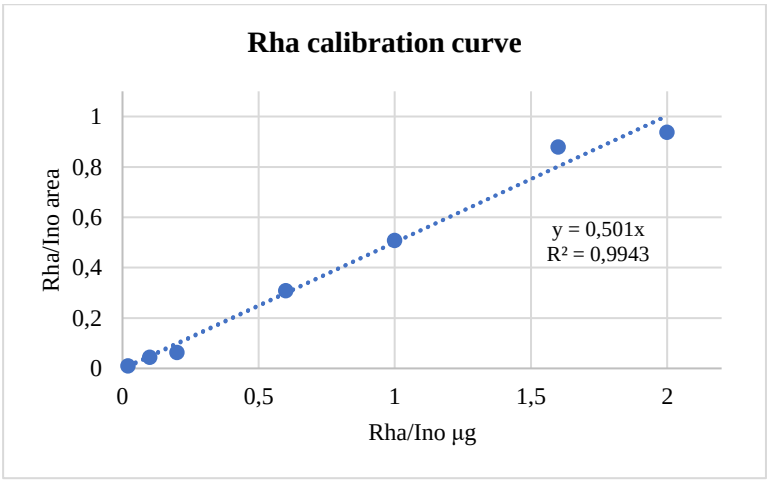

All of these derivatives were analysed on an Agilent Technologies gas chromatograph 7820A equipped with a mass selective detector 5977B and an HP-5 capillary column (Agilent, 30 m x 0.25 mm i.d.; flow rate, 1 mL min^{-1}, He as carrier gas), by using an appropriate temperature program reported in Table 9.3

Table 9.4 – Temperature programs for the derivatives.

Derivatives	Temperature programs
Acetylated Methyl Glycosides	150 °C for 3 min, 150 °C → 240 °C at 3 °C/min.
Methyl Esters Fatty Acids	140 °C for 3 min, 140 °C → 280 °C at 10 °C/min, 280 °C for 20 min.
Alditol acetates	150°C for 3 min, 150°C→240°C at 3°C/min.
Octyl Glycosides	150 °C for 5 min, then 150 °C → 240 °C at 6 °C/min, and 240 °C for 5 min.
Methylation analysis (AAPMs)	90 °C for 1 min, 90 °C → 140 °C at 25 °C/min, 140 °C → 200 °C at 5 °C/min, 200 °C → 280 °C at 10 °C/min, at 280 °C for 10 min.

9.5 Mild acid hydrolysis

The LPSs were hydrolysed with 1% CH_3COOH aq. (10mg/mL, 100°C, 3h) and the obtained suspensions were centrifuged (7500 rpm, 4 °C, 30 min). The precipitates (Lipid As) were washed twice with water and then lyophilized. The supernatant layers containing the saccharidic portions were then fractionated on a Biogel P-10 column (Biorad, 1.5 x 130 cm, flow rate 17 mL/h, fraction volume 2.5 mL) eluted with water and monitored with a Knauer refractive index.

9.6 De-*O* and de-*N*-acylation of LPS

The LPS samples were first dried under vacuum over P_2O_5 (3 h) and then treated with hydrazine (20mg/mL, 37°C, 2 h). The O-deacylated LPSs were precipitated by adding cold acetone. The pellets, collected by centrifugation (4°C, 7500 rpm, 30 min), were washed three times with acetone, suspended in water and finally lyophilized. The O-deacylated LPSs were treated with 4 M KOH at 120°C for 16 h. KOH was neutralized with 2 M HCl until pH 6 and the mixtures were extracted three times with $CHCl_3$. The water phases were recovered and desalted on a column Sephadex G-10 (GE Healthcare, 1.5 × 130 cm, 17 mL/h, fraction volume 2.5 mL, eluent water).

9.7 Ammonium hydroxide hydrolysis of lipid A

The lipid A (200 μg) were incubated with NH_4OH (200 μL), as reported (Silipo A. et al., 2002). The product was dried and analysed by mass spectrometry.

9.8 Isolation of Shewanosamine (ShewN)

The CPS sample (11.7 mg), isolated from *S. vesiculosa* sp. HM13 Rif^r cells, was treated with aq. NH_3 (12%, 170 μl) at 80 °C for 16 h (Kilcoyne et al., 2005) and the obtained mixture was simply dried under air flow. Then the product was fully hydrolysed with triflic acid (TfOH, 600 μl) under anhydrous conditions at room temperature for 24 h (Perepelov A. V. et al., 2000, Kocharova N. A. et al., 2001). The reaction mixture was neutralized with aq. NH_3 (16.5 %) and desalted on a Bio-Gel P-

2 column (Sigma, 16 × 0.5 cm, flow rate 8.4 mL/h, fraction volume 1 mL) using water as eluent. The desalted mixture was further purified on a HPLC Synergi™ 4 μm Polar-RP 80 Å column with methanol:water (4:1 v/v) as eluent.

9.9 Absolute configuration determination

The optical rotation was recorded on a JASCO P-1010 polarimeter using a sodium lamp (589 nm) as the light source.

9.10 Mass spectrometry

All the MS and the MS/MS experiments were performed in reflectron mode and negative ion polarity on an ABSCIEX TOF/TOF 5800 Applied Biosystems mass spectrometer equipped with an Nd:YAG laser (λ = 349 nm), with a 3 ns pulse width and a repetition rate of up to 1000 Hz, and also equipped with delayed extraction technology. Mass calibration was obtained with a hyaluronan oligosaccharides mixture. Spectra were calibrated and processed under computer control by using the Applied Biosystems Data Explorer software.

LOS sample was first suspended in a mixture of methanol/water (1:1) containing 5 mM ethylenediaminetetraacetic acid (EDTA). A few microliters of the obtained mixture were then desalted with some grains of cation-exchange beads (Dowex 50WX8-200, Sigma–Aldrich), previously converted into the ammonium form. To 0.5 μL of this solution was added the same volume of 20 mM dibasic ammonium citrate solution. While Lipid A and NH_4OH-treated Lipid A samples were dissolved in $CHCl_3/CH_3OH$ (4:1, v/v) at a concentration of about 25 pmol/μL. The matrix is a solution prepared by dissolving 2,4,6-trihydroxyacetophenone (THAP) in CH_3OH/H_2O (1:1, v/v) at a concentration of 10 mg/mL. In all the cases, 0.5 μL of the sample and 0.5 μL of the matrix solution were deposited onto a stainless-steel plate and dried at room temperature.

9.11 NMR spectroscopy

1D and 2D NMR (^{1}H-^{1}H COSY, ^{1}H-^{1}H TOCSY, ^{1}H-^{1}H ROESY, ^{1}H-^{1}H NOESY, ^{1}H,^{13}C HSQC-DEPT, F*2*-coupled HSQC, and ^{1}H,^{13}C HMBC) spectra were recorded using a Bruker 600 MHz spectrometer equipped with a cryo-probe(Billerica, MA, USA). All these experiments were performed by using standard pulse sequences available in the Bruker software. The mixing time for TOCSY, ROESY and NOESY experiments was 100 ms. ^{13}C, ^{31}P and ^{1}H-^{31}P spectra were recorded at 298 K using a Bruker Ascend 400 MHz spectrometer (Billerica, MA, USA).

Chemical shifts were measured in D_2O using acetone as internal standard (δ_H 2.225 and δ_C 31.45) or sodium 3-trimethylsilyl-(2,2,3,3-^{2}H4)-propanoate (TSP, δ_H 0.00) and 1,4-dioxane (δ_C 67.40) as external references. Phosphoric acid was used as an external reference (δ 0.00) for ^{31}P NMR spectroscopy.

9.12 Ice Recrystalization Inhibition (IRI) assays

A 10 µL droplet of sample in PBS solution was dropped from 1.4 meters into a glass microscope coverslip, which was placed on top of an aluminum plate cooled to -78 °C using dry ice. The droplet froze instantly upon impact with the plate, spreading out and forming a thin wafer of ice. This wafer was placed on a liquid nitrogen cooled cryostage held at -8 °C and left to anneal for 30 minutes at -8 °C. The number of crystals in the image was counted using ImageJ, and the area of the field of view divided by this number of crystals to provide the average crystal size per wafer and reported as a percentage (%) of area compared to PBS control. Standard deviation was calculated from three independent repeat measurements.

Table 9.5 Mean grain size (MGS) of the ice crystals measured at different concentrations of CPS. The MGS is expressed as a percentage of PBS buffer.

Concentration (mg/mL)	CPS from *S.vesiculosa* HM13		CPS from *P. nigrifaciens* Sq02	
	MGS (% of PBS)	Standard Deviation	MGS (% of PBS)	Standard Deviation
1.25	88.0	7.1	96.1	6.5
2.5	91.6	5.6	92.4	6.6
5	84.2	6.5	86.2	4.5
10	63.6	2.5	76.3	2.5

9.13 Physico-chemical measurements

9.13.1 Static and Dynamic Light Scattering (SLS and DLS) characterization

Static and Dynamic Light Scattering (SLS and DLS) measurements were performed at scattering angle θ=90°, by using a home-made instrument composed by a Photocor compact goniometer, a SMD 6000 Laser Quantum 50 mW light source operating at 532.5 nm, a photomultiplier (PMT120-OP/B) and a correlator (Flex02-01D) from Correlator.com. Measurements were performed at 25 °C with the temperature controlled by means of a thermostat bath.

DLS measurements has been conducted at polymer concentration of 5.0 mg/ml. For SLS measurements a concentration range between $2.5 \cdot 10^{-3}$ and $5.0 \cdot 10^{-4}$ g/ml has been chosen.

The mass-average molecular weight M_w and the second virial coefficient B of each polysaccharide were determined by means of Zimm plot analysis

$$\frac{Kc}{R_\theta} = \frac{1}{M_w} + 2B$$

where c is the sample mass concentration, $K = \frac{4\pi^2 n_0^2 (dn/dc)^2}{N_A \lambda^4}$ with n_0 = 1.33 the refractive index of water, *dn/dc* = 0.185 the refractive index increment with concentration, N_A the Avogadro's number, λ the laser wavelength in vacuum, R_θ the excess Rayleigh ratio at 90°. The value of R_θ was obtained from $R_\theta = (I_s - I_{s,0}) / I_{s,R} (n_0^2 / n_R^2) R_{\theta,R}$ where I_s is the scattered intensity of the solution, $I_{s,0}$ is the scattered intensity of water, $I_{s,R}$ is the scattering intensity of toluene (the standard) and, n_R = 1.496 and $R_{\theta,R}$= 2.85 10^{-5} cm^{-1} are the refractive index and the Rayleigh ratio of toluene, respectively.

9.13.2 Zeta potential measurements

Surface charge (zeta potential) was evaluated by means of electrophoretic light scattering using a Zetasizer Nano ZSP (Malvern Instruments, England) using polystyrene Folded Capillary Zeta cells (Malvern Instruments). Each measurement was performed at 25 °C upon a 120 s equilibration time, and the average of three measurements at a stationary level was taken. The zeta potential was calculated by applying the Smoluchowski model.

9.13.3 Vesicles preparation

The vesicles composed of POPE, POPG, and LPS were prepared with compositions70/30 and 56/24/20 mol % (named POPE/POPG and POPE/POPG/LPS, respectively).

The phospholipids and LPS were independently dissolved in chloroform (10 mg/mL lipid concentration). Proper volumes of these solutions were used to form lipid films with the above reported lipid molar. The lipid films were produced by evaporating the organic solvents under nitrogen flow. Final traces of the solvents were removed by storing the sample under vacuum for at least 3 h. The lipid films were re-suspended with 1 mL of bidistilled water and repeatedly vortexed. The produced multilamellar vesicles (MLVs) were repeatedly extruded through polycarbonate membranes of 100 nm pore size, for at least 21 times, before the DLS measurements to produce SUV (small unilammellar vesicles) suspensions.

9.14 Biological assays

9.14.1 Cell culture

The tumorous cell lines, human colorectal carcinoma cell line (HCT-116) and human colon cancer cells (CaCo-2), were cultured on RPMI (Roswell Park Memorial Institute) media and Dulbecco Modified Eagle medium (DMEM), respectively. All the media were additional supplemented with 200 mM L-glutamine, 10% fetal bovine serum (FBS; Gibco), and 1% penicillin/streptomycin. Cell culture was performed in 25 cm^2 or 75 cm^2 cell culture flasks at 37 °C in a humidified incubator with 5% CO_2 atmosphere. Cell culture medium was changed every 48 h, and cells were harvested by 0.05% trypsin/EDTA (Thermo Fisher Scientific) after reaching 80–90% confluence.

Caco-2 cells (Human Caucasian colon adenocarcinoma cells, ATCC® HTB-37™) were grown in Dulbecco's modified eagle medium (DMEM) containing glucose and glutamine and supplemented with 10% (v/v) fetal bovine serum (FBS). The cells were grown in a sterile 25 cm^2 flask at a concentration of 3 x 10^5 to confluence for 21 days to reach full differentiation in normal enterocytes. THP1-Blue™ NF-κB reporter cells were obtained from InvivoGen (Toulouse, France) and maintained in RPMI 1640 medium containing glucose (2 g/L) and glutamine (0.3 g/L), supplemented with 10% (v/v) FBS, 100µg/ml, Normocin™, and Pen-Strep (100 U/ml). Cells were incubated at 37 °C in a humidified atmosphere of air/CO_2 (95:5, v/v).

9.14.2 RNA extraction and gene expression using qRT-PCR analyses

The total RNA was extracted from treated cells, using TRIzol® Reagent (Thermo Fisher Scientific, Waltham, MA USA) (Stellavato A. et al., 2016). By using Reverse Transcription System Kit (Promega, Milan, Italy), cDNA was synthesized, according to the manufacturer's instructions. The Quantitative real-time polymerase chain reactions (qRT-PCR) were performed using the IQ™ SYBR® Green Supermix (Bio-Rad Laboratories, Milan, Italy) and forward and

reverse primers (Table 10.5), according to the manufacturer's protocol. The PCR reactions were run in triplicate and glyceraldehyde-3-phosphate dehydrogenase (GAPDH) housekeeping gene was used to normalize the mRNA expression of analysed genes. The variations were calculated using the comparative threshold method (ΔΔCt = difference in ΔCt between CPS-treated cells and control) and the results are reported as the normalized fold expression through $2^{-\Delta\Delta Ct}$ quantification method (Stellavato A. et al., 2016) by Bio-Rad iQ5 software (Bio-Rad Laboratories, Italy).

Table 9.6 - Primer sequences used for qRT-PCR analyses

Gene Name (symbol)	PCR primer sequence 5′→ 3′	Annealing Temperature (°C)
Glyceraldehyde-3-phosphate dehydrogenase (GAPDH)	TGCACCACCAACTGCTTAGC GGCATGGACTGTGGTCATGAG	57
Caspase 3	ATGGAAGCGAATCAATGGAC ATCACGCATCAATTCCACAA	57
Caspase 9	GCGAACTAACAGGCAAGCA CCAAATCCTCCAGAACCAAT	57
Toll like receptor 4 (TLR-4)	TCCCAggAATTggTgATAAAgTAgA CTggCATgACgCgAACAATA	55
Interleukin 6 (IL-6)	GTGGAGATTGTTGCCATCAACG CAGTGGATGCAGGGATGATGTTCTG	55

9.14.3 Protein levels evaluation by western blotting analyses

After treatment western blotting analyses were performed. Cells were lysed in Radio-Immunoprecipitation Assay (RIPA buffer 1x; Cell Signaling Technology) and intracellular protein concentration was quantified using the Bradford method.

In the case of TLR-4 and NF-κB level evaluation, 50 µg of proteins for each sample were resolved on a 10% SDS–PAGE gel and transferred onto

nitrocellulose membrane (GE, Amersham, UK). Then, the membrane was blocked by 5% w/v non-fat milk in Tris-buffered saline and 0.05% v/v Tween-20 (TTBS) for 30 min and incubated overnight at 4 °C with primary antibodies against TLR-4 (Abcam, Cambridge, UK) and NF-κB (Santa Cruz, Dallas, TX, USA) diluted 1:500. Then the membrane was incubated with secondary antibodies, horseradish peroxidase-conjugated donkey anti-rabbit and goat anti-mouse, diluted 1:5000 for 2h at room temperature. Anti-β-tubulin antibody diluted 1:1000 was used as loading control. The signal was detected using the ECL system (Chemicon-Millipore, Milano, Italy) and the semi-quantitative analyses of protein expression were carried out with the ImageJ program.

While in the case of Caspase 3, 9, Bax, and Bcl-2 level evaluation, 20 µg of proteins were resolved on 12% SDS-PAGE and transferred to a nitrocellulose membrane (GE, Amersham, UK). The membrane was blocked with 5% non-fat milk in Tris-buffered saline and 0.05% Tween-20 (TBST) and primary antibodies to detect Caspase 3, 9, Bax, and Bcl-2 (Cell Signaling Technology, Inc., Danvers, MA) were used at 1:1000 dilutions and incubated overnight at 4°C. The nitrocellulose membrane was extensively washed with TBST and immunoreactive bands were detected by chemiluminescence using corresponding horseradish peroxidase-conjugated secondary antibodies (Santa Cruz Biotechnology, CAUSA) diluted 1:10000 for 1 h, at room temperature and an ECL system (Millipore). Protein levels were normalized versus the signal obtained with an anti-tubulin antibody 1:500 dilutions (Santa Cruz Biotechnology, CA, USA). The semi-quantitative protein level analysis was performed using the Gel Doc 2000 UV System according to the manufacturer's protocol.

9.14.4 Quanti- THP1-Blue assay, Caco-2/THP-1 co-culture

Caco-2 monolayers were cultured to confluence (triplicates for each condition) for 21 days to reach full differentiation according to previously reported

protocols. In order to obtain a gut inflammation model, these monolayers were incubated with commercial LPS (LPS-from *Salmonella minnesota* S-form, Enzo Life Sciences NY, USA) and LPS isolated from *P. nigrifaciens* at 20 µg/mL for 24h. Successively, THP1-Blue™ cells were added to start co-culture. Specifically, monocytes (THP-1) were added to the LPS-treated monolayers at a concentration of 5×10^4 cells mL^{-1} to obtain a co-culture model (Calatayud M. et al., 2021; Rakshit et al., 2021). Supernatants were collected after 6h incubation for NF-κB quantification (Quanti-Blue reagent, InvivoGen, Toulouse, France). The assay was performed following manufacturer's instructions and luminescence intensity was quantified at 655 nm using Microplate Reader (Biorad Laboratories, Milan Italy) to determine SEAP (secreted embryonic alkaline phosphatase) levels.

9.14.5 Cell viability assay

CaCo-2 and HCT-116 cells were incubated in FBS supplemented with DMEM (untreated cells, CTR), and in the presence of the CPS samples at two different concentrations (600 and 200 µg mL^{-1}) in triplicate. The cells were incubated for 72 h, and their viability was assessed at 24 h, 48h, and at the end of the experiment using Cell Counting Kit-8 (CCK8) (Dojindo, EU GmbH) following the manufacturer's protocol. The optical densities were measured at 450 nm using a Beckman DU 640 spectrometer (Beckman, Milano, Italy). The relative cell viability was calculated as a percentage of the maximal absorbance, considering average values on triplicate of each specific condition tested:

$$\text{Vitality} = (100\text{x mean OD treated cells})/(\text{mean OD control})$$

9.15 Molecular genetic techniques

9.15.1 Materials

9.15.1.1 Growth media

To make 1 L of LB broth, 20 g of LB (Sigma-Alrdich) powder were dissolved in deionised water. For 1 L of LB agar 15 g of Technical agar No. 3 were used. LB broth and agar were autoclaved.

To make 1 L of MB broth and agar, 37.4 g or 55.1 g of Marine Broth 2216 or Marine Agar 2216 (Difco) powder were added to deionised water. The mixture was stirred during heating and boiled for 5 min. MB broth and agar were autoclaved.

9.15.1.2 Antibiotics

Antibiotics dissolved in water were filtered through 0.2 µm pore sterile filter; those dissolved in ethanol or DMSO were not filtered. Antibiotic aliquots were stored at -20°C.

Table 9.7 - Antibiotic stock solution used in this study

Antibiotic	Stock concentration (mg ml^{-1})	Solvent
Ampicillin (Amp)	100	water
Chloramphenicol (Cm)	50	ethanol
Kanamycin (Kan)	50	water
Rifampicin (Rif)	50	DMSO

9.15.2 Methods

9.15.2.1 DNA isolation

The genomic DNA of *Idiomarina zobellii* KMM231^T was isolated by using the E.Z.N.A. Bacterial DNA Kit (omegabiotek), following the procedure indicated

by the kit. The DNA amount was evaluated by absorbance measurements using NanoDrop™ Lite Spectrophotometer (Thermo Scientific).

9.15.2.2 Plasmid isolation

5 ml of bacterial culture was centrifuged at 4000 × g for 10 min. The supernatant was discarded and the cell pellet used to isolate plasmid DNA with the SmartPure Plasmid Kit (Eurogentec) according to manufacturer's protocol. Plasmid DNA was eluted in 50 µl of EB buffer provided with the kit. Plasmid isolation was confirmed using the agarose gel electrophoresis.

9.15.2.3 Agarose gel electrophoresis

DNA was analysed on 0.7-1.2% (w/v) agarose gels prepared with 1x TAE buffer (50x TAE buffer, PanReac AppliChem). To detect the DNA, RedSafe Nucleic Acid Staining Solution (0.5 µg/ml) was added to the gel. Gel Loading Dye Purple (New England BioLabs) was added to the DNA sample in proportion 1:6 prior to electrophoresis, and either the 1 kb DNA ladder (NEB) or 1000 bp DNA ladder (Eurogentec) were used as molecular size markers. Gels were run at 80 V and the DNA fragments were visualized using a ChemiDoc MP Imaging System (BioRad).

9.15.2.4 Purification of DNA fragments from agarose gel

The purification of DNA fragments excised from agarose gel is performed using the QIAquick Gel Extraction Kit (QIAGEN), according to manufacturer's protocol.

9.15.2.5 Polymerase chain reaction (PCR)

PCR reactions were performed using the protocol provided by the Red Diamond *Taq* DNA Polymerase (Eurogentec). The 20 mM dNTP mix (Eurogentec) was used in all the PCR reactions. Colonies or purified DNA were used as templates

for the PCR reaction. If colonies served as a template, they were resuspended in 25 µl of lysis buffer (1% Triton X-100, 20 mM Tris, 2 mM EDTA, pH 8), incubated at 100 °C for 5 minutes. Then 2 µl of this latter suspension was added to a 48 µl PCR reaction. In case of purified plasmid or genomic DNA, 50 ng of DNA was used in the PCR reaction.

Table 9.8 - PCR reactions mixtures

Reagent	**DNA PCR**	**Colonies PCR**
	Amount	**Amount**
*Reaction buffer 10x	5 µl	5 µl
*MgCl2 solution 1.5 mM	3 µl	3 µl
*****Red Diamond *Taq* (5U/µl)	0.25 µl	0.25 µl
dNTPs 20 mM	2 µl	2 µl
Primer F 10 µM	1 µl	1 µl
Primer R. 10 µM	1 µl	1 µl
DNA template	50 ng	2 µl of lysis
H_2O dd	Fill up to 50 µl	Fill up to 50 µl

* asterisks indicate the product provided by the kit

PCR reactions were performed in a T100 Thermal Cycler (BIO RAD). The lid was pre - heated to 105°C and after completion PCR reactions were incubated at 4°C in the PCR machine. Then the PCR products were visualised by agarose gel electrophoresis.

Table 9.9 - Cycling conditions provided by the Red Diamond *Taq* DNA Polymerase (Eurogenetec). Steps 2) – 4) are repeated 25 times. X = annealing temperature (T_a) varied based on the primers length (for **A** and **B** fragments PCR reaction was 65 °C). Y = extension time varied depending on length of amplicon, generally 1kb per minute (for **A** and **B** fragments PCR reaction was 30 sec).

Step	time	temperature
1) Initial Denaturation	10 min	95°C
2) Denaturation	30 sec	94 °C
3) Annealing	30 sec	X = Tm – 2 °C
4) Elongation	Y = 1 min/kb	72 °C
5) Final Elongation	7 min	72 °C
6) Hold	4 °C	end time

9.15.2.6 Suicide plasmid construction

The suicide plasmids for O-antigen ligase gene deletion was constructed starting from pAT-eGPF (provided by prof. M. L. Tutino and E. Parrilli). Two DNA fragments of this gene (**A** and **B**) were amplified by PCR using bacterial genomic DNA as template with two primer pairs designed to amplify a 180 bp region (**RS11405-fw_A**, **RS11405-rv_A**) and a 151 bp region (**RS11405-fw_B**, **RS11405-rv_B**) of the gene. In addition, the primers **RS11405-fw_B** and **RS11405-rv_A** were designed to include an EcoRI-High-Fidelity (HF®) restriction site, primer **RS11405-fw_A** an NotI- HF® site and **RS11405-rv_B** an AscI site. To obtain pVS C-RS11405 plasmid the **A** fragment was digested with EcoRI-HF® and NotI-HF®, while **B** with EcoRI-HF® and AscI. Then these two digested fragments were cloned into pAT-eGPF (provided by prof. M.L Tutino and E. Parrilli laboratory), previously digested with AscI and NotI-HF® and isolated from agarose gel using the QIAquick Gel Extraction Kit (QIAGEN).

Table 9.10 - List of primers used in this study

Primer name	Primer sequence 5'→3'	T_m
RS22405-fw_A	GAGCGGCCGCAAGATAACGAAAGGGAA	68.0 °C
RS22405-rv_A	CGATGAATTCTTGAAGTTTGGTCTGACGCCT	66.8 °C
RS22405-fw_B	CGATGAATTCGAATCCGATCGCACGATCCACA	69.5 °C
RS22405-rv_B	AGGCGCGCCTCTGGGATTTACTTCGGAGCA	72.2 °C

9.15.2.7 DNA ligation

Ligations were set up using 50 ng of linear vector. The calculated amounts of the DNA inserts (10.2 ng of **A** and 8.72 ng of **B**) were ligated using T4 DNA ligase (Promega) in the supplied buffer. The reaction was incubated over night at 15 °C. The ligation reaction was set up in a volume of 20 µl.

9.15.2.8 Transformation of *E. coli* (Top10)

15 µl of ligation mixture was added to 90 µl of competent Top10 *E. coli* (chemically competent strain, provided by prof. M. L. Tutino and E. Parrilli laboratory). This was incubated on ice for 30 minutes, before heated to 42°C for 1 minute and finally incubated on ice for 1 minute. To the mixture was then added 0.9 ml of LB with 34 µg/ml of Cm and incubated at 37°C for 1 hour. The cells were collected by centrifugation and resuspended in 100 µl LB and spread into an LB agar plate containing 34 µg/ml of Cm and incubated over night at 37°C.

9.15.2.9 Electroporation

2mL of a culture grown at 25°C for 48h was inoculated into 10 ml of fresh MB with and incubated continued under the same conditions until an $OD_{600} \sim 0.5$ was reached. The cells were washed four times in decreasing volumes of pre-chilled buffers (20 ml, 10 ml, 1 ml and 0.5 ml) and each time collected by centrifugation at 4000 rpm for 15 min at 4°C. Cells were then kept on ice until electroporation.

Table 9.11 - Composition of buffers used to made competent the cells

Buffers composition
Hepes 7 mM (pH 7), Sucrose 252 mM, 20% glycerol; Hepes 7 mM (pH 7), Sucrose 252 mM;
Sucrose 252 mM, 20% glycerol;
20% glycerol.

100 µl (2 OD) of electro-competent cells were mixed with 1 µg of isolated pVS C-RS11405 plasmid and transferred into a 2 mm electroporation cuvette (Eurogentec). Electroporation was performed in an MicroPulser Electroporator (BIORAD) with 2.5 kV. Immediately after electroporation 0.9 ml of freshly prepared growth medium (MB) was added to the cuvette and the reaction was transferred to a 1.5 ml eppendorf. Then the mixture was incubated at 25°C, 200 rpm for 24 hours. Then 100 µl of mixture was spread into MB plates containing Cm (12 µg/ml). The remaining cells were collected in a centrifuge at 2500 × g for 10 min and resuspended in 100 µl of MB, and spread into MB plates containing Cm (12 µg/ml).

Appendix

In this appendix is reported the RS11405 sequence, which is derived by automated computational analysis using gene prediction method (Protein Homology).

CTAATCATCACTCATACTCTTAAGTTTTTTATACTCGTAAATAAACATCGT
AAAAAAAATAAATATAGGGGCGTTATAATAAAAAATATTAACATCGACG
GCCATAGCATAGATCAAAAGGAATACTAGCAAAGATATCAGCGGTCGAT
TAAAAGCATTTATTTTTTTATAAGATAACGAAAGGGAAAATATGAAAAC
CGCCCAAACTATGACAGTAAGCAGAGGGATCAATCCAAACTTCAACCAA
ATATTCAACAACTCATTGTCTAAAGAATGAAGTCTCGCGTCTGCTGGAAG
ACCTAAAAACCACTCGTTATTGACTGTCGATAAGGCGTCAGACCAAACT
TCAAAAACACGAGCTTTGAAACTACTCATATTTACAAATCGATCATAAAT
TTTTTCGTAAATATCAGTAACAAAAAACGCAGAAAGTACACATATGATG
AAAAGGATAAAATAAAGAACTCTCTTGGGTTTTAGCCTTTTTGAAAAGT
AATAAAAGCCGAACGACACAGTTAAAGCTATCCAGACGGATCTCGACTG
AGAAGAAACTATGGCTAAGAAAAACAAACTAGTCAAAGTTAATTCTAAG
ATATTACTTGCCTTTCTTAAATGATTGTTAATCATAAAAATAAAGGCTAA
ACCCATTACAAAACCAGCTTCGTTAGGGTTTCCGTAGAATCCGATCGCAC
GATCCACATTATTGTCTGCATAGTGTAATGCACGTTCAGCGCCAAGCAAC
TCATAGTATAATGAGTTAATCCCATAAGGATTAAAAAATTGGACAATCA
TGATAATAGACAGGAGCATTGCTCCGAAGTAAATCCCAGATTTAACTTT
CTTCTTGTAGTTTTCCACATCAAAAGCCTTTAATAAGACTATGCAGTAAA
TTATCATCCCACTAATCGTGACTATTCTAGCAATGCTAACATCGGAAGCT
GCTCTTATTTGCGAAAAAGCTTCGAAGGCCAGAAATATAAAAAATGGAG
ATAATACATATATGTCATAACGAGATAATGTTACCTTTTCTATTTTTAAT
AAAAAATAGAAAATAGATATAGTAGAAAACAAGATAAAGAAAGACAAG
TTAATAGGTTGTAAACGAATCGGAAGAATAAATGCAATTAACAGGCAAA
AAGCAATAGATAATACAAAAAGACTCTCAACCGAAAATCTAATACGCTT
TATAGTTGAGTTGGCGGTTGTGTTATTATAATTTTTTTGAAGCAT

Bibliography

Adanitsch F., Shi J., Shao F., Beyaert R., Heine H., Zamyatina A. "Synthetic glycan-based TLR4 agonists targeting caspase-4/11 for the development of adjuvants and immunotherapeutics." Chem. Sci. 9 (2018) 3957.

Adeyeye A., Jansson P., Lindberg B., Abaas S., Svenson, S. B. "Structural studies of the *Escherichia coli* O-149 O-antigen polysaccharide." Carbohydr. Res., 176 (1988) 231–236.

Adinolfi M., Corsaro M. M., De Castro C., Evidente A., Lanzetta R., Lavermicocca P., Parrilli M. "Analysis of the polysaccharide components of the lipopolysaccharide fraction of *Pseudomonas caryophylli*." Carbohydr. Res. 284 (1996) 119-133.

Agrawal, P. K. "NMR spectroscopy in the structural elucidation of oligosaccharides and glycosides." Phytochemistry, 31(10) (1992) 3307-3330.

Agrawal P. K., Bush C. A., Takayama K., Qureshi N. "Structural analysis of lipid A and Re-lipopolysaccharides by NMR spectroscopic methods" Adv. Biophys. Chem. 4 (1994) 179-236.

Alexander C. and Rietschel E. T. "Bacterial lipopolysaccharides and innate immunity." J. Endotoxin Res., 7 (2001) 167–202.

Al-Hakim, A. and Linhardt R. J. "Isolation and recovery of acidic oligosaccharides from polyacrylamide gels by semi-dry electrotransfer." Electrophoresis. 11(1) (1990) 23-8.

Arbizu S., Chew B., Mertens-Talcotta S. U., Noratto G. "Commercial whey products promote intestinal barrier function with glycomacropeptide enhanced activity in downregulating bacterial endotoxin lipopolysaccharides (LPS)-induced inflammation *in vitro*." Food Funct. 11(7) (2020) 5842-5852.

Assmy P., Ehn J. K., Fernández-Méndez M., Hop H., Katlein C., Sundfjord A., Bluhm K., Daase M., Engel A., Fransson A., Granskog M. A., Hudson S. R., Kristiansen S., Nicolaus M., Peeken I., Renner A. H. H., Spreen G., Tatarek A., Wiktor J. "Floating ice-algal aggregates below melting Arctic sea ice." PLoS ONE 8 (2013) e76599.

Ayala-del-Río H. L., Chain P. S., Grzymski J. J., Ponder M. A., Ivanova N., Bergholz P. W., Di Bartolo G., Hauser L., Land M., Bakermans C., Rodrigues D., Klappenbach J., Zarka D., Larimer F., Richardson P., Murray A., Thomashow M., Tiedje J. M. "The Genome Sequence of *Psychrobacter arcticus* 273-4, a Psychroactive Siberian

Permafrost Bacterium, Reveals Mechanisms for Adaptation to Low-Temperature Growth.” Appl. Environ. Microbiol. 76(7) (2010) 2304–2312.

Barr K., Ward S., Meier-Dieter U., Mayer H., Rick P. D.“Characterization of an *Escherichia coli* rff mutant defective in transfer of N-acetylmannosaminuronic acid (ManNAcA) from UDP-ManNAcA to a lipid-linked intermediate involved in enterobacterial common antigen synthesis.” J. Bacteriol. 170 (1988) 228−233.

Barria C., Malecki M., Arraiano C. M. “Bacterial adaptation to cold.” Microbiology 159 (2013) 2437–2443.

Barroca M., Santos G., Gerday C., Collins T. “Biotechnological aspects of cold-active enzymes.” In: Margesin R (ed) Psychrophiles: from biodiversity to biotechnology. 2nd edn. Springer, Cham,. (2017a) 461–475.

Bayer, M. E. “Visualization of the bacterial polysaccharide capsule.” In K. Jann and B. Jann (ed.), Bacterial capsules. Springer Verlag, Berlin, Germany (1990) 129–157.

Benforte F. C., Colonnella M. A., Ricardi M. M., Solar Venero E. C., Lizarraga L., López N. I., Tribelli P. M. „Novel role of the LPS core glycosyltransferase WapH for cold adaptation in the Antarctic bacterium *Pseudomonas extremaustralis*.“ PLoS ONE 13(2) (2018) e0192559.

Beveridge T. J. and Graham L. L. “Surface layers of bacteria.” Microbiol. Mol. Biol. Rev. 55 (1991) 4684-705.

Białkowska A., Majewska E., Olczak A., Twarda-Clapa A. “Ice Binding Proteins: Diverse Biological Roles and Applications in Different Types of Industry.” Biomolecules 10(2) (2020) 274.

Biggs C. I., Stubbs C., Graham B., Fayter A. E. R., Hasan M., Gibson M. I. "Mimicking the Ice Recystallization Activity of Biological Macromolecules. When is a New Polymer 'Active'?" Macromol Biosci. 7 (2019) 1900082

Birnbaum G. I., Roy R., Brisson J.-R., Jennings H. J. “Conformations of ammonium 3-deoxy-D-*manno*-2-octulosonate (KDO) and methyl α-and β-ketopyranosides of KDO: X-ray structure and ^{1}H NMR analyses.” Carbohydr. Chem. 6 (1987) 17–39.

Bock K. and Pedersen C. J. “Carbon-13 Nuclear Magnetic Resonance Spectroscopy of Monosaccharides.” Adv Carbohydr Chem Biochem 41 (1983) 27-66.

Bock, K. and Pedersen C. J. “A study of ^{13}CH coupling constants in hexopyranoses.” J. Chem. Soc., Perkin trans. 2 (1974) 293–297.

Bock K., Vinogradov E. V., Holst O., Brade H. “Isolation and structural analysis of oligosaccharide phosphates containing the complete carbohydrate chain of the lipopolysaccharide from *Vibrio cholerae* Strain H11 (Non-O1).” Eur. J. Biochem. 225 (1994)1029–1039.

Boland K., Flanagan L., Prehn, J. H. “Paracrine control of tissue regeneration and cell proliferation by Caspase-3.” Cell Death Dis. 4(7) (2013) e725.

Brade H. and Rietschel E.T. “α-2→4-Interlinked 3-deoxy-D-*manno*-octulosonic acid disaccharide A common constituent of enterobacterial lipopolysaccharides.” Eur. J. Biochem. 145 (1984) 231 -236.

Branefors-Helander P. “Structural studies of two capsular polysaccharides elaborated by different strains of *Haemophilus influenzae* type e.” Carbohydr. Res., 88 (1981) 77-84.

Bushell S. R., Mainprize I. L., Wear M. A., Lou H., Whitfield C., Naismith J. H.“Wzi Is an Outer Membrane Lectin that Underpins Group 1 Capsule Assembly in *Escherichia coli*” Structure 21 (2013) 844–853.

Cai W., Kesavan K. D., Wan J., Abdelaziz M. H., Su Z., Xu H. “Bacterial outer membrane vesicles, a potential vaccine candidate in interactions with host cells based” Diagn Pathol 13 (2018) 95.

Calatayud M., Verstrepen L., Ghyselinck J., Van den Abbeele P., Marzorati M., Modica S., Ranjanoro T., Maquet V. “Chitin Glucan Shifts Luminal and Mucosal Microbial Communities, Improve Epithelial Barrier and Modulates Cytokine Production In Vitro.” Nutrients 13(9) (2021) 3249.

Carillo S., Casillo A., Pieretti G., Parrilli E., Sannino F., Bayer-Giraldi M., Cosconati S., Novellino E., Ewert M., Deming J. W., Lanzetta R., Marino G., Parrilli M., Randazzo A., Tutino M. L., Corsaro M. M. “A unique capsular polysaccharide structure from the psychrophilic marine bacterium *Colwellia psychrerythraea* 34H that mimics antifreeze (Glyco)proteins” J. Am. Chem. Soc. 137 (2015) 179–189.

Carillo S., Pieretti G., Lindner B., Parrilli E., Sannino F., Tutino M. L., Lanzetta R., Parrilli M., Corsaro M. M. “Structural characterization of the core oligosaccharide isolated from the lipopolysaccharide of the psychrophilic bacterium *Colwellia psychrerythraea* strain 34H” Eur. J. Org Chem. 18 (2013) 3771–3779.

Carillo S., Pieretti G., Parrilli E., Tutino M. L., Gemma S., Molteni M., Lanzetta R., Parrilli M., Corsaro M. M.. “Structural investigation and biological activity of the lipooligosaccharide from the psychrophilic bacterium *Pseudoalteromonas haloplanktis* TAB 23.” Chem. Eur. J. 17 (2011) 7053–7060.

Caroff, M. and Karibian, D. “Structure of bacterial lipopolysaccharides.” Carbohydr. Res. 338 (2003) 2431–2444.

Carty S. M., Sreekumar K. R., Raetz C. R. H.“Effect of Cold Shock on Lipid A Biosynthesis in *Escherichia coli* Induction At 12 °C of an acyltransferase specific for palmitoleoyl-acyl carrier protein.” J. Biol. Chem 274 (14) (1999) 9677–9685.

Caruso C., Rizzo C., Mangano S., Poli A., Di Donato P., Finore I., Nicolaus B., Di Marco G., Michaud L., Lo Giudice A. “Production and biotechnological potential of extracellular polymeric substances from sponge-associated Antarctic bacteria.” Appl Environ Microbiol 84(4) (2018) e01624-17.

Casillo A., Ricciardelli A., Parrilli E., Tutino M. L., Corsaro M. M. “Cell-wall associated polysaccharide from the psychrotolerant bacterium *Psychrobacter arcticus* 273-4: isolation, purification and structural elucidation.” Extremophiles 24 (2020) 63–70.

Casillo A., Lanzetta R., Parrilli M., Corsaro M. M. “Exopolysaccharides from Marine and Marine Extremophilic Bacteria: Structures, Properties, Ecological Roles and Applications” Mar. Drugs 16 (2018) 1948–1957.

Casillo A., Ståhle J., Parrilli E., Sannino F., Mitchell D. E., Pieretti G., Gibson M. I., Marino G., Lanzetta R., Parrilli M., Widmalm G., Tutino M. L., Corsaro M. M. “Structural characterization of an all-aminosugar-containing capsular polysaccharide from *Colwellia psychrerythraea* 34H.” Antonie Leeuwenhoek 110 (2017a) 1377–1387.

Casillo A., Di Guida R., Carillo S., Chen C., Kamasaka K., Kawamoto J., Kurihara T., Corsaro M. M. “Structural elucidation of a novel lipooligosaccharide from the cold-adapted bacterium OMVs producer *Shewanella* sp. HM13.” Mar. Drugs 17 (2019) 34.

Casillo A., Parrilli E., Sannino F., Lindner B., Lanzetta R., Parrilli M., Tutino M. L., Corsaro M. M. “Structural investigation of the oligosaccharide portion isolated from the lipooligosaccharide of the permafrost psychrophile *Psychrobacter arcticus* 273-4.” Mar. Drugs 13 (2015) 4539–4555.

Casillo A., Parrilli E., Sannino F., Mitchell D. E., Gibson M. I., Marino G., Lanzetta R., Parrilli M., Cosconati S., Novellino E., Randazzo A., Tutino M. L., Corsaro M. M.“Structure-activity relationship of the exopolysaccharide from a psychrophilic bacterium: A strategy for cryoprotection” Carbohydr. Polym. 156 (2017b) 364–371.

Casillo A., Parrilli E., Tutino M. L, Corsaro M. M. “The outer membrane glycolipids of bacteria from cold environments: isolation, characterization, and biological activity.” FEMS Microbiol 95 (2019) fiz094.

Casillo A., Ziaco M., Lindner B., Parrilli E., Schwudke D., Holgado A., Verstrepen L., Sannino F., Beyaert R., Lanzetta R., Tutino M. L., Corsaro M. M. “Unusual lipid A from a cold adapted bacterium: Detailed structural characterization.” ChemBioChem 18 (2017) 1845–1854.

Cavicchioli, R. “Cold-adapted archaea” Nat. Rev. Microbiol. 4 (2006) 331-343.

Cavicchioli, R. “Extremophiles and the search for extraterrestrial life.” Astrobiology 2 (2002) 281-292.

Chaisuwan, W., Jantanasakulwong K., Wangtueai S., Phimolsiripol Y., Chaiyaso T., Techapun C., Phongthai S., You S. G., Regenstein J. M., Seesuriyachan P. “Microbial exopolysaccharides for immune enhancement: Fermentation, modifications and bioactivities.” Food Biosci 35 (2020) 100564.

Chen C., Kawamoto J., Kawai S., Tame A., Kato C., Imai T., Kurihara T. “Isolation of a novel bacterial strain capable of producing abundant extracellular membrane vesicles carrying a single major cargo protein and analysis of its transport mechanism.” Front. Microbiol. 10 (2020) 3001.

Cheptsov V. S., Vorobyova E. A., Manucharova N. A., Gorlenko M. V., Pavlov A. K., Vdovina M. A., Lomasov V. N., Bulat S. A.“100 kGy gamma-affected microbial communities within the ancient Arctic permafrost under simulated Martian conditions.” Extremophiles 21 (2017) 1057–1067.

Ciucanu I., Kerek F. “A simple and rapid method for the permethylation of carbohydrates.” Carbohydr. Res.1984, 131, 2 209–217.

Cócera M., Lópeza O., Parraa J. L., Mercadé M. E., Guineab J., la Mazaa A. “Protective effect caused by the exopolymer excreted by *Pseudoalteromonas antarctica* NF(3) on liposomes against the action of octyl glucoside.” Int. J. Pharm 207(1-2) (2000) 39-47.

Cochet N. and Widehem, P. “Ice crystallization by *Pseudomonas syringae*.” Appl Microbiol Biotechnol 54(2) (2000) 153–161.

Collins T. and Margesin, R. “Psychrophilic lifestyles: mechanisms of adaptation and biotechnological tools.” Appl. Microbiol 103 (2019) 2857–2871.

Corsaro M. M., Pieretti G., Lindner B., Lanzetta R., Parrilli E., Tutino M. L., Parrilli M."Highly phosphorylated core oligosaccharide structures from cold-*adapted Psychromonas arctica*" Chem. Eur. J. 14 (2008) 9368–9937.

Corsaro M. M., Lanzetta R., Parrilli E., Parrilli M., Tutino M. L., Ummarino S. "Influence of Growth Temperature on Lipid and Phosphate Contents of Surface Polysaccharides from the Antarctic Bacterium *Pseudoalteromonas haloplanktis* TAC 125" J. Bacteriol. 186(1) (2004) 29–34.

Corsaro M. M., Dal Piaz F., Lanzetta R., Parrilli M. "Lipid A structure of *Pseudoalteromonas haloplanktis* TAC 125: use of electrospray ionization tandem mass spectrometry for the determination of fatty acid distribution." J. Mass Spectrom. 37 (2002) 481–488.

Corsaro M. M., Nicolaus B., Poli A., Corsaro M. M., Lanzetta R., Parrilli M. "Structural determination of the O-chain polysaccharide from the lipopolysaccharide of the haloalkaliphilic *Halomonas pantelleriensis* bacterium" Eur. J. Org Chem. 7 (2006) 1801–1808.

Corsaro M. M., Lanzetta R., Parrilli E., Parrilli M., Tutino M. L. "Structural investigation on the lipooligosaccharide fraction of psychrophilic *Pseudoalteromonas haloplanktis* TAC 125 bacterium." Eur. J. Biochem. 268 (2001) 5092–5097.

Corsaro M. M., Angela C., Parrilli E., Tutino M. L."Structure of lipopolysaccharides of cold-adapted bacteria." In Psychrophiles: From Biodiversity to Biotechnology; Margesin, R., Ed.; Springer International Publishing AG: Cham, Switzerland, 2017; Chapter 13;285–303.

Costerton J. W., Cheng K. J., Geesey G. G., Ladd T. I., Nickel J. C., Dasgupta M., Marrie T. J. "Bacterial Biofilms in Nature and Disease" Annual Review of Microbiology 41 (1987) 435-464.

Cronan J. E. Jr, "Thermal regulation of the membrane lipid composition of *Escherichia coli*. Evidence for the direct control of fatty acid synthesis." J. Biol. Chem. 250(17) (1975) 7074-7077.

D'Amico, S., Collins T., Marx Jean-Claude, Feller G., Gerday C. "Psychrophilic microorganisms: challenges for life" EMBO reports 7 (2006) 385-389.

De Castro C., Parrilli M., Holst O., Molinaro A."Microbe-associated molecular patterns in innate immunity: Extraction and chemical analysis of gram-negative bacterial lipopolysaccharides." Methods Enzymol., 480 (2010) 89-115.

De Castro C., Lanzetta R., Leone S., Parrilli M., Molinaro A."The structural elucidation of the *Salmonella enterica* subsp. enterica, reveals that it contains both O-factors 4 and 5 on the LPS antigen." Carbohydr. Res. 370 (2013)9–12.

De Maayer P., Anderson D., Cary C., Cowan1 D. A., "Some like it cold: understanding the survival strategies of psychrophiles" EMBO reports, 15 (2014) 508-517.

De Soyza A., Silipo A., Lanzetta R., Govan J. R., Molinaro A. "Chemical and biological features of Burkholderia cepacia complex lipopolysaccharides." Innate Immun. 14 (2008) 127-144.

Deming, J. W. and Young, J. N. "The role of exopolysaccharides in microbial adaptation to cold habitats. In: Margesin R (ed). Psychrophiles: From Biodiversity to Biotechnology." Cham: Springer International Publishing (2017) 259–84.

Di Guida R., Casillo A., Corsaro M. M. "O-specific polysaccharide structure isolated from the LPS of the Antarctic bacterium *Pseudomonas* ANT_J38B" Carbohydr. Res. 497 (2020) 108125.

Di Lorenzo F., Crisafi F., La Cono V., Yakimov M. M., Molinaro A., Silipo A. "The Structure of the Lipid A of Gram-Negative Cold-Adapted Bacteria Isolated from Antarctic Environments." *Mar. Drugs 18 (*2020) 592.

Domon, B. and Costello, C. E., "A systematic nomenclature for carbohydrate fragmentations in FABMS/MS of glycoconjugates." Glycoconj. J. 5 (1988) 397-409.

Elhenawy W., Debelyy M. O., Feldman M. F. . "Preferential packing of acidic glycosidases and proteases into Bacteroides outer membrane vesicles." mBio 5 (2014) e00909–e00914.

El-Zayat S. R., Sibaii H., Mannaa F. A."Toll-like receptors activation, signaling, and targeting: an overview." Bull. Natl. Res. Cent. 43 (2019) 187.

Erridge C., Bennett-Guerrero E., Poxton I. R. "Structure and function of lipopolysaccharides." Microbes Infect. 4(8) (2002) 837-51.

Fairman J. W., Noinaj N., Buchanan S. K. "The structural biology of β-barrel membrane proteins: a summary of recent reports." Curr. Opin. Struct. Biol. 21(4) (2011) 523-531.

Feller G. "Protein stability and enzyme activity at extreme biological temperatures." J. Phys. Condens. Matter 22 (2010) 323101.

Fernández-Méndez M., Wenzhöfer,Ilka F,. Heidi P., L. Sørensen, Glud R. N., Boetius A. “Composition, buoyancy regulation and fate of ice algal aggregates in the central Arctic Ocean.” PLoS ONE 9 (2014) e107452.

FiebigT. Freiberger F., Pinto V., Romano M. R., Black A., Litschko C., Bethe A., Yashunsky D., Adamo R., Nikolaev A., Berti F., Gerardy-Schahn R. “Molecular Cloning and Functional Characterization of Components of the Capsule Biosynthesis Complex of *Neisseria meningitidis* serogroup A.” J. Biol. Chem 289(28) (2014) 19395–19407.

Fletcher M. and Floodgate G. D. “An electron microscopic demonstration of an acidic polysaccharide involved in the adhesion of a marine bacterium to solid surfaces.” J. Gen. Microbiol. 74 (1973) 325-334.

Fomsgaard A., Freudenberg M. A., Galanos C. Modification of the silver staining technique to detect lipopolysaccharide in polyacrylamide gels. J. Clin. Microbiol 28(12) (1990). 2627-2631.

Fonseca F., Meneghel J., Cenard S., Passot S., Morris G. J. “Determination of intracellular vitrification temperatures for unicellular microorganisms under conditions relevant for cryopreservation.” PLoS One 11(4) (2016) e0152939.

Francius G., Lebeer S., Alsteens D., Wildling L., Gruber H. J., Hols P., De Keersmaecker S., Vanderleyden J., Dufrêne Y. F. “Detection, Localization, and Conformational Analysis of Single Polysaccharide Molecules on Live Bacteria.” ACS Nano 2 (2008) 1921−1929.

Fresno S., Jiménez N., Izquierdo L., Merino S., Corsaro M. M., De Castro C., Parrilli M., Naldi T., Regué M., Tomás J. M. “The ionic interaction of *Klebsiella pneumoniae* K2 capsule and core lipopolysaccharide.” Microbiology 152 (2006) 1807–1818.

Frias A,. Manresa A., de Oliveira E., López-Iglesias C., Mercade E.“Membrane Vesicles: A Common Feature in the Extracellular Matter of Cold-Adapted Antarctic Bacteria.” Microb Ecol 59 (2010) 476–486.

Galanos C., Lüderitz O., Westphal O. “A new method for the extraction of R lipopolysaccharides.” Eur. J. Biochem. 9 (1969) 245-249.

Gauthier G., Gauthier M., Christen R. “Phylogenetic analysis of the genera *Alteromonas, Shewanella* and *Moritella* using genes coding for small-subunit r RNA sequences and division of the genus *Alteromonas* into two genera, *Alteromonas* (emended) and *Pseudoalteromonas* gen. nov., and proposal of twelve new species combinations.” Int. J. Syst. Bacteriol. 45 (1995) 755-76.

Gauthier M. J. "*Alteromonas* rubra sp. nov., a new marine antibiotic-producing bacterium." Int. J. Syst. Bacteriol. 26 (1979) 459-466.

Georlette D., Blaise V., Collins T., D'Amico S., Gratia E., Hoyoux A., Marx J. C., Sonan G., Feller G., Gerday C. "Some like it cold: biocatalysis at low temperatures." FEMS Microbiol. Rev. 28 (2004) 25–42.

Ghobakhlou A. F., Johnston A., Harris L., Antoun H., Laberge S. "Microarray transcriptional profiling of Arctic *Mesorhizobium* strain N33 at low temperature provides insights into cold adaption strategies." BMC Genomics 16(1) (2015) 383.

Ghosh M., Pulicherla K. K., Rekha V. P. B., P. Kumar Raja P., Sambasiva Rao K. R. S. "Cold active betagalactosidase from Thalassospira sp. 3SC-21 to use in milk lactose hydrolysis: a novel source from deep waters of Bay-of-Bengal." World J Microbiol Biotechnol 28(9) (2012) 2859–2869.

Gibson B.W. ; Engstrom J. J., John C. M., Hines W., Falick A. M. "Characterization of bacterial lipooligosaccharides by delayed extraction matrix-assisted laser desorption ionization time-of-flight mass spectrometry." J. Am. Soc. Mass. Spectrom. 8 (1997) 645–658.

Giuliani M., Parrilli E., Pezzella C., Rippa V., Duilio A., Marino G., Tutino M. L. "A novel strategy for the construction of genomic mutants of the Antarctic bacterium *Pseudoalteromonas haloplanktis* TAC125." Methods Mol Biol. 824 (2012) 219-33.

Glud R. N., Rysgaard S., Turner G., McGinnis D. F., Leakey R. J. G. "Biological- and physical-induced oxygen dynamics in melting sea ice of the Fram Strait." Limnol. Oceanogr. 59, (2014) 1097–1111 (2014).

Goordial J., Raymond-Bouchard I., Zolotarov Y., de Bethencourt L., Ronholm J., Shapiro N., Woyke T., Stromvik M., Greer C. W., Bakermans C., Whyte L. "Cold adaptive traits revealed by comparative genomic analysis of the eurypsychrophile *Rhodococcus* sp. JG3 isolated from high elevation McMurdo Dry Valley permafrost, Antarctica." FEMS Microbiol Ecol 92(2) (2016).

Graham L. L., Harris R., Villiger W., Beveridge T. J. "Freezesubstitution of gram-negative eubacteria: general cell morphology and envelope profiles." J. Bacteriol. 173 (1991) 1623–163.

Grazioso T. P., Tözün N. "Diet, Microbiota, and Colorectal Cancer." *iScience*, 21 (2019) 168-187.

Haag A. P., Geesey G. G., Mittleman Marc W. “Bacterially derived wood adhesive” Int J Adhes Adhes 26 (2006) 177–183.

Hakomori S. “A rapid permethylation of glycolipid, and polysaccharide catalyzed by methylsulfinyl carbanion in dimethyl sulfoxide.” J. Biochem. 55 (1964) 205-208.

Haurat M. F., Aduse-Opoku J., Rangarajan M., Dorobantu L., Gray M. R., Curtis M. A., Feldman M. F. “Selective sorting of cargo proteins into bacterial membrane vesicles.” J. Biol. Chem. 286 (2011) 1269–1276.

Hoffman J., Bøgwald J., Andersson R., Kenne L. “Structural studies of the lipopolysaccharide of *Moritella viscosa* strain M2-226” Carbohydr. Res. 347 (2012) 164–167.

Holmström, C. and Kjelleberg, S. “Marine *Pseudoalteromonas* species are associated with higher organisms and produce biologically active extracellular agents.” FEMS Microbiol Ecol 30 (1999) 285-293.

Holst, O. “Chemical Structure of the Core Region of Lipopolysaccharides” Brade H., Opal S. M., Vogel S. N., Morrison D. C. (Eds.), Endotoxins in Health and Disease, Marcel Dekker, New York Chapter 8 (1999) 115-154.

Holst, O. “De-acylation of lipopolysaccharides and isolation of oligosaccharide phosphates. In Bacterial Toxins: Methods and Protocols.” Methods in Molecular Biology, Ed.; Humana Press: Totowa, NJ, USA, 145 (2000) 345–353.

Holst O., Ulmer A. J., Brade H., Flad H. D., Rietschel E. T. “Biochemistry and cell biology of bacterial endotoxins.” FEMS Immunol. Med. Microbial. 16 (1996) 83-104.

Holst O., Muller-Loennies S., Lindner B., Brade H.“Chemical structure of the lipid A of *Escherichia coli* J-5. Eur. J. Biochem.” 214 (1993) 695–701.

Hoyoux A., Jennes I., Dubois P., Genicot S., Dubail F., François J. M., Baise E., Feller G., Gerday C. “Cold-adapted beta-galactosidase from the Antarctic psychrophile *Pseudoalteromonas haloplanktis*.” Appl Environ Microbiol 67(4) (2001) 1529–1535.

Huston A. L. “Biotechnological Aspects of Cold-Adapted Enzymes.” In: Margesin R., Schinner F., Marx J. C., Gerday C. (eds) Psychrophiles: from Biodiversity to Biotechnology. Springer, Berlin, Heidelberg (2008).

Ivanova, E. P., Romanenko L. A., Chun J., Matte M. H., Matte G. R., Mikhailov V. V., Svetashev V. I., Huq A., Maugel T., Colwell R. R. “*Idiomarina* gen. nov., comprising novel indigenous deep-sea bacteria from the Pacific Ocean, including

descriptions of two species, *Idiomarina abyssalis* sp. nov. and *Idiomarina zobellii* sp. nov." IJSEM 50 (2000) 901–907.

Ivanova E. P., Flavier S., Christen R. "Phylogenetic relationships among marine Alteromonas-like proteobacteria: emended description of the family Alteromonadaceae and proposal of *Pseudoalteromonadaceae* fam. nov., *Colwelliaceae* fam. nov., *Shewanellaceae* fam. nov., *Moritellaceae* fam. nov., *Ferrimonadaceae* fam. nov., *Idiomarinaceae* fam. nov. and *Psychromonadaceae* fam. nov." IJSEM 54 (2004) 1773–1788.

Jouault S. C., Chevolot L., Helley D., Ratiskol J., Bros A., Sinquin C., Roger O., Fischer A. M. "Characterization, chemical modifications and in vitro anticoagulant properties of an exopolysaccharide produced by *Alteromonas infernus*." Biochim Biophys Acta Gen Subj 1528(2) (2001) 141–151.

Kamasaka K., Kawamoto J., Chen C., Yokoyama F., Imai T., Ogawa T., Kurihara T. "Genetic characterization and functional implications of the gene cluster for selective protein transport to extracellular membrane vesicles of *Shewanella vesiculosa* HM13." Biochem. Biophys. Res. Commun. 526(2) (2020) 525-531.

Kamio, Y. and Nikaido, H. "Outer membrane of Salmonella typhimurium: accessibility of phospholipid head groups to phospholipase C and cyanogen bromide activated dextran in the external medium." Biochemistry 15(12) (1976) 2561–2570.

Kandror, O., DeLeon A., Goldberg A.L."Trehalose synthesis is induced upon exposure of *Escherichia coli* to cold and is essential for viability at low temperatures." Proc. Natl. Acad. Sci. U.S.A. 99(15) (2002) 9727-9732.

Karlyshev A. V., McCrossan M. V., Wren B. W."Demonstration of polysaccharide capsule in *Campylobacter jejuni* using electron microscopy." Infect. Immun. 69 (2001)5921–5924.

Kaszowska M., Wojcik M., Siednienko J., Lugowski C., Lukasiewicz J. "Structure-Activity Relationship of *Plesiomonas shigelloides* Lipid A to the Production of TNF-α, IL-1β, and IL-6 by Human and Murine Macrophages." Front Immunol. 8 (2017) 1741.

Kawamura T., Ishimoto N., Ito E. "Enzymatic synthesis of uridine diphosphate N-acetyl-D-mannosaminuronic acid." J. Biol. Chem. *The Journal of Biological Chemistry*, 254 , (1979). 7457−7465.

Keenleyside, W. J. and Whitfield, C. “A novel pathway for O-polysaccharide biosynthesis in *Salmonella enterica* serovar Borreze.” J Biol Chem. 271(45) (1996) 28581-92.

Kilcoyne M., Shashkov A. S., Senchenkova S. A., Knirel Y. A., Vinogradov E.V., Radziejewska-Lebrecht J., Galimska-Stypa R., Savage A. V. “Structural investigation of the O-specific polysaccharides of *Morganella morganii* consisting of two higher sugars” Carbohydr. Res. 337 (2002) 1697–1702.

Kilcoyne M., Perepelov A. V., Tomshich S. V., Komandrova N. A., Shashkov A. S., Romanenko L. A., Knirel Y. A., Savage A. V. “Structure of the O-polysaccharide *Idiomarina zobellii* KMM 231^T containing two unusual amino sugars with the free amino group, 4-amino-4,6-dideoxy-D-glucose and 2-amino-2-deoxy-L-guluronic acid” Carbohydr. Res. 339 (2004) 477–482.

Kilcoyne M., Shashkov A. S., Knirel Y. A., Gorshkova R. P., Nazarenko E.,L., Ivanova E. P., Gorshkova N. M., Senchenkova S. N., Savage AV. “The structure of the O-polysaccharide of the *Pseudoalteromonas rubra* ATCC 29570^T lipopolysaccharide containing a keto sugar” Carbohydr. Res. 340 (2005) 2369–2375.

Kittelberger R. and Hilbink F. “Sensitive silver-staining detection of bacterial lipopolysaccharides in polyacrylamide gels.” J. Biochem. Biophys. Methods 26 (1) (1993) 81-86.

Knirel Y. A. “Cold temperature-induced modifications to the composition and structure of the lipopolysaccharide of *Yersinia pestis*.” Carbohydr. Res. 340 (2005) 1625–1630

Knirel Y. A. “O-Specific polysaccharides of Gram-negative bacteria” in: A.P. Moran, O. Holst, P.J. Brennan, M. von Itzstein (Eds.), Microbial Glycobiology: Structures, Relevance and Applications, Academic Press (2009) 57–73.

Knirel Y. A., H. Molla, J. H. Helbigc, Zähringera U. “Chemical characterization of a new 5,7-diamino-3,5,7,9-tetradeoxynonulosonic acid released by mild acid hydrolysis of the *Legionella pneumophila* serogroup 1 lipopolysaccharide” Carbohydr. Res. 304(1) (1997) 77-79.

Knirel Y.A. Vinogradov E. V., Shashkov A. S., Dmitriev B. A., Kochetkov N. K., Stanislavsky E. S., Mashilova G. M. “Somatic antigens of *Pseudomonas aeruginosa*. The structure of the O-specific polysaccharide chain of the lipopolysaccharide from *P. aeruginosa* O13 (L´anyi)” Eur. J. Biochem. 163 (1987) 627–637.

Kocharova N. A., Perepelov A. V., Zatonsky G. V., Shashkov A. S., Knirel Y. A., Jansson P. E., Weintraub A. “Structural studies of the O-specific polysaccharide of

Vibrio cholerae O8 using solvolysis with triflic acid" Carbohydrate Research 330 (2001) 83 – 92.

Koller, M. "Production of Poly Hydroxyalkanoate (PHA) biopolyesters by extremophiles?" MOJ Poly Sci., 1 (2017), 69–85.

Kondakova A .N., Novototskaya-Vlasova K. A., Drutskaya M. S., Senchenkova S. N., Shcherbakova V. A., Shashkov A. S., Gilichinsky D. A., Nedospasov S. A., Knirel Y. A. "Structure of the O-polysaccharide chain of the lipopolysaccharide of *Psychrobacter muricolla* 2pS(T) isolated from overcooled water brines within permafrost" Carbohydr. Res. 349 (2012) 78–81.

Korenevsky A. A, Vinogradov E., Gorby Y., Beveridge T. J. "Characterization of the lipopolysaccharides and capsules of *Shewanella* spp." Appl. Environ. Microbiol. 68 (2002) 4653–4657.

Krasikova, I. N., Kapustina N. V., Isakov V. V., Gorshkova N. M., Solov'eva T. F. "Elucidation of structure of lipid A from the marine Gram-negative bacterium *Pseudoalteromonas haloplanktis* ATCC 14393T." Russ. J. Bioorgan. Chem. 30 (2003) 367-373.

Kulp, A. and Kuehn, M. J. "Biological Functions and Biogenesis of Secreted Bacterial Outer Membrane Vesicles" Annu. Rev. Microbiol. 64 (2010) 163-184.

Kumar G. S., Jagannadham M. V., Ray M. K. "Low-temperatureinduced changes in composition and fluidity of lipopolysaccharides in the Antarctic psychrotrophic bacterium *Pseudomonas syringae*." J. Bacteriol. 184 (2002) 6746–6749.

Laemmli, U .K. "Most commonly used discontinuous buffer system for SDS electrophoresis." Nature 227 (1970) 680–685.

Larsen, B. D. and Sørensen, C. S. "The caspase-activated DNase: apoptosis and beyond." The FEBS Journal 284(8) (2017) 1160-1170.

Lauro F. M., Tran K., Vezzi A., Vitulo N., Valle G., Bartlett D. H."Physiology and Metabolism Large-Scale Transposon Mutagenesis of *Photobacterium profundum* SS9 Reveals New Genetic Loci Important for Growth at Low Temperature and High Pressure." J. Bacteriol. 190(5) (2008) 1699-1709.

Lehrer J., Vigeant K. A., Tatar L. D., Valvano M. A. "Functional characterization and membrane topology of *Escherichia coli* WecA, a sugar-phosphate transferase initiating the biosynthesis of enterobacterial common antigen and O-antigen lipopolysaccharide." J. Bacteriol. 189 (2007) 2618−2628.

Leontein K., Lindberg B., Lönngren J,"Determination of the absolute configuration of sugars by Gas-Liquid Chromatography of their acetylated 2-octyl glycosides." Carbohydr. Res. 62 (1978) 359-362.

Lerouge I., Laeremans T., Verreth C., Vanderleyden J., Van Soom C., Tobin A., Carlson R. W. "Identification of an ATP-binding Cassette Transporter for Export of the O-antigen across the Inner Membrane in *Rhizobium etli* Based on the Genetic, Functional, and Structural Analysis of an lps Mutant Deficient in O-antigen." J Biol Chem 276(20) (2001) 17190–17198, 2001

Leroy F. and De Vuyst, L. "Advances in production and simplified methods for recovery and quantification of exopolysaccharides for applications in food and health." J Dairy Sci 99(4) (2016) 3229–3238.

Li J., Izquierdo M. P., Lee Tung-Ching "Effects of ice-nucleation active bacteria on the freezing of some model food systems." Int J Food Sci Technol 32(1) (1997) 41–49.

Li W., Xia X., Tang W., Ji J., Rui X., Chen X., Jiang M., Zhou J., Zhang Q., Dong M. "Structural Characterization and Anticancer Activity of Cell-Bound Exopolysaccharide from *Lactobacillus helveticus* MB2-1" J. Agric. Food Chem. 63(13), (2015) 3454-3463.

Li W.W., Zhou W. Z., Zhang Y. Z., Wang J., Zhu X. B. "Flocculation behavior and mechanism of an exopolysaccharide from the deep-sea psychrophilic bacterium *Pseudoalteromonas* sp. SM9913." Bioresour 99 (2008) 6893–6899.

Li Z., Clarke A. J., Beveridge T. J. "A major autolysin of *Pseudomonas aeruginosa*: Subcellular distribution, potential role in cell growth and division and secretion in surface membrane vesicles." J. Bacteriol. 178 (1996) 2479–2488.

Lindell K., Fahlgren A., Hjerde E., Willassen Nils-Peder, Fällman M., Milton D. L. "Lipopolysaccharide O-Antigen Prevents Phagocytosis of *Vibrio anguillarum* by Rainbow Trout (*Oncorhynchus mykiss*) Skin Epithelial Cells" PLoS ONE 7(5) e37678.

Link A. J., Phillips D., Church G. M. "Methods for Generating Precise Deletions and Insertions in the Genome of Wild-Type *Escherichia coli*: Application to Open Reading Frame Characterization." J. Bacteriol. 179(20) (1997) 6228–6237.

Lipkind G. M., Shashkov A. S., Knirel Y. A., Vinogradov E. V., Kochetkov N. K. "A computer-assisted structural analysis of regular polysaccharides on the basis of ^{13}C-NMR data." Carbohydr. Res. 175 (1988) 59–75.

Liu Z., Jiao Y., Lu H., Shu X., Chen Q. “Chemical characterization, antioxidant properties and anticancer activity of exopolysaccharides from *Floccularia luteovirens*.” Carbohydr. Polymers 229 (2020) 115432.

Lo Giudice A., Poli A., Finore I., Rizzo C. “Peculiarities of extracellular polymeric substances produced by Antarctic bacteria and their possible applications.” Appl. Microbiol. Biotechnol. 104 (2020) 104:2923–2934.

Lugowski C., Romanowska E., Kenne L., Lindberg B.“Identification of a trisaccharide repeating-unit in the enterobacterial common-antigen.” Carbohydr. Res. 118 (1983) 173-181.

MacDonell, M. T. and Colwell, R. R. “Phylogeny of the Vibrionaceae and recommendation for two new genera, *Listonella* and *Shewanella*.” Syst Appl Microbiol 6 (1985) 171-182..

Margesin, R. and Miteva, V. “Diversity and ecology of psychrophilic microorganisms.” Research in Microbiology 162 (2011) 346-361

Marx J. C., Collins T., D'Amico S., Feller G., Gerday C. “Cold adapted enzymes from marine Antarctic microorganisms.” Mar. Biotechnol. 9 (2007) 293–304.

Marx J. G., Carpenter S. D., Deming J. W. “Production of cryoprotectant extracellular polysaccharide substances (EPS) by the marine psychrophilic bacterium *Colwellia psychrerythraea* strain 34H under extreme conditions.” Can. J. Microbiol. 55(1) (2009) 63–72.

Mastascusa V., Romano I., Di Donato P., Poli A., Della Corte V., Rotundi A., Bussoletti E., Quarto M., Pugliese M., Nicolaus B. “Extremophiles Survival to Simulated Space Conditions: An Astrobiology Model Study.” Orig Life Evol Biosph 44 (2014) 231–237.

Mayer H., Bhat U. R., Masoud H., Radziejewska-Lebrecht J., Widemann C., Krauss J. H. “Bacterial lipopolysaccharide.” Pure Appl. Chem. 61 (1989) 1271–1282.

Merino S. and Tomas J. M. “Bacterial capsules and evasion of immune responses,” in Encyclopedia of Life Sciences, John Wiley & Sons, New York, NY, USA, 3rd edition (2010).

Michon F., Brisson J. R., Roy R., Ashton F. E., Jennings H. J. “Structural determination of the capsular polysaccharide of *Neisseria meningitidis* group I: a two-dimensional NMR analysis” Biochemistry 24 (1985) 5592–5598.

Micoli F., Costantino P., Adamo R. “Potential targets for next generation antimicrobial glycoconjugate vaccines.” FEMS Microbiol. Rev. 42 (2018) 388–423.

Miyake K. “Innate recognition of lipopolysaccharide by Toll-like receptor 4-MD-2” Trends Microbiol. 12(4) (2004) 186-92.

Molinaro A., Bedini E., Ferrara R., Lanzetta R., Parrilli M., Evidente A., Lo Cantore P., Iacobellis N. S.“Structural determination of the O-specific chain of the lipopolysaccharide from the mushrooms pathogenic bacterium *Pseudomonas tolaasii*” Carbohydr., Res. 338 (2003) 1251–1257.

More T. T., Yadava J. S. S., Yan S., Tyagia R. D., Surampalli R. Y.“Extracellular polymeric substances of bacteria and their potential environmental applications.” J. Environ. Manag. 144 (2014) 1–25.

Morgan P. M., Sala R. F., Tanner M. E. “Eliminations in the reactions catalyzed by UDP-N-acetylglucosamine 2-epimerase.” J. Am. Chem. Soc. 119 (1997) 10269−10277.

Morita R. Y. “Psychrophilic bacteria.” Bacteriol. Rev. 39 (1975) 144-167.

Moule A. L., Galbraith L., Cox A. D., S. G. Wilkinson “Characterisation of a tetrasaccharide released on mild acid hydrolysis of LPS from two rough strains of *Shewanella* species representing different DNA homology groups.” Carbohydr. Res. 339 (2004) 1185–1188.

Mozaheb N. and Mingeot-Leclercq, M. P. “Membrane Vesicle Production as a Bacterial Defense Against Stress.” Front. Microbiol. 11 (2020) 600221.

Müller-Loennies S., Lindner B., Brade H. “Structural analysis of deacylated lipopolysaccharide of Escherichia coli strains 2513 (R4 core-type) and F653 (R3 core-type).” Eur J Biochem 269 (2002) 5982–5991

Muñoz P. A., Márquez S. L., González-Nilo F. D., Márquez-Miranda V., Blamey J. M. “Structure and application of antifreeze proteins from Antarctic bacteria.” Microb Cell Factories 16 (2017) 138.

Muralidharan J. and Jayachandran, S. “Physicochemical analyses of the exopolysaccharides produced by a marine biofouling bacterium, *Vibrio alginolyticus*.” Process Biochem 38(6) (2003) 841–847.

Mykytczuk N. C. S., Foote S. J., Omelon C. R., Southam G., Greer C. W., Whyte L. G. “Bacterial growth at −15 °C; molecular insights from the permafrost bacterium *Planococcus halocryophilus* Or1.” ISME J 7 (2013) 1211–1226.

NeoY-L, Li R., Howe J., Hoo R., Pant A., Ho S., Alonso S. “Evidence for an intact polysaccharide capsule in *Bordetella pertussis*.” Microbes and Infect. 12 (2010) 238-45.

Netea M. G., van Deuren M., Kullberg B. J., Jean-Marc Cavaillon, J. W.M Van der Meer “Does the shape of lipid A determine the interaction of LPS with Toll-like receptors?.” Trends Immunol. 23 (2002) 135–139.

Nevot M., Deroncelé V., Messner P., Guinea J., Mercadé E. “Characterization of outer membrane vesicles released by the psychrotolerant bacterium *Pseudoalteromonas antarctica* NF.” Environ. Microbiol. 8 (2006) 1523–1533.

Nicolaus B., Kambourova M., Oner E. T. “Exopolysaccharides from extremophiles: from fundamentals to biotechnology” Environ. Technol. 31 (2010) 1145-1158.

Nyati K. K., Masuda K., Zaman M. M., Dubey P. K., Millrine D., Chalise J. P., Higa M., Li S., Standley D. M., Saito K., Hanieh H., Kishimoto T. “TLR4-induced NF-κB and MAPK signaling regulate the IL-6 mRNA stabilizing protein Arid5a.” Nucleic Acids Res. 45(5) (2017) 2687-2703.

Ophir, T. and Gutnick, D. L. “A role for expolysaccharides in the protection of microorgansims from desiccation.” Appl Environ Microbiol 60 (1994) 740-745.

Pance A., Reisser D., Jeannin J. F. “Antitumoral Effects of Lipid A: Preclinical and Clinical Studies.” J. Investig. Med. 50 (2002)173-178.

Parrilli E., Tedesco P., Fondi M., Tutino M. L. Lo Giudice A., de Pascale D., Fani R. “The art of adapting to extreme environments: The model system *Pseudoalteromonas*.” Phys. Life Rev. 36 (2021) 137-161.

Pawlowska M. K., Ciok A., Decewicz P., Uhrynowski W., Budzik K., Nieckarz M., Pawlowska J., Zdanowski M. K., Bartosik D., Dziewit L. “Insight into heavy metal resistome of soil psychrotolerant bacteria originating from King George Island (Antarctica)” Polar Biol. 41 (2018) 1319–1333.

Peix A., Ramírez-Bahena M. H., Velázquez E. “Historical evolution and current status of the taxonomy of genus *Pseudomonas* Infection” Genetics and Evolution 9 (2009) 1132–1147.

Perepelov A. V., Senchenkova S., Shashkov A. S., Komandrova N. A., Tomshich S. V., Shevchenko L., Knirel Y., Kochetko N. K. “First application of triflic acid for selective cleavage of glycosidic linkages in structural studies of a bacterial polysaccharide from *Pseudoalteromonas* sp. KMM 634 J” Chem. Soc., Perkin Trans. 1 (2000)363-366.

Perez-Cruz C., Carrión O., Delgado L., Martinez G., López-Iglesias C., Mercadè E. "New type of outer membrane vesicle produced by the Gram-negative bacterium *Shewanella vesiculosa* M7T: implications for DNA content." Appl Environ Microbiol 79 (2013) 1874–81.

Phadtare, S. "Recent Developments in Bacterial Cold-Shock Response" Curr. Issues Mol. Biol. 6 (2004) 125-136.

Pieretti G., Corsaro M. M., Lanzetta R., Parrilli M., Canals R., Merino S., Tomás J. M. "Structural studies of the O-chain Polysaccharide from *Plesiomonas shigelloides* Strain 302–73 (Serotype O1)." Eur. J. Org. Chem 18 (2008) 3149–3155.

Pieretti G., Carillo S., Lindner B., Kim K. K., Lee K. C., Lee J.-S, Lanzetta R., Parrilli M., M. M. Corsaro "Characterization of the core oligosaccharide and the O-antigen biological repeating unit from *Halomonas stevensii* LPS: The first case of O-antigen linked to the inner core." Chem. Eur. J. 18 (2012) 3729–3735.

Plötz B. M., Lindner B., Stetter K. O., Holst O. "Characterization of a Novel Lipid A Containing D-Galacturonic Acid That Replaces Phosphate Residues." J. Biol. Chem 275(15) (2000) 11222–11228.

Poli A., Di Donato P., Abbamondi G. R., Nicolaus B. "Synthesis, Production, and Biotechnological Applications of Exopolysaccharides and Polyhydroxyalkanoates by Archaea" Archaea 2011 (2011) 1-13.

Prasanna, G. L. and T. Panda, T. "Electroporation: basic principles, practical considerations and applications in molecular biology." Bioprocess Biosyst Eng 16 (1997) 261–264.

Pummer B. G., Budke C., Augustin-Bauditz,S., Niedermeier D., Felgitsch L., Kampf C. J., Huber R. G., Liedl K. R., Loerting T., Moschen T., Schauperl M., Tollinger M., Morris C. E., Wex H., Grothe H., Pöschl U., Koop T., Fröhlich-Nowoisky J. "Ice nucleation by water-soluble macromolecules." Atmos Chem Phys 15(8) (2015) 4077–409.

Qin G., Zhu L., Chen X., Wang P. G., Zhang Y. "Structural characterization and ecological roles of a novel exopolysaccharide from the deep-sea psychrotolerant bacterium *Pseudoalteromonas* sp. SM9913" Microbiology 153 (2007) 1566–1572.

Que N., Lin S., Cotter R. J., Raetz C. R. "Purification and mass spectrometry of six lipid A species from the bacterial endosymbiont *Rhizobium etli*." J. Biol. Chem. 275 (2000) 28006-28016.

Raetz, C. R. and Whitfield, C. “Lipopolysaccharide endotoxins.” Annu Rev Biochem. 71 (2002) 635-700.

Rakshit M., Darwitan A., Muktabar A., Das P., Nguyen L. T. H., Cao Y., Vizetto-Duarte C., Tang J., Wong Y. S., Venkatraman S., Ng K. W. “Anti-inflammatory potential of simvastatin loaded nanoliposomes in 2D and 3D foam cell models.” Nanomedicine 37 (2021) 102434.

Ray M. K., Kumar G. S., Shivaji S. “Phosphorylation of lipopolysaccharides in the Antarctic psychrotroph *Pseudomonas syringae*: a possible role in temperature adaptation.” J. Bacteriol. 176 (1994) 4243–4249.

Reddy G. P., Hayat U., Abeygunawardana C., Fox C., Wright A. C., Maneval D. R., Jr, Bush C. A., Morris J. G., Jr “Purification and determination of the structure of capsular polysaccharide of *Vibrio vulnificus* M06-24.” J. Bacteriol. 174(8) (1992). 2620–2630.

Regand A. and Goff H. D. “Ice recrystallization inhibition in ice cream as affected by ice structuring proteins from winter wheat grass.” J Dairy Sci 89(1) (2006) 49–57.

Restaino O. F., Finamore R., Diana P., Marseglia M. C., Vitiello M., Casillo A., Bedini E., Parrilli M., Corsaro M. M., Trifuoggi M., De Rosa M., Schiraldi C. “A multianalytical approach to better assess the keratan sulfate contamination in animal origin chondroitin sulfate” Anal. Chim. Acta 958 (2017) 59–70.

Roberts I. S., “The biochemistry and genetics of capsular polysaccharide production in bacteria” Annu. Rev. Microbiol 50 (1996) 285–315.

Romaniuk K., Ciok A., Decewicz P., Uhrynowski W., Budzik K., Nieckarz M., Pawlowska J., Zdanowski M. K., Bartosik D., Dziewit L. “Insight into heavy metal resistome of soil psychrotolerant bacteria originating from King George Island (Antarctica).” Polar Biol. 41 (2018) 1319–1333.

Rosenfeld Y. and Shai Y. “Lipopolysaccharide (Endotoxin)-host defense antibacterial peptides interactions: Role in bacterial resistance and prevention of sepsis.” Biochimica et Biophysica Acta 1758 (2006) 1513–1522.

Sankaran, K. and Wu, H. C. “Lipid modification of bacterial prolipoprotein. Transfer of diacylglyceryl moiety from phosphatidylglycerol.” J. Biol. Chem 269(31) (1994) 19701-19706.

Sarmiento F., Peralta R., Blamey J. M. “Cold and hot extremozymes: industrial relevance and current trends.” Front Bioeng Biotechnol 3 (2015) 148.

Schulz G. E. “The structure of bacterial outer membrane proteins.” Biochim Biophys Acta Biomembr 1565(2) (2002) 308-317.

Schwechheimer C. and Kuehn M. J. “Outer-membrane vesicles from Gram-negative bacteria: biogenesis and functions” Nat Rev Microbiol. 13(10) (2015) 605–619.

Seydel U., Oikawa M., Fukase K., Kusumoto S., Brandenburg K. I. “Intrinsic conformation of lipid A is responsible for agonistic and antagonistic activity.” Eur. J. Biochem. 267 (2000) 3032-3039.

Sharpe J. C., Arnoult D., Youle R. J. “Control of mitochondrial permeability by Bcl-2 family members.” Biochim Biophys Acta Bioenerg, 1644, 2-3, (2004) 107–13.

Shashkov S., Torgov V. I., Nazarenko E. L., Zubkov V. A., Gorshkov N. M., Gorshkov R. P., Widmalma G.“Structure of the phenol-soluble polysaccharide from *Shewanella putrefaciens* strain A6” Carbohyd. Res. 337 (2002) 1119–1127.

Siddiqui K. S., Williams T. J., Wilkins D., Yau S., Allen M. A., Brown M. V., Lauro F. M., Cavicchioli R.“Psychrophiles” Annu. Rev. Earth Planet. Sci., 41 *(*2013), 87–115.

Silipo A., Lanzetta R., Amoresano A., Parrilli M., Molinaro A. “Ammonium hydroxide hydrolysis: a valuable support in the MALDI-TOF mass spectrometry analysis of Lipid A fatty acid distribution.” J. Lipid Res. 43 (2002) 2188–2195.

Silipo A., Leone S., Molinaro A., Sturiale L., Garozzo D., Nazarenko E. L., Gorshkova R. P., Ivanova E. P., Lanzetta R., Parrilli M. “Complete structural elucidation of a novel lipooligosaccharide from the outer membrane of the marine bacterium *Shewanella pacifica*.” Eur. J. Org. Chem. 11 (2005) 2281–2291.

Silipo A., Molinaro A., Comegna D., Sturiale L., Cescutti P., Garozzo D., Lanzetta R., Parrilli M. “Full Structural Characterisation of the Lipooligosaccharide of a *Burkholderia pyrrocinia* Clinical Isolate” Eur. J. Org. Chem 2006 (21) (2006) 4874-4883

Skovhus T. L., C. Holmström, S. Kjelleberg, I. Dahllöf “Molecular investigation of the distribution, abundance and diversity of the genus *Pseudoalteromonas* in marine samples.” FEMS Microbiol Ecol 61 (2007) 348–361.

Spina E., Sturiale L., Romeo D., Impallomeni G., Garozzo D., Waidelich D., Glueckmann M. “New fragmentation mechanisms in matrix-assisted laser desorption/ionization time-of-flight/time-of-flight tandem mass spectrometry of carbohydrates.” Rapid Comm. Mass Spec. 18 (2004) 392-398.

Srivastava G. K., Alonso-Alonso M. L., Fernandez-Bueno I., Garcia-Gutierrez M. T., Rull F., Medina J., Coco R. M., Pastor J. C. "Comparison between direct contact and extract exposure methods for PFO cytotoxicity evaluation." Sci. Rep 23 (2018) 1425.

Stellavato A., Abate L., Vassallo V., Donniacuo M., Rinaldi B., Schiraldi C. "An in vitro study to assess the effect of hyaluronan-based gels on muscle-derived cells: Highlighting a new perspective in regenerative medicine." PLoS One 15(8) (2020) e0236164.

Stellavato A., Tirino V., de Novellis F., Della Vecchia A., Cinquegrani F., De Rosa M., Papaccio G., Schiraldi C. "Biotechnological chondroitin a novel glycosamminoglycan with remarkable biological function on human primary chondrocytes." J. Cell. Biochem 117 (2016) 2158–2169.

Strittmatter W., Weckesser J., Salimath P. V., Galanos C. "Nontoxic lipopolysaccharide from *Rhodopseudomonas sphaeroides* ATCC 17023." J Bacteriol. 155(1) (1983) 153-8.

Sweet C. R., Sweet C. R., Alpuche G. M., Landis C. A., Sandman B. C. "Endotoxin structures in the psychrophiles Psychromonas marina and *Psychrobacter cryohalolentis* contain distinctive acyl features." Mar. Drugs 12 (2014) 4126–47.

Szewzyk U., Holmström C., Wrangstadh M., Samuelsson M. O., Maki J. S., S. Kjelleberg "Relevance of the exopolysaccharide of marine *Pseudomonas* sp. strain S9 for attachment of *Ciona intestinalis* larvae." Mar. Ecol. Prog. Ser. 75 (1991) 259-265.

Taborda M., Antunes A., Tiago I., Veríssimo A., Nobre M. F., da Costa M. S.. "Description of *Idiomarina insulisalsae* sp. nov., isolated from the soil of a sea salt evaporation pond, proposal to transfer the species of the genus *Pseudidiomarina* to the genus *Idiomarina* and emended description of the genus *Idiomarina*." Syst Appl Microbiol 32 (2009) 371–378.

Tamaru Y., Takani Y., Yoshida T., Sakamoto T. "Crucial role of extracellular polysaccharides in desiccation and freezing tolerance in the terrestrial cyanobacterium Nostoc commune." Appl Environ Microbiol 71 (2005) 7327- 7333.

Tomshich S. V., Kokoulin M. S., Kalinovsky A. I., Nedashkovskaya O. I., Komandrova N. A. "Structure of the O-specific polysaccharide from a marine bacterium *Echinicola pacifica* KMM 6172T containing 2,3-diacetamido-2,3-dideoxy-D-glucuronic acid" Carbohydr. Res. 425 (2016) 22–27.

Trent M. S., "Biosynthesis, transport, and modification of lipid A." Biochem Cell Biol. 2004 82(1) 71-86.

Tsai C. M. and Frasch C. E. “A sensitive silver stain for detecting lipopolysaccharides in polyacrylamide gels.” Anal Biochem 119 (1982) 115-119.

Tukenmez U., Aktas B., Aslim B., Yavuz S. “The relationship between the structural characteristics of lactobacilli-EPS and its ability to induce apoptosis in colon cancer cells in vitro.” Sci. Rep 4;9(1) (2019) 8268.

Vaara M. “Agents that increase the permeability of the outer membrane.” Microbiol Rev 56 (1992) 395–411.

Van De Walle J., Hendrickx A., Romier B., Larondelle Y., Schneider Y.-J. “Inflammatory parameters in Caco-2 cells: Effect of stimuli nature,concentration, combination and cell differentiation.” Toxicl. in Vitro 24 (2010) 1441–1449.

Velegol, S. B. and Logan, B. E.; “Contributions of Bacterial Surface Polymers, Electrostatics, and Cell Elasticity to the Shape of AFM Force Curves.” Langmuir 18 (2002) 5256−5262.

Vinogradov E., St Michael F., Cox A. D. “Structure of the LPS O-chain from *Fusobacterium nucleatum* strain ATCC23726 containing a novel 5,7-diamino-3,5,7,9-tetradeoxy-L-gluco-non-2-ulosonic acid presumably having the D-glycero-L-gluco configuration” Carbohydrate Research 468 (2018) 69–7271

Vinogradov E., Bock K., Petersen B. O., Holst O., Brade H. “The structure of the carbohydrate backbone of the lipopolysaccharide from *Acinetobacter* strain ATCC 17905.” Eur. J. Biochem. 243(1-2) (1997) 122-7.

Vinogradov E., Kubler-Kielb J., Korenevsky A. “The structure of the carbohydrate backbone of the LPS from *Shewanella putrefaciens* CN32.” Carbohydr. Res. 337 (2002) 1285–1289.

Vinogradov E., Korenevsky A., Beveridge T. J.“The structure of the rough-type lipopolysaccharide from *Shewanella oneidensis* MR-1, containing 8-amino-8-deoxy-Kdo and an open-chain form of 2-acetamido-2-deoxy-D-galactose” Carbohydr. Res. 338 (2003) 1991–1997.

Vinogradov E., Kubler-Kielb J., Korenevsky A. “The structure of the carbohydrate backbone of the LPS from *Shewanella* spp. MR-4.” Carbohydr. Res. 343 (2008) 2701–2705.

Vinogradov E., Korenevsky A., Beveridge T. J. “The structure of the core region of the lipopolysaccharide from *Shewanella algae* BrY, containing 8-amino-3,8-dideoxy-D-mannooct-2-ulosonic acid.” Carbohydr. Res. 339 (2004) 737–740.

Voets I. K. “From ice-binding proteins to bio-inspired antifreeze materials.” Soft Matter 13(28) (2017) 4808–4823.

Volk A. S., Krasikova I. N., Anastyuk S. D., Solov’eva T. F. “Structure of lipid A from the marine gram-negative bacterium *Pseudoalteromonas nigrifaciens* IAM 13010^{T}.” Chem. Nat. Compd. 43 (2007) 519–524.

Volk W. A., Salomonsky N. L., Hunt D. “*Xanthomonas sinensis* cell wall lipopolysaccharide. I. Isolation of 4,7-anhydro- and 4,8-anhydro-3-deoxy-octulosonic acid following acid hydrolysis of Xanthomonas sinensis lipopolysaccharid” J. Biol. Chem. 247(12) (197) 3881-3887.

Wang X., Preston J. F. 3rd, Romeo T.“The *pgaABCD* locus of *Escherichia coli* Promotes the Synthesis of a Polysaccharide Adhesin Required for Biofilm Formation.” J. Bacteriol. (2004)724–2734

Wang P., Yu Z., Li B., Cai X., Zeng Z., Chen X., Wang X. “Development of an efficient conjugation-based genetic manipulation system for *Pseudoalteromonas*.” Microb Cell Fact 14 (2015) 1–11.

Wanga J., Salem D. R., Sani R. K. “Extremophilic exopolysaccharides: A review and new perspectives on engineering strategies and applications.” Carbohydr. Polymers 205 (2019) 8–26.

Westphal O. and Jann K. “Bacterial lipopolysaccharides: extraction with phenol-water and further applications of the procedure.” Methods Carbohydr. Chem. 5 (1965) 83–91.

Whitfield C. “Bacterial extracellular polysaccharides.” Can J Microbiol 34(4) (1988) 415-420

Whitfield C. “Biosynthesis and Assembly of Capsular Polysaccharides in *Escherichia coli*” Annu. Rev. Biochem. 75 (2006) 39-68.

Whitfield C. and Valvano M. A. “Biosynthesis and expression of cell-surface: polysaccharides in gram-negative bacteria.” Adv Microb Physiol 35 (1993) 135–246.

Whitfield C., Wear S. S., Sande C. “Assembly of Bacterial Capsular Polysaccharides and Exopolysaccharides.” Annu Rev Microbiol. 8(74) 2020 521-543.

Wishart D.S., Knox C., Guo A. C., Eisner R., Young N., Gautam B., Hau D. D., Psychogios N., Dong E., Bouatra S., Mandal R., Sinelnikov I., Xia J., Jia L., Cruz J. A., Lim E., Sobsey C. A., Shrivastava S., Huang P., Liu P., Fang L., Peng J., Fradette R., Cheng D., Tzur D., Clements M., Lewis A., De Souza A., Zuniga A., Dawe M.,

Xiong Y., Clive D., Greiner R., Nazyrova A., Shaykhutdinov R., Li L., Vogel H. J., Forsythe I. “HMDB: A knowledgebase for the human metabolome.” Nucleic Acids Res. 37 (2009) 603–610.

Wrangstadh M., P. L. Conway, S. Kjelleberg “The production and release of an extracellular polysaccharide during starvation of a marine *Pseudomonas* sp. and the effect thereof on aadhesion.” Arch. Microbiol. 145 (1986) 220-227.

Xie L., Shen M., Hong Y., Ye H., Huang L., Xie J. “Chemical modifications of polysaccharides and their anti-tumor activities.” Carbohydr. Polymers 229 (2020) 115436.

Yu Y., Shen M., Song Q., Xie J. “Biological activities and pharmaceutical applications of polysaccharide from natural resources: A review.” Carbohydr. Polymers, 183, (2018). 91–101.

Zdorovenko E. L., Kadykova A. A., Shashkov A. S., Kiselev E. P., Savich V. V., Novikc G. I.“O-specific polysaccharides structures of *Pseudomonas* strains isolated from the strawberry leaves” Carbohydr. Res. 489 (2020) 1079322.

Zeaiter Z., Mapelli F., Crotti E., Borin S. “Methods for the genetic manipulation of marine bacteria.” Electron. J. Biotechnol. 33 (2018) 17–28.

Zeth K. and Thein, M. “Porins in prokaryotes and eukaryotes: common themes and variations.” Biochem J 431(1) (2010) 13–22.

Zhao J. S., Deng Y., Manno D., Hawari J.“*Shewanella* spp. genomic evolution for a cold marine lifestyle and in-situ explosive biodegradation.” Plos one 5(2) (2010) e9109.

Zhong Q., Wei B., Wang S., Ke S., Chen J., Zhang H., Wang H. “The Antioxidant Activity of Polysaccharides Derived from Marine Organisms: An Overview.” Mar Drugs. 17(12) (2019) 674.